VOL. 657 NO. 1 DECEMBER 24, 1993

JOURNAL OF CHROMATOGRAPHY A

INCLUDING ELECTROPHORESIS AND OTHER SEPARATION METHODS

ELSEVIER

JOURNAL OF CHROMATOGRAPHY A

INCLUDING ELECTROPHORESIS AND OTHER SEPARATION METHODS

Scope. The *Journal of Chromatography A* publishes papers on all aspects of **chromatography, electrophoresis** and related methods. Contributions consist mainly of research papers dealing with chromatographic theory, instrumental developments and their applications. In the *Symposium volumes*, which are under separate editorship, proceedings of symposia on chromatography, electrophoresis and related methods are published. *Journal of Chromatography B: Biomedical Applications* —This journal, which is under separate editorship, deals with the following aspects: developments in and applications of chromatographic and electrophoretic techniques related to clinical diagnosis or alterations during medical treatment; screening and profiling of body fluids or tissues related to the analysis of active substances and to metabolic disorders; drug level monitoring and pharmacokinetic studies; clinical toxicology; forensic medicine; veterinary medicine; occupational medicine; results from basic medical research with direct consequences in clinical practice.

Submission of Papers. The preferred medium of submission is on disk with accompanying manuscript (see *Electronic manuscripts* in the Instructions to Authors, which can be obtained from the publisher, Elsevier Science Publishers B.V., P.O. Box 330, 1000 AH Amsterdam, Netherlands). Manuscripts (in English; *four* copies are required) should be submitted to: Editorial Office of *Journal of Chromatography A*, P.O. Box 681, 1000 AR Amsterdam, Netherlands, Telefax (+31-20) 5862 304, or to: The Editor of *Journal of Chromatography B: Biomedical Applications*, P.O. Box 681, 1000 AR Amsterdam, Netherlands. Review articles are invited or proposed in writing to the Editors who welcome suggestions for subjects. An outline of the proposed review should first be forwarded to the Editors for preliminary discussion prior to preparation. Submission of an article is understood to imply that the article is original and unpublished and is not being considered for publication elsewhere. For copyright regulations, see below.

Publication information. *Journal of Chromatography A* (ISSN 0021-9673): for 1994 Vols. 652–682 are scheduled for publication. *Journal of Chromatography B: Biomedical Applications* (ISSN 0378-4347): for 1994 Vols. 652–662 are scheduled for publication. Subscription prices for *Journal of Chromatography A*, *Journal of Chromatography B: Biomedical Applications* or a combined subscription are available upon request from the publisher. Subscriptions are accepted on a prepaid basis only and are entered on a calendar year basis. Issues are sent by surface mail except to the following countries where air delivery via SAL is ensured: Argentina, Australia, Brazil, Canada, China, Hong Kong, India, Israel, Japan, Malaysia, Mexico, New Zealand, Pakistan, Singapore, South Africa, South Korea, Taiwan, Thailand, USA. For all other countries airmail rates are available upon request. Claims for missing issues must be made within six months of our publication (mailing) date. Please address all your requests regarding orders and subscription queries to: Elsevier Science Publishers, Journal Department, P.O. Box 211, 1000 AE Amsterdam, Netherlands. Tel.: (+31-20) 5803 642; Fax: (+31-20) 5803 598. Customers in the USA and Canada wishing information on this and other Elsevier journals, please contact Journal Information Center, Elsevier Science Publishing Co. Inc., 655 Avenue of the Americas, New York, NY 10010. USA, Tel. (+1-212) 633 3750, Telefax (+1-212) 633 3764.

Abstracts/Contents Lists published in Analytical Abstracts, Biochemical Abstracts, Biological Abstracts, Chemical Abstracts, Chemical Titles, Chromatography Abstracts, Current Awareness in Biological Sciences (CABS), Current Contents/Life Sciences, Current Contents/Physical, Chemical & Earth Sciences, Deep-Sea Research/Part B: Oceanographic Literature Review, Excerpta Medica, Index Medicus, Mass Spectrometry Bulletin, PASCAL-CNRS, Referativnyi Zhurnal, Research Alert and Science Citation Index.

US Mailing Notice. *Journal of Chromatography A* (ISSN 0021-9673) is published weekly (total 52 issues) by Elsevier Science Publishers (Sara Burgerhartstraat 25, P.O. Box 211, 1000 AE Amsterdam, Netherlands). Annual subscription price in the USA US$ 5132.25 (US$ price valid in North, Central and South America only) including air speed delivery. Second class postage paid at Jamaica, NY 11431. **USA POSTMASTERS**: Send address changes to *Journal of Chromatography A*, Publications Expediting, Inc., 200 Meacham Avenue, Elmont, NY 11003. Airfreight and mailing in the USA by Publications Expediting.

See inside back cover for Publication Schedule, Information for Authors and information on Advertisements.

0021-9673/94/$07.00

Printed in the Netherlands

VOL. 657, NO. 1 JOURNAL OF CHROMATOGRAPHY A DECEMBER 24, 1993

CONTENTS

(Abstracts/Contents Lists published in Analytical Abstracts, Biochemical Abstracts, Biological Abstracts, Chemical Abstracts, Chemical Titles, Chromatography Abstracts, Current Awareness in Biological Sciences (CABS), Current Contents/Life Sciences, Current Contents/Physical, Chemical & Earth Sciences, Deep-Sea Research/Part B: Oceanographic Literature Review, Excerpta Medica, Index Medicus, Mass Spectrometry Bulletin, PASCAL-CNRS, Referativnyi Zhurnal, Research Alert and Science Citation Index)

REVIEW

REGULAR PAPERS

Column Liquid Chromatography

Gas Chromatography

(Continued overleaf)

BOOK REVIEW

JOURNAL OF CHROMATOGRAPHY A

VOL. 657 (1993)

JOURNAL OF CHROMATOGRAPHY A

INCLUDING ELECTROPHORESIS AND OTHER SEPARATION METHODS

ELSEVIER

AMSTERDAM — LONDON — NEW YORK — TOKYO

0021-9673/93/$06.00

This issue is printed on acid-free paper.

Printed in the Netherlands

Journal of Chromatography A, 657 (1993) 1–15
Elsevier Science Publishers B.V., Amsterdam

CHROM. 25 521

Review

Programmed-temperature gas chromatographic retention index

Yiliang Sun*, Ruiyan Zhang and Qingqing Wang

Department of Chemistry, Beijing University, Beijing 100871 (China)

Bingjiu Xu

School of Pharmaceutical Sciences, Beijing Medical University, Beijing 100083 (China)

(First received April 26th, 1993; revised manuscript received August 16th, 1993)

ABSTRACT

Thirty years of studies on the definitions and calculation methods of the gas chromatographic programmed-temperature retention index values and the various conversion methods between retention values under different gas chromatographic conditions have been reviewed. The programmed-temperature retention value databases compiled in various laboratories are listed. Special emphasis is placed on the recent advances in reproducing programmed-temperature retention indexes under different chromatographic conditions.

CONTENTS

* Corresponding author.

0021-9673/93/$06.00

1. INTRODUCTION

Since its advent in the early 1950s [1], gas chromatography (GC) has long been an extraordinarily important and active field in analytical chemistry. Being an excellent separation method, it also serves as an identifying means. Retention values, especially retention indices (I) are generally used for identification in GC. It is usually impossible, however, to obtain unambiguous results solely by means of I identification. In practical analyses, it has to be used in conjunction with other identification means. A number of coupled techniques, such as GC–MS, GC–Fourier transform IR spectrometry and GC–atomic emission spectrometry, have been developed in parallel. Nevertheless, identification by I still attracts much attention owing to several of its characteristic advantages: (1) it is very effective in differentiating isomers giving similar mass spectra; (2) it is the most inexpensive identification method as no special facilities are needed; (3) it is easy in manipulation and (4) it is extremely sensitive, especially when the sample size is too small to be analysed by other techniques, such as MS. These justify the continuous efforts in the study of I values along with the development of the chromatographic technique as a whole. Moreover, the repeatability of I measurements has improved steadily in step with the improvements in chromatographic instrumentation and capillary column technology.

The Kováts retention index system [2] put forward in 1958 has been commonly accepted. It is a very important parameter in the identification of compounds is isothermal GC analysis. Very abundant data on isothermal GC I values have been accumulated over several decades of practical research work.

There have been numerous reports on the study of GC I values in the literature. In 1983 and 1989, Budahegyi *et al.* [3] and Tarjan *et al.* [4] published two exhaustive reviews to commemorate the 25th and 30th anniversaries of the GC I system, respectively. Nearly 1400 and 500 references were cited respectively, and the advent and subsequent development of the I system and its applications and research on various aspects of the system were put into retrospect. Evans and Haken [5] reviewed research work on I under isothermal conditions.

Programmed-temperature gas chromatography (PTGC), especially linear PTGC (LPTGC), has become the most important technique in GC. About 75% of GC studies were done under programmed-temperature conditions [3]. Retention indices under PTGC conditions (I_{PT}) were studied almost immediately after Kováts put forward his I concept. Judging from the importance of the PTGC technique, however, this kind of study has not won as much popularity. The studies published account for only a small fraction of those on I systems as a whole.

It is known that I values under PTGC conditions depend not only on the characteristics of the stationary phase as in isothermal GC, but also on the conditions prevailing in a PTGC process (initial temperature, programming rate r, column geometry, flow-rate of the carrier gas and its change during the temperature programme, etc.). As a result, without a knowledge of the relationship between I_{PT} values and the numerous parameters involved, they can be reproduced only when all the parameters in a "standard process" are followed rigorously. The problems are that it is difficult to duplicate strictly some parameters of the conditions (exact inner diameter of the column and capillary deactivation are two examples) under which the literature I values were measured, and that it is difficult to define a standard temperature programme that is universally applicable and will win common acceptance by chromatographers who measure I values and who use them for identification. These problems caused some difficulties in reproducing I_{PT} values and applying them for identification.

Nevertheless, studies on I_{PT} systems have been

pushed forward by numerous chromatographers the world over. The first approach to an I_{PT} system was to define it by replacing the log t'_R terms in Kováts' I definition with retention temperature or time, T_R or t_R, as measured in a PTGC process (see below). On the basis of this system, numerous modifications were put forward. Later, with a better understanding of an I system as a function of the programmed-temperature conditions, different approaches to I_{PT} systems were proposed in an attempt to convert between I values obtained under different conditions. Recently, by allowing for all the relevant parameters in the calculation, has been shown that more fundamental parameters (*e.g.*, enthalpies and entropies of solution of solutes in the stationary phase) can be obtained from the measured retention times under one set of conditions, by using such parameter the I values of the same solutes under any conditions can be calculated.

To commemorate the 35th anniversary of the Kováts I system, studies on I_{PT} systems are reviewed in this paper. It can be seen that, as in science research in general, by studying more and more the fundamentals of the subject, research is pushed continuously forward.

2. DEFINITIONS OF VALUES

2.1. Van den Dool and Kratz equation

The first equation for calculating I_{PT} values was put forward by Van den Dool and Kratz [6] in 1963:

$$I_{PT,x} = 100z + 100 \cdot \frac{T_{R,x} - T_{R,z}}{T_{R,z+1} - T_{R,z}} \quad (1a)$$

$$I_{PT,x} = 100z + 100 \cdot \frac{t_{r,x} - t_{r,z}}{t_{rz+1} - t_{r,z}} \quad (1b)$$

where $I_{PT,x}$ is the value of the solute being measured, T_R and t_R are retention temperature and retention time, respectively, and x, z, and $z + 1$ denote the solute being measured and two adjacent n-alkanes that elute just before and after the solute, respectively.

It is easier, however, to calculate I values with eqn. 1b. These equations imply a linear relationship between retention temperatures of the n-alkanes and the number of carbon atoms in their molecules. Actually, this linear relationship is only approximate, so the range of validity of the equation is limited. Moreover, this equation is applicable only to temperature programmes without an isothermal period. Nevertheless, I_{PT} values in the literature were generally calculated with this equation.

2.2. Generalized retention index (GI)

In an effort to find the correlation between z and T_R, a number of researchers adopted the method of curve fitting. The term generalized retention index (GI) was first put forward by Zenkevich and Ioffe [7]. In this paper, GI systems will be discussed in a broader sense, including all I_{PT} systems using the curve-fitting method for I definition.

Halang *et al.* [8] adopted a T_R cubic spline interpolation for the calculation of retention. Cubic splines are functions composed of third-order polynomials pieced together in the data points. It is claimed that this method offers the following advantages: smoothness, no introduction of extraneous oscillations, easy computability and good fit to both non-linear and linear data sets.

Messadi *et al.* [9] compared the retention indices computed by the spline and the linear methods. It was found that retention indices computed by the two methods may differ by as much as 49 index units (i.u.), generally the spline method yields better results. Zenkevich and Ioffe [7] obtained

$$I_{pt} = at'_R + b \log t'_R + c$$
$$= a(t'_R + q \log t'_R) + c \quad (2a)$$

where t'_R is the adjusted retention time of an n-alkane. On the basis of the above relationship, the so-called linear–logarithmic (generalized) retention index was defined:

$$GI = 100z + \Delta I \cdot \frac{(t'_{R,x} + q \log t'_{R,x}) - (t'_{R,z} + q \log t'_{R,z})}{(t'_{R,z+k} + q \log t'_{R,z+k}) - (t'_{R,z} + q \log t'_{R,z})} \quad (2b)$$

where a, b, c and $q = b/a$ are constants, ΔI is the difference between the I_{PT} values of two n-alkanes and k is the difference between the carbon numbers in two n-alkane molecules ($k \geqslant 1$). Similarly, Wang and Sun [10] obtained a relationship between I_{PT} and parameters such as retention volume or its ratio with carrier gas velocity or partition coefficient of the solute, and defining their GI on the basis of I_{PT}, they obtained

$$\begin{aligned} I_{PT} &= a_0 + a_1 \ln Y + a_2 10^{b \ln Y} \\ &= a_0 + a_1 \ln Y + a_2 Y^B \\ &= a_0 + a_2(q \ln Y + Y^B) \end{aligned} \tag{3a}$$

where $q = a_1/a_2$, a_0, a_1, a_2, b, B and q are constants. Y could be one of the parameters V, V/F or V/K, where F is the carrier gas velocity, V the retention volume and K the partition coefficient of the solute, respectively. On the basis of the linear relationship shown above, GI can be defined as

$$GI(x) = 100z + 100 \cdot \frac{(q \ln Y_x + Y_x^B) - (q \ln Y_z + Y_z^B)}{(q \ln Y_z + 1 + Y_{z+1}^B) - (q \ln Y_z + Y_z^B)} \tag{3b}$$

Although these GI systems have some advantages, they both have the shortcoming that the constants a, b, c and q (or a_0, a_1, a_2, q and B) have to be re-calibrated every time the temperature programme changes.

Podmaniczky *et al.* [11] rewrote Van den Dool and Kratz's equation using the capacity factor, k', as follows:

$$I_{PT} = 100z + 100 \cdot \frac{k'_x - k'_z}{k'_{z+1} - k'_z} \tag{4a}$$

They tried to correlate k'_{PT} *vs.* z by different functions. The best correlation was obtained by parabolic regression:

$$k'_{PT} = b_2 z^2 + b_1 z + b_0 \tag{4b}$$

where b_0, b_1 and b_2 are constants. The I_{PT} value can be calculated as

$$I_{PT} = 100\left(\sqrt{\frac{k'_{PT} - b_0}{b_2} + \frac{b_1^2}{4b_2^2}} - \frac{b_1}{2b_2}\right) \tag{4c}$$

2.3. Extended Kováts retention index

This definition is so-called in this paper only because of its resemblance in form to the Kováts isothermal I. It is applicable to complex programmed-temperature processes with isothermal periods:

$$I_v(x) = 100z + 100 \cdot \frac{\ln V_{N,x} - \ln V_{N,z}}{\ln V_{N,z+1} - \ln V_{N,z}} \tag{5}$$

where $V_{N,x}$, $V_{N,z}$ and $V_{N,z+1}$ are the net retention volume of the solute being measured and those of the n-alkanes with z and $z + 1$ carbon atoms, respectively.

In the calculation of I_{PT} with this equation, it is critical to obtain the correct net retention volume. For a constant flow-rate-controlled chromatograph, V_N can be obtained with Majlat *et al.*'s method [12]:

$$V_N(A) = F\left[j_1 t_1 + t_2 \int_{P_1}^{P_2} j \, dP/(P_2 - P_1) + j_3 t_3\right] \tag{6}$$

where F is the carrier gas velocity, J is the gas compressibility correction factor and t_1, t_2 and t_3 are times (see Fig. 1).

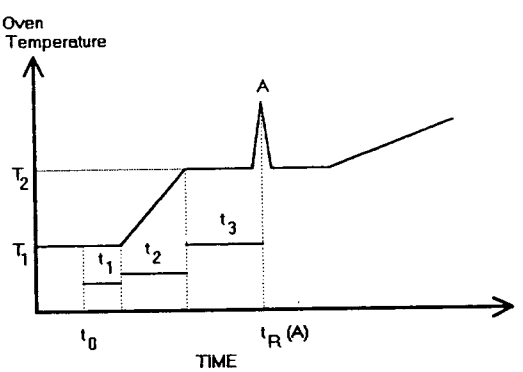

Fig. 1. Schematic diagram of a temperature programme.

Zhu [13] suggested calculating the retention volume on a constant pressure-controlled chromatograph with the following equation:

$$V_N(A) = K\left[(AT_1^{-1/2} - BT_1^{1/2})t_1 + \left(\frac{2A}{T_1^{1/2} + T_2^{1/2}} - \frac{2B}{3}\cdot\frac{[T_1 + T_2 + (T_1T_2)^{1/2}]}{T_1^{1/2} + T_2^{1/2}}\right)t_2 + (AT_2^{-1/2} - BT_2^{1/2})t_3\right] \quad (7)$$

where K, A and B are constants and T_1 and T_2 are column temperatures (see Fig. 1).

For programmed-temperature processes other than that shown in Fig. 1, the calculation equation for $V_N(A)$ should be modified accordingly.

Chen *et al.* [14] proposed calculating the I_{PT} values with Kováts' definition:

$$I_{PT} = 100\left(z + \frac{\log t'_{R,x} - \log t'_{R,z}}{\log t'_{R,z+1} - \log t'_{R,z}}\right) \quad (8a)$$

However, in a temperature programme the temperature ranges to which the compounds of interest and the *n*-alkanes are exposed are different from each other. Therefore, the influences of carrier gas velocity (which is in turn influenced by temperature) on the retention times of the compound of interest and the *n*-alkanes are also different. In order to obtain results comparable with the isothermal retention indices, the influence of the gas velocity due to temperature change should be considered. They suggested to use the adjusted retention times $t'_{R,z}(T)$ and $t'_{R,z+1}(T)$ instead of $t'_{R,z}$ and $t'_{R,z+1}$, respectively. $t'_{R,z}(T)$ and $t'_{R,z+1}(T)$ can be calculated with the equations

$$t'_{R,z}(T) = t'_{R,z}(T_z)10^{B(1/T - 1/T_z)} + \alpha t'_{R,z}(T_z)(T^m T_z^m) \quad (8b)$$

$$t'_{R,z+1}(T) = t'_{R,z+1}(T_{z+1})10^{B(1/T - 1/T_{z+1})} + \alpha t'_{R,z+1}(T_{z+1})(T^m T_{z+1}^m) \quad (8c)$$

where T is the average retention temperature of the compound, T_z and T_{z+1} are the average retention temperatures of the respective *n*-alkanes, α and B can be obtained from the gas hold-up times at two or more different temperatures and from the adjusted retention times for the *n*-alkanes at two or more different programming rates and m is a constant, the value of which is 0.725 for nitrogen. The data calculated by this method are in good agreement with the isothermal retention indices.

The extended Kováts I system has the advantage of being applicable to those programming processes having an isothermal period, even those having multi-ramps with more than one isothermal period. The calculations involved are very tedious, however, and no reports on the application of these calculation methods have appeared in the literature.

Jennings and Shibamoto [15] used a simplified calculation method on the basis of the extended Kováts concept:

$$I_{Pt,x} = 100z + 100\cdot\frac{\ln t'_{R,x} - \ln t'_{r,z}}{\ln t'_{R,z+1} + \ln t'_{R,z}} \quad (9)$$

where $t'_{R,x}$, $t'_{R,z}$ and $t'_{R,z+1}$ are the adjusted retention times of the solute under investigation and the *n*-alkanes with z and $z+1$ carbon atoms, respectively. However, they did not give a sound proof for the justification of using $t'_{R,x}$ as a substitute for $V_{N,x}$ for calculating I_{PT} with eqn. 5. Wang and Sun [16] showed experimentally that there were only slight differences between the results of the exact (with eqns. 5–7) and the approximate (with eqn. 9) calculation methods under different temperature programming conditions (the maximum deviation is less than 0.5 i.u. in extreme cases). A mathematical explanation of this result was also given. This substitution of adjusted retention time for net retention volume greatly simplifies the calculation of extended Kováts I values.

2.4. Other methods

Janssens [17] suggested adding *n*-alkanes with only odd or even numbers of carbon atoms to the sample. The larger systematic error introduced by fewer reference compounds could be compensated for by a proposed improved linear

interpolation, *i.e.*, setting an imaginary reference point between two consecutive *n*-alkanes.

Watts and Kekwick [18] defined retention index by a simple parameter, the relative elution temperature (T_{re}), *i.e.*, the ratio of the elution temperature of any compound to that of a standard. They found that both the logarithms of the retention volume, log V_R, and T_{re} vary with boiling points in an identical manner. This implies that there is a direct relationship between log V_R and T_{re}. They derived a relationship between I_{PT} and the elution temperature T_e.

2.5. Comparison of retention index definitions

Wang and Sun [19] made a comparison of the values calculated according to three definitions (eqns. 1a, 3b and 5). The advantages and shortcomings of these definitions were discussed in terms of their theoretical basis, accuracy, ease of calculation and applicability. They found that eqn. 3b seems to be the best definition of I_{PT} except for its complexity in calculation, while eqns. 1a and 5 are approximate methods for calculating I_{PT} and can be applied only to simple temperature programmes. In the early stages of a simple temperature programme without an initial isothermal step, the I_{PT} values calculated by eqn. 1a may be 7 i.u. smaller than those given by eqn. 3b and may give rise to anomalous results in the correlation between I_{PT} and I_{iso}, while the difference in the I_{PT} values calculated with eqns. 3b and 5 is about 1–3 i.u.

Garcia Dominguez and Santiuste [20] compared I_{PT} values obtained with the cubic spline method, which they considered to be the most reliable, with those calculated with the methods of Van den Dool and Kratz [6], Halang *et al.* [8], Zenkevich and Ioffe [7], Pdmaniczky *et al.* [11], Wang and Sun [10] and Chen *et al.* [14] and with the isothermal Kováts method. They concluded that Van den Dool and Kratz's method is consistently one of the surest methods, but it works worse with high-T_R solutes. The log t_R cubic interpolation appeared to be the most reliable method. As comparison is made with Halang *et al.*'s T_R cubic spline interpolation, this seems to be natural. Zenkevich and Ioffe's and Wang and Sun's methods are also reliable, and all these methods have the advantage that they need only retention times in their calculations. The Podmaniczky *et al.* method appears to be less reliable.

In summary, in order to establish a widely applicable I_{PT} system, numerous proposals have been made, but most of the I_{PT} values reported in the literature were still calculated with Van den Dool and Kratz's definition of I_{PT}.

3. CONVERSIONS BETWEEN RETENTION VALUES UNDER DIFFERENT GC CONDITIONS

3.1. Conversion of I values under isothermal conditions or other isothermal retention values into values under PTGC conditions I_{pt}

Although PTGC has received widespread application, the lack of standard PTRI data results in inconvenience in identification by means of I_{PT}. It is logical, therefore, to find the relationship between I_{PT} and I_{iso} (or other isothermal retention values, such as k or t'_R), so that widely accepted and accumulated isothermal data can be used for PTGC identification. This was for a long time one of the focal points in research and many papers have been published on this topic.

Since the 1960s in studies on the relationship between I_{PT} and I_{iso}, many researchers have tried to find a certain equivalent temperature T_e, so that $I_{PT} = I_{iso}$ (T_e). Among the earlier chromatographers who tried to find T_e with empirical or semi-empirical approximation are Guiochon [21], Giddings [22] and Habgood and Harris [23]. Guiochon proposed that $T_e = T_R - 20°C$. Giddings suggested that $T_e = 0.92\ T_R$. Harris and Habgood, on the basis of many of their investigations on cyclohydrocarbons, pointed out that T_e should be 30–50°C lower than T_R. Lee and Taylor [24] showed that T_e should be the harmonic mean between retention temperature T_R and the initial oven temperature T_0: $T_e = 2T_RT_0/(T_R + T_0)$. Later, Akporhonor *et al.* [25] compared the fitness of the calculated I_{PT} with $T_e = 0.92\ T_R$ and $T_e = 2T_RT_0/(T_R + T_0)$. The results showed that under the condition of lower T_0, I_{PT} corresponds better with I_{iso} if the former T_e values are applied, whereas under higher T_0 the latter gives better results. When the initial

temperatures are the same, at higher programming rates the former T_e and at lower programming rates the latter give better results.

All the above workers based their conclusion on experiments, but as the ranges of solutes under investigation were limited and the precision of I_{PT} measurements on packed columns is less satisfactory than on capillary columns, the conclusions are of limited validity. The approximate calculations proposed by these workers are easy to perform, but they are truly empirical. The influence of some important parameters such as programming rate, geometry of the column, film thickness of the stationary phase and other operating conditions on equivalent T_e has not been taken into consideration.

Said *et al.* [26] tried to make a theoretical study of the problem. They deduced the relationship between the programmed-temperature and isothermal retention indices in chromatography. The relationship was given in the form of a chart from which the equivalent isothermal temperature T_e is plotted *vs.* $\Delta T'$ with I_{PT} as the parameter, $\Delta T'$ is a function of both the inlet and outlet temperatures during the temperature programme and T_e is the temperature at which the isothermal retention index is equal to the programmed-temperature retention index I_{PT}.

In order to reflect the overall dependence of retention temperature in LPTGC on various chromatographic parameters, Grant and Hollis [27] derived the following equation:

$$\int_{T_0}^{T_R} \frac{dT}{[1+\alpha/\beta \exp(\Delta H/RT)]} = \int_0^L r \cdot \frac{dx}{ux} \qquad (10a)$$

where u_x is the linear gas velocity at point x, β column phase ratio, ΔH the molar heat of solution of the solute in the stationary phase at the column temperature T, $a = \exp(\Delta S/R)$ is constant for a given solute, ΔS the molar entropy of solution at the column temperature, r the programming rate (°C/min), L the column length, R the gas constant, T_0 the initial programme temperature (K) and T_r retention temperature of the solute (K). In order to simplify the treatment, the following assumptions are made: during a period corresponding to the column dead time, the solute is transported a negligible distance; and the dead time is assumed to be constant during temperature programming.

On the basis of the assumptions, for aromatic compounds the following equation was determined by the authors:

$$T_R = \frac{T_b}{A + 0.22 \log(0.0012 T_b/A^2)} \qquad (10b)$$

where T_b is the boiling point of the solute, $A = 0.44 - 0.22 \log r\phi$, $\phi = aL/\beta\bar{u}$, L is the column length and $\bar{u}$ is the average linear velocity of the carrier gas.

Curvers *et al.* [28] stressed that the first assumption will not hold for components with relatively short retention times except when an extremely low (sub-ambient) initial temperature is used. The second assumption is not valid owing to changes in the carrier gas viscosity and thermal expansion of the carrier gas. They continued the treatment without any simplifications and derived the following equation:

$$\int_{T_0}^{T_R} \frac{dT}{t_0(T)[1+\alpha/\beta \exp(\Delta H/RT)]} = r \qquad (11a)$$

where $t_0(T)$, the dead retention time, is a function of temperature. They further pointed out [28] that the parameters in eqn. 11a could be obtained as follows without any preconditions:

(1) Calculation of a/β and $\Delta H/RT$: for an isothermal GC process,

$$\ln k = \ln(a/\beta) + \Delta H/RT \qquad (11b)$$

From measurements at two or more temperatures, a ln k *versus* $1/T$ curve can be obtained; α/β and $\Delta H/RT$ in turn can be obtained from the slope and the intercept of the regression line.

(2) Calculation of $t_0(T)$: according to Ettre's theory [29], there is a linear relationship between the viscosity of a gas and temperature T. Hence $t_0(T)$ can be obtained from the following equation:

$$t_0(T) = \frac{4L^2(P^3-1)}{3P_0(P^2-1)} \cdot \frac{32}{d_c^2} \cdot \eta(T) \qquad (11c)$$

and experiments, where $P = P_i/P_0$, P_0 and P_i are the pressures at the outlet and the inlet of the column, respectively, and d_c and L are the inner diameter and the length of the column, respec-

tively. By using the above-mentioned relationships, the retention temperature of the solute T_R can be calculated with the temperature programme parameters T_0 and r provided and I_{PT} can be further calculated by Van den Dool and Kratz's equation. This procedure for calculating linear programmed temperature retention indices was evaluated using five different non-polar columns with OV-1 as the stationary phase. The results were compared with the measured values (*e.g.*, see Table 1). It was believed that the isothermal retention information obtained on one column can be transferred to another column containing the same stationary phase with different phase ratio.

Guan *et al.* [30] pointed out, however, that the entropy and enthalpy terms in eqn. 11a are not independent of the stationary phase film thickness or even of the carrier gas velocity. Hence it is not correct to transfer the entropy and enthalpy terms obtained from one column to those for another as proposed by Curvers *et al.* They suggested evaluating these terms from two or more isothermal Kováts I measurements with some new equations:

$$\ln k_i = \frac{I_i - 100z}{100} \cdot \ln\left(\frac{k_{z+1}}{k_z}\right) + \ln K_z \qquad (12a)$$

$$\ln k_{i,T} = \ln\left(\frac{a_i}{\beta}\right) - \frac{\Delta H_i}{RT} \qquad (12b)$$

Together with eqn. 12a, they obtained the desired equations:

$$-\frac{\Delta H_i}{R} = (\ln k_{i,T_1} - \ln k_{i,T_2})\frac{T_1 T_2}{T_2 - T_1} \qquad (12c)$$

and

$$\frac{a_i}{\beta} = \exp\left(\ln k_{i,T} - \frac{\Delta H_i}{RT}\right) \qquad (12d)$$

where T can be T_1 or T_2. The differences between calculated and experimentally determined I_{PT} values usually fall within 0.5 i.u. (*e.g.*, see Table 2).

Guan and Zhou [31] used their modified calculation method to evaluate retention times obtained under multi-step temperature programmes with equal success (*e.g.*, see Table 3). Guan *et al.* [32] applied their calculation method to the identification of unknown components in a simple mixture.

Similarly, on the basis of the work of Grant and Hollis [27], Podmaniczky *et al.* [33] developed a method for the calculation of k'_{PT} (capacity factor in a PTGC process) and then calculated the retention indices using eqn. 4c. The mean difference in the retention indices measured and calculated is 5 i.u.

Krupcik and co-workers [34,35] derived an equation for the prediction of T_R for a compound of interest, measured by LPTGC, from isothermal Kováts retention indices I. The temperature coefficient, dI/dT, and retention temperatures of n-alkanes, $T_{R,z}$, $T_{R,z+1}$, were found via LPTGC.

$$T_R = \frac{[I_{T_0} - 100z + (dI/dT)T_0][T_{R,z+1} - T_{R,z}] + 100T_{R,z}}{100 - (dI/dT)(T_{R,z+1} - T_{R,z})} \qquad (13)$$

where I_{T_0} is the isothermal retention index at the initial temperature. The predicted retention temperature can be used to calculate I_{PT} with Van den Dool and Kratz's eqn. 1a.

Examples of other methods without using T_e are as follows:

$$I_{T_0/r} = (I_{T_r} + I_{T_0})/2 \qquad (14)$$

This equation was put forward by Golovnya and Uraletz [36], where $I_{T_0/r}$ is the PTGC retention index under the conditions of programming rate r and initial temperature T_0 and I_{T_R} and I_{T_0} are the isothermal retention indices at temperatures of T_R and T_0, respectively.

Erdey *et al.* [37] put forward

$$I_{PT} = A + \frac{2.3B \log[(T_R + C)/(T_0 + C)]}{T_R - T_0} \qquad (15)$$

where A, B and C are constants in Antoine-type equations.

Further, Akporhonor *et al.* [38–40] described procedures for the calculation of programmed-temperature retention times, elution tempera-

TABLE 1

PREDICTION OF RETENTION VALUES ACCORDING TO CURVERS *ET AL.*'S [28]

Comparison between measured and calculated retention temperatures and retention indices for column 2. Reproduced from Table 8 in ref. 28.

Retention parameter	Component	Programming rate (°C/min)								
		2			4			8		
		Measured	Calculated	Difference	Measured	Calculated	Difference	Measured	Calculated	Difference
Retention temperature	*n*-Octane	345.13	345.12	−0.11	360.26	360.37	−0.12	384.08	363.82	+0.28
	n-Dodecane	401.24	400.78	+0.46	423.42	422.95	+0.46	453.39	452.11	+1.28
	Heptanol	363.90	400.78	−0.33	382.99	383.02	−0.04	410.13	409.06	+1.06
	Decanol	409.36	409.04	+0.32	431.88	431.39	+0.49	462.32	460.69	+1.63
	3-Pentanone	336.24	336.34	−0.11	347.49	347.62	−0.13	367.48	367.38	+0.10
	3-Octanone	359.74	360.08	−0.34	378.48	378.61	−0.13	405.46	404.68	+0.78
	2,4,4-Trimethyl-1-pentene	338.18	338.29	−0.12	350.52	350.64	−0.12	371.78	371.62	+0.15
	1-Tridecene	414.31	414.04	+0.27	437.08	436.49	+0.59	467.72	465.91	+1.81
	Toluene	341.29	341.44	−0.16	355.16	355.32	−0.16	378.04	377.87	+0.17
	1,2-Dimethylbenzene	353.98	354.24	−0.26	371.94	372.09	−0.16	398.53	397.98	+0.54
	Isobutylbenzene	370.10	370.34	−0.25	Coincides with $n-C-10$			419.52	418.07	+1.45
Retention index	Heptanol	951.56	952.07	−0.51	951.56	951.97	−0.42	–		
	Decanol	1255.19	1255.40	−0.21	1255.32	1255.64	−0.32	–		
	3-Pentanone	670.49	672.79	−2.30	660.58	662.59	−2.01	672.89	673.41	−0.52
	3-Octanone	922.24	923.06	−0.82	923.72	924.33	−0.61	925.57	925.51	+0.06
	2,2,4-Trimethyl-1-pentene	709.05	710.09	−1.04	710.32	710.98	−0.66	911.96	711.61	+0.35
	1-Tridecene	1288.85	1288.93	−0.08	1289.36	1289.31	+0.05	1289.70	1289.81	−0.11
	Toluene	749.73	750.84	−1.12	753.06	753.80	−0.74	756.98	756.40	+0.58
	1,2-Trimethylbenzene	877.19	877.92	−0.73	881.20	881.62	+0.41	885.87	885.60	+0.17
	Isobutylbenzene	995.33	994.95	+0.37	Coincides with $n-C-10$			1004.21	1003.88	+0.33

TABLE 2

PREDICTION OF RETENTION VALUES ACCORDING TO GUAN *ET AL.*'S METHOD [30]

Comparison of calculated and measured LPTGC I values on column 4. $T_0 = 40°C$. Reproduced from Table V in ref. 30.

Component	Isothermal		Programming rate (°C/min)					
	45.0°C	65.0°C	2		4		8	
			$I_{calc.}$	ΔI	$I_{calc.}$	ΔI	$I_{calc.}$	ΔI
2-Methyl-2-butene	520.0	519.8	513.7	0.0	514.1	0.1	514.7	0.1
4-Methyl-1-pentene	556.7	557.1	546.0	0.2	546.9	0.3	548.2	0.4
2,3-Dimethylbutane	566.3	567.2	556.2	0.2	557.1	0.2	558.6	0.3
2-Methyl-1-pentene	588.0	588.0	583.0	0.1	583.5	−0.1	584.1	0.0
Methylcyclopentane	628.2	631.3	620.9	0.1	622.3	0.1		
2,4-Dimethylpentane	630.4	631.3	623.0	0.0	624.2	0.0		
Benzene	651.3	655.4	642.0	0.2	644.2	0.5	647.2	0.6
Cyclohexane	660.6	665.6	651.6	0.2	654.0	0.4	657.3	0.6
2-Methylhexane	667.6	667.7	659.5	0.1	661.0	0.0	662.8	0.0
1-Heptane	688.6	688.7	684.7	0.0	685.5	0.0	686.4	0.0

ture, retention indices and two kinds of equivalent temperature from isothermal chromatographic data. The first equivalent temperature, $T_e(1)$, is the temperature at which the isothermal retention time t_{iso} equals t_{PT}, the programmed temperature retention time, and the second, $T_e(2)$, is the temperature at which the isothermal retention index I_{iso} equals the programmed-temperature retention index I_{PT}.

Engewald and Maurer [41] used the retention index concept in systems of series-coupled columns without intermediate trapping for the identification of individual components in a complex mixture. Recently, Wright and Walling [42] demonstrated the calculation of retention times for temperature-programmed serially linked capillary columns from isothermal chromatographic data.

In summary, many researchers have made contributions to the study of the relationships between I_{PT} and isothermal retention values in an effort to make use of the I_{iso} standard data system in LPTGC analysis. However, the equivalent temperature approach gave less accurate predictions than those given by the approaches of Curvers *et al.* [28] and Guan *et al.* [30].

3.2. Conversion of I_{PT} values under one set of PTGC conditions into those under another set of PTGC conditions

All studies on the conversion of I_{PT} values under one set of PTGC conditions into those under another set of conditions are based on Golovnya and Uraletz's work [36]. On studying the relationship between I_{iso} and I_{PT}, they obtained

$$I_{PT} = I_{T_0} + \frac{T_R - T_0}{2} \cdot \frac{dI}{dT} \tag{16}$$

where T_R is the retention temperature of the solute, T_0 is the initial temperature, I_{T_0} is the isothermal retention index of the solute at T_0 and dI/dT is the temperature coefficient of the isothermal retention index.

On the basis of eqn. 16, Wang and Sun [43] derived the following equation to define the LPTGC I values of a certain solute under different temperature programming conditions:

$$I_{PT}(1) = I_{T_{0\,1}} + \frac{T_{R1} - T_{01}}{2} \cdot \frac{dI}{dT} \tag{17a}$$

and

TABLE 3

PREDICTION OF RETENTION TIMES ACCORDING TO GUAN AND ZHOU'S METHOD [31]

Retention time (min) calculation for column 2. Temperature programming conditions as indicated. Reproduced from Tables IV and V in ref. 31.

Component	Programme A		Programme B		Programme C		Programme D	
	Calculated	Measured	Calculated	Measured	Calculated	Measured	Calculated	Measured
Decane	2.32	2.35	–	–	1.88	1.90	2.60	2.63
o-Cresol	3.57	3.50	3.53	3.50	2.68	2.62	4.04	4.05
p-Cresol	4.10	4.04	3.95	3.94	3.01	2.94[a]	4.60	4.62
Undecane	3.91	2.92	3.80	3.81	2.91	2.94[a]	4.39	4.39
Dodecane	6.59	6.60	5.54	5.55	4.88	4.88	7.33	7.34
1-Decanol	8.55	8.53	6.85	6.84	7.12	7.13	10.57	10.56
Tridecane	9.07	9.09	7.22	7.22	7.84	7.90	11.48	11.49
Tetradecane	11.21	11.20	8.76	8.76	11.15	11.21	15.82	15.82
Methyl dodecanoate	11.76	11.75	9.15	9.15	12.06	12.09	16.75	16.73
Pentadecane	13.53	13.52	10.17	10.17	14.74	14.79	18.72	18.72
Methyl deodecanoate	14.31	14.29	10.55	10.57	15.97	15.99	19.33	19.34
Hexadecane	16.98	16.94	11.78	11.81	20.23	20.22	20.80	20.84

Temperature programming conditions

Programme	Step No.	Temperature (°C)	Hold time (min)	Programming rate (°C/min)
A	1	87.0	5.0	8.0
	2	137.0	Hold	
B	1	87.0	3.0	10.0
	2	157.0	Hold	
C	1	97.5	5.0	4.0
	2	127.5	Hold	
D	1	82.5	2.0	2.0
	2	90.0	2.0	4.2
	3	107.0	2.0	8.0
	4	200.0	Hold	

[a] Peaks overlap.

$$I_{PT}(2) = I_{T_{02}} + \frac{T_{R2} - T_{02}}{2} \cdot \frac{dI}{dT} \quad (17b)$$

From eqns. 17a and 17b, the following equation can be derived to calculate $I_{PT}(2)$ under PTGC conditions 2 from $I_{PT}(1)$ under conditions 1, assuming dI/dT to be constant:

$$I_{PT}(2) = I_{PT}(1) + \frac{T_{02} - T_{01}}{2} \cdot \frac{dI}{dT} + \frac{T_{R2} - T_{R1}}{2} \cdot \frac{dI}{dT} \quad (17c)$$

Eqn. 17c opens up a new way to expand the application of the PTGC I system.

Chen and Peng [44] obtained the following equation from Kováts' isothermal definition:

$$I_{T_2} = I_{T_1} + \frac{T_2 - T_1}{A + BT_2} \quad (18a)$$

where A and B are constants. Under programmed temperature conditions, if I_{PT} is calculated from eqn. 8a, eqn. 18a can be extended as follows:

$$I_{PT}(2) = I_{PT}(1) + \frac{T_2 - T_1}{A + BT_2} \quad (18b)$$

where T_1 and T_2 are retention temperatures.

3.3. Conversion of I values under PTGC conditions into those under isothermal conditions

A method of calculating I_{iso} from different PTGC I systems was also put forward by Chen *et al.* [45]. This seems to be the only work concerned with the conversion of I_{PT} into I_{iso}.

4. I_{PT} DATABASES

Comparing the measured I values of the solutes to be identified with those in I databases is a very important auxiliary means of identification. Currently, there are two main programmed-temperature retention index data bases.

4.1. Quantitative Analysis of Flavor and Fragrance Volatiles by Glass Capillary Gas Chromatography [15]

The book of the above title collected I values of 1193 organic compounds on PEG-20M and OV-101 columns under programmed-temperature GC conditions. This data system is valuable as a reference to researchers on chromatographic analyses of flavours and fragrances. However, in compiling this data system, glass capillary columns were applied, which are different from fused-silica capillary columns that currently are predominantly used, and some of the chromatographic conditions such as stationary phase film thickness and carrier gas flow-rates are not specified, so it is difficult to reproduce the conditions prevailing in the measurements of the I values. The I_{PT} used in the book was calculated by the extended Kováts definition, which is different from that in other databases using Van den Dool and Kratz's definition.

4.2. Sadtler Standard Capillary Gas Chromatographic Retention Index Library [46]

In 1984, Sadtler Research Laboratories put forward a series of standard capillary chromatographic retention index data. This database is composed of four volumes with retention indices of about 2000 organic compounds under isothermal and temperature-programmed conditions. This database can serve as a valuable reference in GC identification. The Sadtler data system has the advantage that the experimental conditions are more clearly listed, which might facilitate its application. Weber [47] made use of this database in micropollution monitoring, and discussed the effects of various factors on I_{PT} measurements.

4.3. Others

In addition to the above two larger databases, many laboratories have collected and compiled their own I_{PT} databases for some specific purposes.

Lee and co-workers [48,49] established a linear retention index for capillary PTGC of polycyclic aromatic hydrocarbons (PAHs), polycyclic aromatic heterocyclic and nitrogen-containing polycyclic compounds using naphthalene, phenanthrene, chrysene and picene as reference standards. This system of 310 compounds has been applied to the analysis of diesel particulate material, coal extracts, synthetic fuels, tissues, sediments, air particulate matter and combustion effluents.

Hayes and Pitzer [50] established a I_{PT} library of over 200 hydrocarbons and applied it in the analysis of unknown jet fuel samples.

Emergence (elution, retention) temperature indices and relative retention times of nearly 600 pesticides and industrial chemicals were sequentially tabulated by Saxton [51–53] to provide a basis for the identification of unknowns detected on methylsilicone columns when PTGC is used.

White *et al.* [54] compiled retention indices for 480 compounds, including all possible alkylbenzenes containing ten or fewer carbon atoms, and over 150 monoenes and dienes. The library can be applied to measure gasoline derived from either petroleum or synthetic reactions. The bases of all the above databases are given in Table 4.

Hancock and Peters [55] presented a database of GC retention indices for chemical warfare agents and stimulants, which was applied to the identification of triethyl phosphate, tributyl phosphate and diethyl malonate in water and soil samples.

TABLE 4

PROGRAMMED-TEMPERATURE RETENTION VALUE DATABASES

Compiler(s)	No. of compounds	Compound class	Retention value	Definition equation	Column used	Reference standards	Year	Ref.
Jennings and Shibamoto	1193	Flavours and fragrances	I_{PT}	1a	OV-101, PEG-20M	*n*-Alkanes	1980	15
Sadtler Labs.	2000	Various	I_{PT}	1a	OV-1, SE-54, Carbowax 20M	*n*-Alkanes	1984	46
Lee *et al.*	310	Polycyclic aromatics	I_{PT}	1a	SE-52	PAHs	1979	48
Hayes and Pitzer	200	Hydrocarbons	I_{PT}	Kováts	OV-1, OV-17	*n*-Alkanes	1982	50
White *et al.*	480	Hydrocarbons	I_{PT}	1a	OV-1	*n*-Alkanes	1992	54
Saxton	600	Pesticides	T_r, t_r		Methylsilicones	*n*-Alkanes	1987	51–53

5. STUDY ON THE REPRODUCIBILITY AND TRANSFERABILITY OF I_{PT} VALUES

Compared with I_{iso} measurement, the repeatability of I_{PT} is equally good. However, the reproducibility of I_{PT} measurements between different laboratories or between different groups in a laboratory is usually poor because many authors did not specify exhaustively all the experimental parameters necessary for reproducing their I_{PT} data used in their measurement. In most instances, the poor reproducibility of I_{PT} measurements can be compensated for by using standard samples, although their procurement is often expensive and time consuming. The dependence of this identification method on standard samples is a serious drawback in comparison with spectroscopic identification methods. Also, transferring I_{PT} data obtained under one set of experimental conditions to those under another set even by the same person is considered to be impossible by most chromatographers.

The reliability of the identification by retention indices is based on the reproducibility of retention index measurements. Chromatographs of high quality with highly stable performance have long been available. In addition, capillary columns 0.1–0.53 mm inner diameter, 10–60 m in length and 0.10–5.0 μm film thickness and of high performance are manufactured on a large scale. With high-quality chromatographs and columns, the repeatability of I_{PT} values has attained new levels. Under identical chromatographic conditions, provided that the characteristics of the stationary phases are stable and the samples are not overloaded, the standard deviations of the measurements of I_{PT} can be lower than 0.1 i.u.

Currently, an attractive point in the study of application of I_{PT} values is to increase its reproducibility and to achieve their transferability in order to make full use of their high repeatability. However, many chromatographers pessimistically consider that it is impossible to reproduce I_{PT} values under different experimental conditions. For instance, after a careful study on the effects of column inner diameter, r, $P(P_i/P_o)$, F (gas volumetric velocity), T_0 and the film thickness of the stationary phase, d_f, on measured I_{PT} values, Weber [47] concluded that only on strictly identical columns and with advanced chromatographs was it possible to reproduce standard I_{PT} values, and it was meaningless to compare I_{PT} values obtained in different laboratories and under different conditions.

As early as 1960, Habgood and Harris [56] derived a basic equation for LPTGC:

$$\int_{T_0}^{T_R} \frac{1}{V} \cdot dT = \frac{r}{F} \tag{19}$$

where V is the retention volume of the solute.

In 1983 Knoeppel *et al.* [57], starting from Habgood and Harris's basic equation, proposed that in order to obtain standard I_{PT} values under

different conditions, it was not necessary to standardize all the column characteristics and temperature programming parameters, but only to make the parameters satisfy the condition $raL^2/D^2 = \text{constant}$, where $a = (P^3 - 1)/(P^2 - 1)$, $P = P_i/P_o$, P_i and P_o are the inlet and outlet pressure of the column, respectively, D is the inner diameter of the column, L is the length of the column and r is the programming rate. The authors verified their proposition and found that, when D and L were constants and r and a were adjusted according to aforementioned condition, the reproducibility of I_{PT} values obtained was excellent, but when L changed the reproducibility of I_{PT} suffered.

To solve this problem, Saxton [51–53] proposed a technique of simultaneous parameter compensation: to obtain reproducible I_{PT} values for components in a mixture under different conditions, all the parameters should be adjusted appropriately so as to make the retention temperature T_R of a certain reference compound in the mixture remain unchanged. This simultaneous parameter compensation method seems straightforward and convenient to use but needs a theoretical explanation.

In 1985, Wang and Sun [58] pointed out that it was possible to obtain reproducible I_{PT} values in the I_{PT} measurements on a capillary column heated from the same initial oven temperature. Both the programming rate r and the carrier gas flow-rate F can be varied, but their ratio r/F should be kept constant. In 1987, Wang and Sun [59] furthered their study and also starting from the basic equation of Habgood and Harris they obtained

$$\int_{T_0}^{T_R} \left(V_g + \frac{273V_d}{Tw}\right)^{-1} dT = \frac{rw}{F} \qquad (20)$$

where w is the mass of the stationary phase in the column, V_g the specific retention volume of the solute and V_d the column dead retention volume; rw/F is a characteristic parameter for the measurement of retention indices under LPTGC conditions. The authors pointed out that when T_0 and rw/F were kept constant, reproducible I_{PT} values could be obtained with different columns and under different temperature programming conditions. Yin and Sun [60] improved and simplified the previous work and pointed out that the ratio rt_0/β, where t_0 is the dead retention time, and β the phase ratio of the column, had the same characteristic in reproducing I_{PT} values as rw/F, while the new characteristic parameter is more convenient to use. Recently, De Paoli *et al.* [61] succeeded in reproducing values on two columns with different phase ratios using Yin and Sun's method.

It can therefore be concluded that reproducing or transferring I_{PT} values under non-identical conditions can be achieved if all the important chromatographic parameters are clearly specified in the original I_{PT} database.

Apart from the work mentioned above, the effects of sample size [62–66] and the amount of the neighbouring solute (large neighbour effect) [67] on reproducing measurements have also been studied. They emphasized the importance of avoiding overloading of injected sample and reference *n*-alkanes and the presence of large neighbouring peaks in order to obtain reproducible I_{PT} measurements. All these studies could help to deepen the understanding on this topic and are of practical significance.

The aforementioned are the main directions in I_{PT} studies in the literature. It should be stated that there are also some publications on studies of the relationship between I_{PT} and molecular structure and thermodynamic parameters. The aim of these studies is to calculate I_{PT} values from structure and thermodynamic parameters. With recent developments in computer technology, more and more chromatographers are following this direction of research. In this review, however, studies in this direction were not included.

6. ACKNOWLEDGEMENT

This work was kindly supported by the National Natural Science Foundation of China.

REFERENCES

1 A.T. James and A.J.P. Martin, *Biochem. J.*, 50 (1952) 679.
2 E.sz. Kovats, *Helv. Chim. Acta*, 41 (1958) 1915.

3 M.V. Budahegyi, E.R. Lombosi, T.S. Lombosi, S.Y. Meszaros, Sz. Nyiredy, G. Tarjan, I. Timar and J.M. Takacs, *J. Chromatogr.*, 271 (1983) 213.
4 G. Tarjan, Sz. Nyiredy, M. Gyoer, E.R. Lombosi, T.S. Lombosi, M.V. Budahegyi, S.Y. Meszaros and J.M. Takacs, *J. Chromatogr.*, 472 (1989) 1.
5 M.B. Evans and J.K. Haken, *J. Chromatogr.*, 472 (1989) 93.
6 H. Van den Dool and P.D. Kratz, *J. Chromatogr.*, 11 (1963) 463.
7 I.G. Zenkevich and B.V. Ioffe, *J. Chromatogr.*, 439 (1988) 185.
8 W.A. Halang, R. Langlais and E. Kugler, *Anal. Chem.*, 50 (1978) 1829.
9 D. Messadi, F. Helaimia, S. Ali-Kokhnache and M. Boumahraz, *Chromatographia*, 29 (1990) 429.
10 T.S. Wang and Y.L. Sun, *J. Chromatogr.*, 390 (1987) 261.
11 L. Podmaniczky, L. Szepesy, K. Lakszner and G. Schomburg, *Chromatographia*, 21 (1986) 397.
12 P. Majlat, Z. Erdoes and J. Takacs, *J. Chromatogr.*, 91 (1974) 89.
13 A. Zhu, *J. Chromatogr.*, 331 (1985) 229.
14 B.J. Chen, X.J. Guo and S.Y. Peng, *Chromatographia*, 23 (1987) 888.
15 W. Jennings and T. Shibamoto, *Qualitative Analysis of Flavor and Fragrance Volatiles by Glass Capillary Gas Chromatography*, Academic Press, New York, 1980, p. 9.
16 T.S. Wang and Y.L. Sun, *J. Chromatogr.*, 390 (1987) 275.
17 G. Janssens, *Anal. Chim. Acta*, 95 (1977) 153.
18 R.B. Watts and R.G.O. Kekwick, *J. Chromatogr.*, 88 (1974) 165.
19 T.S. Wang and Y.L. Sun, *J. Chromatogr.*, 390 (1987) 269.
20 J.A. Garcia Dominguez and J.M. Santiuste, *Chromatographia*, 32 (1991) 116.
21 G. Guiochon, *Anal. Chem.*, 36 (1964) 661.
22 J.C. Giddings, *Gas Chromatography*, Academic Press, New York, 1963, p. 57.
23 H.W. Habgood and W.E. Harris, *Anal. Chem.*, 36 (1964) 663.
24 J. Lee and D.R. Taylor, *Chromatographia*, 16 (1982) 286.
25 E.E. Akporhonor, J. Lee and D.R. Taylor, *Anal. Proc.*, 23 (1986) 163.
26 A.S. Said, A.M. Jarallah and R.S. Al-Ameeri, *J. High Resolut. Chromatogr. Chromatogr. Commun.*, 9 (1986) 345.
27 D.W. Grant and M.G. Hollis, *J. Chromatogr.*, 158 (1978) 3.
28 J. Curvers, J. Rijks, C. Cramers, K. Knauss and P. Larson, *J. High Resolut. Chromatogr. Chromatogr. Commun.*, 8 (1985) 607, 611.
29 L.S. Ettre, *Chromatographia*, 18 (1984) 243.
30 Y.F. Guan, J. Kiraly and J. Rijks, *J. Chromatogr.*, 472 (1989) 129.
31 Y.F. Guan and L.M. Zhou, *J. Chromatogr.*, 552 (1991) 187.
32 Y.F. Guan, P. Zheng and L.M. Zhou, *J. High Resolut. Chromatogr.*, 15 (1992) 18.
33 L. Podmaniczky, L. Szepesy, K. Lakszner and G. Schomburg, *Chromatographia*, 21 (1986) 91.
34 J. Krupcik, P. Cellar, D. Repka, J. Garaj and G. Guiochon, *J. Chromatogr.*, 351 (1986) 111.
35 J. Krupcik, D. Repka, T. Hevesi and J. Garaj, *J. Chromatogr.*, 406 (1987) 117.
36 R.V. Golovnya and V.P. Uraletz, *J. Chromatogr.*, 36 (1968) 276.
37 L. Erdey, J. Takacs and E. Szalanczy, *J. Chromatogr.*, 46 (1970) 29.
38 E.E. Akporhonor, S. LeVent and D.R. Taylor, *J. Chromatogr.*, 405 (1987) 67.
39 E.E. Akporhonor, S. LeVent and D.R. Taylor, *J. Chromatogr.*, 463 (1989) 271.
40 E.E. Akporhonor, S. LeVent and D.R. Taylor, *J. Chromatogr.*, 504 (1990) 269.
41 W. Engewald and T. Maurer, *J. Chromatogr.*, 520 (1990) 3.
42 L.H. Wright and J.F. Walling, *J. Chromatogr.*, 540 (1991) 311.
43 T.S. Wang and Y.L. Sun, *J. Chromatogr.*, 407 (1987) 79.
44 B.J. Chen and S.Y. Peng, *Chromatographia*, 25 (1988) 731.
45 B.J. Chen, Y.J. Guo and S.Y. Peng, *Chromatographia*, 25 (1988) 539.
46 *The Sadtler Standard Gas Chromatography Retention Index Library*, Sadtler Laboratories, Philadelphia, 1984.
47 L. Weber, *J. High Resolut. Chromatogr. Chromatogr. Commun.*, 9 (1986) 446.
48 M.L. Lee, D.L. Vassilaros, C.M. White and M. Novotny, *Anal. Chem.*, 51 (1979) 768.
49 D.L. Vassilaros, R.C. Kong, D.W. Later and M.L. Lee, *J. Chromatogr.*, 252 (1982) 1.
50 P.C. Hayes, Jr. and E.W. Pitzer, *J. Chromatogr.*, 253 (1982) 179.
51 W.L. Saxton, *J. Chromatogr.*, 312 (1984) 59.
52 W.L. Saxton, *J. Chromatogr.*, 357 (1986) 1.
53 W.L. Saxton, *J. Chromatogr.*, 393 (1987) 175.
54 C.M. White, J. Hackett, R.R. Anderson, S. Kail and P.S. Spock, *J. High Resolut. Chromatogr.*, 15 (1992) 105.
55 R. Hancock and G.R. Peters, *J. Chromatogr.*, 538 (1991) 249.
56 H.W. Habgood and W.E. Harris, *Anal. Chem.*, 32 (1960) 450.
57 H. Knoeppel, M. De Bortoli, A. Peil and H. Vissers, *J. Chromatogr.*, 279 (1983) 483.
58 T.S. Wang and Y.L. Sun, *Sepu*, 3 (1985) 226.
59 T.S. Wang and Y.L. Sun, *J. Chromatogr.*, 407 (1987) 79.
60 H.F. Yin and Y.L. Sun, *Chromatographia*, 29 (1990) 39.
61 M. De Paoli, M. Taccheo-Barbina and G. Bontempelli, *J. Chromatogr.*, 547 (1991) 355.
62 T.S. Wang and Y.L. Sun, *J. High Resolut. Chromatogr. Chromatogr. Commun.*, 10 (1987) 603.
63 G. Schomburg and G. Dielmann, *J. Chromatogr. Sci.*, 11 (1973) 151.
64 R.V. Golovnya, M.B. Terenina and V.P. Uraletz, *J. Chromatogr.*, 91 (1974) 127.
65 L. Mathiasson, J.A. Jansson, A.M. Olsson and L. Haraldson, *J. Chromatogr.*, 153 (1978) 11.
66 F. Vernon and J.B. Struatmann, *Chromatographia*, 17 (1983) 597.
67 H.F. Yin, Y. Zhu and Y.L. Sun, *Chromatographia*, 28 (1989) 502.

Journal of Chromatography A, 657 (1993) 17–24
Elsevier Science Publishers B.V., Amsterdam

CHROM. 25 562

Quantitative structure–retention relationships for secondary interactions in cation-exchange liquid chromatography

Brian Law* and Steven Weir

Zeneca Pharmaceuticals, Drug Kinetics Group, Safety of Medicines Department, Alderley Park, Macclesfield, Cheshire SK10 4TG (UK)

(First received July 7th, 1993; revised manuscript received September 15th, 1993)

ABSTRACT

Eighty-three aryl alkyl amines with a range of substituents in the aromatic ring were chromatographed on a silica stationary phase in the ion-exchange mode using a non-polar eluent which promotes hydrogen bonding interactions. The increase in retention due to the presence of the polar substituents was quantified using the functional group contribution value τ. The correlation between τ and a range of substituent physical and quantum chemical parameters was investigated using multiple regression.

The increase in retention could be attributed to a hydrogen bonding interaction between the polar substituents and unionised silanols. This could be quantified in terms of the hydrogen bonding acceptor properties of the substituent (log K_β) and it size, although the quality of the correlations was poor. A superior correlation was obtained using the lipophilicity (π) of the substituent. The correlations, which gave an R^2 of 0.8423 at best were unsuited to accurate retention prediction.

INTRODUCTION

The findings presented here arose from chance observations in other areas of analytical work carried out in this laboratory [1,2]. Firstly, in the development of a rational approach to solid-phase extraction for drugs [1], using nominally reversed-phase cartridges, we observed anomalies in the elution order of some compounds which we attributed to a hydrogen bonding interaction between acceptor atoms in the solute and donor groups (presumably unbonded unionised silanols) on the stationary phase.

The second observation arose from our interest in the use of silica as a cation exchanger for the analysis of basic compounds [2]. Although it has been shown that retention is controlled in the main by the pK_a of the solute [3], to account for the good separation between compounds of similar pK_a, necessitated invoking some, as yet, unexplained interaction. For example [2], the four β-blockers propranolol, atenolol, alprenolol and practolol all have the same oxypropanolamine side chain and pK_a values within 0.05 units of 9.5 [4]. On silica however they show good separation with k' ranging from 1.5 to 2.5. Examination of the data in the light of the above findings [1] indicated that the two compounds showing the greatest retention (atenolol and practolol) possessed an amide substituent; a strong hydrogen bond acceptor group in the aromatic ring. In contrast, propranolol has an unsubstituted naphthalene and alprenolol a simple allyl substituted phenyl ring, neither of which are strong hydrogen bond acceptors. It seemed possible therefore that the longer retention of the more polar compounds (atenolol and prac-

* Corresponding author.

tolol) was due to some form of hydrogen bonding. The silica cation-exchange system, with its methanol rich eluent which favours hydrogen bonding between the solute and the stationary phase [5], appeared to be a good vehicle to allow the study of these secondary hydrogen bond interactions.

The recent publication [6] of hydrogen bond acceptor values (log K_β) for a wide range of structural fragments commonly used in drug design, facilitated this investigation. These values were used with some caution since they were generated under conditions which are quite different to the chromatographic conditions employed here.

We generated retention data for 83 compounds with substituents covering a wide range of log K_β values with the aim of correlating the increase in retention with the hydrogen bond acceptor potential of the molecules. In so doing we hoped to gain a clearer understanding of the factors controlling retention on silica when used with methanol–aqueous eluents. This information could then be used for the prediction of retention, thus minimising method development work.

EXPERIMENTAL

Equipment

The HPLC system consisted of a Perkin-Elmer 250 pump, a 135 variable-wavelength UV detector, and a ISS 200 autosampler. Chromatographic data were recorded using a Hewlett-Packard HP 3392A integrator.

Materials

Acetic acid and ammonia (25%, w/v) were AnalaR grade from BDH (Liverpool, UK), methanol was HPLC grade from Fisons (Loughborough, UK). The test solutes were obtained from the ICI compound collection and were used as received. These compounds were of four structural types. Types I–III were β-blockers and type IV were phenethylamine derivatives, the structures of which are shown in Fig. I. With the exception of the four parent compounds they were all substituted in the 4-position of the aromatic ring. The substituents studied are given in Table I.

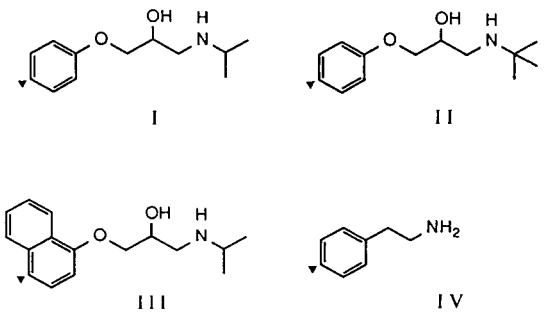

Fig. 1. The parent structures for the four sets of compounds studied (I to IV). The site of substitution is indicated by a closed triangle

Chromatography

The column was 100 × 4.6 mm I.D. packed with Spherisorb S5W silica (Phase Separations, Deeside, UK). The eluent was methanol–aqueous ammonium acetate buffer (9:1), pH 9.1. The buffer was prepared from ammonia (65 ml, 25%), acetic acid (11 ml) and water (924 ml).

Methods

The test solutes were dissolved in methanol (*ca.* 0.1 mg/ml) and a minimum of duplicate injections (1 to 10 μl) made to give k' data with reproducibility of better than 1%. Diphenylamine was used as the t_0 marker in the calculation of k' as described previously [3]. Hydrogen bond acceptor values (log K_β) were obtained from the literature [6] or from other sources [7]. Where the substituent had more that one hydrogen bond acceptor atom *e.g.* 11 and 36, only the log K_β of the stronger hydrogen bond acceptor was considered.

Computational work was carried out using a Vax computer running an "in-house" molecular modelling system, based on MOPAC and AMPAC software. The following parameters were calculated for the 4-substituents; charge on the donor atom (QM), fragment volume (FV), fragment polarisability (FPO), moment of fragment polarisability (FPM), fragment dipole (DCM), the dipole vectors (DCX, DCY and DCZ), the Verloop steric parameters (L, B1, B2,

TABLE I

HPLC RETENTION DATA AND SUBSTITUENT π AND LOG K_β VALUES FOR THE 83 COMPOUNDS STUDIED

NA = Not applicable.

No.	Substituent	k'	τ	π^a	Log $K_\beta{}^b$	Core structure
1	H	0.97	NA	0.00	NA	I
2	CH_3	0.97	0.00	0.56	−1.3	I
3	OCH_2CHCH_2	1.02	0.02	0.43	−0.8	I
4	Cl	0.99	0.01	0.71	−0.7	I
5	OCH_2CCH	0.97	0.00	−0.43	0.3	I
6	OCH_3	1.09	0.05	−0.02	0.3	I
7	NO_2	1.22	0.10	−0.28	0.7	I
8	NH_2	1.40	0.16	−1.23	1.0	I
9	CN	1.17	0.08	−0.57	1.0	I
10	CHO	1.31	0.13	−0.65	1.2	I
11	$O(CH_2)_4CN$	1.14	0.07	−0.12	1.2	I
12	$COOCH_3$	1.02	0.02	−0.01	1.2	I
13	$COCH_3$	1.31	0.13	−0.55	1.4	I
14	OCH_2COCH_3	1.34	0.14	−0.77	1.6	I
15	CH_2COCH_3	1.22	0.10	−0.23	1.6	I
16	$NHCOCH_3$	1.28	0.12	−0.97	2.5	I
17	$NHCOCH_2CH_3$	1.17	0.08	−0.46	2.5	I
18	$NHCOCH(CH_3)_2$	1.09	0.05	−0.15	2.5	I
19	$NHCO(CH_2)_2CH_3$	1.09	0.05	0.07	2.5	I
20	$NHCO(CH_2)_3CH_3$	1.02	0.02	0.60	2.5	I
21	$CONHCH_2CH_3$	1.37	0.15	−0.76	2.8	I
22	$CONH(CH_2)_2CH_3$	1.17	0.08	−0.23	2.8	I
23	$CONHCH_2CH(CH_3)_2$	1.09	0.05	0.17	2.8	I
24	CH_2CONH_2	1.43	0.17	−1.69	3.0	I
25	OCH_2CONH_2	1.34	0.14	−1.67	3.0	I
26	$CH_2NHCOCH_3$	1.34	0.14	−1.45	3.0	I
27	$(CH_2)_2NHCOCH_3$	1.28	0.12	−1.13	3.0	I
28	$CH_2NHCOCH_2CH_3$	1.28	0.12	−0.92	3.0	I
29	$(CH_2)_2NHCOCH_2CH_3$	1.17	0.08	−0.60	3.0	I
30	$CH_2CON(CH_2CH_3)_2$	1.47	0.18	−0.12	3.0	I
31	$CH_2CONH(CH_2)_3CH_3$	1.04	0.03	0.13	3.0	I
32	$CH_2NHCONH_2$	1.43	0.17	−1.41	3.2	I
33	$NHCONH_2$	1.40	0.16	−1.30	3.2	I
34	$NHCONHCH_3$	1.37	0.15	−0.93	3.2	I
35	$NHCONHCHCH_2$	1.1	0.07	−0.68	2.8	I
36	$O(CH_2)_2NHCONHCH_3$	1.34	0.14	−0.60	3.2	I
37	$CH_2NHCONHCHCH_2$	1.14	0.07	−0.60	2.8	I
38	$NHCONHCH_2CH_3$	1.25	0.11	−0.52	3.2	I
39	$NHCONHCH(CH_3)_2$	1.11	0.06	−0.21	3.2	I
40	$NHCONH(CH_2)_2CH_3$	1.1	0.09	0.01	3.2	I
41	$CH_2NHCONH(CH_2)_2CH_3$	1.11	0.06	0.13	3.2	I
42	$(CH_2)_2NHCONH(CH_2)_2CH_3$	1.09	0.05	0.46	3.2	I
43	$NHCONH(CH_2)_3CH_3$	1.06	0.04	0.54	3.2	I
44	$CH_2NHCONH(CH_2)_3CH_3$	1.06	0.04	0.66	3.2	I
45	$NHCONH(CH_2)_5CH_3$	0.97	0.00	1.60	3.2	I
46	$CH_2NHCONH(CH_2)_5CH_3$	0.95	−0.01	1.72	3.2	I
47	H	0.91	NA	0.00	NA	II
48	Br	0.85	−0.03	0.86	−0.9	II
49	F	0.91	0	0.14	−0.7	II
50	Cl	0.91	0	0.71	−0.7	II
51	NO_2	1.07	0.07	−0.28	0.7	II
52	NH_2	1.23	0.13	−1.23	1.0	II
53	CN	1.12	0.09	−0.57	1.0	II
54	$O(CH_2)_2CN$	1.07	0.07	−0.68	1.2	II
55	CH_2CN	1.15	0.1	−0.59	1.2	II
56	$(CH_2)_2CN$	1.09	0.08	−0.43	1.2	II

(Continued on p. 20)

TABLE I (*Continued*)

No.	Substituent	k'	τ	π^a	Log K_β [b]	Core structure
57	$O(CH_2)_4CN$	1.04	0.06	−0.12	1.2	II
58	$O(CH_2)_5CN$	0.98	0.03	0.42	1.2	II
59	SO_2CH_3	1.48	0.21	−1.63	1.4	II
60	$NHSO_2CH_3$	1.26	0.14	−1.62	1.4	II
61	$NHCOCH_3$	1.12	0.09	−0.98	2.5	II
62	$CONH_2$	1.26	0.14	−1.49	2.8	II
63	$CONHCH_3$	1.26	0.14	−1.27	2.8	II
64	$N(CH_3)COCH_3$	1.41	0.19	−1.04	2.8	II
65	CH_2CONH_2	1.26	0.14	−1.69	3.0	II
66	$CH_2CONHCH_3$	1.29	0.15	−1.46	3.0	II
67	H	0.83	NA	0.00	NA	III
68	CH_3	0.79	−0.02	0.56	−1.3	III
69	Cl	0.81	−0.01	0.71	−0.7	III
70	OH	0.89	0.03	−0.69	0.2	III
71	OCH_3	0.91	0.04	−0.02	0.3	III
72	OCH_2CH_3	0.87	0.02	0.45	0.3	III
73	$COCH_3$	1.17	0.15	−0.55	1.4	III
74	$SO_2N(CH_2CH_3)_2$	0.95	0.06	0.25	1.4	III
75	$NHCOCH_3$	1.09	0.12	−0.97	2.5	III
76	$NHCOCH_2CH_3$	1.02	0.09	−0.45	2.5	III
77	OCH_2CONH_2	1.00	0.08	−1.67	3.0	III
78	H	1.58	NA	0.00	NA	IV
79	Br	1.47	−0.03	0.86	−0.9	IV
80	OH	1.73	0.04	−0.72	0.2	IV
81	OCH_3	1.77	0.05	−0.02	0.3	IV
82	NH_2	2.28	0.16	−1.23	1.0	IV
83	SO_2CH_3	2.39	0.18	−1.63	1.4	IV

[a] Obtained from refs. 9 and 10.
[b] Obtained from refs. 6 and 7.

B3 and B4) [8] and the charge on the acceptor atom (QM). The fragment lipophilicity (π) was obtained from the literature [9] or calculated using standard methods [10]. The pseudo cross-sectional area (CSA) was generated from FV and the Verloop length parameter L. The square of the Verloop parameters and π were also generated as has been the practice of some workers [8,11 and references cited therein].

Multiple regression analysis was carried out using the program SAS which also ran on a VAX computer.

RESULTS AND DISCUSSION

The four sets of compounds (I to IV) had clearly defined through overlapping retention ranges which were ultimately a function of the pK_a and the substituents of the basic nitrogen. The influence of the different core structures was eliminated through calculation of the retention increments or functional group contribution values (τ) for the substituents in each compound, where;

$$\tau = \log k'_s - \log k'_p$$

and the subscripts p and s refers to the parent compound (X = H, *i.e.* compounds 1, 47, 67 and 78) and the substituted compounds, respectively. This allowed the data for the four groups of compounds to be combined and analysed together. The validity of this approach was confirmed by the data in Table II which shows good agreement between τ values for compounds of differing basic type but having the same substituents.

Correlations using log K_β

Superficial examination of the raw data (Table I) showed that compounds with high log K_β

TABLE II

RETENTION INCREMENTS (τ) FOR COMPOUNDS WHERE THE SUBSTITUENT WAS COMMON TO SEVERAL OF THE CORE STRUCTURES

Substituent	τ			
	Core I	Core II	Core III	Core IV
-Cl	0.01	0.00	−0.01	NA
$-NH_2$	0.16	0.13	NA	0.16
$-NHCOCH_3$	0.12	0.09	0.12	NA
-OH	NA	NA	0.03	0.04
$-SO_2Me$	NA	0.21	NA	0.18
$-NO_2$	0.10	0.07	NA	NA
-CN	0.08	0.09	NA	NA
-Br	NA	−0.03	NA	−0.03

tended to give higher τ values, *i.e.* they showed increased retention over the parent compound. However for a range of homologues with the same log K_β, but with a range of substituent sizes (*e.g.* the amides; 16 to 20, and 21 to 23 and also the N-alkyl ureas; 38, 40, 43 and 45) the smaller substituents clearly produced a greater positive effect on retention. At the extreme the bulky N-hexyl substituent on the urea 46 completely eliminated the effect of the strong hydrogen bond acceptor such that the τ value for this compound was actually negative!

On the basis of the above observation the initial analysis of the data was based on correlations using log K_β and steric terms *e.g.* FV, L, etc. The result of this analysis for the 79 substituted compounds was only partially successful as only 57% of the variability in the data could be explained. The best correlations were observed using log K_β and L^2 ($R^2 = 0.5792$) and log K_β and L ($R^2 = 0.5724$).

Examination of the residuals showed a number of systematic deviations. The two amino compounds (8 and 52) showed higher τ values that predicted as did the sulphones (59 and 83). In other experiments [12] we have observed unusually long retention for dibasic compounds.

In the case of the sulphones it is believed that the quoted log K_β values [6] may be an underestimation of the hydrogen bond acceptor ability under the present conditions. The data of Abraham *et al.* [6] are based on a one-to-one interaction between a donor atom and the acceptor under study. Sulphones however are capable of simultaneous interaction with two donor atoms given the right conditions. It would seem probable therefore that under the present chromatographic conditions the two sulphone compounds are forming one-to-two complexes resulting in greater retention than predicted by the log K_β values.

Removal of the four compounds discussed above (8, 52, 59 and 83) led to no overall change in the analysis, although as expected the correlation coefficients improved slightly. The best equation was

$$\tau = 0.0384(\pm 0.0034)\log K_\beta - 0.00128(\pm 0.00016)L^2 + 0.0617(\pm 0.0072)$$

$$R^2 = 0.6428 \quad n = 75 \quad F = 64.8 \quad s = 0.0339$$

Correlations with the lipophilicity parameter π

It was obvious from the analysis above that the currently available log K_β values in combination with steric terms were unable to fully describe the variation in the observed retention data. Further multiple regression analysis was therefore carried out using the full set of substituent parameters described in the Methods. Using all 79 observations gave a result which initially seemed surprising. The lipophilicity of the substituents (π) was able to account for around 71% of the variability in the data. A plot of the

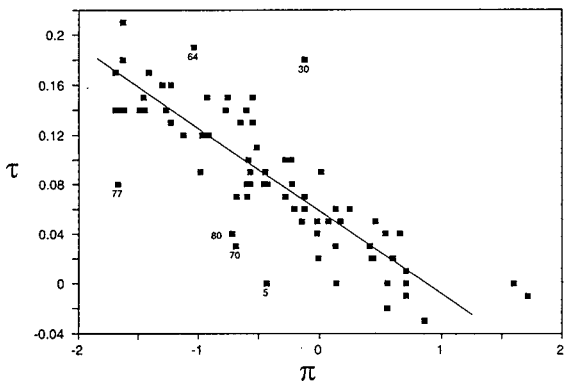

Fig. 2. A plot of τ *versus* π for the 79 substituted compounds. The identity of the six major outliers is indicated, and the best fit line excluding these compounds is shown.

correlation is shown in Fig. 2 and a number of significant outliers are highlighted. These outliers include the two phenolic compounds 70 and 80 which appear to be deviating in a systematic manner. In other work [3,12] it has been found that analytes carrying a negative charge have much reduced retention. Under the present conditions (eluent pH 9.1) the phenols would be partially ionised which could account for the observed deviation. Compounds 30, 64 and 77 were also found to be significant outliers in the correlations with log K_β. These compounds along with compound 5 all showed Studentised Residuals in excess of 2.0 and were therefore considered to be statistical outliers. Deleting these six points and repeating the analysis gave the expected improvement in the correlation and the equation shown below.

$$\tau = -0.0654(\pm 0.0035)\pi + 0.0585(\pm 0.0041)$$

$$r^2 = 0.8275 \quad n = 73 \quad F = 341 \quad s = 0.0241$$

The ability of π to describe what is essentially a polar interaction can, in retrospect, be rationalised in one of two ways. Firstly the parameter π is the lipophilicity of a molecular fragment or the 4-substituent in this particular case. These fragmental π values can be summed to generate molecular lipophilicity or log P values. It has been shown [13] that the log P can be described by an equation with three major terms, *viz.*

$$\log P = \text{cavity term} + \text{dipolar term} + \text{hydrogen bonding terms}$$

In the present context, what is of interest is the capacity term which is actually a molecular volume, either the molar volume or the intrinsic molecular volume [14] of the solute in question. The hydrogen bonding term contains a hydrogen bond acceptor contribution related to log K_β. The fact that π alone gave a similar correlation to log K_β in combination with a volume term, is therefore easily understood. It should be noted however that the coefficient in the equation relating τ and π is negative, in contrast to that for log K_β which was positive. This indicates that the effect of π is not related to a hydrophobic or reversed-phase type interaction with the stationary phase.

A second possible explanation for the observed inverse correlation with π relates to the effect and properties of the mobile phase. In the present case the eluent, which is 90% methanol is probably more lipophilic or hydrophobic than the polar ionised stationary phase. Thus it is possible that the compounds with the more lipophilic substituents (*i.e.* higher π) may partition more readily into the mobile phase and hence show more rapid elution than comparable polar compounds with substituents that have lower π values. In fact it is also possible that the exact mechanism could be a mixture of both a hydrogen bonding interaction with the stationary phase and a lipophilic interaction with the mobile phase. The present experiments however do not allow the exact mechanism to be determined.

Analysing the whole data set with all variables using stepwise multiple regression gave the equation shown below.

$$\tau = -0.0599(\pm 0.00421)\pi + 0.00878(\pm 0.00245)\log K_\beta + 0.0278(\pm 0.0079)\mathrm{B2} - 0.0118(\pm 0.0158)$$

$$R^2 = 0.7989 \quad n = 79 \quad F = 99.3 \quad s = 0.0270$$

The quality of the fit is only slightly improved over that between τ and π alone. Adding an extra two variable has only increased the R^2 by approximately 8%. Examination of the residuals

once again showed compounds 5 and 77 to be significant outliers and compounds 30 and 64 to be moderate outliers. Removing these four data points modified the equation to that shown below.

$$\tau = -0.0603(\pm 0.0036)\pi + 0.00763(\pm 0.00214)\log K_\beta + 0.0179(\pm 0.0075)\mathrm{B2} - 0.00979(\pm 0.01420)$$

$$R^2 = 0.8432 \quad n = 75 \quad F = 127 \quad \mathrm{s} = 0.0232$$

Collinearity of variables

The above approach using log K_β and π, which contain similar information, in a single equation is only valid if the variables are totally independent. Examining the collinearity of the variables showed the correlation between π and log K_β for the full set of 79 compounds to be very poor with an r^2 of only 0.1077. This can be explained by the fact that whereas π varies more or less continuously between −1.69 and 1.72, log K_β takes discrete values, showing little variation with substitution. For example the ureas (compounds 32 to 46) have log K_β values of 3.2, or in two instances 2.8. The π values of these compounds however varies between −1.41 for compound 32 to +1.72 for compound 46. The correlation between π and the steric terms is similarly poor $r^2 < 0.1598$. In combination however certain parameters correlate reasonably well with π. For example log K_β and fragment volume (FV) gives an R^2 or 0.6232. For the most part however introducing a steric parameter into the correlation between π and log K_β has little effect. On this basis therefore it would seem justified to use π, selected steric parameters and log K_β is a single equation as carried out above.

CONCLUSIONS

The selectivity differences observed between compounds with the same pK_a when chromatographed in an ion-exchange system are due to the polarity of the substituents in the solute molecule.

Increasing polarity of the substituent generally leads to an increase in retention relative to an unsubstituted parent compound. This increase in retention correlates with the size and hydrogen bond acceptor potential (log K_β) of the substituent. Increasing log K_β leads to an increase in retention whilst increasing size of the substituent leads to a decrease in retention. As this secondary interaction involves hydrogen bonding between an acceptor atom in the substituent and unionised silanols, the effect of substituent size can be rationalised in steric terms.

The increase in retention was also correlated with the lipophilicity of the substituent (π) which was able to explain around 71% of the variability in the data. Unlike the correlations with log K_β the coefficient of the π term was negative. This suggests that a lipophilic interaction is taking place between the solute and the mobile phase. The data rules out any reversed-phase interaction with the silica stationary phase as has been suggested by other workers [14].

Overall the quality of the correlations were poor. This can be explained by a number of factors such as the inherent variability in the retention data (shown by a number of significant outliers) and the narrow retention range. More importantly however the terms log K_β and π although relatively useful are probably not a true measure of the interactions involved. The hydrogen bond acceptor values are based on one-to-one interactions, which in the case of the sulphones at least, appears to be an over simplification of the situation in the present chromatographic conditions. It is possible that other substituents are also capable of multiple interactions. Furthermore no account was taken of the substituents which had multiple hydrogen bonding atoms (*e.g.* 11 and 25).

The substituent lipophilicity values π obviously contain information that partially describes the secondary interactions observed here. However, as the concept of lipophilicity was originally designed to explain biochemical phenomenon, in particular the passage across lipid membranes [9], it is hardly surprising that π values are of only limited values in describing a phenomenon involving polar interactions.

Refinement of the data and additional studies will be necessary before retention of a novel solute can be accurately predicted.

ACKNOWLEDGEMENTS

We would like to thank Jeff Morris and David Leahy of the Molecular Design Group, Zeneca Pharmaceuticals and Brian Middleton for help with statistical matters.

REFERENCES

1 B. Law and S. Weir, *J. Pharm. Biomed. Anal.*, 10 (1992) 181.
2 B. Law, *Trends Anal. Chem.*, 9 (1990) 31.
3 B. Law, *J. Chromatogr.*, 407 (1987) 1.
4 ICI, unpublished results.
5 K.E. Bij, Cs. Horváth, W.R. Melander and A. Nahum, *J. Chromatogr.*, 203 (1981) 65.
6 M.H. Abraham, P.P. Fuce, D.V. Prior, D.G. Barrett, J.J. Morris and P.J. Taylor, *J. Chem. Soc., Perkin Trans. 2*, (1989) 1355.
7 J.J. Morris, personal communication.
8 A. Verloop, Q. Hoogenstraaten and J. Tipker, in E.J. Ariens (Editor), *Drug Design*, Vol. 7, Academic Press, New York, 1976, p. 165.
9 C. Hansch and A. Leo, *Substituent Constants for Correlation Analysis in Chemistry and Biology*, Wiley, New York, 1979.
10 *Medchem Software Manual*, Version 3.4, Pomona College, Claremont, CA, 1986.
11 A. Verloop, in E.J. Ariens (Editor), *Drug Design*, Vol. 3, Academic Press, New York, 1972, p. 133.
12 B. Law, unpublished results.
13 R.W. Taft, M.H. Abraham, G.R. Famini, R.M. Doherty, J.-L.M. Abboud and M.J. Kamlet, *J. Pharm. Sci.*, 74 (1985) 807.
14 D.E. Leahy, *J. Pharm. Sci.*, 75 (1986) 629.
15 B.A. Bidlingmeyer, J.K. Del Rios and J. Korpl, *Anal. Chem.*, 54 (1982) 442.

Journal of Chromatography A, 657 (1993) 25–31
Elsevier Science Publishers B.V., Amsterdam

CHROM. 25 310

Development of an analytical procedure to study linear alkylbenzenesulphonate (LAS) degradation in sewage sludge-amended soils ☆

L. Comellas*, J.L. Portillo and M.T. Vaquero

Secció de Cromatografia, C.E.T.S. Institut Químic de Sarrià (Universitat Ramon Llull), Institut Químic de Sarrià s/n, 08017 Barcelona (Spain)

(First received December 10th, 1992; revised manuscript received May 12th, 1993)

ABSTRACT

A procedure for determining linear alkylbenzenesulphonates (LASs) in sewage sludge and amended soils has been developed. Extraction by sample treatment with 0.5 *M* potassium hydroxide in methanol and reflux was compared with a previously described extraction procedure in Soxhlet with methanol and solid sodium hydroxide in the sample. Repeatability results were similar with savings in extraction time, solvents and evaporation time. A clean-up method involving a C_{18} cartridge has been developed. Analytes were quantified by a reversed-phase HPLC method with UV and fluorescence detectors. Recoveries obtained were higher than 84%. The standing procedure was applied to high doses of sewage sludge-amended soils (15%) with increasing quantities of added LASs. Degradation data for a 116-day period are presented.

INTRODUCTION

Linear alkylbenzenesulphonates (LASs) are the major surfactants currently used. Commercial LASs are complex mixtures of homologues of C_{10}–C_{13} chain-lengths compounds and phenyl positional isomers, except those isomers with the aromatic ring bonded to the two terminal methyl groups. Their formula is presented in Fig. 1.

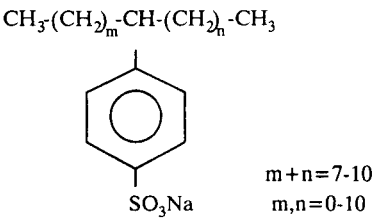

Fig. 1. Structural formula of LASs.

As LASs are extensively used as household laundry detergents, their direct disposal results in high concentrations in waste water, about 5–20 mg/l [1,2]. Sewage treatment plants break down LASs only partly; some of them remain in effluent and other fraction is adsorbed in sewage solids, in which LASs are major synthetic compounds in quantities between 2 and 5 g/kg [3–5]. Through waterways and sewage sludge disposal LASs are discharged into the environment.

The potential fertility of sewage sludge is well known, and in order to avoid health and environmental hazards guidelines [6] have been developed regarding its heavy metal content for agricultural land utilization. Our research team has been studying the possibility of exploiting greater sludge quantities in limy soil [7–9], including a laboratory study that takes into account degradation or accumulation of sewage sludge organic pollutants in soils, including LASs.

An experiment involving limy soils amended

* Corresponding author.

☆ Presented at the *21st Scientific Meeting of the Spanish Group of Chromatography and Related Techniques*, Granada, October 21–23, 1992.

0021-9673/93/$06.00

with high doses of sewage sludge (15%) and increasing quantities of added LASs has been designed. The aim was to evaluate the effects of high surfactant concentrations on the degradation of LASs. This required an analytical procedure to analyse LASs in sewage sludge and amended soils.

Although there is a well-established analytical method to determine LASs in water samples [1,2], a variety of procedures have been used to analyse them in solid samples: methanol reflux and anionic exchange and C_{18} cartridge clean-up [2]; methanol Soxhlet extraction and anionic exchange and C_{18} cartridge clean-up [5]; and methanol in Soxhlet with solid sodium hydroxide in the sample (20%, w/w) [10]. Each procedure uses an HPLC separation for the final analysis.

We have previously tested the existing methods of analysing LASs in sewage sludge and amended soils. Soxhlet extraction with methanol and sodium hydroxide gave the best results. We attribute this to the ability of basic medium to prevent LAS sorption on sewage sludge lipid organic matter. Based on our previous experience in lipid analysis of sewage sludge, we tested a direct basic treatment with potassium hydroxide in methanol under reflux.

This report compares both methods, extraction through sample treatment with methanolic 0.5 *M* potassium hydroxide under reflux and methanol Soxhlet extraction with sodium hydroxide in the sample, with a C_{18} cartridge clean-up in both cases. Analyses were completed with a reversed-phase HPLC method with UV and fluorescence detection.

EXPERIMENTAL

Reagents and materials

Acetonitrile and methanol were of HPLC grade and were supplied by Merck (Darmstadt, Germany). Milli-Q water was obtained with a Millipore system from Waters (Milford, MA, USA). HCl (0.1 *M*) was prepared from concentrated hydrochloric acid from Panreac (Barcelona, Spain). Potassium hydroxide and sodium perchlorate analytical grade were obtained from Merck. Sep-Pak C_{18} cartridges were supplied by Waters. A commercial mixture of linear alkylbenzenesulphonic acids with C_{10}–C_{13} chain lengths was used as received from K.A.O. (Barcelona, Spain): 50, 100, 500 and 1000 μg/ml standard solutions were made in methanol.

Instruments

An analytical LiChrospher 100 RP-18, 125 × 4 mm, 5-μm column and a LiChroCART 4-4, 100 RP-18, 5-μm precolumn, both from Merck, were used. The chromatography system consisted of a Waters 600E pump with a Rheodyne (Cotati, CA, USA) sample 20-μl loop injector. A Model 991 photodiode-array detector ($\lambda = 225$ nm) with integration software from Waters, a Model 470 fluorescence detector ($\lambda_{ex}/\lambda_{em} = 225/295$ nm) from Waters and a Model D-2000 integrator from Hitachi (Tokyo, Japan) were also used.

Chromatography conditions

Acetonitrile and acetonitrile–water (25:75) containing 0.1 *M* $NaClO_4$ were used as gradient eluents with a 1 ml/min flow-rate. After 1 min of 15% acetonitrile, a linear gradient elution was applied for 19 min leading to 40% acetonitrile, followed by a 2-min isocratic elution and a 3-min linear gradient elution to 70% acetonitrile, which was maintained for 10 min.

Procedure

About 0.5 g of sewage sludge or 2 g of amended soil were treated with 50 ml of 0.5 *M* potassium hydroxide in methanol under reflux for 4 h. The extract was vacuum evaporated to 1 ml on a 35°C bath and dried under a gentle stream of nitrogen on a 70°C bath. About 10 ml of methanol–water (30:70) were added and the pH adjusted to 1.0 with concentrated hydrocloric acid. The sample was sonicated for at least 1 min, to dissolve potassium chloride. A C_{18} cartridge was rinsed with 2 ml of methanol and 3 ml of 0.1 *M* HCl before use. The entire sonicated solution was percolated through the octadecylsilica cartridge. The column was washed with 2 ml of 0.1 *M* HCl. LASs were eluted with exactly 10 ml of methanol. The methanol eluate could be injected directly into the HPLC system. LAS concentration could be quantified by measuring peak heights and comparing them with external standards.

TABLE I

SPIKED AND TOTAL AMOUNT OF LASs IN SEWAGE SLUDGE (15%)-AMENDED SOIL EXPERIMENTS

Experiment	LAS spiked amount (g/kg)	LAS total amount (g/kg)
COA	0.00	1.87
COB	0.00	1.87
LAS 1A	3.59	5.46
LAS 1B	3.59	5.46
LAS 10A	18.00	19.87
LAS 10B	18.00	19.87

Experiment design to assess LAS degradation in sewage sludge-amended soils

Anaerobically digested sewage sludge came from Dargisa, a sewage aerobic treatment plant in Girona (Spain). Sludge was air-dried and ground to less than 0.4 mm before analysis or soil addition. Limy soil from Bellaterra (Vallés Occidental, Spain) was ground and sieved to less than 2 mm.

High doses of sewage sludge (15%)-amended soil were prepared in 6-kg polyethylene containers. LASs were added to sludge in the form of sodium linear alkylbenzenesulphonate and homogenized by grinding. Three experiments were performed in duplicate: the first used sewage sludge-amended soil with no added LASs (COA, COB), the second amended soil to which LASs were added to three times the normal concentration (LAS 1A, LAS 1B) and the third used amended soil to which LASs were added to ten times the normal concentration (LAS 10A, LAS 10B). The added and total amounts of LASs used in the experiments are reported in Table I.

Experimental soils were watered to maintain 20% humidity. Homogeneous samples were guaranteed by sampling and mixing throughout the container depth. The samples were preserved by the addition of 1% (w/w) formaldehyde and stored in the dark at +4°C. They were also dried at 70°C for 12 h before analysis.

RESULTS AND DISCUSSION

High-performance chromatography

An eluent gradient was developed to separate LAS homologues and the greater part of their isomers. Individual LASs were quantified by comparing their peak heights with those of an external standard injected daily. UV detection ($\lambda = 225$ nm) provides a linear response between 20 and 2000 μg/ml and a detection limit of 20 μg/ml. Fluorescence detection (225/295 nm) reduces the detection limit to 16 ng/ml.

Procedure

Basic methanol treatment of samples improves LAS extraction because LAS sorption on lipid organic matter decreases. Soxhlet extraction with solid sodium hydroxide provides these conditions only in first cycles. When the sample is submitted to a continuous basic methanolic treatment, lipids are saponified, scission of the lipid organic fraction of sewage sludge occurs and interactions between organic matter and mineral matrix are abolished. Therefore, associations between surfactants and lipid and mineral sludge fractions are reduced and extraction is made easier.

The strong basic medium after saponification or the subsequent increase in salt content that a neutralization would represent makes direct injection of the extract on HPLC impossible. Therefore, it is advisable to perform a C_{18} microcolumn cleaning to obtain LAS elution in a clear methanol solution. This purification allows the elimination of polar compounds and inorganic salts simultaneously.

Direct methanolic extract clean-up is not possible, because LASs are too soluble in methanol and would not interact with the C_{18} phase in the microcolumn. However, addition of water to the methanolic solution to be cleaned improves the affinity of LASs for the stationary phase. Cartridge behaviour has been studied as a function of methanol–water proportion in the solution to be cleaned. LAS standards (100 μg/ml) were prepared with methanol contents between 0 and 70% (v/v). The pH of standards was adjusted to 1.0 in order to protonate surfactant sulphonic group, to increase the affinity for the stationary reversed phase.

Results are reported in Fig. 2. Quantitative LAS recoveries were obtained with methanol contents of 0–30%. However, 30% methanol in water must be used when applying purification to sewage sludge extract, as only 30% methanol

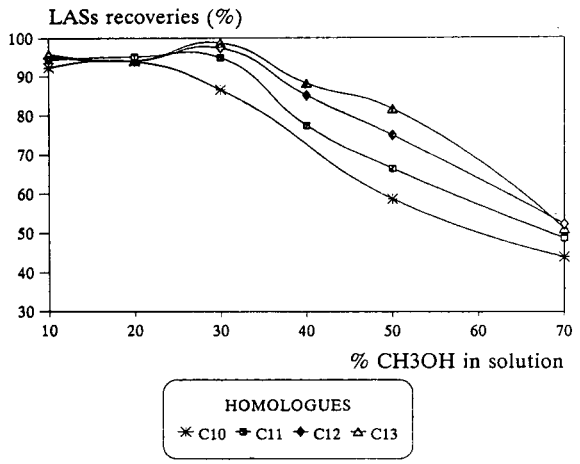

Fig. 2. LAS recoveries in C_{18} cartridge clean-up according to the methanol–water proportion in the solution before cleaning.

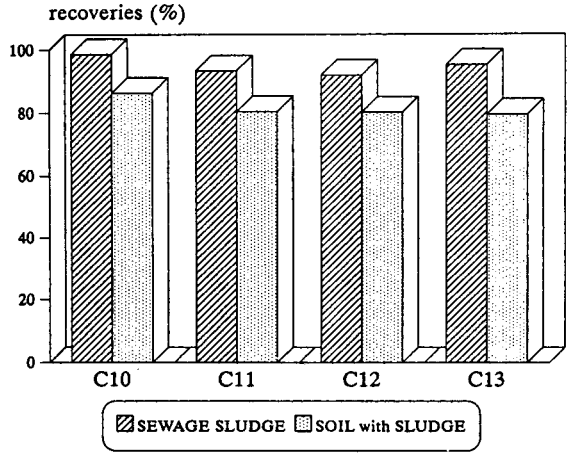

Fig. 3. Recoveries of various homologues in sewage sludge and amended soils.

completely dissolves the sludge-extracted fraction. In lower proportions methanol would form emulsions that would envelop LASs and prevent their interaction with the stationary phase.

A sample basic treatment for 4 h is enough to extract all LASs in sewage sludge: 14.8 g of LAS per kg in four replicates [$s_{n-1} = 0.8$, relative standard deviation (R.S.D.) = 6%]. A second extraction of the same samples recovers only 0.6% of total LASs.

Table II compares the proposed procedure with the one described in literature [10] using Soxhlet extraction and solid sodium hydroxide within the sample. Each procedure with C_{18} clean-up was applied in triplicate to 2 g of sewage sludge-amended soil. The repeatability obtained is similar in both methods.

The accuracy of the procedure was measured by a standard additions analysis. Sewage sludge and sludge-amended soils (15%) were spiked with increasing quantities of LASs (0, 15, 30 and 45 g of LAS per kg of sewage sludge) in order to ensure medium recoveries in samples with different LAS concentrations. The recoveries obtained were 94% and 81% for sewage sludge and for amended soils, respectively. There is no difference between LAS homologues in extraction as similar recoveries were obtained for them all (Fig. 3).

Finally, the results of the proposed method are consistent with those obtained by a previous method [10]. This new procedure reduces solvent use and analysis time. Only 4 h are needed in comparison with the 7 h required for the procedure described in literature.

LAS degradation results

LAS degradation in sewage sludge-amended soils over a 116-day period was studied. The degradation of LASs varied depending on the

TABLE II

REPEATABILITY[a] OF THE PROCEDURES APPLIED TO SEWAGE SLUDGE-AMENDED SOIL

Procedure	Mean (g of LAS per kg)	n[b]	s_{n-1}[b]	R.S.D.[b]
Reflux/KOH 0.5 M/C_{18} clean-up	2.2	3	0.32	14.5
Soxhlet/solid NaOH/C_{18} clean-up	2.7	3	0.30	10.9

[a] Repeatability, in 1 day.

[b] n = Repetitions; $s_{n-1} = n - 1$ standard deviation; R.S.D. = relative standard deviation (%).

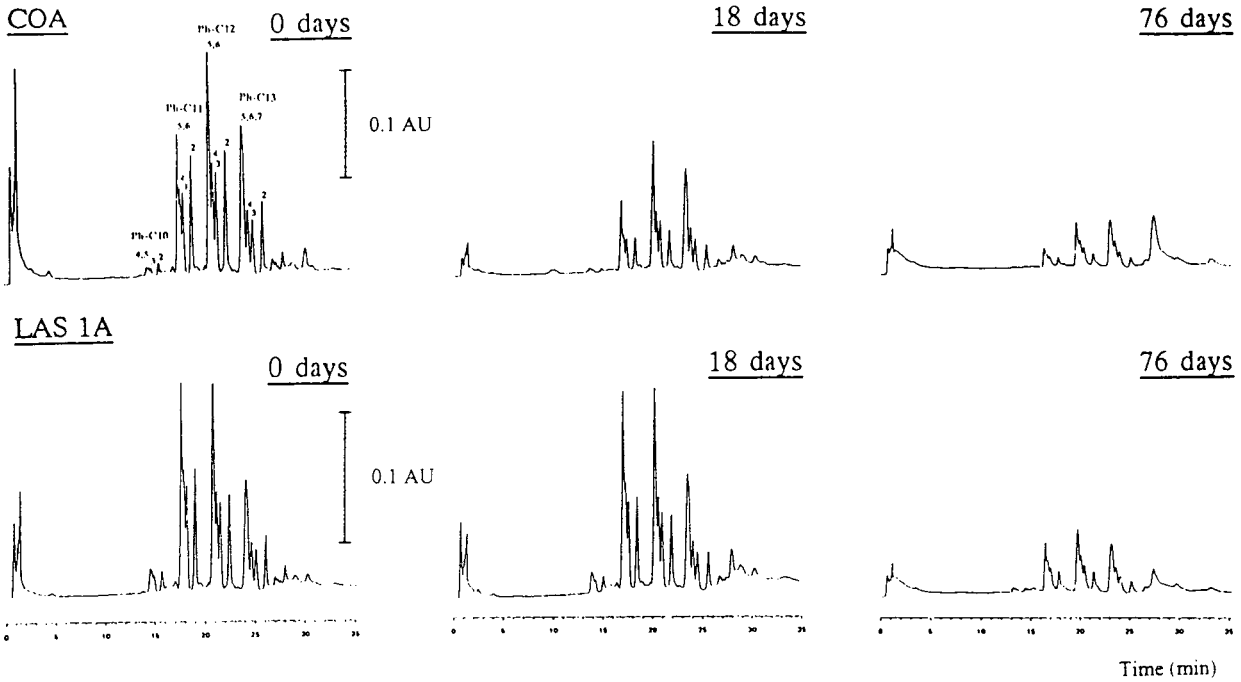

Fig. 4. Chromatograms of LASs in COA and LAS 1A samples after 0, 8 and 16 days of degradation. Peaks: Ph-C_{10}, Ph-C_{11}, Ph-C_{12} and Ph-C_{13} are groups of LAS homologues; the numbers above each peak show the phenyl position on the alkyl chain for every isomer.

amount added, as shown in the chromatograms in Fig. 4. In soils with no added LASs (COA) degradation was 50% in 18 days, whereas no degradation occurred in soils spiked with three times the normal concentration of LASs (LAS 1A). However, after 76 days both soil types exhibited low surfactant levels, only about 15% of the initial concentration. Quantitative results were subjected to statistical treatment to produce an evolution curve. Moreover, there was a variation in homologue and isomer distribution during degradation. Homologues with small number of carbon atoms and external phenyl positional isomers appeared to be more degraded. These results will be reported in the near future.

Results treatment

A period of time with no LAS variation was observed in every experiment when mathematically evaluated. It was named accommodation time (t_0). There is no statistical difference between the initial points as they do not fit any curve. They only reflect method deviation. This means that there is no immediate degradation of LASs. An initial period of time without LAS degradation is reported to be usual when organic compounds are submitted to microbial breakdown [11].

In order to study LAS degradation times, the curve that provides the minor error was adjusted to experimental points with degradation. Every experiment seemed to follow:

$$C_t = e^a \cdot t^{-b}$$

for $t > t_0$

where C_t is the concentration of LAS (g of LAS per kg of sewage sludge-amended soil) and t the time (days) elapsed from the beginning of the experiment as the only parameter. Fig. 5 presents adjusted curves and experimental data. Relative errors were generally less than 11% (Table III).

Table IV reports degradation parameters of spiked experiments: accommodation time (t_0), half-life time to 50% degradation ($t_{1/2}$) and apparent time to 95% degradation ($t_{0.05}$).

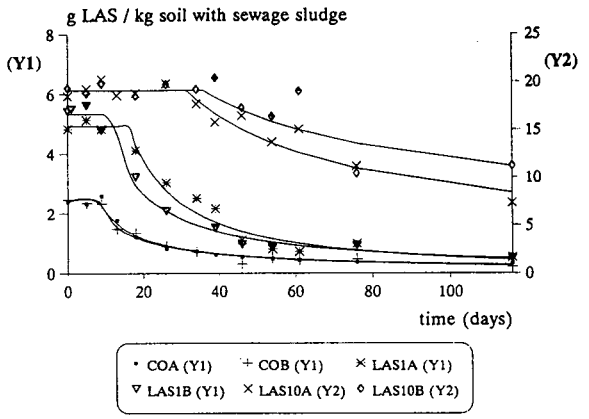

Fig. 5. Variation in LAS concentration in sewage sludge amended soil for every experiment (COA, COB, LAS 1A and LAS 1B on axis Y1, LAS 10A and LAS 10B on axis Y2) versus the time elapsed from the start of the experiment. Points correspond to experimental values and curves have been mathematically adjusted.

In degradation:

(1) Accommodation time until surfactant degradation begins (t_0) increases with initial LAS concentration in sewage sludge.

(2) Half-life time to 50% degradation of surfactants ($t_{1/2}$), increases with LAS quantities in sludge.

(3) Apparent degradation time until 5% LAS remains ($t_{0.05}$) is greater for experiments with higher surfactant concentrations.

TABLE IV

EVOLUTION PARAMETERS IN LASs EVOLUTION EXPERIMENTS

Experiment	t_0 (days)[a]	$t_{1/2}$ (days)[b]	$t_{0.05}$ (days)[c]
COA	7	18	335
COB	8	19	292
LAS 1A	16	29	196
LAS 1B	10	20	225
LAS 10A	31	94	3665
LAS 10B	35	162	24 698

[a] t_0 = Accommodation time.
[b] $t_{1/2}$ = Half-life time.
[c] $t_{0.05}$ = Apparent degradation time.

CONCLUSIONS

The procedure described appears to be suitable for the study of LAS degradation in sewage sludge-amended soils. LAS degradation can be predicted when amending soil. The higher the LAS concentration in sewage sludge, the lower the LAS biodegradation rate in amended soil.

TABLE III

CURVES ADJUSTED TO LAS DEGRADATION EXPERIMENTS

Experiment	$C_t = e^a \cdot t^{-b}$ ☆		Average error	
	a	b	ϵ_A [a] (g of LAS per kg)	e_r (%)[b]
COA	2.4388	0.781538	0.049	6.9
COB	2.66719	0.842782	0.059	8.0
LAS 1A	4.92125	1.197900	0.290	21.0
LAS 1B	3.82776	0.950372	0.137	10.9
LAS 10A	5.12006	0.629331	1.047	7.6
LAS 10B	4.59151	0.458242	1.602	9.9

☆ C_t = LAS concentration (g of LASs per kg of sewage sludge-amended soil); t = time from experiment start (days).
[a] ϵ_A = Absolute error.
[b] e_r = Relative error.

However, complete LAS elimination is always predictable.

ACKNOWLEDGEMENTS

We thank the CICYT in Spain for financial support (Project No. NAT91-0340) and M.T.V. gratefully acknowledges the support of the CIRIT, Generalitat de Catalunya.

REFERENCES

1 D. Prats, F. Ruiz, B. Vázquez and D. Zarso, *Jorn. Com. Deterg.*, 22 (1991) 479.
2 J.L. Berna, A. Moreno and J. Ferrer, *J. Chem. Tech. Biotechnol.*, 50 (1991) 387.
3 E. Matthijs and H. De Henau, *Tenside Deterg.*, 24 (1987) 193.
4 W. Giger, A.C. Alder, P.H. Brunner, A. Marcomini and H. Siegrist, *Tenside Deterg.*, 26 (1989) 95.
5 M.S. Holt, E. Matthijs and J. Waters, *Wat. Res.*, 23 (1989) 749.
6 *Official Journal of the European Community L181/6-L181/12 (86/278/EEC)*, European Commission, Brussels, Barcelona, 1986.
7 M. Pujolà, *Quaderns Agraris ICEA*, 6 (1985) 97.
8 J.M. Alcañiz, M. Jorba, R. Josa, A. Solé and R. Vallejo, *Guía Provisional per a la Restauració de Sòls de Pedreres de Roca Calcària*, Edició interna Dpt. Política Territorial i Obres Públiques, Generalitat de Catalunya, July 12th, 1989, p. 46.
9 J. Ll. Lliberia, S. Borrós, L. Comellas and J.M. Alcañiz, *Afinidad*, 49 (1992) 227.
10 A. Marcomini and W. Giger, *Tenside Deterg.*, 25 (1988) 4.
11 R.D. Swisher, *Surfactant Biodegradation*, Marcel Dekker, New York, 1987.

Journal of Chromatography A, 657 (1993) 33–41
Elsevier Science Publishers B.V., Amsterdam

CHROM. 25 539

Determination of the molecular mass of heparin samples by size-exclusion chromatography applying non-identical standards

M. Bergman*, R. Dohmen, H.A. Claessens and C.A. Cramers

Laboratory of Instrumental Analysis, Eindhoven University of Technology, P.O. Box 513, 5600 MB Eindhoven (Netherlands)

(First received March 19th, 1993; revised manuscript received July 5th, 1993)

ABSTRACT

The influence of three experimental parameters, temperature, pH and ionic strength of the eluent, on the retention of specific heparin samples and polysaccharides as calibration standards in size-exclusion chromatography was investigated applying chemometric techniques. The results allowed the adjustment of the retention volumes of the studied heparin samples in such a way that the average molecular masses of these compounds could be calculated using polysaccharides as the standards. This approach shows the possibilities of determining average molecular masses of biopolymers using non-identical commercially available standards.

INTRODUCTION

The anticoagulant heparin is a polydisperse polysaccharide that is widely used therapeutically for the prevention of thrombo-embolic disorders. Heparin is a copolymer of uronic acid (glucuronic acid or iduronic acid) and glucosamine, either N-acetylated or N-sulphated. It is highly substituted with O-sulfate residues at the 6-positions of the glucosamine residues and at the 2-positions of the iduronic acid residues [1–3].

It has been shown that a relationship between the molecular mass and the biological activity of heparin [4] exists. Therefore, the characterization of heparin samples by the determination of the average molecular masses and molecular mass distributions of heparin samples is very important. One of the techniques suitable to provide this information is size-exclusion chromatography (SEC) [5–10]. However, a disadvantage of this technique is the lack of well defined heparin standards with narrow molecular mass distributions. In some reports the use of these standards was mentioned to determine the average molecular mass [number-average (M_n) or mass average (M_w)] and the molecular mass distribution of heparin samples [5,7–10]. However, these heparin standards are not yet commercially available.

A possible solution to overcome this general problem is the use of standards not similar to heparin, *e.g.*, polystyrene sulphonates [6]. These standards can be used to obtain an estimate of the average molecular mass (M_n or M_w) and the molecular mass distribution of biopolymer samples such as heparins. A problem may occur when an accurate determination of the average molecular mass or the molecular mass distribution of the biopolymer sample must be made. SEC is based on differences in molecular sizes [10], and not on differences in molecular masses. It is well known that different types of polymers

* Corresponding author.

0021-9673/93/$06.00

of the same molecular mass, may have different conformational structures and consequentially show different molecular sizes. Also, these conformational structures may depend on a number of experimental conditions. Therefore, the calibration of the SEC analysis of biopolymers such as heparins with non-identical standards may lead to erroneous results.

An improvement can be achieved by the use of calibration standards belonging to the same chemical group as the sample substances. For example, from a physico-chemical point of view, commercially available polysaccharides are relative similar to heparin molecules. However, the charged groups on the heparin molecules may influence considerably the hydrodynamic volume of these molecules. This is mainly caused by the mutual electrostatic repulsion of the negatively charged groups on the heparin molecules. Therefore, the hydrodynamic volume of polyelectrolytes can be influenced by the experimental conditions. The effect of ionic strength and pH on the conformation of polyelectrolytes in SEC has already been studied [11–14]. However, polystyrene sulphonates [12–14] and proteins [11] were used.

In this study, an attempt was made to reduce the difference in hydrodynamic volume between a number of standard polysaccharide molecules and the studied heparin molecules by manipulating a number of experimental conditions. Three experimental parameters, ionic strength, pH and temperature of the eluent, were investigated. The influence of the investigated parameters on the retention volume was studied by applying chemometric techniques. Finally, with these data the molecular mass distribution of the studied heparin samples was calculated.

EXPERIMENTAL

Equipment

The chromatographic system consisted of a Model 100A HPLC pump (Beckman, Palo Alto, CA, USA) with a Model R-401 differential refractometer detector (Waters Millipore, Milford, MA, USA). All experiments were performed on a Zorbax GF-250 column (200 × 9.4 mm I.D.) (Rockland Technologies, Newport, DE, USA). The column was packed with 5-μm silica-based particles with a 150 Å pore size (pH range 3–8.5). The column was thermostated with a laboratory-constructed water-jacket, connected with an ultra-thermostat (Colora, Germany). Injections were made with a Model 7125 injector (Rheodyne, Cotati, CA, USA) equipped with a 20-μl injection loop. A guard column (PL Aquagel, 75 × 7.5 mm I.D.) (Polymer Laboratories, Church Stretton, Shropshire, UK) was placed between the injector and the Zorbax column.

Chemicals

The heparin samples and heparin standards used were a kind gift from Professor Dr. H.C. Hemker of the Department of Biochemistry, University of Limburg, (Maastricht, Netherlands). Two different heparin samples were used, Fraxiparine (Sanofi, Maassluis, Netherlands) with an average molecular mass of 5090 g/mol [15], and Calparine (Sanofi) with an unknown average molecular mass. The heparin standards, with mass-average molecular masses of 3000, 4200, 6000, 9200 and 11200 g/mol, were prepared by fractionation of a low-molecular-mass heparin (enoxaparin) by gel permeation chromatography [16]. The polysaccharide standards of M_w 5800, 12 200, 23 700, 48 000 and 100 000 g/mol were obtained from Polymer Labs. Sodium dihydrogenphosphate and sodium chloride were purchased from Merck (Darmstadt, Germany). Water was demineralized with a Milli-Q water-purification system (Waters Millipore). The eluents were filtrated over a 0.45-μm membrane filter and degassed with helium prior to use.

In all analyses, the concentration of the samples and the injection volume were kept constant.

RESULTS AND DISCUSSION

In the linear range of a specific size-exclusion column, the retention volume V_r is a parameter for the molecular size of a compound. Therefore, in this work the influence of the ionic strength, pH and temperature of the eluent on

TABLE I

EXPERIMENTAL SETTINGS USED IN THE CENTRAL COMPOSITE DESIGN FOR THE DETERMINATION OF THE INFLUENCE OF THE IONIC STRENGTH, TEMPERATURE AND pH OF THE ELUENT ON THE RETENTION VOLUME OF HEPARIN

Setting No.	Temperature (°C)	pH	Ionic strength
1	25	4	0.01
2	25	4	1
3	25	7	1
4	45	7	1
5	45	4	1
6	45	7	0.01
7	25	7	0.01
8	45	4	0.01
9	35	5.5	0.1
10	35	5.5	2
11	35	5.5	0.005
12	35	7.45	0.1
13	35	3.55	0.1
14	48	5.5	0.1
15	22	5.5	0.1

TABLE II

RESULTS OF THE ANALYSIS OF VARIANCE (ANOVA) OF THE RETENTION MODEL FOR HEPARIN

The total sum of squares [SS(Total)] is calculated by comparing the experimental and calculated data. The total sum of squares can be divided into a contribution of the mean [SS(Mean)] and a contribution of the correction [SS(Corrected)]. The latter can be considered as the sum of the contribution of the factors [SS(Factors)] and a residual sum of squares [SS(Residue)]. The latter value can be separated into a sum of squares caused by pure experimental error [SS(Pure Error)] and by lack of fit [SS(Lack of Fit)]. DF = degrees of freedom.

Sums of squares (SS)	Fraxiparine (M_w = 5090 g/mol)	Heparin standard (M_w = 9200 g/mol)
SS(Total)	4742.7 (41 DF)	2274.1 (22 DF)
SS(Mean)	4658.85 (1 DF)	2250.69 (1 DF)
SS(Corrected)	83.85 (40 DF)	23.45 (21 DF)
SS(Factors)	83.7861 (9 DF)	23.41 (4 DF)
SS(Residue)	0.05868 (31 DF)	0.03605 (17 DF)
SS(Pure Error)	0.04048 (15 DF)	0.01280 (9 DF)
SS(Lack of Fit)	0.01820 (16 DF)	0.02325 (8 (DF)

the retention volume of heparins and polysaccharides was investigated.

Heparin model

First the influence of the experimental parameters on the retention volume of both Fraxiparine and the heparin standard with an average molecular mass of 9200 g/mol was investigated. Then the remaining heparin standards were used to validate the method. A central composite design was used to determine these influences more rapidly. The design is shown in Table I. All levels were measured twice, except for the centre point, which was measured ten times. The pure experimental error could be calculated from the measurements in the centre point. The influences of the investigated parameters were calculated from the results of the experiments under different conditions. For Fraxiparine (M_w = 5090, with a peak maximum at molecular mass 4500 g/mol [15]), the equation describing the dependence of the retention volume of this heparin on these parameters is

$$V_R = 25.845 - 0.422T - 5.131 \cdot \mathrm{pH} + 0.889 \log I - 0.0517 \cdot \mathrm{pH} \cdot \log I + 0.0126T^2 + 0.971(\mathrm{pH})^2 - 0.424(\log I)^2 - 0.120 \cdot 10^{-3}T^3 - 0.060(\mathrm{pH})^3 \quad (1)$$

where V_R is the retention volume (ml) of Fraxiparine under the experimental conditions, T the temperature (°C) and I the ionic strength of the eluent. With the assumption of homoscedasticity, the model can be checked with a goodness-of-fit (GOF) and a lack-of-fit (LOF) test. The results of these tests for the calculated model of Fraxiparine are given in Tables II and III.

The experiments with the heparin standard (M_w = 9200 g/mol) resulted in the following equation for the retention volume as a function of the experimental parameters:

$$V_R = 11.410 - 0.0208 \cdot \mathrm{pH} + 1.162 \log I - 0.0458 \cdot \mathrm{pH} \cdot \log I - 0.148(\log I)^2 \quad (2)$$

The results of the GOF and LOF tests are given in Tables II and III. To obtain a more detailed insight into the calculated models, the influence

TABLE III

RESULTS OF THE VALIDATION OF THE MODEL FOR HEPARIN WITH A GOODNESS OF FIT AND A LACK OF FIT TEST

The calculated F-values are compared with F-values in ref. 17 at the 95% confidence level (F^*). The degrees of freedom (DF) are calculated with the number of independent measurements (f), the number of model parameters (p) and the number of experiments (n).

Parameter	Fraxiparine (M_w = 5090 g/mol)	Heparin standard (M_w = 9200 g/mol)
F_{GOF}	4918.43	2760.33
F^*	2.56	3.68
DF ($p-1, n-p$)	9, 31	4, 17
F_{LOF}	0.42	2.04
F^*	2.85	4.10
DF ($f-p, n-f$)	16, 15	8, 9

of the ionic strength, pH and temperature on the retention volume of heparin are plotted separately in the Figs. 1, 2 and 3, respectively. The results show that the ionic strength of the eluent has a relatively large influence on the retention volume of heparin, while the influence of the temperature and pH of the eluent on the retention volume of heparin is of minor importance in the investigated pH and temperature ranges.

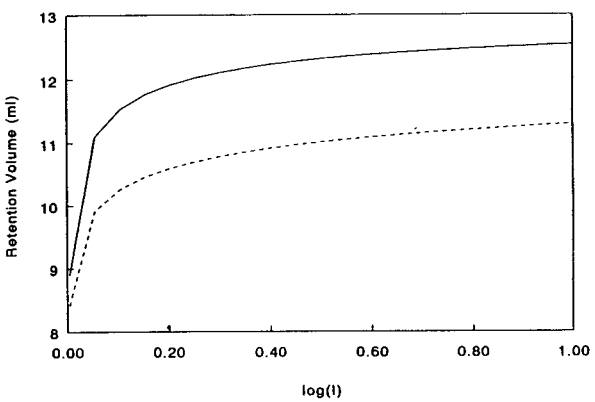

Fig. 1. Calculated influence of the ionic strength of the eluent on the retention volume (ml) of two specific heparin samples, M_w = 5090 (solid line) and 9200 (dotted line). The temperature and pH of the eluent were 35°C and 5.5, respectively.

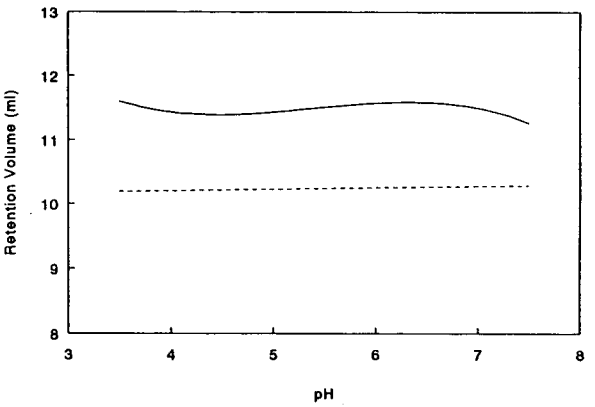

Fig. 2. Calculated influence of the pH of the eluent on the retention volume (ml) of two specific heparin samples, M_w = 5090 (solid line) and 9200 (dotted line). The temperature and ionic strength of the eluent were 35°C and 0.1, respectively.

Polysaccharide model

The influence of the ionic strength, pH and temperature of the eluent on the retention volume of five polysaccharide standards of M_w = 5800, 12 200, 23 700, 48 000 and 100 000 g/mol was also investigated. A 3^3 factorial design was used, which indicates that three factors were measured at three different levels. The factorial

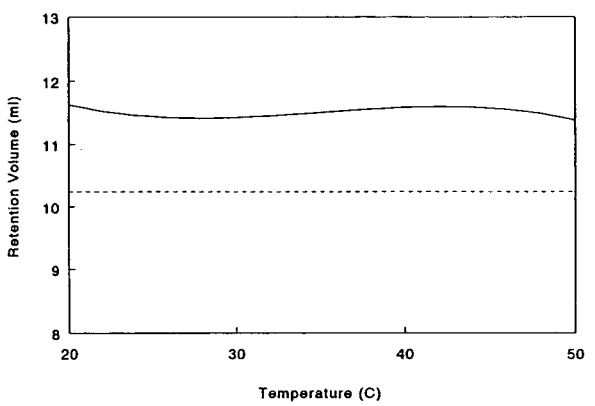

Fig. 3. Calculated influence of the temperature of the eluent on the retention volume (ml) of two specific heparin samples, M_w = 5090 (solid line) and 9200 (dotted line). The pH and ionic strength of the eluent were 5.5 and 0.1, respectively.

TABLE IV

EXPERIMENTAL SETTINGS USED IN THE FACTORIAL DESIGN FOR THE DETERMINATION OF THE INFLUENCE OF THE IONIC STRENGTH, TEMPERATURE AND pH OF THE ELUENT ON THE RETENTION VOLUME OF POLYSACCHARIDES

Setting No.	Temperature (°C)	pH	Ionic strength
1	25	4	0.01
2	25	4	1
3	25	7	1
4	45	7	1
5	45	4	1
6	45	7	0.01
7	25	7	0.01
8	45	4	0.01
9	35	5.5	0.1

design is given in Table IV. All levels were measured twice, except the centre point (35°C, pH 5.5, ionic strength = 0.1), which was measured ten times. The pure experimental error could be calculated from the measurements in the centre point.

From the experimental results, the influences of the three parameters on the retention volume of the polysaccharide standards could be calculated. In the investigated experimental framework, no significant influence of the ionic strength, pH and temperature of the eluent on the retention volume of the polysaccharide standards with average molecular masses of 12 200, 23 700 and 100 000 g/mol was observed.

The results from the calculations of the influence of the three parameters under study on the retention volume of the polysaccharide standard with an average molecular mass of 5800 g/mol can be expressed as

$$V_R = 12.192 + 0.00154 \log I \quad (3)$$

From the results for the polysaccharide standard with an average molecular mass of 48 000 (g/mol), a slightly different equation was derived:

$$V_R = 9.929 + 0.04875 \log I \quad (4)$$

These two expressions were validated with a GOF and an LOF test. The results of these tests are given in Table V. From eqns. 3 and 4 it can be concluded that the temperature, pH and ionic strength of the eluent have almost no influence on the retention volume of the polysaccharide standards.

Fig. 4 shows the retention volume of the polysaccharide standards as a function of the molecular mass of the polysaccharide standards. Under the assumption that the polysaccharide standard with an average molecular mass of 100 000 g/mol is totally excluded from the pores of the stationary phase of the size-exclusion column, the measured values can be fitted with the following logarithmic function:

$$\log M_w = -0.282 V_R + 7.209 \quad (5)$$

TABLE V

RESULTS OF THE VALIDATION OF THE RETENTION VOLUME EXPRESSION OF THE POLYSACCHARIDE STANDARDS WITH A GOODNESS OF FIT AND A LACK OF FIT TEST

Parameters defined as in Table III.

Parameter	Polysaccharide standard (M_w = 5800 g/mol)	Polysaccharide standard (M_w = 48 000 g/mol)
F_{GOF}	24.24	10.83
F^*	5.76	5.72
DF ($p-1, n-p$)	1, 24	1, 24
F_{LOF}	0.44	0.87
F^*	3.77	3.77
DF ($f-p, n-f$)	15, 9	15, 9

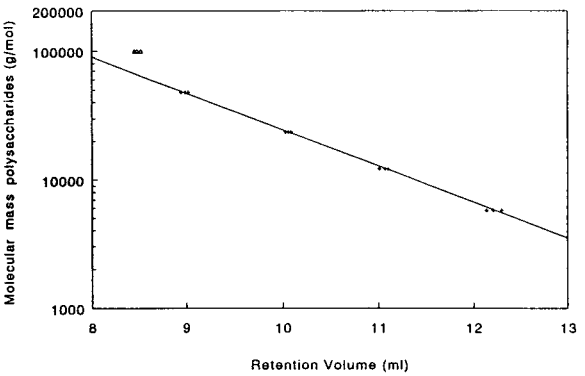

Fig. 4. Calibration graph for the polysaccharide standards. The experiments were performed with water as the eluent at 35°C. The polysaccharide standard with an average M_w = 100 000 is excluded from the pores in the column.

So far the results showed that the molecular size of heparins can be controlled by the composition of the mobile phase, while the retention volumes of polysaccharide standards are hardly influenced by the eluent composition. In principle, this observation offers the possibility of calculating the optimum composition of the eluent at which the retention volume of heparin samples approaches that of a polysaccharide standard with the same molecular mass.

Calculation of optimum ionic strength

Eqn. 5 expresses the relationship between the molecular mass and the retention volume of polysaccharide standards. In order to be able to calibrate the average molecular mass of heparin samples, the retention volume of a heparin standard of a certain average molecular mass should be the same as that of a polysaccharide with the same molecular mass under specific conditions. To determinate the molecular mass of heparin samples from eqn. 5, the optimum eluent composition must be calculated from eqns. 1 and 2, in order to manipulate the molecular sizes of the heparin compounds to values comparable to those of the polysaccharide standards. However, the error made by the interpolation should also be taken into account [18]. The results from these calculations are given in Table VI, where it can be seen that two different optimum values for the ionic strength of the eluent were obtained. We assume that this may be due to the different nature of the heparins. However, because the difference between the two optimum ionic strengths is small, the mildest separation condition ($I = 1.42$) was selected for the calibration of the heparin samples.

At this calculated optimum ionic strength, the retention volume of the heparin standards can be measured, and the molecular masses of the heparin standards can be calculated from eqn. 5. The results are summarized in Table VII. As can be seen, this method provides a fairly good estimate of the molecular masses of the heparin standards. All the calculated molecular masses are slightly higher than the true values but especially for the higher molecular masses the difference between the true and calculated values is small.

With the help of the presented model, the molecular mass distribution of a commercially

TABLE VI

RESULTS OF THE CALCULATION OF THE OPTIMUM IONIC STRENGTH OF THE ELUENT FOR THE STUDIED HEPARIN SAMPLES

Temperature = 35°C; pH of the eluent = 5.5.

Sample	V_R (calculated) (ml)	Standard deviation ($n = 36$) of calculated V_R (ml)	Ionic strength (calculated)
Fraxiparine (M_w = 5090 g/mol)	12.62	0.0872	1.42
Heparin standard (M_w = 9200 g/mol)	11.52	0.0847	1.77

TABLE VII

RESULTS FROM THE VALIDATION OF THE CALIBRATION MODEL FOR HEPARIN

Retention volumes measured at 35°C and an eluent pH of 5.5.

Ionic strength	Real average molecular mass (g/mol)	Calculated average molecular mass (g/mol) from eqn. 5
1.42	3000	$4.5 \cdot 10^3$
	4200	$5.4 \cdot 10^3$
	6000	$7.0 \cdot 10^3$
	9200	$10.7 \cdot 10^3$
	11 200	$12.7 \cdot 10^3$
1.77	6000	$7.1 \cdot 10^3$
	9200	$10.2 \cdot 10^3$
	11 200	$13.1 \cdot 10^3$

available heparin, Calparine, was calculated from a chromatogram of a Calparine sample (Fig. 5). The chromatogram was divided into slices, and for each slice the corresponding molecular mass was calculated using both the polysaccharide and the heparin calibration graph. Fig. 6 shows the results of both calibration methods for the calibration of Calparine. The data from these experiments are in good agreement with the expected results. The molecular mass of the different oligosaccharides of commercially available heparin, such as Calparine, normally ranges from 2000 to 40 000 g/mol [2].

CONCLUSIONS

It has been shown that by adjusting experimental parameters such as the pH, ionic strength and temperature of the eluent, the molecular masses of specific heparin samples can be calculated by applying other biopolymers, *e.g.*, polysaccharides, as standards. An advantage of this approach is that these calibrations

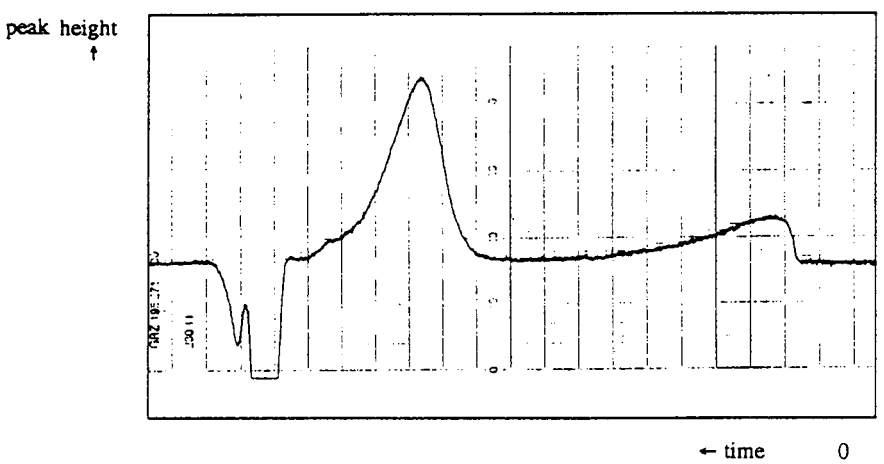

Fig. 5. Size-exclusion chromatogram of a specific heparin sample (Calparine) on a Zorbax GF-250 column (200 mm × 9.4 mm I.D.) with RI detection. Flow-rate, 1.0 ml/min; temperature, 35°C; buffer composition, Na_2HPO_4–NaCl; pH of buffer, 5.5; ionic strength of buffer, 1.42.

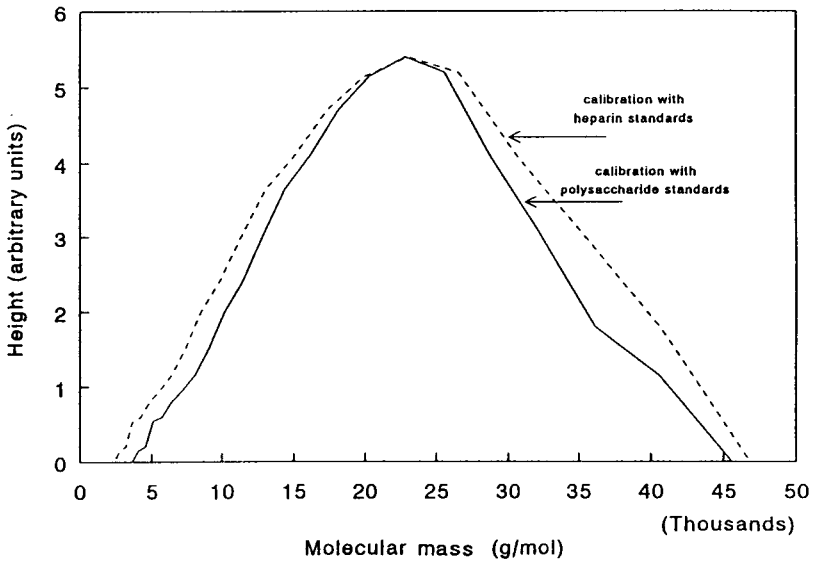

Fig. 6. Molecular mass distribution of a specific heparin sample (Calparine), calculated from a polysaccharide and a heparin calibration graph.

can be performed with commercially available standards, consisting of other chemical substances, when standards of the target compounds are not available. A satisfactory agreement in the molecular mass distribution of a Calparine sample was observed for both the calibration with polysaccharide standards and the calibration with heparin standards. However, it should be mentioned that, because of possible secondary separation mechanisms, the results presented in this study may only be valid for this size-exclusion column.

The use of chemometrics was found to be very helpful in setting up the experimental design and the calculation of the data. As a consequence, the effects of the different parameters could be investigated with a relatively small number of experiments. Applying chemometric techniques to the results also allowed the calculation of the influence of the separation variables and additionally the determination of the interaction effects of these variables.

The approach described here for measuring the molecular masses of heparin samples by applying standards of other chemical classes as standards may also be useful for other biopolymers.

ACKNOWLEDGEMENT

The authors gratefully acknowledge Professor Dr. H.C. Hemker of the Department of Biochemistry, University of Limburg (Maastricht, Netherlands), for providing the heparin samples and standards.

REFERENCES

1 B. Casu, *Adv. Carbohydr. Chem. Biochem.*, 43 (1985) 51–134.
2 D.A. Lane, I. Björk and U. Lindahl, *Heparin and Related Polysaccharides (Advances in Experimental Medicine and Biology*, Vol. 313), Plenum Press, New York, London, 1992.
3 L. Oscarsson, G. Pejlel and U. Lindahl, *J. Biol. Chem.*, 264 (1989) 296–304.
4 R. Lasito, H. Gattiker and G. Bilodeau, *J. Chromatogr.*, 226 (1981) 61–67.
5 J. Harenberg and J.X. de Vries, *J. Chromatogr.*, 261 (1983) 287–292.
6 D. Muller, M.N. Doume-Nze and J. Jozefonvicz, *J. Chromatogr.*, 297 (1984) 351–358.
7 J.X. de Vries, *J. Chromatogr.*, 465 (1989) 297–304.
8 H.I. Kirstinsen, E.M. Tomborg, J.R. Nielsen, J.I. Nielsen, K.B. Johansen and P.B. Ostergaard, *Thromb. Res.*, 64 (1991) 131–141.
9 L. Rosenfeld, M.T. Prior and L.M. Girardi, *Thromb. Res.*, 64 (1991) 203–211.

10 W.W. Yau, J.J. Kirkland and D.D. Bly, *Modern Size Exclusion Liquid Chromatography*, Wiley, New York, 1979.
11 M. Potschka, *J. Chromatogr.*, 441 (1988) 239–260.
12 P.K. Dubin and M.N. Tecklenburg, *Anal. Chem.*, 57 (1985) 275–279.
13 P.L. Dubin, C.M. Speck and J.I. Kaplan, *Anal. Chem.*, 60 (1988) 895–900.
14 E. Pérez-Payá, L. Braco, A. Campos, V. Soria and C. Abad, *J. Chromatogr.*, 461 (1989) 229–242.
15 S. Béguin, S. Wielders, J.C. Lormeau and H.C. Hemker, *Thromb. Haemostasis*, 67 (1992) 33–41.
16 A.V. Bendetowicz, E. Pacaud, S. Béguin, A. Uzan and H.C. Hemker, *Thromb. Haemostasis*, 67 (1992) 556–562.
17 D.L. Massart, B.G.M. Vandeginste, S.N. Deming, Y. Michotte and L. Kaufman, *Chemometrics, a Textbook*, Elsevier, Amsterdam, 1988.
18 J.C. Miller and J.N. Miller, *Statistics for Analytical Chemistry*, Ellis Horwood, Chichester, 2nd ed., 1992.

Journal of Chromatography A, 657 (1993) 43–54
Elsevier Science Publishers B.V., Amsterdam

CHROM. 25 503

Chiral separation of unmodified amino acids by ligand-exchange high-performance liquid chromatography using copper(II) complexes of L-amino acid amides as additives to the eluent

Gianni Galaverna, Roberto Corradini, Eriberto de Munari, Arnaldo Dossena and Rosangela Marchelli*

Dipartimento di Chimica Organica e Industriale dell' Università, Viale delle Scienze, I-43100 Parma (Italy)

(First received May 6th, 1993; revised manuscript received August 12th, 1993)

ABSTRACT

Copper(II) complexes of L-amino acid amides added to the eluent in reversed-phase high-performance liquid chromatography are able to perform chiral discrimination of unmodified amino acids with high enantioselectivity. The mechanism is consistent with a ligand exchange between the binary initial copper(II) complex and the enantiomers. Evidence is provided that the exchange of the ligand is actually occurring during the chromatographic separation. The system involves a series of equilibria of exchange in the aqueous solution, in the stationary phase and between the two phases. Enantioselectivity is essentially due to the adsorption of the diastereomeric ternary species on the column, whereas the relative stabilities of the mixed complexes in the mobile phase seem to be negligible with respect to the overall discrimination process. The structural features of the initial copper complexes greatly affect the stereoselectivity of the process. The chromatographic parameters (pH, selector concentration, eluent polarity, ionic strength) are examined.

INTRODUCTION

Chiral separation of amino acids is of great interest in many research fields, from geochronological to pharmaceutical and biomedical areas [1–3]. Recently, we have found surprisingly large amounts of D-amino acids in foods, not only in connection with heat or alkali treatments, but also with the most common fermentation processes, such as cheese and yoghurt preparations [4]. Whether D-amino acids are derived from the lysis of the bacterial cell walls and/or other microbiological transformations is an intriguing question, as also is their biological significance at the nutritional, toxicological and organoleptic levels [5].

In the last decade, the enantiomeric separation of unmodified amino acids by HPLC has received much attention. In particular, ligand-exchange chromatography (LEC) [6] has proved to be successful with a variety of copper(II) complexes of amino acids or amino acid derivatives either chemically bonded to the stationary phases [7–9] or as additives to the eluent [10–23]. The addition of chiral metal complexes to the eluent is particularly useful in analytical applications, being very easy to handle, flexible, and efficient [24]. In fact, achiral columns can be used in combination with different optically active complexes with high enantioselectivity and efficiency.

Several years ago [25–27] we started an exten-

* Corresponding author.

0021-9673/93/$06.00

sive investigation on the mechanism of chiral discrimination by ligand exchange with copper(II) complexes of bidentate, tridentate and tetradentate ligands of the amino amide type. In fact, whether chiral discrimination occurs via a total or partial displacement of one ligand from a binary complex is still a matter of discussion. Alternative mechanisms have been proposed, involving also apical and outer-sphere interactions [28]. In particular, in a previous paper [26] we reported that with copper(II) complexes of bidentate ligands (L-amino acid amides) added to the mobile phase, very good chiral separations of D,L-dansyl (Dns)-amino acids in reversed-phase HPLC were obtained. We now report that copper(II) complexes of the same (or slightly modified) ligands when added to the eluent are able to perform chiral separations of unmodified amino acids in reversed-phase HPLC with either postcolumn derivatization with *o*-phthalaldehyde (OPA) and fluorescence detection or with UV detection. The effects of ligand hydrophobicity and structure, complex concentration, pH, solvent polarity and ionic strength were investigated.

L-Amino acid amides are commercially available or can be easily synthesized [29], with retention of configuration. Their ability to form copper(II) complexes, both in aqueous solution and in the solid state, was also studied. The distribution pattern of the various complexes existing at different pHs and their thermodynamic stabilities were established by potentiometry and spectroscopy [30]. The crystal structures of several copper complexes with L-phenylaninamide, L-N^2-methyl- and L-N^2,N^2-dimethylphenylalaninamide [31] and L-prolinamide [32] were determined by X-ray crystallography and may provide important clues regarding the eventual interactions involved in chiral discrimination. Whether the mechanism of chiral discrimination proceeds via ligand exchange in the chromatographic system was investigated by using copper(II) complexes of L-tryptophanamide.

EXPERIMENTAL

Equipment

Chromatographic analyses were performed on a Waters Model 440 chromatograph equipped with a Model 420 fluorescence detector and a Waters 745 data module or with a UV detector set at 254 or 280 nm. A C_{18} Spherisorb ODS-2 (3 μm) column (150 × 4.6 mm I.D.) was used.

Reagents

The D,L- and L-amino acids and L-amino acid amides were obtained from Sigma (St. Louis, MO, USA), OPA from Fluka (Buchs, Switzerland) and acetonitrile (LC grade), methanol (LC grade) and copper acetate (RPE ACS grade) from Carlo Erba (Milan, Italy). Doubly distilled water was produced in our laboratory utilizing an Alpha-Q system (Millipore).

Synthesis of ligands

N^2-Methyl-L-amino acid amide hydrochlorides. N-Methylamino acids were synthesized from Cbz-amino acids using McDermott and Benoiton's procedure [33] or were obtained from Sigma (St. Louis, MO, USA). The amidation procedure was performed according to an original method developed in our laboratory [29] by reacting the N-hydroxysuccinimidyl ester with diaminomethane dihydrochloride in dioxane. Compounds synthesized were N^2-methyl-L-phenylalaninamide hydrochloride (L-MePhe-A · HCl) [30] and N^2-methyl-L-valinamide hydrochloride (L-MeVal-A · HCl) [29].

N^2,N^2-Dimethyl-L-amino acid amide hydrochlorides. These ligands were obtained from the corresponding L-amino acid amide hydrochlorides and formaldehyde in methanol by stirring under hydrogen in the presence of 10% Pd–C at 40°C for 3 h. Compounds synthesized were N^2,N^2-dimethyl-L-phenylalaninamide hydrochloride (L-Me_2Phe-A · HCl) [30] and N^2,N^2-dimethyl-L-valinamide hydrochloride (L-Me_2Val-A · HCl). Data for the latter compound were as follows: yield, 85%; m.p., 262–264°C; $[\alpha]_D^{25°C}$ = +24.3 (c = 1, 95% EtOH). IR (KBr): ν = 3310, 3150, 2980, 1690 cm^{-1}. ^1H NMR (C^2HCl_3, free amine): δ 1.0 (dd, 6H, 2 CH_3), 2.0–2.2 (m, 1H, CH_β), 2.3 [s, 6H, $N(CH_3)_2$], 2.45 (d, 1H, CH_α), 5.7 (broad s, 1H, CONH), 6.3 (broad s, 1H, CONH) ppm. ^{13}C NMR (C^2HCl_3, free amine): δ 18 (CH_3), 20 (CH_3), 28 (CH_β), 43 [$N(CH_3)_2$], 75 (CH_α), 195 (CO) ppm. Mass spectrum: m/z

144 (traces, M^+), 100 (100), 85 (38), 70 (18), 56 (10).

Preparation of derivatizing agent

Boric acid (18.55 g) was dissolved in doubly distilled water (1 l) and the pH was adjusted to 10 by addition of solid KOH (pellets). EDTA (2.5 g) was added and the pH was readjusted to 10. OPA (0.8 g) was dissolved in mercaptoethanol (4 ml) and then added to the former solution with a syringe under vigorous magnetic stirring. The resulting solution was filtered and degassed under reduced pressure on HPLC filters (0.45 μm; Millipore).

Mobile phase preparation

The ligand and copper acetate were carefully weighed to give the ratios required and dissolved in water or in a water–organic solvent (methanol or acetonitrile) mixture. When needed, sodium acetate (0.1–0.3 *M*) was added. The solutions were adjusted to the desired pH with acetic acid or sodium hydroxide, then filtered and degassed under reduced pressure. Before starting the analysis, the mobile phase was allowed to flow until reproducible retention times were obtained. The column efficiency was checked by calculating the number of theoretical plates per metre; 25 000–50 000 plates per metre were obtained, depending on the amino acid and on the selector. The column dead volume (V_0) was determined from the elution time of an unretained solute (acetic acid).

Ligand-exchange experiment

L-Tryptophanamide (L-Trp-A) and copper(II) acetate were dissolved in water in the appropriate ratio (2:1) to obtain a 0.2 m*M* complex concentration. The pH was adjusted at 5.8 and the solution was filtered and degassed under reduced pressure on HPLC filters (0.45 μm). The mobile phase was allowed to flow on a C_{18} Spherisorb 3 ODS-2 column and, after equilibration (2 h), the analysis was started. A fluorescence detector, set at the excitation and emission wavelengths of tryptophan ($\lambda_{exc.}$ = 295 nm, $\lambda_{em.}$ = 359 nm), or a UV detector, set at 254 or 280 nm, was used.

RESULTS AND DISCUSSION

We utilized copper(II) complexes of L-prolinamide (L-Pro-A), L-phenylalaninamide (L-Phe-A), N^2-methyl-L-phenylalaninamide (L-MePhe-A), N^2,N^2-dimethyl-L-phenylalaninamide (L-Me_2Phe-A), L-valinamide (L-Val-A), N^2-methyl-L-valinamide (L-MeVal-A), N^2,N^2-dimethyl-L-valinamide (L-Me_2Val-A) and L-tryptophanamide (L-Trp-A) as additives to the eluent. All ligands were easily prepared in high yield and optical purity [29].

Chromatographic results

Copper(II) complexes of L-Phe-A and L-MePhe-A in aqueous solution in the pH range 5–7.5 in reversed-phase HPLC proved to be enantioselective towards polar and non-polar amino acids, except glutamic acid and serine. All other amides were able to separate only non-polar amino acids. Results are reported in Tables I and II and in Figs. 1 and 2.

Effect of ligand hydrophobicity

By taking the hydrophobic parameters π for the amino acid side-chains [34] as a measure of the lipophilicity of the selectors and selectands, it appears that the more lipophilic selectors Phe-A and MePhe-A (π_{Phe} = 1.63) gave the best enantioselectivity factors with most amino acids, whereas the least lipophilic Pro-A (π_{Pro} = 0.77) gave very good results only with non-polar amino acids. The analogous MeVal-A (π_{Val} = 1.27) gave very poor results.

Effect of N-substitution on the amino group of the ligand

The introduction of one methyl group on the amino nitrogen of the ligand improved the enantioselectivity, whereas the presence of a second methyl group enhanced the separation factors of non-polar amino acids, but it prevented the separation of the polar compounds. Accordingly, the best separation factors with non-polar amino acids were obtained with the more hindered ligand Me_2Phe-A and with Pro-A, which has a rigid cyclic moiety. Polar amino acids were separated only by Phe-A and MePhe-A, which

TABLE I

CHIRAL SEPARATION OF AMINO ACIDS WITH COPPER(II) COMPLEXES OF L-AMINO ACID AMIDES: CAPACITY FACTORS (k'), ENANTIOSELECTIVITY FACTORS ($\alpha = k'_L/k'_D$) AND HYDROPHOBIC CONSTANTS (π) FOR AMINO ACID SIDE-CHAINS

Conditions: 2 m*M* amino acid amide–1 m*M* copper (II) acetate; pH 6.0; column, Spherisorb 3 ODS-2 (3 μm, 15 × 0.46 cm I.D.); fluorescence detection (postcolumn derivatization with OPA); UV detection at 254 nm for Pro; flow-rate, 0.5 ml/min; room temperature; $t_0 = 3.24$ min (retention time of CH_3COOH).

Amino acid	π	Phe-A			MePhe-A			Me_2Phe-A		
		k'_L	k'_D	α	k'_L	k'_D	α	k'_L	k'_D	α
Glu	−0.98	6.54	6.54	1.00	2.40	2.40	1.00	0.58	0.58	1.00
Asp	−1.05	1.65	1.88	0.88	1.28	1.57	0.82	0.35	0.35	1.00
Ser	−0.08	0.85	0.85	1.00	0.20	0.20	1.00	0.06	0.06	1.00
Thr	0.33	1.23	1.46	0.84	0.29	0.52	0.56	0.13	0.13	1.00
His	−0.40	2.62	2.62	1.00	0.84	1.68	0.50	0.14	0.38	0.37
Ala	0.40	1.62	1.38	1.17	0.54	0.37	1.50	0.23	0.12	1.92
α-NBu	0.83[a]	4.38	3.38	1.30	2.33	1.46	1.60	1.24	0.49	2.53
Met	1.42	20.92	16.54	1.27	12.84	9.77	1.31	6.81	4.28	1.59
Val	1.18	16.77	9.08	1.85	7.61	4.31	1.77	4.24	1.77	2.40
Leu	1.64	47.69	31.31	1.52	33.74	18.41	1.83	12.77	6.05	2.11
Pro	0.77	17.54	14.46	1.21	3.75	0.82	4.57	2.41	0.50	4.82
Nval	1.37	17.85	11.15	1.60	5.96	3.19	1.87	4.33	1.96	2.21
Tyr	0.88	43.00	22.69	1.90	29.04	13.82	2.10	14.95	6.16	2.43

[a] Sum of fragmental contributions π_f [34].

give a good compromise between lipophilicity and steric hindrance. With the latter, a reversal of elution order was observed: L > D for the non-polar and L < D for the polar amino acids.

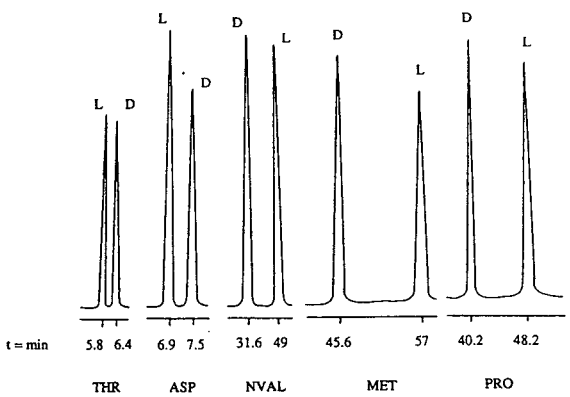

Fig. 1. Chromatographic separation of D,L-amino acids with L-Phe-A–Cu(II). Conditions: 2 m*M* L-Phe-A, 1 m*M* copper(II) acetate dissolved in water; pH = 6; column, Spherisorb ODS-2 (3 μm, 15 × 0.46 cm I.D.); room temperature; flow-rate, 0.5 ml/min; UV detection at 254 nm.

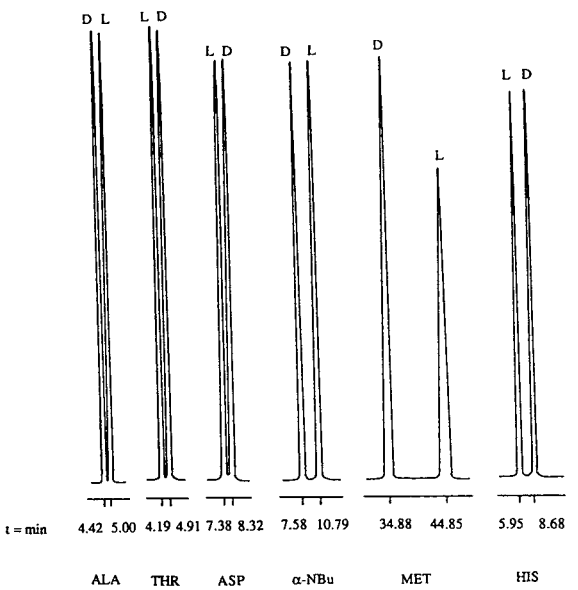

Fig. 2. Chromatographic separation of D,L-amino acids with L-MePhe-A–Cu(II). Conditions: 2 m*M* L-MePhe-A, 1 m*M* copper(II) acetate dissolved in water; pH 6; column, Spherisorb ODS-2 (3 μm, 15 × 0.46 cm I.D.); room temperature; flow-rate, 0.5 ml/min; fluorescence detection (postcolumn derivatization with OPA).

TABLE II

CHIRAL SEPARATION OF AMINO ACIDS WITH COPPER(II) COMPLEXES OF L-AMINO ACID AMIDES: CAPACITY FACTORS (k'), ENANTIOSELECTIVITY FACTORS ($\alpha = k'_L/k'_D$) AND HYDROPHOBIC CONSTANTS (π) FOR AMINO ACID SIDE-CHAINS

Conditions: 2 m*M* amino acid amide–1 m*M* copper (II) acetate; pH 6.0; column, Spherisorb 3 ODS-2 (3 μm, 15 × 0.46 cm I.D.); fluorescence detection (postcolumn derivatization with OPA); UV detection at 254 nm for Pro; flow-rate, 0.5 ml/min; room temperature; $t_0 = 3.24$ min (retention time of CH_3COOH).

Amino acid	π	Pro-A			MeVal-A			Me_2Val-A		
		k'_L	k'_D	α	k'_L	k'_D	α	k'_L	k'_D	α
Glu	−0.98	0.33	0.33	1.00	0.05	0.05	1.00	0.28	0.28	1.00
Asp	−1.05	0.31	0.31	1.00	0.03	0.03	1.00	0.29	0.29	1.00
Ser	−0.08	0.18	0.18	1.00	0.09	0.09	1.00	0.30	0.30	1.00
Thr	0.33	0.30	0.30	1.00	0.17	0.17	1.00	0.48	0.48	1.00
His	−0.40	0.55	0.71	0.78	0.42	0.63	0.67	1.15	1.15	1.00
Ala	0.40	0.36	0.28	1.29	0.18	0.18	1.00	0.55	0.55	1.00
α-NBu	0.83[a]	1.10	0.54	2.04	0.62	0.62	1.00	1.13	1.03	1.10
Met	1.42	5.90	3.43	1.72	3.13	2.96	1.06	4.19	3.82	1.10
Val	1.18	5.50	1.80	3.05	2.49	2.16	1.15	3.22	2.74	1.18
Leu	1.64	6.55	3.28	2.00	6.48	6.08	1.07	8.33	7.06	1.18
Pro	0.77	5.29	2.21	2.39	2.39	1.85	1.29	3.09	2.25	1.37
NVal	1.37	4.61	2.38	1.94	2.28	2.07	1.10	3.08	2.70	1.14
Tyr	0.88	10.31	6.07	1.70	6.83	6.53	1.05	8.13	6.82	1.19

[a] Sum of fragmental contributions π_f [34].

Effect of pH

Chiral discrimination occurs in the pH range 5.0–7.5. By increasing the pH, the capacity factors of both enantiomers increased, especially that of the most retained enantiomer, so that the selectivity factors also increased, as reported in Fig. 3 for L-Pro-A and in Fig. 4 for MePhe-A.

From potentiometric titrations, we have found [30] that in the pH range considered several copper(II) complexes are present: CuL^{2+}, CuL_2^{2+}, $CuLH^{+}_{-1}$, $CuL_2H^{+}_{-1}$ and CuL_2H_{-2}. In Fig. 5 the species distribution for the Cu(II)–MePhe-A system and in Fig. 6 the structures of the complexes are reported.

As shown by Dallavalle *et al.* [30] and in agreement with Sigel and Martin [35], deprotonation of the amide starts at about pH 5 in the presence of the copper(II) ion. Therefore, it is difficult to ascribe enantioselectivity to a single species, as several equilibria co-exist in the pH range considered. The better enantioselectivity factors (α) obtained at higher pH can be accounted for by the presence of a neutral initial Cu(II) complex or by the formation of neutral ternary species, which may display a better affinity for the column.

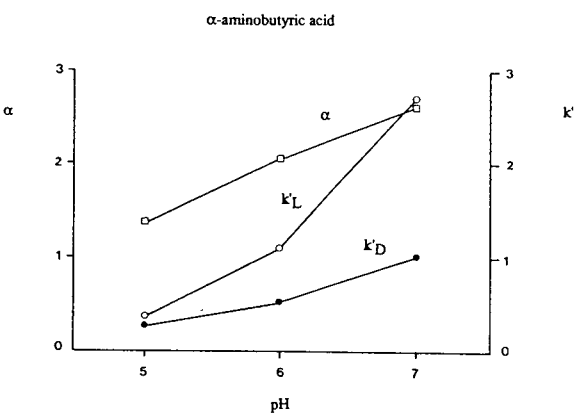

Fig. 3. Variation of the capacity factors (k') and enantioselectivity factors (α) as a function of pH with L-Pro-A–Cu(II). Conditions: 4 m*M* L-Pro-A, 2 m*M* copper(II) acetate dissolved in water; room temperature; column, Spherisorb ODS-2 (3 μm, 15 × 0.46 cm I.D.); flow-rate, 0.5 ml/min.

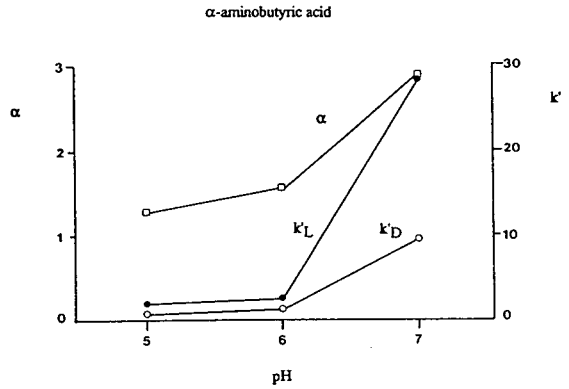

Fig. 4. Variation of the capacity factors (k') and enantioselectivity factors (α) as a function of pH with L-MePhe-A–Cu(II). Conditions: 4 m*M* L-MePhe-A, 2 m*M* copper(II) acetate dissolved in water; room temperature; column, Spherisorb ODS-2 (3 μm, 15 × 0.46 cm I.D.); flow-rate, 0.5 ml/min.

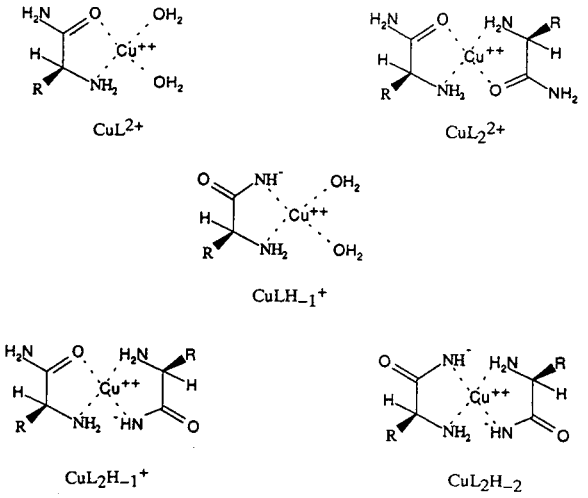

Fig. 6. Structures of the complexes of L-amino acid amides with copper(II).

Effect of amino acid side-chain

We have considered the effect of the length of the amino acid side-chain (R) on the enantioselectivity factor (α) in the case of Pro-A (Fig. 7): as the length (and therefore the hydrophobic constant) of the linear side chain increased (Ala < α-NBu < NVal < NLeu), α also increased, owing to the stronger interaction of the more retained enantiomer with the non-polar C_{18} column (solvophobic effect) (Table II). Moreover, branching at C_β (Val, Ile) enhanced the enantioselectivity factor, on account of an enhanced steric discriminating effect. Branching at further positions (C_γ, Leu) had negligible effects. The same trend was observed with the ligand MePhe-A.

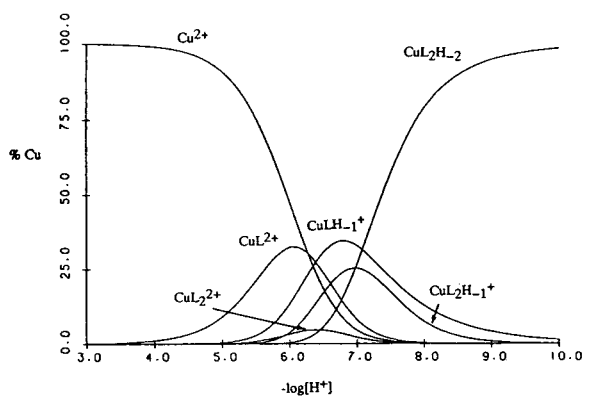

Fig. 5. Species distribution for the Cu(II)–MePhe-A system with c_{Cu} = 0.002 *M* and c_L = 0.004 *M* as a function of $-\log[H^+]$.

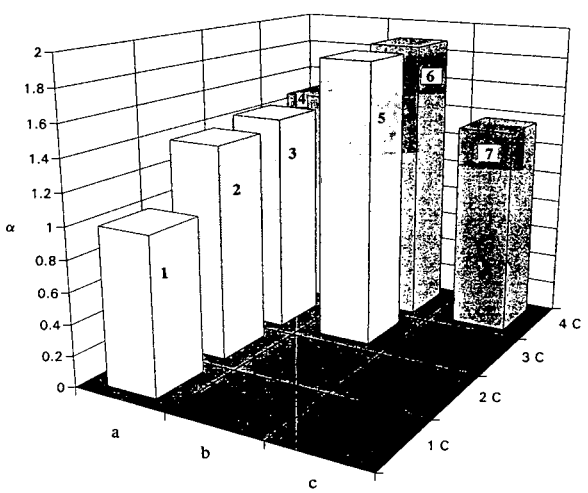

Fig. 7. Three-dimensional representation of the effect of the side-chain of the amino acids on the enantioselectivity factor (α) with L-Pro-A–Cu(II). 1C, 2C, 3C, 4C = number of carbon atoms in the amino acid side-chain; (a) linear side-chain; (b) β-branching; (c) γ-branching. 1 = Ala; 2 = α-NBu; 3 = NVal; 4 = NLeu; 5 = Val; 6 = Ile; 7 = Leu.

Effect of concentration of initial Cu(II) complexes

The concentration effect was studied with Pro-A and MePhe-A at pH 7 in the concentration range 1–8 m*M*. As shown in Fig. 5, the main species present at this pH are $CuLH^{+}_{-1}$, $CuL_2H^{+}_{-1}$ and CuL_2H_{-2}. First, the chromatographic system was conditioned with the copper complex at a given molarity for 30 min. Then the experiment was performed with the selector in the mobile phase at the same concentration. The results are different with the selectors L-Pro-A and L-MePhe-A. With the former, the enantioselectivity factor (α) increased from a concentration of 1 m*M*, reached a maximum at 4 m*M* and then decreased. In contrast, with the latter the best enantioselectivity factor was obtained at 1 m*M*. It is evident that a higher concentration of the complex with the less lipophilic Pro-A is needed to saturate the column. The experimental details are reported in Figs. 8 and 9 for the separation of D,L-α-aminobutyric acid.

Effects of eluent polarity and ionic strength

On adding sodium acetate to the eluent both polar and non-polar amino acids were less retained, so that α decreased. The same effect was observed on addition of an organic modifier (acetonitrile) to the aqueous solution containing the chiral copper(II) complex. However, acetonitrile must be used to reduce retention times for the separation of the most lipophilic amino acids

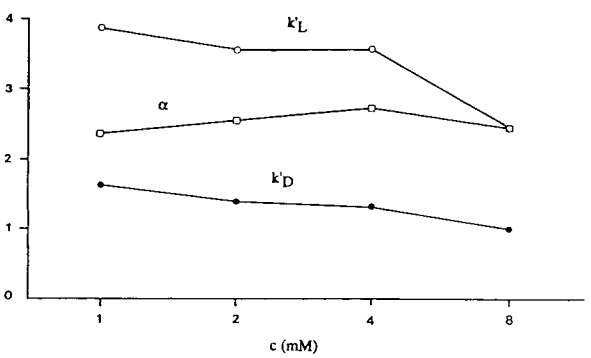

Fig. 8. Variation of the capacity factors (k') and enantioselectivity factors (α) as a function of the initial complex concentration in the eluent: L-Pro-A–Cu(II); amino acid = α-aminobutyric acid.

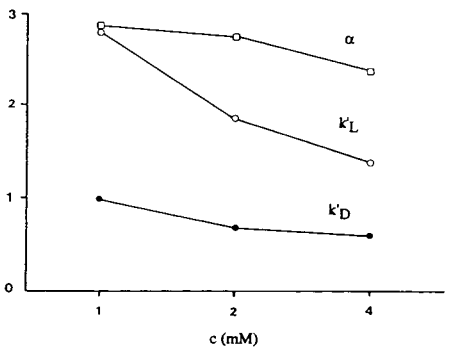

Fig. 9. Variation of the capacity factors (k') and enantioselectivity factors (α) as a function of the initial complex concentration in the eluent: L-MePhe-A–Cu(II); amino acid = α-aminobutyric acid.

such as phenylalanine and tryptophan, as shown in Fig. 10.

Separation of a mixture of amino acids

By using MePhe-A and copper(II) acetate, it was possible to obtain the separation of a mix-

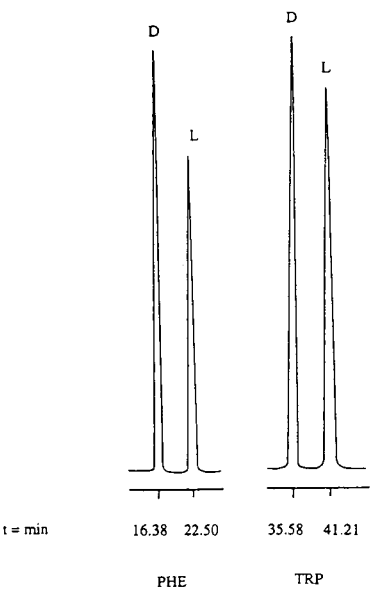

Fig. 10. Chromatographic separation of D,L-Phe and D,L-Trp with L-MePhe-A–Cu(II). Conditions: 2 m*M* L-MePhe-A, 1 m*M* copper(II) acetate; eluent, water–acetonitrile (90:10); pH 6; column, Spherisorb ODS-2 (3 μm, 15 × 0.46 cm I.D.); room temperature; flow-rate, 0.5 ml/min; fluorescence detection (postcolumn derivatization with OPA).

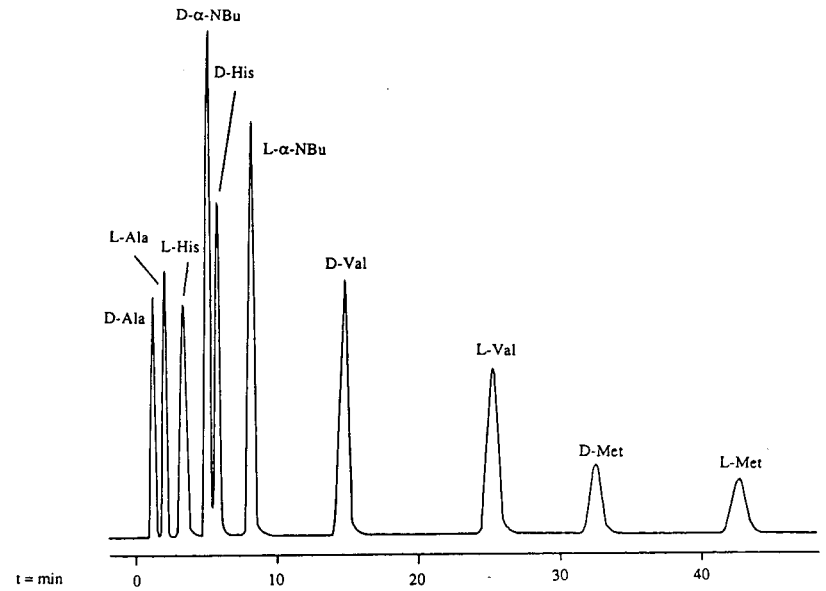

Fig. 11. Isocratic separation of a mixture of D,L-amino acids with L-MePhe-A–Cu(II). Conditions: 2 m*M* L-MePhe-A, 1 m*M* copper(II) acetate dissolved in water; pH 6; column, Spherisorb ODS-2 (3 μm, 15 × 0.46 cm I.D.); room temperature; flow-rate, 0.5 ml/min; fluorescence detection (postcolumn derivatization with OPA).

ture of amino acids with fairly good chemoselectivity and high enantioselectivity (Fig. 11). However, we have not developed the method further, because in the meantime we envisaged an alternative two-dimensional system that allowed the chiral separation of one amino acid at a time (single amino acid analysis) [36].

Mechanism of chiral discrimination

Generally, chiral discrimination is ascribed to a reaction of ligand exchange between the initial copper complex and the enantiomers with formation of diastereomeric ternary complexes of different stabilities and/or different affinities for the column.

Evidence was obtained for the first time that a ligand-exchange mechanism is indeed occurring in the chromatographic system with copper(II) complexes of these bidentate ligands (L:Cu = 2:1). The experiment was performed with L-Trp-A, which is fluorescent. As copper(II) is a fluorescence quencher, in the binary complex bis(L-tryptophanamidato)copper(II), fluorescence was almost completely quenched (only 10% of the initial fluorescence was retained). When using this complex as eluent and a fluorescence detector, a unique signal was observed with the same retention time for all D,L-amino acids, corresponding to free L-Trp-A. The mixed copper complexes, being non-fluorescent, were not detectable under the conditions used (Fig. 12). Indeed, fluorescence was induced by displacement of one Trp-A ligand from the initial bis(amino acid amidato) complex, according to the equilibrium

$$[\mathrm{Cu(Trp\text{-}A)_2}] + \mathrm{AA} \rightleftharpoons [\mathrm{Cu(Trp\text{-}A)} \cdot (\mathrm{AA})] + \mathrm{Trp\text{-}A}$$

Moreover, when a UV detector was used at 254 nm, three positive signals were obtained, one corresponding to L-Trp-A and the other two to the diastereomeric ternary complexes. Absorption in this wavelength range is due to a charge-transfer band characteristic of these copper(II) complexes. When the UV detector was set at 280 nm, the absorption wavelength of the indole moiety of tryptophanamide, the signal corresponding to free L-Trp-A was present, whereas the two diastereomeric mixed complex-

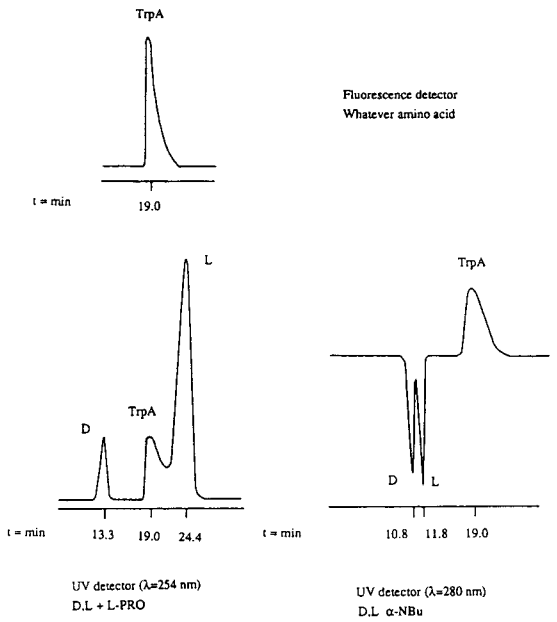

Fig. 12. Ligand-exchange experiment with L-Trp-A–Cu(II) system. Conditions: 0.4 m*M* L-Trp-A, 0.2 m*M* copper(II) acetate dissolved in water; pH 5.8; column, Spherisorb ODS-2 (3 μm, 15 × 0.46 cm I.D.); room temperature; flow-rate, 1 ml/min.

es gave rise to two negative peaks as they have a lower absorbance than the initial bis-tryptophanamidato complex, being deprived of a tryptophanamide moiety. The experiment unequivocally shows that one of the two ligands is displaced from the original binary complex to give rise to mixed species.

Whether ligand exchange occurs on the stationary phase or in the aqueous phase depends on the structural features of the selector [37]. With lipophilic selectors the chiral initial complex is completely adsorbed on the stationary phase and the recognition process occurs entirely in this phase [38,39]. With hydrophilic selectors, such as cyclodextrins, chiral discrimination is assumed to occur mainly in the mobile phase [40]. In a more general case, complex formation equilibria are relevant in both the mobile and stationary phases and partitioning of all species between the two phases must be taken into account to explain enantiomeric discrimination.

In the case of amino acidato–copper(II) complexes as chiral additives [41], the three fundamental interactions accounting for the separation were assumed to be the coordination of the α-carboxy and the α-amino groups of the solute to the copper(II) ion and the hydrophobic interactions between the side-chains of the selector and the solute, which determine the stability of the ternary complexes in aqueous solution. According to our results with amino acid amidato–copper(II) complexes, the enantioselectivity observed in the chromatographic system is not accounted for by the formation equilibria of the diastereomeric complexes in solution [42], but rather by a complex series of equilibria in both aqueous and organic (stationary) phases. Whether one predominates leading to enantiomeric discrimination depends on the structural features of the initial complex and to the partitioning of the mixed complexes between the two phases. In agreement with Davankov *et al.* [43], the solvophobic interactions between the non-polar side-chains of the selector and the solute with the stationary phase of the column appear to be fundamental.

As for the structures of the ternary complexes, we must consider that, in the pH range considered, three species are present: $CuLH^{+}_{-1}$, $CuL_2H^{+}_{-1}$ and CuL_2H_{-2}. However, if a ligand-exchange mechanism is occurring, the three species give rise to the same diastereomeric ternary complexes: Cu(II)(LH_{-1})(L-amino acid) and Cu(II)(LH_{-1})(D-amino acid). We assume that the diastereomeric complexes, formed by amino acid amides and amino acids, are *trans*, in agreement with the crystallographic data for the binary complexes of bis(amino acid amidato)– [31,32] and bis(amino acidato)–copper(II) complexes [44]. Accordingly, in the ternary L,L-

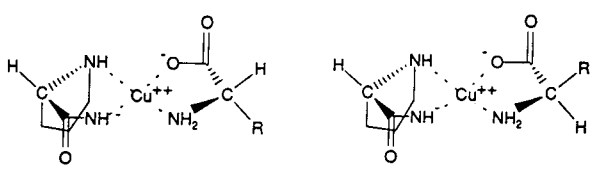

Fig. 13. Structures of the mixed ternary complexes L-Pro-A–Cu(II)–amino acid.

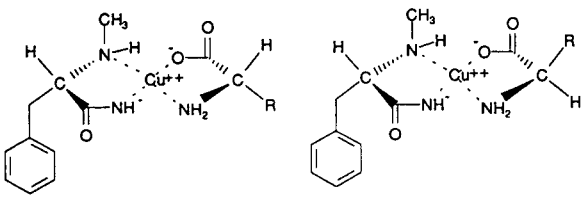

Fig. 14. Structures of the mixed ternary complexes L-MePhe-A–Cu(II)–AA.

species, the side-chains of both the selector and the enantiomer are situated on the same side of the copper coordination plane, thus allowing a strong interaction with the column when R is non-polar, and a less favourable interaction when R is hydrophilic; the opposite occurs with the D-enantiomers (Figs. 13 and 14). This interpretation accounts for the reversed elution order observed for polar and non-polar amino acids.

In fact, non-polar amino acids can interact strongly with the stationary phase of the column and are well separated by all ligands (in particular by more hindered ligands such as Me_2Phe-A and Pro-A). Polar amino acids were separated only by the more hydrophobic ligands (Phe-A and MePhe-A), whereas MeVal-A, Me_2Val-A and Pro-A do not ensure sufficient solvophobic interactions with the stationary phase. With Me_2Phe-A, polar amino acids were eluted too fast from the column, probably on account of the low stability of the complexes, without separation.

The behaviour of each polar amino acid is worth examining. Lysine and arginine were not separated, probably because in the pH range considered the protonated side-chain inferred too low a hydrophobicity ($\pi_{Lys} = -1.14$, $\pi_{Arg} = -0.90$) to the amino acid and to the mixed complexes, thus preventing enantioseparation. In contrast, histidine ($\pi_{His} = -0.40$) was very well separated, as imidazole may form a five-membered chelate ring with the copper(II) ion at the apical position.

The possibility of apical interaction is probably the reason for the different chromatographic behaviour of aspartic and glutamic acid. In fact, it was possible to obtain the enantioselective separation of the former whereas the latter was not resolved. Although the two charged amino acids have very close hydrophobic coefficients ($\pi_{Asp} = -1.05$, $\pi_{Glu} = -0.98$), only the former can form a five-membered chelate ring with copper(II) at the apical position.

For threonine ($\pi_{Thr} = 0.33$) it is probably the presence of the methyl group in the side-chain which accounts for the separation; in contrast, serine is too hydrophilic ($\pi_{Ser} = -0.08$) and unhindered to be discriminated.

The addition of sodium acetate increases the ionic strength of the mobile phase and favours ionization of both the selector and the amino acids and their solubility in the aqueous phase. Thus, the ligand-exchange equilibria preferentially occur in the mobile phase and are less stereoselective. The organic modifier induces the same effect on the enantioselectivity, decreasing the solvophobic interactions with the column and favouring partitioning of the initial chiral complex and of the mixed species towards the mobile phase.

Enantioselectivity increases with increasing concentration of the initial complex up to a certain value, then it decreases at higher concen-

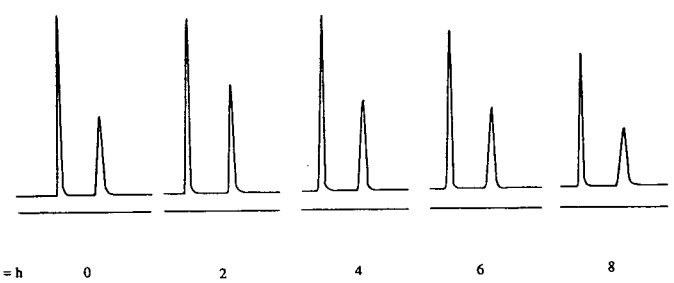

Fig. 15. Enantiomeric separation of D,L-α-aminobutyric acid with L-MePhe-A–Cu(II) adsorbed on the stationary phase of the C_{18} column. Conditions: 2 m*M* L-MePhe-A, 1 m*M* copper(II) acetate dissolved in water at pH 7 adsorbed on the column; eluent, water at pH 7; room temperature; column, Spherisorb ODS-2 (3 μm, 15 × 0.46 cm I.D.); flow-rate, 1 ml/min.

tration, suggesting that chiral discrimination mainly occurs on the saturated stationary phase. Accordingly, the lipophilic MePhe-A easily saturates the column at a 1 m*M* concentration, whereas a higher concentration is needed for Pro-A (4 m*M*). By further increasing the concentration of the initial complex in the mobile phase, the ligand-exchange reaction occurs also in solution, leading to faster elution of both enantiomers and to a decrease in α.

To confirm that the separation occurs on the stationary phase, we performed an experiment in which the complex with MePhe-A was previously adsorbed on the column and elution was carried out with water at pH 7. The column retained its efficiency and enantioselectivity for at least 8 h (Fig. 15). By adding a small amount of copper(II) acetate to the eluent, the enantioselectivity could be maintained for several weeks.

CONCLUSIONS

In conclusion, we have provided a novel, simple method for the enantiomeric separation of unmodified amino acids by HPLC. The selectors are easily available and give very good enantioselectivity factors. It has been shown unequivocally for the first time in HPLC that, in the case of bis(amino acid amidato) complexes, the mechanism proceeds via the exchange of one ligand from the binary complex. The system involves a series of equilibria of exchange in the aqueous solution, in the organic phase and between the two phases. The enantioselectivity due to complex formation in the mobile phase appears to be negligible with respect to the overall discrimination process, whereas the solvophobic interactions of the species with the column is of the utmost importance.

ACKNOWLEDGEMENTS

This paper was supported by a grant from CNR (Consiglio Nazionale delle Ricerche, Rome), Progetto Finalizzato Chimica Fine e Secondaria II, and by MURST (Ministero dell' Università e della Ricerca Scientifica e Tecnologica). NMR and mass spectra were recorded at CIM (Centro Interdipartimentale di Misure), University of Parma.

REFERENCES

1 J.S. Davies, in B. Weinstein (Editor), *Chemistry and Biochemistry of Amino Acids, Peptides and Proteins*, Marcel Dekker, New York, 1977, p. 1.
2 R.L. Preston, *Comp. Biochem. Physiol. B*, 87 (1987) 55.
3 A. D'Aniello and A. Giuditta, *J. Neurochem.*, 29 (1977) 1053.
4 G. Palla, R. Marchelli, A. Dossena and G. Casnati, *J. Chromatogr.*, 475 (1989) 45.
5 M. Friedman, in M. Friedman (Editor), *Nutritional and Toxicological Consequences of Food Processing*, Plenum Press, New York, 1991, p. 447.
6 V.A. Davankov, J.D. Navratil and H.F. Walton, *Ligand Exchange Chromatography*, CRC Press, Boca Raton, FL, 1988.
7 G. Gübitz, W. Jellenz and W. Santi, *J. Chromatogr.*, 203 (1981) 377.
8 P. Roumeliotis, K.K. Unger, A.A. Kurganov and V.A. Davankov, *Angew. Chem., Int. Ed. Engl.*, 21 (1982) 930.
9 A.A. Kurganov, A.B. Tevlin and V.A. Davankov, *J. Chromatogr.*, 261 (1983) 223.
10 P.E. Hare and E. Gil-Av, *Science*, 204 (1979) 1226.
11 E. Gil-Av, A. Tishbee and P.E. Hare, *J. Am. Chem. Soc.*, 102 (1980) 5115.
12 R. Wernicke, *J. Chromatogr. Sci.*, 23 (1985) 39.
13 S. Weinstein, M.H. Engel and P.E. Hare, *Anal. Biochem.*, 121 (1982) 370.
14 S. Weinstein, *Angew. Chem., Int. Ed. Engl.*, 21 (1982) 218.
15 V.A. Davankov and A.A. Kurganov, *Chromatographia*, 17 (1983) 686.
16 C. Gilon, R. Leshem, Y. Tapuhi and E. Grushka, *J. Am. Chem. Soc.*, 101 (1979) 7612.
17 C. Gilon, R. Leshem and E. Grushka, *Anal. Chem.*, 52 (1980) 1206.
18 C. Gilon, R. Leshem and E. Grushka, *J. Chromatogr.*, 203 (1981) 365.
19 E. Grushka, R. Leshem and C. Gilon, *J. Chromatogr.*, 255 (41) 1983.
20 N. Nimura, T. Suzuki, Y. Kasahara and T. Kinoshita, *Anal. Chem.*, 53 (1981) 1380.
21 N. Nimura, A. Toyama and T. Kinoshita, *J. Chromatogr.*, 234 (1982) 482.
22 N. Nimura, A. Toyama, Y. Kasahara and T. Kinoshita, *J. Chromatogr.*, 239 (1982) 671.
23 N. Nimura, A. Toyama and T. Kinoshita, *J. Chromatogr.*, 316 (1984) 547.
24 R. Marchelli, A. Dossena, G. Palla, M. Audhuy-Peaudecerf, S. Lefeuvre, P. Carnevali and M. Freddi, *J. Sci. Food Agric.*, 59 (1992) 217.
25 R. Marchelli, A. Dossena, G. Casnati, F. Dallavalle and S. Weinstein, *Angew. Chem., Int. Ed. Engl.*, 24 (1985) 336.

26 E. Armani, L. Barazzoni, A. Dossena and R. Marchelli, *J. Chromatogr.*, 441 (1988) 287.
27 E. Armani, A. Dossena, R. Marchelli and R. Virgili, *J. Chromatogr.*, 441 (1988) 275.
28 S. Weinstein and L. Leiserowitz, *Isr. J. Chem.*, 25 (1985) 334.
29 G. Galaverna, A. Dossena, R. Corradini and R. Marchelli, *Int. J. Pept. Protein Res.*, 42 (1993) 53.
30 F. Dallavalle, E. Fisicaro, R. Corradini and R. Marchelli, *Helv. Chim. Acta*, 72 (1989) 1479.
31 R. Corradini, G. Gasparri Fava, M. Belicchi Ferrari, A. Dossena, R. Marchelli and G. Pelosi, *Tetrahedron: Asymmetry*, 3 (1992) 387.
32 G. Gasparri Fava, M. Belicchi Ferrari, G. Pelosi, E. De Munari, R. Corradini, R. Marchelli and A. Dossena, *Acta Crystallogr., Sect. C*, 49 (1993) 1449.
33 J.R. McDermott and N.L. Benoiton, *Can. J. Chem.*, 51 (1973) 1915.
34 V. Pliska, M. Schmidt and J.L. Fauchère, *J. Chromatogr.*, 216 (1981) 79.
35 H. Sigel and R.B. Martin, *Chem. Rev.*, 82 (1982) 385.
36 A. Dossena, G. Galaverna, R. Corradini and R. Marchelli, *J. Chromatogr.*, 653 (1993) 229.
37 V.A. Davankov, A.A. Kurganov and T.M. Ponomareva, *J. Chromatogr.*, 452 (1988) 309.
38 J.N. Le Page, W. Lindner, G. Davies, D.E. Seitz and B.L. Karger, *J. Chromatogr.*, 185 (1979) 323.
39 V.A. Davankov, A.S. Bochkov, A.A. Kurganov, P. Roumeliotis and K.K. Unger, *Chromatographia*, 13 (1980) 677.
40 J. Debowski, D. Sybilska and J. Jurczak, *Chromatographia*, 16 (1982) 198.
41 C. Gilon, R. Leshem and E. Grushka, *J. Chromatogr.*, 203 (1981) 365.
42 F. Dallavalle, G. Folesani, R. Corradini, G. Galaverna and R. Marchelli, in preparation.
43 V.A. Davankov, V.R. Meyer and M. Rais, *Chirality*, 2 (1990) 208.
44 P. Van der Helm, M.B. Lawson and E.L. Enwall, *Acta Crystallogr., Sect. B*, 27 (1971) 2411.

Journal of Chromatography A, 657 (1993) 55–61
Elsevier Science Publishers B.V., Amsterdam

CHROM. 25 554

Single-step purification of a bacterially expressed antibody F_v fragment by immobilized metal affinity chromatography in the presence of betaine

Lars-Oliver Essen and Arne Skerra*

Max-Planck-Institut für Biophysik, Abt. Molekulare Membranbiologie, Heinrich-Hoffmann-Strasse 7, D-60528 Frankfurt/Main (Germany)

(First received June 1st, 1993; revised manuscript received August 30th, 1993)

ABSTRACT

A procedure was developed for the rapid isolation of an antibody F_v fragment expressed in *Escherichia coli* via immobilized metal affinity chromatography. Metal affinity was mediated by fusing hexahistidine tails to both the V_L and the V_H domain and was thus independent of the antigen-binding specificity. Unexpectedly, it was not possible to isolate the F_v fragment with correct stoichiometric composition of the two variable domains under standard chromatographic conditions. Proper non-covalent association of V_L and V_H was, however, maintained when using glycine betaine as electrolyte, thus permitting purification of the intact F_v fragment to homogeneity in a single step.

INTRODUCTION

Since the development of methods for the expression of functional F_v and F_{ab} fragments of antibodies in *Escherichia coli* [1–3] the bacterial production of recombinant immunoglobulin fragments has gained widespread application (for a review see ref. 4). Initially hapten or antigen affinity columns were used for the purification of functional antibody fragments from the periplasmic fraction, whole-cell extract or culture supernatant of *E. coli*. Recently, methods have been developed that permit the affinity purification of bacterially expressed Ig fragments independent of their antigen-binding properties [5,6]. These methods, which rely on C-terminally fused peptide sequences conferring specific affinity properties, are particularly advantageous in cases where antigens are too valuable, unstable or just unavailable for the preparation of affinity matrices.

A sequence of five or six consecutive histidine residues fused to a recombinant protein has been shown to enable specific purification of the polypeptide via immobilized metal affinity chromatography (IMAC) [7,8]. This approach was also successfully employed for the facile purification of an active single-chain F_v fragment produced in *E. coli* [5]. The Ig fragment retained its original antigen-binding properties so that the carboxy-terminal oligohistidine tag did not need to be removed. In contrast, attempts to purify an F_v fragment without a peptide linker connecting the two variable domains using the same strategy did not lead to immediate success, because of

* Corresponding author.

0021-9673/93/$06.00

chain dissociation. We demonstrate here that the non-covalent association of these two polypeptide chains, can, however, be sufficiently stabilized by use of a buffer system containing the osmolyte glycine betaine instead of commonly used inorganic salts, thus enabling IMAC purification of the intact F_v fragment from *E. coli* in a single step.

EXPERIMENTAL

Chemicals

Analytical grade chemicals were purchased from Merck (Darmstadt, Germany) chelating Sepharose fast flow was from Pharmacia (Freiburg, Germany), glycine betaine (monohydrate) and tetramethylammonium chloride from Fluka (Neu-Ulm, Germany), Coomassie brilliant blue R-250 from Serva (Heidelberg, Germany), ampicillin from Sigma (Deisenhofen, Germany) and isopropyl β-D-thiogalactopyranoside (IPTG) from Biomol (Hamburg, Germany).

Bacterial expression of the antibody F_v fragment

The expression plasmid pASK69-M29b was constructed from the vector pASK30 described previously [5] by standard DNA manipulations [9]. Unique restriction sites were introduced at the beginning and the end of the V_H and V_L genes in order to permit the cloning and expression of a variety of different variable domain genes, obtained, for example, by polymerase chain reaction [10]. pASK69-M29b was used for expression of the mutant variant "M29b" of the F_v fragment derived from the anti-lysozyme antibody HyHEL-10 [11]. The coding regions for the variable domains of this Ig fragment were obtained by gene synthesis, as will be described in detail elsewhere [12].

A 2-l culture of *Escherichia coli* strain JM83 [*ara*, Δ(*lac-pro*AB), *rps*L (=*str*A), φ80, *lac*ZΔM15] [13] transformed with the expression plasmid was grown at 22°C in Luria-Bertani (LB) medium [9] containing 100 μg/ml ampicillin. Expression was induced at an A_{550} value of *ca.* 0.5 by the addition of 0.5 m*M* IPTG (final concentration). After an induction period of 3 h the bacterial cells were harvested by centrifugation, resuspended in 20 ml of ice-cold 0.5 *M* NaCl, 50 m*M* sodium phosphate, pH 7.5, 1 m*M* EDTA and stirred for 30 min at 4°C. The spheroplasts were sedimented by centrifugation at 4400 *g* for 30 min at 4°C. The supernatant was recovered as the periplasmic cell fraction and cleared by centrifugation at 27 000 *g* for 15 min at 4°C.

IMAC

A Zn^{2+}/IDA (iminodiacetic acid) Sepharose matrix was prepared by charging a column packed with 2 ml (bed volume) of chelating Sepharose fast flow with 15 ml of 10 m*M* $ZnSO_4$ followed by washing with water. The column was equilibrated with one of the following chromatography buffers (all steps were carried out at 4°C): (i) 1 *M* NaCl, 40 m*M* sodium phosphate, pH 7.0; (ii) 0.5 *M* K_2SO_4, 50 m*M* sodium phosphate, pH 7.0; (iii) 0.5 *M* glycine betaine, 50 m*M* sodium phosphate, pH 7.0. The periplasmic cell fraction from a 2-l *E. coli* culture (*ca.* 20 ml, see above) dialysed against the same buffer was applied to the column, which was subsequently washed with approximately ten bed volumes of the chromatography buffer until absorption of the flow-through reached the baseline. Then bound protein was eluted with a linear gradient of 0 m*M* to 500 m*M* imidazole in the chromatography buffer (during this step the flow-rate was reduced from 20 ml/h to 10 ml/h).

Sodium dodecyl sulphate–polyacrylamide gel electrophoresis (SDS-PAGE)

SDS-PAGE of column fractions was performed using the discontinuous buffer system according to Fling and Gregerson [14] followed by staining with Coomassie brilliant blue. For quantitative determination of V_H/V_L ratios the gel lanes were scanned at 585 nm on a GS300 densitometer (Hoefer Scientific Instruments, San Francisco, CA, USA) connected to an IBM personal computer using analysis software from the same manufacturer.

RESULTS AND DISCUSSION

The experiments described were aimed at the purification of a genetically engineered F_v frag-

ment with a modified amino acid sequence [12] based on the primary structure of the antibody HyHEL-10 [11]. For bacterial production of the F_v fragment in a functional state the two variable domains, V_H and V_L, which are non-covalently associated, were co-secreted into the periplasm of the same *E. coli* cell. In this compartment disulphide bond formation, protein folding and chain association were shown to take place [1]. For this purpose a suitable expression vector, pASK69-M29b, was constructed (Fig. 1). On this plasmid, V_H and V_L were both fused at their N-termini to bacterial signal sequences directing transport across the inner cell membrane, and their structural genes were arranged in an artificial dicistronic operon in order to permit inducible coexpression.

For purification of the recombinant F_v fragment via IMAC, initially a single oligohistidine tail (five or six residues) was fused to the C-terminus of either V_H or V_L. Yet, in preliminary experiments the F_v fragment could not be isolated in either of these cases. Instead, only that variable domain bound to the Zn^{2+}/IDA Sepharose column which carried the C-terminal affinity tag (not shown) and was then individually eluted by the imidazole gradient under standard chromatographic conditions [5].

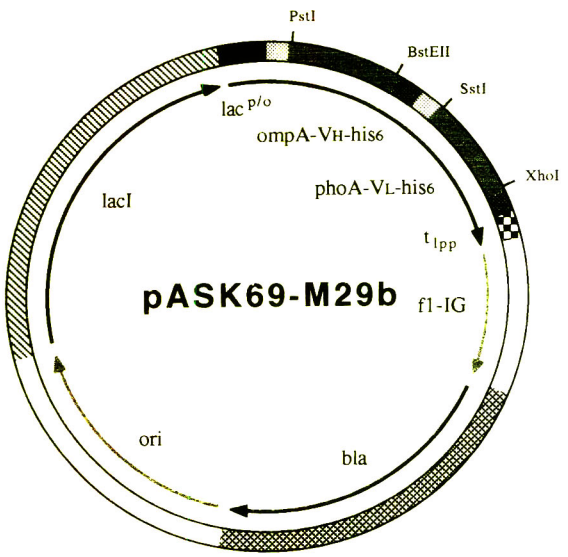

Fig. 1. Schematic drawing of the plasmid pASK69-M29b for the production of the antibody F_v fragment in *E. coli*. The variable domain genes V_H and V_L are bounded by singular restriction sites as indicated. They were both fused at their 5′ ends to nucleotide sequences encoding bacterial signal peptides from the outer membrane protein A (*ompA*) and from alkaline phosphatase (*phoA*), respectively, and at their 3′ ends to six consecutive histidine codons. The two structural genes were arranged in an artificial dicistronic operon under control of the IPTG-inducible *lac* promoter. *lpp*, f1-IG, *bla* and *ori* denote the strong lipoprotein transcription terminator, the intergenic region from the single-stranded bacteriophage f1, the β-lactamase gene for ampicillin resistance and the origin of replication, respectively.

Consequently it was sought to confer similar metal affinities on both polypeptide chains by adding hexahistidine tails to the C-termini of V_H as well as V_L. When the periplasmic cell fraction of *E. coli* cells harbouring the corresponding expression plasmid pASK69-M29b (see Fig. 1) was applied to a Zn^{2+}/IDA Sepharose column, the proteins that bound to the metal chelate matrix were eluted in two peaks by the imidazole gradient (Fig. 2a). The early peak at low imidazole concentrations contained host cell proteins with low affinity for immobilized metal ions (not shown), whereas the two variable domains of the F_v fragment were together specifically eluted in a single symmetric peak at higher eluent concentrations. Unexpectedly, however, an analysis of individual protein fractions by SDS-PAGE revealed a non-stoichiometric ratio for the two polypeptide chains with a large excess of V_L over V_H (Fig. 2b and c).

It was already known that immunoglobulin V_L domains can adopt soluble globular structures by homodimerization to form so-called Bence Jones proteins [15]. A V_L dimer has similar size and shape as an F_v fragment, i.e. the heterodimer of V_H and V_L. Thus, it had to be concluded that a mixture of the F_v fragment and its corresponding V_L dimer was isolated by the chromatographic procedure employed, and the question arose whether it was possible to separate these two protein species by the choice of appropriate buffer conditions.

IMAC of native proteins is generally performed in the presence of high-salt conditions in order to prevent non-specific binding to the charged groups of the affinity matrix via an ion-exchange effect. Ordinarily, NaCl is used for this purpose, but the use of K_2SO_4 has also been reported [16]. Yet, when the same chromatog-

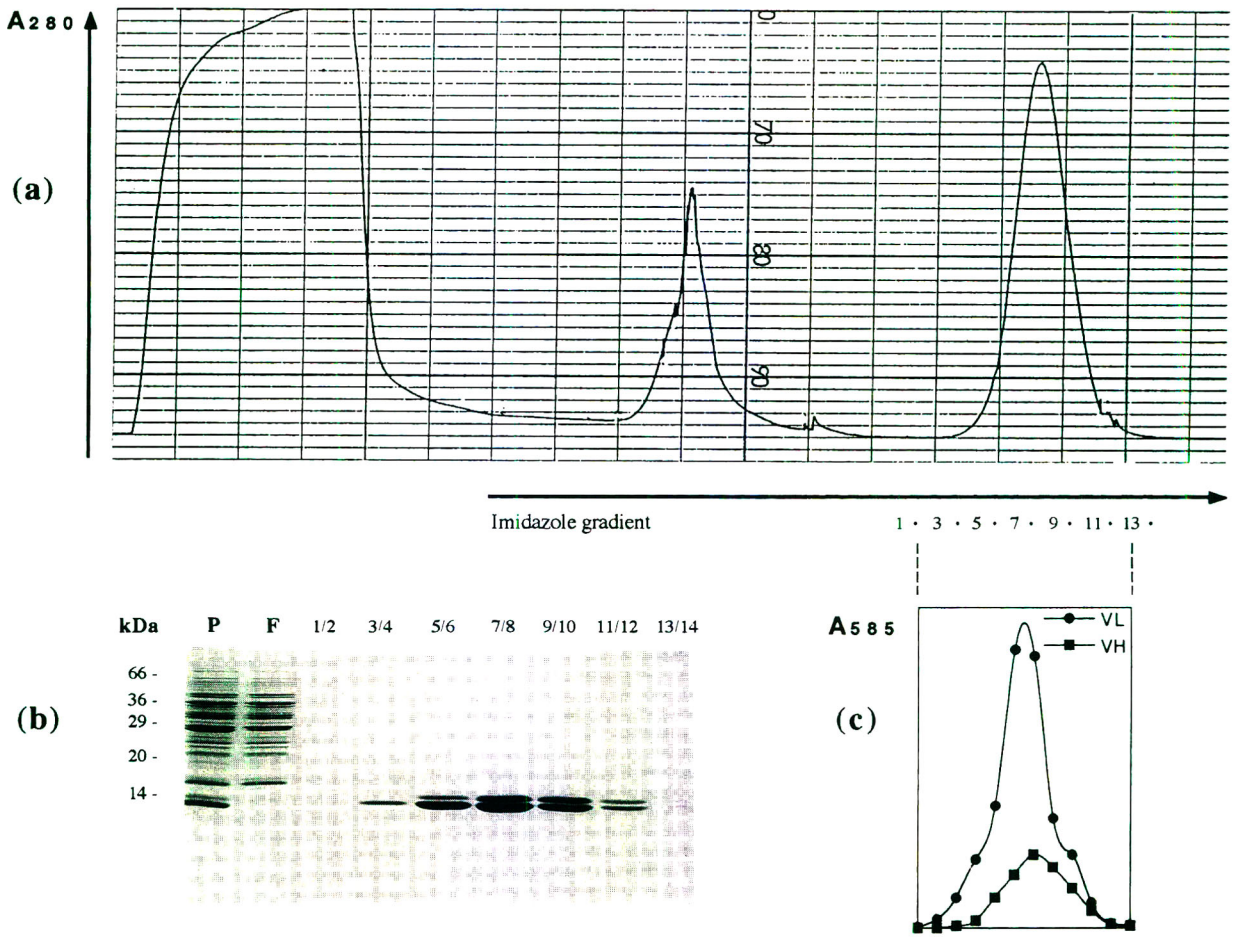

Fig. 2. IMAC in the presence of 1 *M* NaCl of the bacterial periplasmic cell fraction containing recombinant F_v fragment. (a) Elution profile monitored at 280 nm. (b) SDS-PAGE (18%) showing consecutive peak fractions (pooled in pairs) as indicated below (a). Lane P, periplasmic cell fraction; lane F, flow-through. Molecular masses are given to the left in kilodaltons (kDa). V_L corresponds to the lower and V_H to the upper of the two bands in the peak fractions. (c) Elution profiles of the variable domains V_H and V_L separately determined by scanning of peak fractions on an SDS-polyacrylamide gel (absorption in arbitrary units).

raphy experiment was carried out as before with 0.5 *M* K_2SO_4 as electrolyte instead of 1 *M* NaCl, again a single symmetrical elution peak was obtained (Fig. 3a) representing a non-stoichiometric mixture of V_L and V_H (Fig. 3b and c). This time, however, elution occurred at significantly higher imidazole concentrations, and it appeared unlikely that the F_v fragment and the V_L dimer displayed identical metal affinity properties in the presence of both inorganic salts.

Rather, we had to consider the possibility of a dynamic equilibrium between both species that was favoured by the high ionic strength conditions, effectively preventing their separation during chromatography. Thus, in the third experiment an electrolyte was chosen that did not just primarily have an effect on the ionic strength of the buffer but that also potentially contributed to the stabilization of the non-covalent association of the variable immunoglobulin domains. Recently, it has been reported that the osmolyte glycine betaine exerts a stabilizing effect on proteins against thermal denaturation [17]. Glycine betaine is a highly soluble zwitterionic compound that combines a negatively charged carboxylate group and a positively charged

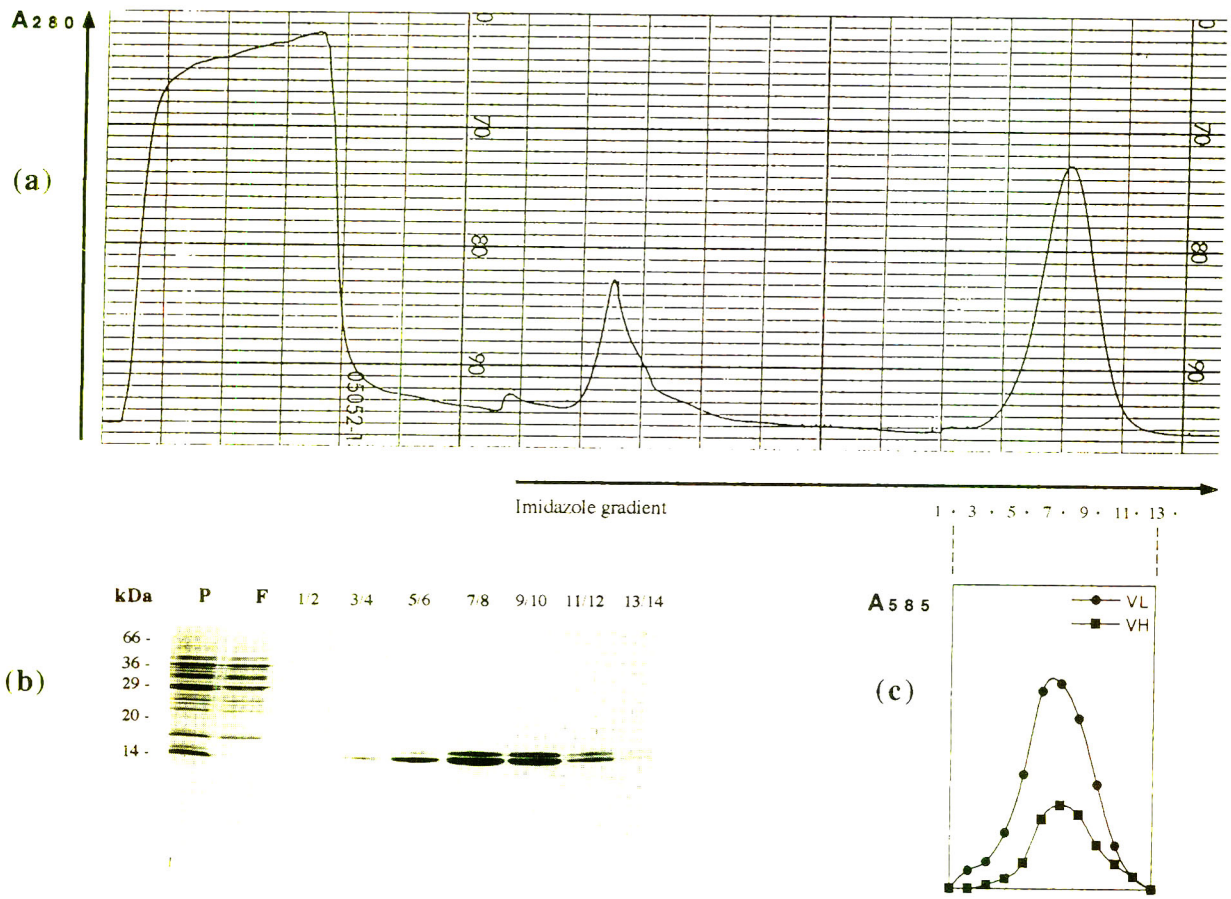

Fig. 3. IMAC in the presence of 0.5 *M* K_2SO_4 of the bacterial periplasmic cell fraction containing recombinant F_v fragment. (a), (b) and (c) as described for Fig. 2.

quaternary ammonium group in the same molecule and thus strongly contributes to the ionic strength of the solution. Since the nitrogen is permethylated in betaine it cannot act as a ligand for metal ions via a free electron pair and was thus not expected to interfere with metal complexation.

When IMAC was carried out in the presence of 0.5 *M* betaine a similar amount of protein bound to the column as before but, remarkably, the recombinant protein was eluted in two distinct peaks by the imidazole gradient under otherwise unchanged conditions (Fig. 4a). SDS-PAGE revealed that the second peak obtained corresponded to the pure F_v fragment with stoichiometric composition of V_H and V_L, whereas the first peak represented the excess amount of the V_L domain (Fig. 4b and c). Upon rechromatography, the isolated F_v fragment appeared to be homogeneous and stable (not shown). Thus, the use of betaine as electrolyte enabled the efficient purification of the intact F_v fragment from the periplasmic cell fraction of *E. coli* in a single step. In order to clarify the precise role of glycine betaine in the observed effect, another IMAC experiment was performed in the presence of 0.5 *M* tetramethylammonium chloride. As a result, exactly the same elution profile was obtained (not shown). Therefore, it has to be concluded that the stabilizing effect of betaine during IMAC is mainly due to the hydrophobic nature of the tetraalkylammonium ion.

Meanwhile, IMAC in the presence of betaine

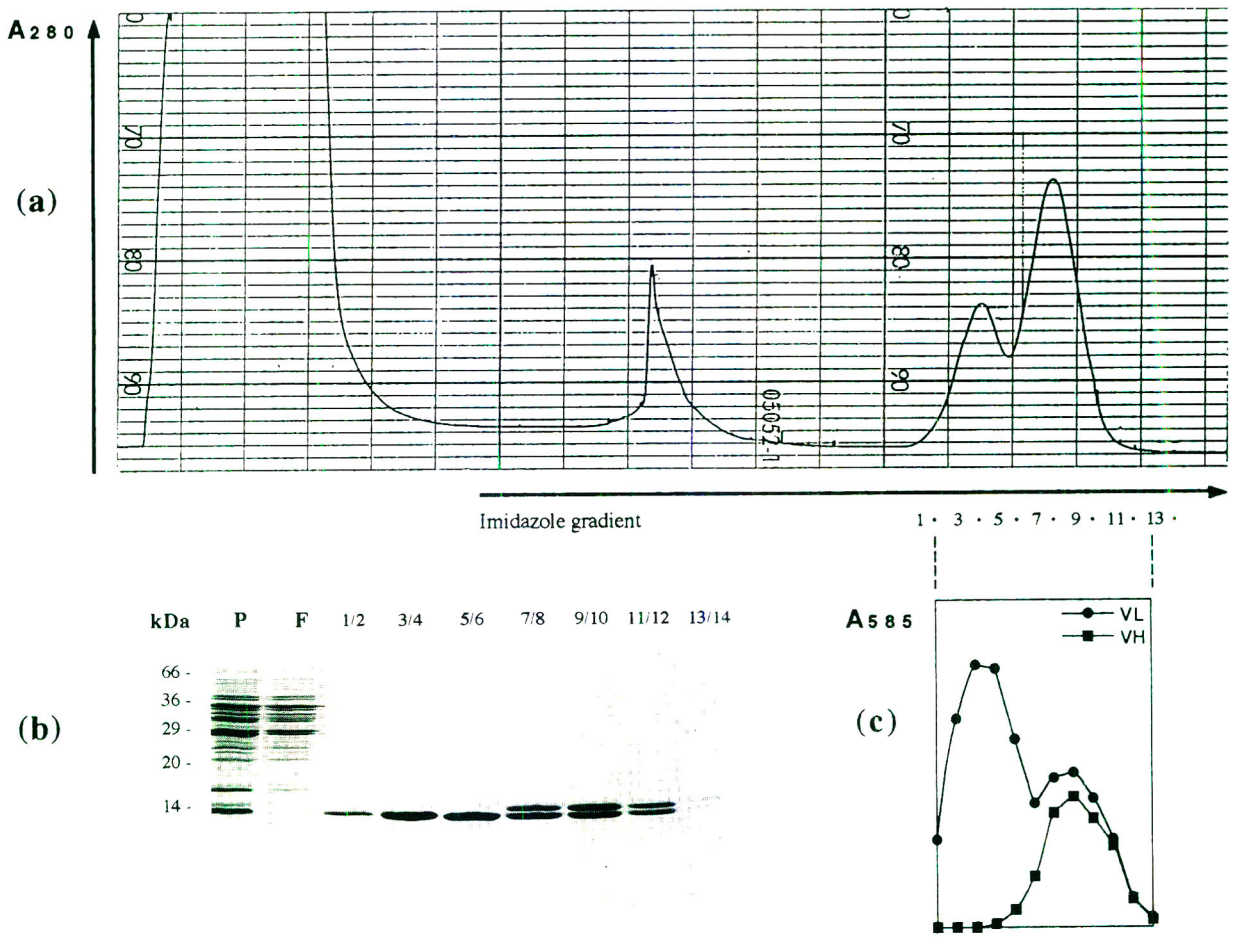

Fig. 4. IMAC in the presence of 0.5 *M* glycine betaine of the bacterial periplasmic cell fraction containing recombinant F_v fragment. (a), (b) and (c) as described for Fig. 2.

was used for the successful isolation of several different F_v fragments in our laboratory, indicating that the chromatographic conditions established here generally serve to stabilize the non-covalent association between the variable immunoglobulin domains. It should be noted that in the purification of a single-chain F_v fragment via IMAC described before [5] the variable domains were covalently connected by a flexible peptide linker so that no special care had to be taken to ensure the integrity of chain dimerization. Nevertheless, the purification of a functional and homogeneous antibody F_v fragment with proper chain stoichiometry had been possible before in a physiological buffer system by fusing a peptide conferring binding affinity towards immobilized streptavidin to the C-terminus of just one of the variable domains [6]. Thus, the dynamic behaviour observed here for the chain association of V_H and V_L could not be expected *a priori* and has to be attributed to the high ionic strength conditions employed for IMAC. The results presented clearly demonstrate the important role of the buffer conditions in the purification of an intact antibody F_v fragment, particularly if the antigen or hapten is absent. The stabilizing effect of betaine and related compounds may be of relevance not only for the isolation of this particular Ig fragment but also for the purification of protein complexes composed of several subunits via IMAC in general.

ACKNOWLEDGEMENTS

The authors wish to thank Christina Wardenberg for technical assistance, Professor Hartmut Michel for continuous encouragement and one of the referees for his critical comments. This work was supported by a grant from the Deutsche Forschungsgemeinschaft to A.S. and a predoctoral fellowship from the Fonds der Chemischen Industrie to L.-O.E.

REFERENCES

1 A. Skerra and A. Plückthun, *Science*, 240 (1988) 1038.
2 M. Better, C.P. Chang, R.R. Robinson and A.H. Horwitz, *Science*, 240 (1988) 1041.
3 A. Plückthun and A. Skerra, *Methods Enzymol.*, 178 (1989) 497.
4 A. Skerra, *Curr. Opin. Immunol.*, 5 (1993) 256.
5 A. Skerra, I. Pfitzinger and A. Plückthun, *Bio/Technology*, 9 (1991) 273.
6 T.G.M. Schmidt and A. Skerra, *Protein Eng.*, 6 (1993) 109.
7 E. Hochuli, H. Döbeli and A. Schacher, *J. Chromatogr.*, 411 (1987) 177.
8 E. Hochuli, W. Bannwarth, H. Döbeli, R. Gentz and D. Stüber, *Bio/Technology*, 6 (1988) 1321.
9 J. Sambrook, E.F. Fritsch and T. Maniatis, *Molecular Cloning: A Laboratory Manual*, Cold Spring Harbor Laboratory Press, Cold Spring Harbor, 1989.
10 R. Orlandi, D.H. Güssow, P.T. Jones and G. Winter, *Proc. Natl. Acad. Sci. U.S.A.*, 86 (1989) 3833.
11 E.A. Padlan, E.W. Silverton, S. Sheriff, G.H. Cohen, S.J. Smith-Gill and D.R. Davies, *Proc. Natl. Acad. Sci. U.S.A.*, 86 (1989) 5938.
12 L.-O. Essen and A. Skerra, in preparation.
13 C. Yanisch-Perron, J. Vieira and J. Messing, *Gene*, 33 (1985) 103.
14 S.P. Fling and D.S. Gregerson, *Anal. Biochem.*, 155 (1986) 83.
15 F.J. Stevens, A. Salomon and M. Schiffer, *Biochemistry*, 30 (1991) 6803.
16 T.-T. Yip, Y. Nakagawa and J. Porath, *Anal. Biochem.*, 183 (1989) 159.
17 M.M. Santoro, Y. Liu, S.M.A. Khan, L.-X. Hou and D.W. Bolen, *Biochemistry*, 31 (1992) 5278.

Journal of Chromatography A, 657 (1993) 63–68
Elsevier Science Publishers B.V., Amsterdam

CHROM. 25 523

Separation of novel polyol surfactants on polystyrene and octadecylsilyl bonded silica columns

Roger M. Smith* and J. Brian Deasy☆

Department of Chemistry, Loughborough University of Technology, Loughborough, Leics. LE11 3TU (UK)

(First received July 6th, 1993; revised manuscript received August 23rd, 1993)

ABSTRACT

The separation of a series of novel basic polyol surfactants, which exist as cations in aqueous solution, and their synthetic precursors have been compared using ion-suppression chromatography at pH 12 on a polystyrene–divinylbenzene column or ion-pair chromatography on an ODS column using hexanesulphonic acid as an ion-pair reagent. The latter method appeared to be the more versatile. Reversed-phase chromatography was also used for the separation of a related non-ionic diamide polyol surfactant.

INTRODUCTION

Surfactants play an important commercial role in many industries and their determination is important in quality control [1,2]. Many are ionised and contain either anionic sulphonic acid groups or cationic quaternary ammonium groups. The latter compounds are usually based on quaternary aliphatic amines, such as cetrimide (hexadecyltrimethyl ammonium bromide) or benzylalkyl ammonium compounds. Many of these products have caused concern as pollutants in water supplies and in recent years a number of biologically based surfactants [3] and carbohydrate- or polyol-based materials have been developed with greater biodegradability [4–6]. Many of these are industrial chemicals but polyol surfactants are now being developed for the biotechnology, biomedical and pharmaceutical fields. This has resulted in an increased interest in their purity and composition.

However, although a number of methods have been reported for anionic and non-ionic surfactants, so far there has been little work on the chromatographic analysis of cationic surfactants [1]. In most cases cation-exchange separation methods have been used but the absence of a chromophore in the quaternary alkyl ammonium compounds means that detection is a problem. Conductometric detectors [7,8], mass evaporative light-scattering detection [9] or post-column ion-pair extraction [10] have been used. In recent papers, capillary isotachophoresis [11] and capillary zone electrophoresis [12] of cationic surfactants have been described but detection was still a problem.

This paper compares ion-suppression and ion-pairing high-performance liquid chromatography (HPLC) for the determination of a series of recently developed basic polyol surfactants [4] (**I–V**), which are present as cations in aqueous solution, their synthetic precursor diepoxides (**VI–VII**) and the related non-ionic polyol amide surfactant [5] (**VIII**) (Fig. 1).

* Corresponding author.
☆ Present address: School of Chemical Sciences, Dublin City University, Dublin, Ireland.

0021-9673/93/$06.00

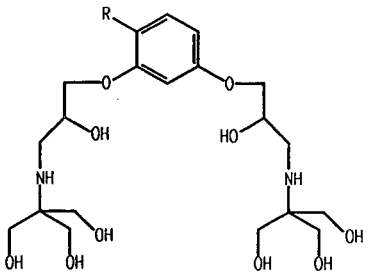

Hexahexaol (I) $R = C_6H_{13}$

Dodecylhexaol (II) $R = C_{12}H_{25}$

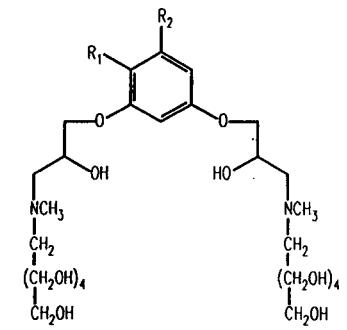

Hexyldecaol (III) $R_1 = C_6H_{13}$ $R_2 = H$

Dodecyldecaol (IV) $R_1 = C_{12}H_{25}$ $R_2 = H$

Pentadecyldecaol (V) $R_1 = H$ $R_2 = C_{15}H_{31}$

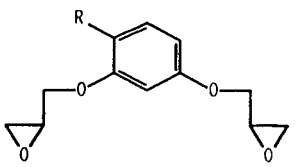

Hexyldiepoxide (VI) $R = C_6H_{13}$

Dodecyldiepoxide (VII) $R = C_{12}H_{25}$

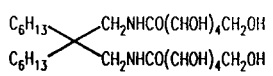

Dihexyldecaol amide (VIII)

Fig. 1. Structure of surfactants and related compounds.

EXPERIMENTAL

Chemicals and materials

The basic surfactants **I–V**, their precursors **VI** and **VII** and the non-ionic surfactant **VIII** were provided by Kodak Research Laboratory, Harrow, UK.

Methanol, acetonitrile and hexanesulphonic acids were of HPLC grade from Fisons Scientific, Loughborough, UK. Acetic acid, ammonium acetate and sodium hydroxide were of laboratory-reagent grade.

HPLC system

The liquid chromatograph consisted of a Waters M600A pump (Millipore, Milford, MA), a Shimadzu GTO-6A column oven (Kyoto, Japan) and a Philips PU4020 variable-wavelength detector (Cambridge, UK). The samples (10 μl) were injected using a Rheodyne 7125 valve (Cotati, CA, USA) fitted with a 20-μl loop onto either a PLRP-S polystyrene–divinylbenzene (PS–DVB) column (5 μm, 150 × 4.6 mm, Polymer Labs., Church Stretton, UK) or a 100 × 4.6 mm column packed with Hypersil 5 ODS (5 μm, Shandon

Scientific, Runcorn, UK). The eluent was degassed before use and was pumped at 1 ml min^{-1}. The peaks were recorded on a Hewlett-Packard 3390A integrator.

Separations using the PS–DVB column

The analytes were separated on the PS–DVB column at 45°C using acetonitrile–pH 12 aqueous sodium hydroxide solutions as the eluents and detection at 210 nm.

Separations using ion-pair reagents

The analytes were separated on the Hypersil ODS column at 35°C using acetonitrile–pH 4.5 buffer solutions containing 0.004 *M* 1-hexanesulphonic acid with detection at 210 nm. The pH 4.5 buffer solution contained ammonium acetate (3.13 g l^{-1}) and acetic acid (3 ml l^{-1}).

Separation of amide surfactants

The amide surfactant (**VIII**) was separated on the Hypersil ODS column at 35°C using acetonitrile–water (50:50) as the eluent and detection at 199 nm.

RESULTS AND DISCUSSION

The basic polyol surfactants (**I–V**, Fig. 1) studied in the present work have novel structures and contain both a prominent alkyl side chain and two secondary amino groups each substituted with a polyhydroxylated side chain. They had been synthesised from the corresponding alkyldiepoxides (*e.g.* **VI** and **VII**). The surfactants had a weak absorbance band at 280 nm but absorbed strongly at short wavelengths and 210 nm was selected as a suitable wavelength for detection.

The amino groups in these surfactants are strongly basic. In preliminary studies by HPLC on a reversed-phase column, it was found that they were protonated over the acceptable pH range (3–8) for ODS bonded silica-based column materials and were not retained even with a 100% aqueous eluent. Two approaches, ion-suppression chromatography at high pH on a polymeric column and ion-pair chromatography on an ODS-silica column, were therefore examined.

Separation using ion-suppression chromatography

When **IV** was examined on a PS–DVB column using acetonitrile–water (50:50) adjusted to pH 10.9 with ammonia as the mobile phase, it was found that the surfactant was retained but the peak shape was poor with considerable tailing. Increasing the basicity of the aqueous solution to pH 12 with 0.2 *M* sodium hydroxide gave a marked improvement in peak shape and reproducible retention times. Raising the column temperature to 45°C also improved the peak shape.

These conditions of acetonitrile–pH 12 sodium hydroxide solution (50:50) were then applied to the two dodecyl (**II** and **IV**) and the pentadecyl surfactants (**V**) and in each case the peak shapes were good. Surprisingly there was only a small difference between the retention times of **II** ($k' = 3.31$) and the more highly hydroxylated **IV** ($k' = 3.18$, Fig. 2a) and a mixture of the two compounds could not be resolved. Both were well separated from **V** ($k' = 9.71$). These results suggested that the retention was dominated by the interaction of the alkyl side chain with the PS–DVB column and that the hydroxyl groups played only a minor part. This would accord with previous studies, which have suggested that hydroxyl groups are strongly excluded from PS–DVB materials causing an enhancement of the

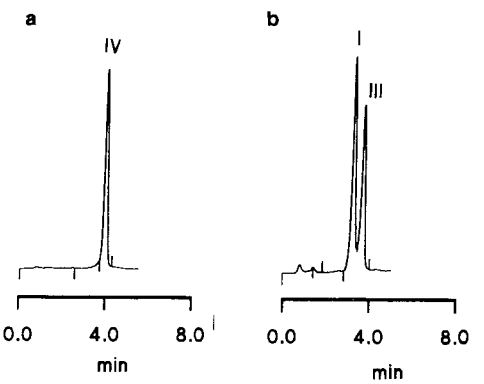

Fig. 2. Separation of the surfactants on a PS–DVB column using ion-suppression chromatography. Conditions: column, PLRP-S at 45°C; detection, 210 nm. (a) **IV**: eluent, acetonitrile–pH 12 sodium hydroxide solution (50:50). (b) **I** and **III**; eluent, acetonitrile–pH 12 sodium hydroxide solution (33:67).

differences between polar and non-polar analytes [13]. However, with these eluents the surfactants with a hexyl side chain (**I** and **III**) were eluted very close to the solvent front.

On increasing the proportion of the aqueous component of the eluent to give acetonitrile–pH 12 sodium hydroxide solution (33:76), these smaller compounds were retained but the order of elution of **I** ($k' = 2.53$) and **III** ($k' = 3.07$) surfactants (Fig. 2b) was unexpected as the latter with more hydroxyl groups was expected to be the more polar and thus to be eluted more rapidly.

A calibration curve was prepared for each of the analytes in the corresponding eluent for a reasonable retention. In each case a linear response was obtained over the concentration ranges 1 to 0.1 mg ml^{-1} with a correlation between 0.9993 and 0.9984 (Table I). However, the calibration curves did not go through the origin suggesting that a small but systematic loss was occurring, up to a maximum of 0.065 mg ml^{-1} for **IV**, although the reason for this could not be determined. The limits of detection corresponded to about 100–300 ng which is similar to the levels reported for other aromatic surfactants [14].

TABLE I

SEPARATION OF THE SURFACTANTS USING ION-SUPPRESSION AND ION-PAIR MODES

Ion-suppression mode conditions: column, PLRP-S; eluent, acetonitrile–pH 12 sodium hydroxide solution; detection, 210 nm. Ion-pair mode conditions: column, Hypersil 5 ODS; eluent, acetonitrile–pH 4.5 ammonium acetate buffer containing 0.004 *M* hexanesulphonic acid; detection, 210 nm. Correlations of calibration curve for solutions of surfactant over the range 0.1 to 1.0 mg ml^{-1}.

Compound	Modifier (%)	k'	Correlation
Ion-suppression mode			
I	33	2.53	0.9989
III	33	3.07	0.9984
II	50	3.31	0.9992
IV	50	3.18	0.9985
V	50	9.71	0.9993
Ion-pair mode			
I	30	4.43	0.9995
III	30	2.42	0.9996
II	50	8.11	0.9992
IV	50	3.62	0.9995
V	70	4.03	0.9945

In order to examine the purity of the surfactants it was also necessary to be able to determine their synthetic alkyldiepoxide precursors. These are relatively much less polar compounds and were highly retained under the conditions used for the corresponding surfactants. It was therefore necessary to employ much higher proportions of acetonitrile to obtain reasonable retentions. The hexyldiepoxide (**VI**) could be eluted with acetonitrile–pH 12 solution (75:25) ($k' = 7.65$) but the corresponding hexyl surfactants were very rapidly eluted (**I**, $k' = 0.60$; **III**, $k' = 0.75$) under these conditions. For **VII**, a stronger eluent acetonitrile–pH 12 solution (90:10) was required ($k' = 11.61$) and the dodecyl surfactants were rapidly eluted (**II**, k' 1.5 and **IV**, $k' = 1.1$). In both eluents it was not practical to quantify the starting materials and surfactants in a single isocratic run because the latter were eluted close to the major solvent disturbance caused by the aqueous solvent used to dissolve the sample.

Separation using ion-pair reagent

Although the PS–DVB column would give a good separation of the surfactants and their starting materials, the differences in their polarities meant that separate assay conditions would be needed. It was therefore decided to examine the potential of ion-pair separations, which might enable both products and starting materials to be assayed in a single determination.

Surfactants **II** and **IV** were chromatographed using an ODS-silica column with acetonitrile–pH 4.5 ammonium acetate buffer (50:50) containing 0.004 *M* hexanesulphonic acid. Unlike the ion-suppression separation **IV** ($k' = 3.62$) was eluted much more readily than **II** ($k' = 8.11$). The pentadecyldecaol (**V**) required a stronger eluent of acetonitrile–buffer (70:30) containing 0.004 *M* hexanesulphonic acid for elution ($k' = 4.03$).

By using a weaker eluent, acetonitrile–buffer (30:70) containing 0.004 *M* hexanesulphonic acid, the hexyl surfactants could be retained and again the decaol (**III**, $k' = 2.42$) was eluted more

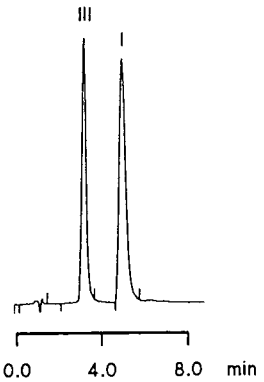

Fig. 3. Separation of hexyl surfactants **I** and **III** using an ion-pair reagent. Conditions: column, Hypersil 5 ODS; temperature, 35°C; eluent, acetonitrile–pH 4.5 ammonium acetate buffer (30:70) containing 0.004 *M* hexanesulphonic acid; detection, 210 nm.

rapidly than the hexaol (**I**, $k' = 4.43$) (Fig. 3). Thus under the ion-pairing conditions the analytes were behaving as expected with the more highly hydroxylated analytes being the more rapidly eluted in each case. For each surfactant a calibration curve showed a linear correlation (r = 0.9995–9945) over the concentration range 1 to 0.1 mg ml^{-1} and a limit of detection of 20–30 ng.

Acetonitrile–buffer (70:30) containing 0.004 *M* hexanesulphonic acid was needed to elute the hexyldiepoxide starting material (**VI**, $k' = 3.71$) but under these conditions the two hexyl surfactants were rapidly eluted with capacity factors of less then 0.5. For the dodecyldiepoxide a stronger eluent of acetonitrile–buffer (80:20) containing 0.004 *M* hexanesulphonic acid was required (**VII**, $k' = 12.12$). Examination of a deliberately impure sample of **IV** showed the product at $k' = 0.9$ and an impurity peak at $k' = 3.13$. When the purified surfactant product was examined this peak was absent but a trace of starting material was present. Thus it appears that ion-pairing separation conditions are better then the ion-suppression technique for the determination of impurities in these products. However, there were still significant differences between the retentions of the starting materials and the ion-paired products. The use of ion-pairing reagents with a longer alkyl side chain or in higher concentrations might give more comparable retentions if these were required.

Methanol–buffer eluents containing the ion-pair reagent were also examined for the chromatography of the surfactants. However, although by using methanol–buffer (65:35) containing 0.004 *M* hexanesulphonic acid the two hexyl polyols were retained, they were unresolved (**I**, $k' = 1.74$ and **III**, $k' = 1.95$) and the two dodecyl surfactants were unresolved in methanol–buffer (85:15) containing 0.004 *M* hexanesulphonic acid (**II**, $k' = 3.00$; **IV**, $k' = 2.94$). The peaks were also not as symmetrical as in the acetonitrile eluents.

Amide surfactants

The related aliphatic amide polyol surfactant (**VIII**) was also examined. Because of its limited chromophore, detection at 199 nm was employed. Using an eluent of acetonitrile–water (40:60) a good retention was obtained on the Hypersil 5 ODS column ($k' = 2.18$) with a symmetrical peak shape. A quantitative determination found a limit of detection of 260 ng. This is poorer than for the earlier surfactants because of the weaker chromophore.

CONCLUSIONS

Alternative methods could be employed for the chromatography of these surfactants. The choice will depend of the levels of detection required, the reason for the analysis and whether it is necessary to resolve the homologues.

ACKNOWLEDGEMENT

The authors thank Polymer Laboratories for a column.

REFERENCES

1 T.M. Schmitt, *Analysis of Surfactants*, Marcel Dekker, New York, 1992.
2 J. Cross, *Nonionic Surfactants: Chemical Analysis*, Marcel Dekker, New York, 1987.
3 N. Kosaric (Editor), *Biosurfactants*, Marcel Dekker, New York, 1993.
4 I.M. Newington and A.R. Pitt, PCT *Pat. Appl.*, PCT/EP90/00606.
5 L.B.A. Brigg and A.R. Pitt, *US Pat.*, 4 892 806 (Jan. 1990).

6 R. Garelli-Calvet, F. Brisset, I. Rico and A. Lattas, *Syn. Commun.*, 23 (1993) 35.
7 V.T. Wee and J.M. Kennedy, *Anal. Chem*, 54 (1982) 1631.
8 L. Nitschke, R. Muller, G. Metzner and L. Huber, *Fresenius' J. Anal. Chem.*, 342 (1992) 711.
9 A.J. Wilkes, G. Walraven and J.M. Talbot, *J. Am. Oil Chem. Soc.*, 69 (1992) 609.
10 J. Kwase, T. Takao and K. Tsuji, *J. Chromatogr.*, 262 (1983) 293.
11 C. Tribet, R. Gaboriaud and P. Gareil, *J. Chromatogr.*, 609 (1992) 381.
12 C.S. Weiss, J, S. Hazlett, M.H. Dalta and M.H. Danzo, *J. Chromatogr.*, 608 (1992) 325.
13 R.M. Smith, *J. Chromatogr.*, 291 (1984) 372.
14 A. Marcomini and W. Giger, *Anal. Chem.*, 59 (1987) 1709.

Journal of Chromatography A, 657 (1993) 69–76
Elsevier Science Publishers B.V., Amsterdam

CHROM. 25 471

Chromatographic separations of metal chelates present in commercial fertilizers

I. Development of a gel permeation chromatographic separation method for the identification of metal chelates in commercial fertilizers

Marian Deacon and Malcolm R. Smyth*

School of Chemical Sciences, Dublin City University, Dublin 9 (Ireland)

Louis G.M.Th. Tuinstra

State Institute for Quality Control of Agricultural Produce, Postbus 230, 6700 AE Wageningen (Netherlands)

(First received June 28th, 1993; revised manuscript received July 30th, 1993)

ABSTRACT

The separation of iron(III) chelates of ethylenediaminetetraacetic acid (EDTA), diethylenetriaminepentaacetic acid (DTPA), hydroxy-2-ethylenediaminetriacetic acid (HEEDTA), ethylenediaminedi(*o*-hydroxyphenyl)acetic acid (EDDHA) and ethylenediaminedi(*o*-hydroxy-*p*-methylphenyl)acetic acid (EDDHMA) and the Cu(II), Zn(II) and Mn(II) chelates of EDTA by gel permeation chromatography on Bio-Gel P2 and Fractogel HW-40(S) was investigated. The chelates FeDTPA, FeHEEDTA, FeEDDHA and FeEDDHMA were separated on a 35 × 1 cm I.D. Fractogel column using 0.05 *M* NaCl–0.005 *M* KH_2PO_4 (pH 8.0) with a total analysis time of 3 h. FeEDTA was not completely resolved from FeDTPA, and FeHEEDTA, CuEDTA, ZnEDTA and MnEDTA were found to co-elute with FeDTPA. The method is applicable to the qualitative analysis of fertilizers containing a single trace element in combination with a single chelating agent. Positive identification of a chelate is achieved by comparison of retention time data and identification of the metal present by atomic absorption spectrometry or inductively coupled plasma mass spectrometry. Quantification can be achieved by comparison of peak height or area with that of standards.

INTRODUCTION

Synthetic chelates are added to commercial fertilizers for the supply of micronutrients to plants. These fertilizers have two main areas of application, *viz.*, hydroponics (the growth of plants in water culture) and the correction of micronutrient deficiencies in soils. The availability of micronutrients to a plant is largely dependent on their solubility at the pH of the soil/hydroponic solution. A pH range of 4–10 is found in hydroponic solutions, whereas soil, in which micronutrient deficiencies are found, is usually alkaline. The chelates supply micronutrients in a soluble form which is accessible to the plant. The chelate form in which the micronutrient is present in the fertilizer will depend on the conditions of use, *e.g.*, pH of the growing media, the stability of the chelate and the cost of

* Corresponding author.

0021-9673/93/$06.00

the chelating agent. The elements most commonly added to fertilizers are iron, copper, zinc and manganese. The 76/116/EC Directive of the European Communities has recommended the use of the chelating agents listed in Table I. These fertilisers may be manufactured in solid or liquid form. This Directive dictates that there are two categories of fertilizer which may be marketed: fertilizers containing only one of the trace elements listed, and those containing at least two different trace elements. To evaluate the trace element content of the fertilizer, the Directive recommends that the total content in respect of each nutrient, the water-soluble content, the chelated form in which the trace element is present and the amount of the trace element which is chelated must be determined. Where a trace element is present in a chelated form, the pH range guaranteeing acceptable stability of the chelated fraction must be stated.

Currently, four methods of analysis have been developed and considered at EC level for the quality control of trace elements in fertilizers. Method 1 details a gel permeation technique and is based on a method developed by Boxma [1]. This method, however, cannot distinguish the chelating agents present and has a very long analysis time. Method 2 identifies the chelating agents present using TLC. Although the amount of chelated metal can be determined using this method, it does not quantify each chelating agent present, and the method may contain metal chelated by any negatively charged chelating agent. Method 3 only applies to the analysis of iron chelates. The method does not identify or determine the chelating agents present. Method 4 identifies the chelating agent present by TLC and determines the amount of chelating agent. The method can only be used, however, when one chelating agent is present, and the quantitative method used cannot distinguish between the different chelating agents.

TABLE I

CHELATING AGENTS RECOMMENDED BY DIRECTIVE 76/116/EC OF THE EUROPEAN COMMUNITIES

Chelating agent	Abbreviation
Ethylenediaminetetraacetic acid	EDTA
Diethylenetriaminepentaacetic acid	DTPA
Hydroxy-2-ethylenediaminetriacetic acid	HEEDTA
Ethylenediaminedi(*o*-hydroxyphenyl) acetic acid	EDDHA
Ethylenediaminedi(*o*-hydroxy-*p*-methyl phenyl)acetic acid	EDDHMA

In this work, the capabilities of gel permeation chromatography (GPC) for the identification and determination of the iron(III) chelates of EDTA, DTPA, HEEDTA, EDDHA and EDDHMA and the Cu(II), Zn(II) and Mn(II) chelates of EDTA was investigated, as these are the chelates most commonly found in commercial fertilizers. As GPC is generally associated with biological applications, very little investigation into its use as a method for the determination of chelates has been carried out. However, GPC provides an alternative mechanism of separation, *i.e.*, separation on the basis of size. Yoza *et al.* [2] showed that a mixture of Mg(II) and Mg(II)–EDTA could be separated on Sephadex G-15 when eluted with sodium chloride solution. Deguchi [3] studied the behaviour of Co(II)–, Ni(II)–, Cu(II)–, Cr(III)–, Fe(III)–Co(III)– and Bi(III)–EDTA on Sephadex columns. It was found that the complexes with an oxidation state of two were separated from those with an oxidation state of three on a Sephadex G-15 column when eluting with sodium chloride. The separation of free and complexed metal developed by Boxma [1], which is the basis of method 1, is currently used for the evaluation of the chelated fraction of metal in fertilizers in the Netherlands. In this method, however, FeDTA co-elutes with FeDTPA and FeEDDHA co-elutes with FeEDDHMA, making it impossible to analyse a mixture of these chelates. Also, FeEDDHA and FeEDDHMA have a very long retention time of 4 h. The present investigation set out to improve both the selectivity of this method and to reduce the time required for separation.

EXPERIMENTAL

Chemicals and Reagents

Deionized water was obtained by passing distilled water through a Waters Milli-Q water-

purification system. Sodium hydroxide solution (40%) was obtained from BDH. Potassium dihydrogenphosphate was obtained from Merck. Sodium chloride was of analytical-reagent grade. FeEDTA was obtained from Koch-Light, FeDTPA from Aldrich, and FeHEEDTA, FeEDDHA and FeEDDHMA from the Instituut voor Bodemvruchtbaarheid (Haren, Netherlands). All standards and samples for analysis were made up in the mobile phase and filtered with a 0.45-μm filter prior to analysis.

Apparatus

A Waters M45 pump, a Waters solvent-select valve and a Gilson Model 231 injector with a 20-μl injection loop were used in conjunction with a Merck–Hitachi L-4000 UV detector was used. The system was interfaced to a Nelson Analytical 900 series interface. Data were processed using a Nelson Analytical 3000 Series chromatography data system. A Corning 450 × 10 mm I.D. adjustable column casing was used. Fractogel TSK HW-40(S) was obtained from Merck and Bio-Gel P2 from Bio-Rad.

Methods

Pretreatment of sample. A sample mass approximately equivalent to 3 mg of the metal present in the chelate is taken. The mass of the sample in grams is estimated from $1/(U/0.3)$, where U is an estimate of the percentage of chelated metal in the sample. The sample is dissolved in approximately 20 ml of deionized water and placed in an ultrasonic bath for 30 min. The solution is diluted to 25 ml in a volumetric flask and filtered with a 0.45-μm filter.

Analysis of sample. A 20-μl volume of the pretreated sample is injected onto a Fractogel column (35 × 1 cm I.D.) in a mobile phase consisting of 0.05 *M* NaCl–0.005 *M* KH_2PO_4 (pH 8) at a flow-rate of 0.5 ml/min. The chromatogram is recorded by measuring the absorbance at 210 nm. The chelate fraction is collected, 1 ml of 5 *M* HCl is added and the sample is diluted to 10 ml with the mobile phase. Analysis of the fraction by atomic absorption spectrometry (AAS) or inductively coupled plasma mass spectrometry (ICP-MS) leads to identification of the metal present. This information, in combination with the retention time of the fraction, may be used to identify the chelate present. Quantification can be achieved by comparison of peak height or area with that of standards.

RESULTS AND DISCUSSION

General considerations

The bioavailability of a nutrient (*i.e.*, the percentage of it that is complexed and thus in soluble form and available to the plant) is dependent on the growing media conditions, *e.g.*, the soil solution pH and the presence of other metal ions and ligands. The analytical method used to evaluate the fertilizer must reflect this. Therefore, while the content of the fertilizer as manufactured is of some practical value in terms of quality control, it must be appreciated that this content must not be used as the absolute "nutrient value" of the fertilizer. A more correct evaluation of the value of the fertilizer in the field would involve both the identification and determination of the chelating agents and the trace elements present. Using this information, together with studies of the behaviour of metal chelates in soil as described, for instance, by Linsay *et al.* [4], the composition of the fertilizer under changing conditions of usage may be predicted. To this end the identification and determination of the chelating agent content of fertilizers should be investigated in addition to the specific chelate composition of the fertilizer as stated by the manufacturer.

The effect of the analytical method on the equilibrium condition of a metal chelate must also be considered. The analytical method imposes its own demands with regard to pH, buffer and solvent conditions on the metal chelate. Within this environment the metal chelate will further equilibrate. For a solid fertilizer, which contains a single trace element in the presence of a single chelating agent, this effect may be accounted for by the use of standards. A standard of FeEDTA of 95% purity, for example, may dissociate on equilibration in the analytical system, such that 80% of the metal remains chelated. The detector response achieved, how-

ever, may be taken as that corresponding to a sample of 95% purity as manufactured. This example illustrates how previous methods, in which an analytical system was used to isolate a chelate, followed by analysis of the fraction for metal content, did not reflect the true chelate content of the sample, but rather the chelate content under the conditions of analysis. However, where a fertilizer contains a mixture of trace elements and chelating agents, the competing reactions of the metal ions and ligands must be considered. Again the mixture of metal ions and chelating agents will achieve an equilibrium dependent upon the conditions employed in the analytical method. However, the analytical conditions not only have an influence on the extent of association/dissociation of the chelate but also on the extent of replacement reactions of metal chelates. Thus, a chelate which is very stable in an alkaline environment, such as FeEDDHA, if analysed at an acidic pH where, owing to the high pK_a values of the free acid the conditional stability constant relative to that of FeEDTA will be considerably less than at pH 11, the iron may be replaced to some extent by EDTA, thus decreasing the FeEDDHA concentration. Hence an incorrect evaluation of the fertilizer will be obtained should this fertilizer be used under alkaline conditions. Another example is the analysis of a mixture of FeEDTA and ZnEDTA. The results of such an analysis will differ if the analysis is carried out at pH 6 or 8, owing to the change in conditional constants as the stability of ZnEDTA increases from pH 6 to 8 whereas that of FeEDTA decreases. Therefore, the analysis of a mixture of metal ions and chelating agents is impossible using a chromatographic method of fixed pH, as the analysis will reflect the equilibrium achieved by the metals under the conditions of analysis and not the composition as manufactured or the composition under the conditions of usage. This paper therefore details the development of a method for the determination of the chelate content of a fertilizer containing one chelating agent in combination with one trace element.

Hydroponic, ionic and structural interactions all play a part in the behaviour observed by Boxma [1] and Deguchi [3]. If the Boxma separation is studied in detail, it is evident that it does not exhibit gel permeation behaviour, *i.e.*, separation on the basis of size. It can be seen that, contrary to GPC where the larger components of a sample have a shorter elution time than the smaller components, in the Boxma separation the smaller chelates FeEDTA and FeDTPA elute before the larger chelates FeEDDHA and FeEDDHMA. There is evidence that FeEDTA and FeDTPA are excluded from the gel owing to the presence of a small number of carboxylic acid groups in the gel matrix. These repel anions from the gel phase when they are applied to the gel in small amounts and eluted with ion-free water. This effect can be removed for inorganic anions by the addition of other electrolytes to the eluent [5]. This is possibly why Boxma and Deguchi both used calcium chloride and sodium chloride. However, this behaviour, or the investigation of it, was not mentioned in either paper. Therefore, this behaviour was investigated in a gel other than Sephadex to see if this phenomenon can be used to help achieve a separation.

The long retention times of FeEDDHA and FeEDDHMA are possibly due to the interaction of their aromatic groups with the Sephadex matrix. This behaviour on Sephadex has been reported in the chromatography of compounds containing aromatic functionalities [6]. Williams [7] has suggested that this is due to the involvement of the electron system of the solute with the other oxygens in the glyceryl bridge of the Sephadex. This effect increases as expected as the pore size of the gel decreases. However, for the smallest pore sizes of Sephadex G-10 and G-15, the retention of aromatics increases dramatically, and cannot be explained alone by interaction of the electron system. Determann and Walters [6] have suggested that the added increase in retention was due to structural considerations. However, they were not able to observe this very large increase for the Bio-Gels. In this study, therefore, Bio-Gel P2 was investigated. Fractogel HW-40(S) was also investigated, as it is a small-pore, very rigid gel that can be used at a relatively high linear flow-rate in GPC.

Separation on Bio-Gel P2

Fig. 1 shows the influence of NaCl concen-

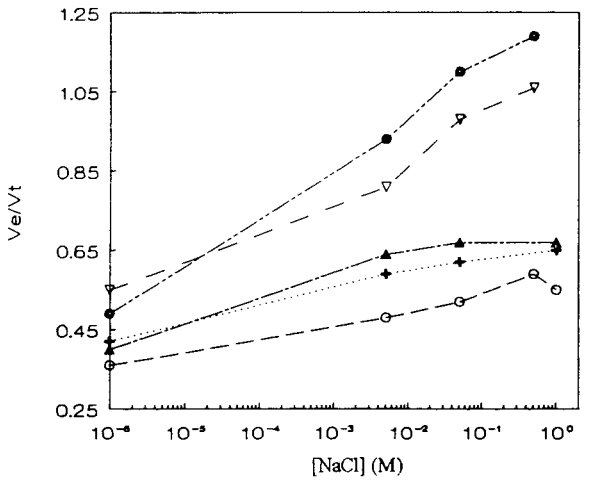

Fig. 1. Influence of sodium chloride concentration on the retention of iron(III) chelates on Bio-Gel P2. Column, 35 × 1 cm. I.D.; flow-rate, 0.25 ml/min; mobile phase sodium chloride solution (pH 7.0). ○ = FeDTPA; + = FeHEEDTA; ▲ = FeEDTA; ● = FeEDDHA; ▽ = FeEDDHMA.

tration on the retention of the chelates on Bio-Gel P2 with an aqueous mobile phase at pH 7 (adjusted with NaOH) at a flow-rate of 0.25 ml/min. The plot of V_e/V_t (elution volume/total common volume) gives a measure of retention independent of column dimension or flow-rate. It can be seen that as the NaCl concentration is increased, the retention of the chelates increased dramatically. This indicates that ionic interactions between the chelates and negatively charged groups in the gel are being overcome and therefore the anions are not being repelled from the column to the same extent. As with the Boxma method, the iron chelates of EDDHA and EDDHMA elute with longer retention times than the chelates of EDTA, DTPA and HEEDTA. However, the retention times of FeEDDHA and FeEDDHMA are significantly shorter than those obtained by us using the Boxma method employing Sephadex G-10 (Table II). The increase in the retention time of both EDDHA and EDDHMA chelates with increased sodium chloride concentration is much more dramatic than that for the EDTA, DTPA and HEEDTA chelates. This is possibly due to the fact that as ionic interactions are overcome, hydrophobic interactions increase and EDDHA and EDDHMA will have a much greater hydrophobic interaction owing to their respective aromatic groups.

TABLE II

COMPARISON OF V_e/V_t VALUES OF IRON(III) CHELATES ON VARIOUS GELS

Chelate	Sephadex	Bio-Gel	Fractogel
FeEDTA	0.44	0.67	0.46
FeDTPA	0.44	0.52	0.40
FeHEEDTA	ND[a]	0.62	0.48
FeEDDHA	1.66	1.1	1.77
FeEDDHMA	1.99	0.98	2.93

[a] ND = Not determined.

There was very little change in retention time once the NaCl concentration had increased above 0.05 M, and therefore it can be concluded that this is the optimum NaCl concentration for separation as there is no further decrease in ionic repulsion with increased NaCl concentration. FeEDTA and FeDTPA are well resolved using this system. FeDTPA and FeHEEDTA have a resolution factor (R_s) of 1.38. FeHEEDTA and FeEDTA are not resolved, having an R_s value of 0.52. FeEDDHA and FeEDDHMA have an R_s value of 0.8.

Separation on Fractogel HW-40(S)

The chelates behaved similarly on Fractogel, the retention time increasing as the sodium chloride concentration was increased (Fig. 2).

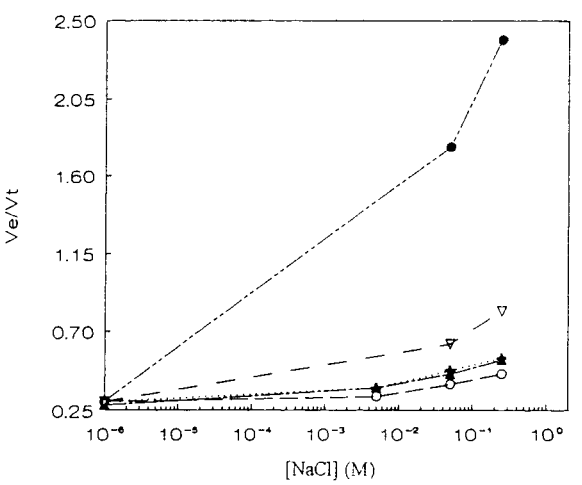

Fig. 2. Influence of sodium chloride concentration on the retention of chelates on Fractogel TSK HW-40(S). Column, 35 × 1 cm I.D.; flow-rate, 0.5 ml/min; mobile phase, sodium chloride solution (pH 7.0). Symbols as in Fig. 1.

The separation increases up to a salt concentration of 0.05 M. A further increase in salt concentration did not bring any improvement in resolution but only caused an increase in retention time; therefore, the optimum salt concentration for separation was found to be 0.05 *M*. Under these conditions, FeDTPA and FeEDTA are resolved, having an R_s value of 2.0. FeEDDHA and FeEDDHMA are also resolved, having an R_s value of 2.1. However, as with Bio-Gel, FeEDTA and FeHEEDTA are not resolved, having an R_s value of 0.3. A comparison of the retentions of the chelates on Fractogel, Bio-Gel and Sephadex is shown in Table II, from which it can be concluded that the behaviour of the chelates on the Fractogel follows more closely that of the Sephadex. The chelates FeEDDHA and FeEDDHMA have a long retention time on Fractogel, suggesting a steric interaction with the gel due to the aromatic functionalities of these chelates, as with Sephadex [6]. However, this interaction is helping to achieve greater resolution than on the Bio-Gel. Owing to the better resolution of FeEDDHA and FeEDDHMA with Fractogel HW-40(S), and the greater rigidity of the gel, which enables higher flow-rates to be employed than with the Bio-Gel, thus decreasing the analysis time, the Fractogel was chosen instead of the Bio-Gel for further study.

As FeEDDHA and FeEDDHMA were well resolved, the improvement of the separation of FeEDTA, FeDTPA and FeHEEDTA was then investigated. As buffer was added to the mobile phase it was found that the order of elution of the chelates changed. It was found that as the buffer concentration decreased, the separation improved for FeDTPA and FeHEEDTA (Fig. 3). The best separation was achieved at a buffer concentration of 0.02 *M*; however, the separation of FeHEEDTA and FeEDTA was still not resolved under these conditions.

Using this buffer concentration, the pH was varied from pH 6.5 to 8.0 to try to improve the separation (Fig. 4). It can be seen that the chelates changed elution order over this pH range. The best separation was found at pH 6.6. However, it was found that if pH 8.0 was used together with a low buffer concentration (Fig. 3), thus encouraging the elution order FeDTPA, FeEDTA, FeHEEDTA, a better separation was achieved (Fig. 5). Fig. 6 shows the separation of FeEDDHA and FeEDDHMA. The double peak for FeEDDHMA shows a partial separation of its diastereomers, but those of FeEDDHA co-elute. The earlier eluting peaks are due to impurities in the standards used. CuEDTA,

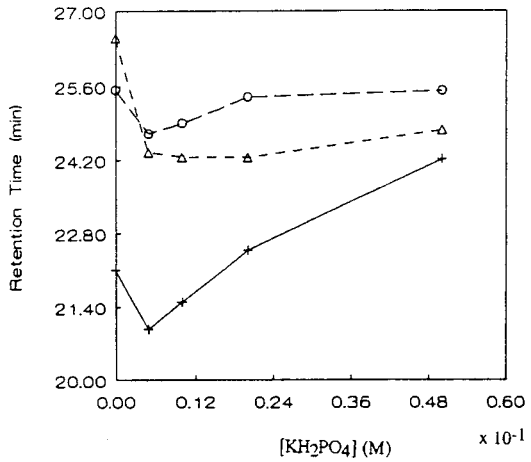

Fig. 3. Influence of phosphate buffer concentration on the retention of iron(III) chelates on Fractogel TSK HW-40(S). Column, 35 × 1 cm I.D.; flow-rate, 0.5 ml/min; mobile phase, 0.05 *M* NaCl (pH 7.0) containing various KH_2PO_4 concentrations. + = FeDTPA; △ = FeHEEDTA; ○ = FeEDTA.

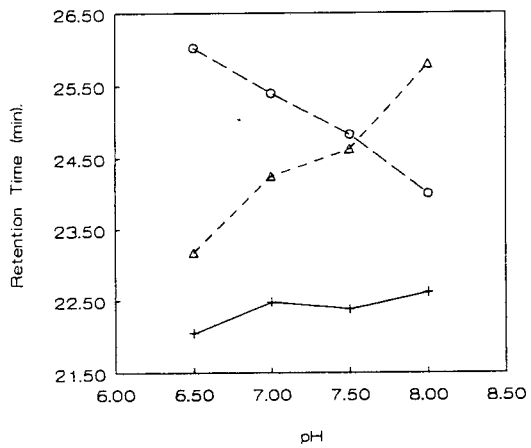

Fig. 4. Influence of pH on the retention of the iron(III) chelates on Fractogel TSK HW-40(S). Column 35 × 1 cm I.D.; flow-rate, 0.5 ml/min; mobile phase, 0.05 *M* NaCl–0.02 *M* KH_2PO_4. Symbols as in Fig. 3.

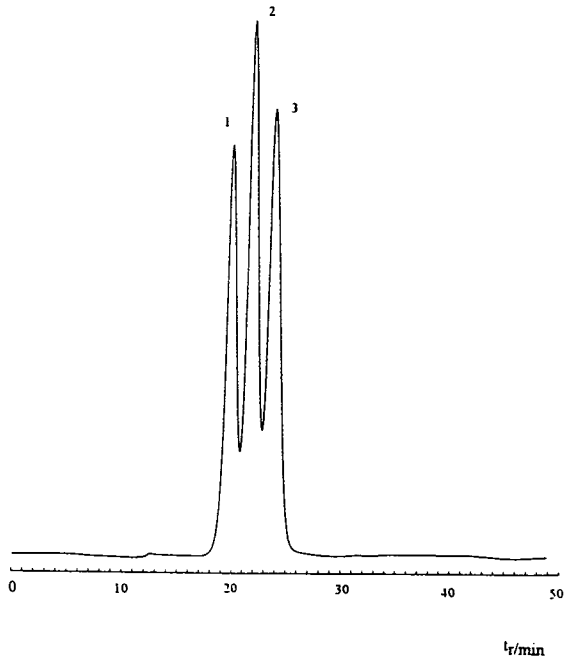

Fig. 5. Separation of (1) 19 μg of FeDTPA, (2) 26 μg of FeEDTA and (3) 28 μg of FeHEEDTA on Fractogel TSK HW-40(S). Column, 35 × 1 cm I.D.; flow-rate, 0.5 ml/min; mobile phase, 0.05 *M* NaCl–0.005 *M* KH_2PO_4 (pH 8.0); injection volume, 20 μl; detection at 210 nm.

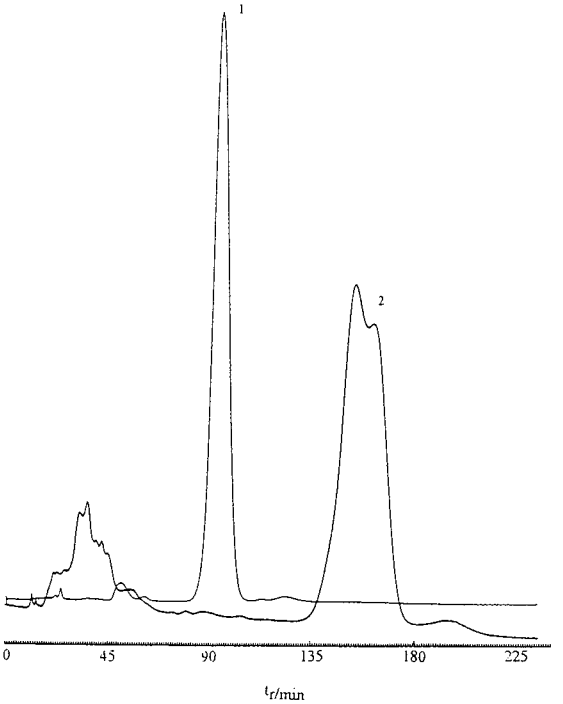

Fig. 6. Separation of (1) 390 μg of FeEDDHA and (2) 44 μg of FeEDDHMA on Fractogel TSK HW-40(S). Column, 35 × 1 cm I.D.; flow-rate, 0.5 ml/min; mobile phase, 0.05 *M* NaCl–0.005 *M* KH_2PO_4 (pH 8.0); injection volume, 20 μl; detection at 210 nm.

ZnEDTA and MnEDTA were found to co-elute with FeDTPA under these conditions.

The relative standard deviation of the retention time based on ten injections of the same standard was less than 1% for the iron(III) chelates of EDTA, DTPA and HEEDTA. The analysis of fertilizer samples showed that matrix interferences were not a problem for the separation as the standard deviation did not increase. However, to avoid matrix interferences, a minimum run time of 50 min is recommended. Quantification using this method should be carried out by a comparison of peak height or area with that of standards as previously discussed, and not by collection and determination of the metal content of chelate fractions.

CONCLUSION

The method developed shows a substantial improvement over the Boxma method. All chelates in a mixture containing FeDTPA, FeHEEDTA, FeEDDHA and FeEDDHMA can be separated. The method is intended for the analysis of fertilizers containing a single micronutrient in combination with a single chelating agent. Therefore, the retention time of the chelate, in combination with identification of the micronutrient present by AAS or ICP-MS, may be used to identify any of the chelates FeEDTA, FeDTPA, FeHEEDTA, FeEDDHA, FeEDDHMA, CuEDTA, ZnEDTA and MnEDTA. Quantification can be achieved by peak height or area analysis. The analysis time of 3 h for a sample containing FeEDDHMA is a disadvantage of the method, however. The most suitable application of the method could be for purification purposes, *i.e.*, the separation of chelated metal from free metal.

ACKNOWLEDGEMENT

This work was supported by the European Commission for Science.

REFERENCES

1 R.Z. Boxma, *Pflanzenernaehr. Bodenkd.*, 142 (1979) 824.
2 N. Yoza, T. Ogata, Y. Ueno and S. Ohashi, *Bull. Chem. Soc. Jpn.*, 41 (1968) 2550.
3 T.J. Deguchi, *J. Chromatogr.*, 120 (1976) 159.
4 W.L. Linsay, J.F. Hodgson and W.A. Norvell, *Int. Soc. Trans. Comm.*, II, IV (Aberdeen) (1966) 305.
5 H. Spitzy, H. Scrube and K. Muller, *Microchim. Acta*, (1961) 296.
6 H. Determann and I. Walters, in L. Fisher (Editor), *Gel Filtration Chromatography*, Elsevier/North-Holland, Amsterdam, 1968, p. 82.
7 K.W. Williams, *Lab. Pract.*, 21, No. 9 (1972) 67.

Journal of Chromatography, A 657 (1993) 77–85
Elsevier Science Publishers B.V., Amsterdam

CHROM. 25 211

Determination of phosphate in samples with high levels of sulphate by ion chromatography☆

M.T. Galceran*, M. Diez and L. Paniagua

Departament de Química Analítica, Universitat de Barcelona, Av. Diagonal 647, 08028 Barcelona (Spain)

(First received December 12th, 1992; revised manuscript received April 11th, 1993)

ABSTRACT

A comparative study of the separation of phosphate from chloride, nitrate, nitrite, bromide and sulphate by ion chromatography with direct conductimetric detection and indirect photometric detection was performed. The best resolution was obtained using borate–gluconate or hydrogenphthalate as the eluent. Indirect photometry using hydrogenphthalate or naphthalenedisulphonate gave the best detection limit for phosphate (1 ng). The use of ion-exchange resins in the barium form for the elimination of high levels of sulphate prior to the determination of trace amounts of phosphate was evaluated. For the elimination of sulphate in samples containing less than 1000 mg/l (SO_4^{2-}:PO_4^{3-} = 100) the column mode can be used, but for samples with high concentrations of sulphate (5000 mg/l) the batch procedure is recommended. The behaviour of commercial cartridges in the barium form was also evaluated. The method was applied to the separation and determination of anions in saline sediments.

INTRODUCTION

The determination of trace components in the presence of major interferents is a common challenge in many areas of analytical chemistry. In ion chromatography (IC) the difficulty becomes particularly severe when the sample is contaminated with high levels of ionic species. Although it may be possible to separate the ionic matrix components from the analyte, this separation becomes difficult to achieve when the concentration of the matrix ions is high because they are eluted as very large peaks, which may obscure the analyte ions and induce retention time variability and loss of chromatographic efficiency. Moreover, high concentrations of ionic compounds result in overloading of the analytical column and shortening of the column lifetime.

Several approaches have been suggested to overcome these adverse effects of high levels of interfering ions. First, the concentration of the matrix ions in the sample can be reduced prior to the analysis by using a suitable precolumn filled with an ion-exchange resin [1,2], hollow-fibre ion-exchange membranes [3] or dialysis through membranes [4]. Other approaches to eliminate matrix contaminants use on-line heart-cutting or recycling methods [5,6]. The use of the interfering ion as the eluent has also been proposed [7]. All these methods are recommended for the elimination of large amounts of chloride in different kinds of sample such as brine [3,8] or sea and polluted water [2,9]. Few methods have been proposed for the elimination of sulphates in highly saline samples, but the use of precolumns in the barium form is generally recommended [10,11]. Few data about their removal capacity or the recoveries of other anions, particularly phosphate, that can coprecipitate or be adsorbed in the resin have been published. In this study the use of precolumns with ion-exchange resins

* Corresponding author.

☆ Presented at the *21st Scientific Meeting of the Spanish Group of Chromatography and Related Techniques*, Granada, October 21–23, 1992.

0021-9673/93/$06.00

in the barium form for the reduction of the sulphate concentration in saline samples before phosphate determination is described.

The determination of phosphate by IC is generally carried out using either direct conductimetric detection in a suppressed system [12] or a non-suppressed system with a low-capacity anion-exchange column and borate–gluconate as eluent [13]. Alternatively, it is possible to use indirect photometric detection with a dilute solution of an aromatic acid anion such as benzoate or phthalate as the eluent [14,15]. Recently, the use of naphthalenesulphonates as mobile phases for anion-exchange chromatography with indirect photometric detection has also been described [16–20], but no information is available about the behaviour of phosphate using these eluents. The applicability of different detection methods for the determination of low concentrations of phosphate was also investigated.

It is generally accepted that phosphate has an important role as nutrient in aquatic systems and its presence could be related to the growth of organisms that can live in hypersaline media. The applicability of the optimized procedure to the determination of phosphate in saline sediments with large amounts of chloride or sulphate is demonstrated.

EXPERIMENTAL

Instruments

The liquid chromatograph consisted of an LKB (Bromma, Sweden) Model 2150 pump, a Rheodyne (Cotati, CA, USA) Model 7125 valve (100-μl loop), a Metrohm (Herisau, Switzerland) Model 690 conductivity detector, an Applied Biosystems (Foster City, CA, USA) Model 757 UV detector and a W + W recorder. The analytical columns used were a Waters (Milford, MA, USA) IC Pak A (50 × 4.6 mm I.D.) packed with a methacrylate-based anion exchanger of 30 ± 3 μequiv/ml capacity and a Vydac 302 IC (250 × 4.6 mm I.D.) packed with a silica-based anion exchanger.

Materials

Salts of the common anions, of analytical-reagent grade or better, were obtained from different suppliers. A 1000 mg/l stock solution of each anion was prepared and used for further dilutions. Water purified using a Culligan water-purification system and filtered through a 0.45-μm membrane filter was used for all solutions.

Sodium gluconate (97%), boric acid, glycerine (87%), potassium hydrogenphthalate, methanesulphonic acid and acetonitrile (HPLC grade) were obtained from Merck (Darmstadt, Germany). Sodium tetraborate was obtained from Carlo Erba (Milan, Italy), 2-naphthalenesulphonic acid of 70% purity, sodium 2-naphthalenesulphonate (NMS) of 90% purity and disodium 1,5-naphthalenedisulphonate (NDS) of 95% purity was obtained from Aldrich (Steinheim, Germany).

Chromatographic conditions

For the determination of nitrate using direct UV detection at 205 nm, a Vydac 302 IC column and 10 m*M* methanesulphonic adjusted to pH 4.2 with 1 *M* sodium hydroxide as eluent at 2 ml/min were used.

Non-suppressed ion chromatography using a Waters IC Pak A and borate–gluconate [1.3 m*M* tetraborate, 5.8 m*M* boric acid, 1.3 m*M* gluconate, 5 g/l glycerine (pH 8.5) and 120 ml/l acetonitrile] at 1 ml/min with conductimetric detection was used for the determination of chloride, nitrite, bromide, nitrate, phosphate and sulphate.

Indirect UV absorption detection at 285 nm using a Waters IC Pak A column and 1 m*M* potassium hydrogenphthalate adjusted to pH 5.5 with 1 *M* sodium hydroxide as eluent at 1 ml/min and 0.3 m*M* NMS–acetonitrile (90:10), 0.3 m*M* 2-naphthalenesulphonic acid–acetonitrile (90:10) and 0.1 m*M* NDS acetonitrile (90:10) adjusted to pH 10 with 1 *M* sodium hydroxide as eluents at 1.2 ml/min was used for the determination of chloride, nitrite, bromide, nitrate, phosphate and sulphate. All eluents were prepared daily, filtered and degassed. Further chromatographic conditions are given in the figure captions.

Chloride and sulphate elimination

Chloride elimination was carried out using a

50W-X8 cation-exchange resin in the Ag^+ form, as described elsewhere [21]. For the elimination of sulphate the strong cation-exchange resin Dowex 50W-X8 in the H^+ form (200–400 mesh) (Fluka, Buchs, Switzerland) was converted into the Ba^{2+} form by soaking in a 1 *M* solution of barium chloride or barium acetate; previously the resin was thoroughly cleaned with water. When the sample clean-up was carried out in the column mode, the resin was packed in a small column (10 × 0.6 cm I.D.) and placed in a suction flask; when the clean-up was carried out in the off-column mode, the resin was dried at 50°C and added to the sample. The resin was regenerated using 1 *M* sodium hydroxide, barium chloride or barium acetate and thoroughly rinsed in water.

Commercial cartridges of purified polystyrene resin in the Ba^{2+} form from Alltech, Maxi-Clean IC Ba^{2+} (0.5 ml) and Maxi-Clean IC Ba^{2+} Plus (1.5 ml) were also used.

Sample preparation

Saline samples were air dried and crushed before use. Amounts between 0.1 and 1 g, according to the anion concentration, were dissolved in water by shaking for 16 h and analysed by IC for nitrate and chloride.

For the determination of sulphate and phosphate, the standard method for the determination of phosphate in soils [22] was used. Samples of sediments were treated with 1 *M* HCl by shaking for 16 h and the solution was then centrifuged at 2000 *g* and neutralized. The excess of chloride was eliminated using a column containing 1 g of 50W-X8 ion-exchange resin in the Ag^+ form. In samples with high concentrations of sulphate (>1000 mg/l), the latter anion was eliminated using the Ba^{2+} ion-exchange resin in the batch mode.

RESULTS AND DISCUSSION

An example of the separation obtained using the Waters IC Pak A polymeric ion-exchange column and hydrogenphthalate as eluent is shown in Fig. 1. The results are in agreement with those published by Sosimenko and Haddad [23] and Haddad and Cowie [24]. For phosphate

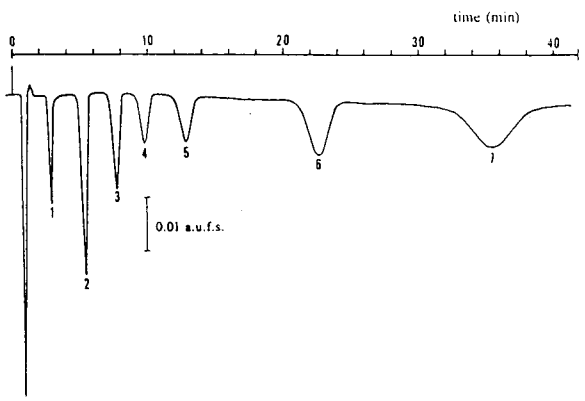

Fig. 1. Separation of a standard mixture of inorganic anions. Peaks: 1 = $H_2PO_4^-$; 2 = Cl^-; 3 = NO_2^-; 4 = Br^-; 5 = NO_3^-; 6 = SO_4^{2-}; 7 = system peak. Column, Waters IC Pak A; eluent, 1.0 m*M* potassium hydrogenphthalate (pH 5.5); flow-rate, 1.0 ml/min; indirect UV detection at 285 nm; sample, 100 μl, 10 mg/l.

a distinct increase in k' at pH 7.5–8 was observed, reflecting the presence of high concentrations of the monohydrogenphosphate ion in the sample (monohydrogen phosphate was eluted at higher k' than the dihydrogenphosphate). The system peak showed a decrease when the eluent pH was increased from 4.5 to 5.5; its height become progressively lower and the peak disappeared at pH 7. These results are in agreement with those published by Jackson and Haddad [25] and Karlson and Frankenberger [26] for other anion chromatographic columns and may be related to the pK_a of the phthalic acid ($pK_1 = 2.95$; $pK_2 = 5.5$).

Considering the resolution, sensitivity and analysis time, the eluent selected was 1 m*M* potassium hydrogenphthalate at pH 5.5. The appearance of the system peak under these conditions can be avoided by injecting the sample dissolved in the mobile phase. The values of k' and resolution under these conditions are given in Table I. It can be seen that resolution was always higher than 1.4.

Naphthalenesulphonate eluents have recently been proposed for the determination of anions with indirect photometric detection [16–20]. The advantages of these eluents include their stability, the use of longer detection wavelengths, non-dependence of the elution strength on pH, absence of system peaks and lower detection

TABLE I

COMPARISON OF RESOLUTIONS AND CAPACITY FACTORS OBTAINED WITH DIFFERENT ELUENTS

Anion	Borate–gluconate[a]		Hydrogenphthalate[b]		Naphthalenesulphonate[c]		Naphthalenedisulphonate[d]	
	k'	R_s	k'	R_s	k'	R_s	k'	R_s
$H_2PO_4^-$	–		6.26		–		–	
		–		1.82		–		–
Cl^-	6.44		12.26		29.50		4.75	
		1.65		2.21		1.00		0.80
NO_2^-	9.33		18.26		36.50		6.00	
		1.59		1.46		1.17		1.33
Br^-	12.69		23.50		45.00		7.00	
		1.52		1.85		0.64		4.36
NO_3^-	16.40		31.26		52.00		9.00	
		1.53		–		0.00		2.80
HPO_4^{2-}	23.30		–		52.00		21.00	
		3.45		1.85		–		3.52
SO_4^{2-}	35.21		56.00		–		31.50	

[a] Borate–gluconate, 1.3 m*M*, pH 8.5.
[b] Hydrogenphthalate, 1.0 m*M*, pH 5.5.
[c] Napthalenesulphonate, 0.3 m*M*, pH 7.
[d] Naphthalenedisulphonate, 0.1 m*M*, pH 10.

limits. Their use for the determination of several anions has been proposed but no information is available about their applicability to the determination of phosphate.

Using 0.3 m*M* 2-naphthalenesulphonate–acetonitrile (90:10) as eluent, phosphate co-eluted with nitrate; the capacity factor for phosphate varied because a non-buffered eluent was used at pH 6.8 (near pK = 7.2 for the dihydrogenphosphate ion). Working at lower pH (4) or using 0.3 m*M* 2-naphthalenesulphonic acid–acetonitrile (90:10) did not help as a system peak appeared that co-eluted with phosphate. Consequently, the determination of phosphate ion was impossible.

The other eluent tested was 1,5-naphthalenesulphonate. The capacity factor for phosphate also varied because a non-buffered mobile phase was used. The behaviour of this eluent at pH 10, at which the monohydrogenphosphate species was predominant, was studied. The chromatogram obtained for the common ions, including phosphate and sulphate, is given in Fig. 2. Complete separation was not achieved but this eluent can be used for the determination of nitrate, phosphate and sulphate. Capacity factors and resolution for these conditions are given in Table I.

The detection limits were calculated as a response higher than twice the standard deviation of the background noise. Table II gives the values obtained with conductimetric and direct or indirect photometric detection using borate–gluconate, methanesulphonic acid, hydrogenphthalate and 1,5-naphthalenesulphonate eluents. Although nitrate had a low detection limit using the 1,5-naphthalenesulphonate eluent, the best result was obtained with direct photometric detection. The detection limits obtained with the 1,5-naphthalenesulphonate eluent are generally lower than those obtained using the other phases, and are in agreement with those previously reported for similar mobile phase concentrations [17,18,20]. The values obtained for phosphate by indirect photometric detection are better than those using conductimetric detection, which may be due to the elution of the dihydrogenphosphate with a low retention time when phthalate is used as eluent or to the higher molar absorptivity and lower

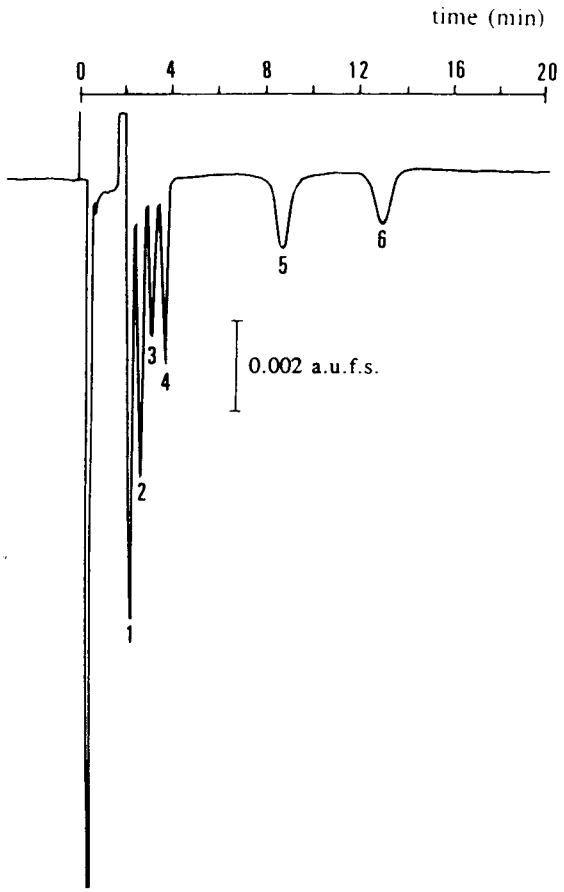

Fig. 2. Separation of a standard mixture of inorganic anions. Peaks: 1 = Cl^-; 2 = NO_2^-; 3 = Br^-; 4 = NO_3^-; 5 = HPO_4^{2-}; 6 = SO_4^{2-}. Column, Waters IC Pak A; eluent, 0.1 m*M* 1,5-naphthalenedisulphonate–acetonitrile (90:10); flow-rate, 1.2 ml/min; indirect UV detection at 285 nm; sample, 100 μl, 1 mg/l.

baseline noise of the 1,5-naphthalenesulphonate. Indirect photometry using phthalate or 1,5-naphthalenesulphonate was the most sensitive detection method for the determination of phosphate.

Calibration for the anions was carried out in each of the solvents with concentrations in the range 0.5–20 mg/l. Peak area was used as the response. The correlation coefficients ranged from 0.9989 to 0.9999 for all analytes.

Ten replicate determinations of 1 mg/l of each anion was carried out under the optimum conditions for each mobile phase to determine the reproducibility. The relative standard deviations (R.S.D.) of retention times and peak areas were 0.4–1.0% and 0.6–2.0%, respectively, when borate–gluconate or hydrogenphthalate was used. For the naphthalenesulphonate eluents higher R.S.D.s were obtained (0.9–3.0%).

Removal of sulphate using ion-exchange resins in Ba^{2+} form

There are some references to the use of ion-exchange resins in the Ba^{2+} form for the removal of sulphate in samples with high levels of this anion [10,11] but few of them give data about the recovery of phosphate; only Henderson *et al.* [10] reported recoveries of 96.5% using phosphate solutions of 30 mg/l.

In this study two reagents were used for the preparation of cation-exchange resin in the Ba^{2+} form: barium chloride and barium acetate. The results obtained using a sample of 100 mg/l of sulphate and 10 mg/l of phosphate were similar and the reagent was chosen depending on the anions to be determined in the sample.

The results obtained for the removal of sulphate and the recovery of phosphate using ion-exchange resins in the barium form in the column mode for different sulphate-to-phosphate concentration ratios are given in Table III. The amount of resin used in each instance was calculated taking into account the concentration of sulphate in the sample. The removal of sulphate was high for low concentration ratios up to a value of 100; when the amount of sulphate increased from 1000 to 5000 mg/l, a large decrease in sulphate removal was observed (recovery 17%). These results could not be improved using large columns (12 g) and may be explained in terms of the kinetics of the column; the flow in the column was too fast to allow effective retention. The recoveries obtained for the phosphate ion was not sufficiently high (see Table III) but the results were reproducible.

To optimize the elimination of sulphate in samples with high levels of this anion, a batch method with the barium ion-exchange resin was used. The amount of resin and the contact time for samples with a sulphate-to-phosphate ratio of 5000:10 (mg/l) were studied and the results are given in Table IV. An increase in the amount of resin gave a better elimination of sulphate, but

TABLE II

COMPARISON OF DETECTION LIMITS WITH CONDUCTIMETRIC AND DIRECT OR INDIRECT PHOTOMETRIC DETECTION

Compound	Detection limit (ng)			
	Conductimetric detection	Direct photometric detection	Indirect photometric detection	
			Phthalate	Naphthalenedisulphonate
Cl^-	0.5	–	0.5	–
NO_2^-	1.0	–	1.5	–
Br^-	2.5	–	5.0	–
NO_3^-	2.5	0.1	5.0	0.5
HPO_4^{2-}	5.0	–	0.9[a]	1.0
SO_4^{2-}	2.5	–	5.0	1.0

[a] As $H_2PO_4^-$.

low recoveries of phosphate were observed for masses above 3 g, probably owing to the co-precipitation of this anion in the barium resin. Moreover, the recovery of phosphate increased with a decrease in the contact time. Therefore, we propose a batch procedure using 3 g of resin, leaving it to stand for 8 h to ensure the elimination of sulphate in samples in which the sulphate-to-phosphate ratio is 500 or higher (calculated as mg/l). The elimination of sulphate in this instance was 97.5% (R.S.D. 1.3%) and the recovery of phosphate was 51.5% (R.S.D. 14.2%).

One of the most versatile means of sample clean-up is the use of commercial disposable cartridges. We studied the behaviour of two different commercial cartridges with different amounts of resin, Maxi-Clean Ba^{2+} and Maxi-Clean Ba^{2+} Plus with 1 and 3 g of resin, respectively. The results obtained are given in Table V. For samples with a sulphate-to-phosphate ratio of 100:10 (mg/l) recoveries of 55% were obtained, but for the other samples, which contained higher concentrations of sulphate, only the Maxi-Clean Ba^{2+} Plus cartridge could be used and the recovery of phosphate was lower than those obtained with the columns prepared in our laboratory. This illustrates one of the most important drawbacks of the method, *i.e.*, that the amount of resin must be adjusted according to the sample composition.

TABLE III

RECOVERIES OF PHOSPHATE WITH Ba^{2+} ION-EXCHANGE RESIN IN COLUMN MODE ($n = 5$)

SO_4^{2-}:PO_4^{3-} (mg/l)	Resin (g)	SO_4^{2-}		PO_4^{3-}	
		Average elimination (%)	R.S.D. (%)	Average recovery (%)	R.S.D. (%)
100:10	0.1	90.70	2.39	73.20	2.95
500:10	0.4	98.84	0.87	48.92	4.80
1000:10	1.5	99.69	0.08	49.67	0.91
5000:10	4.0	17.50	–	–	
	12.0	15.90	–	–	

TABLE IV

RECOVERIES OF PHOSPHATE WITH Ba^{2+} ION-EXCHANGE RESIN IN BATCH MODE ($n = 5$) FOR SO_4^{2-}:PO_4^{3-} = 5000:10 (mg/l)

Resin (g)	Contact time (h)	SO_4^{2-} elimination (%)	PO_4^{3-} recovery (%)
1.0	20	37.3	N.D.[a]
2.0	20	57.1	N.D.
2.5	48	99.9	1.5
2.5	20	99.6	15.0
2.5	14	86.0	34.3
2.5	10	81.0	37.5
3.0	8	97.5	51.5
3.5	4	95.0	19.0

[a] N.D. = Not determined.

Analysis of saline sediments

In order to examine the suitability of the method for the determination of nitrate and phosphate in highly saline samples, several kinds of sediments from a saline circuit with calcite and gypsum domains were analysed. Chloride and nitrate were determined in the water-soluble fraction and their values ranged from 36.4 to 41.2 mg/g for chloride and from 0.20 to 0.50 mg/g for NO_3^-. Sulphate and phosphate were determined in the solution obtained by extraction of the sample with 1 *M* HCl and elimination of chloride using an ion-exchange resin in the Ag^+ form. Their values ranged from 0.07 to 0.22 mg/g for phosphate and from 12.40 to 465.40 mg/g for sulphate. Fig. 3A shows the chromatogram (conductimetric detection) for a sample with a low level of sulphate, where direct determination of nitrate and phosphate was possible.

Figs. 3B and 4A show the chromatograms (conductimetric and indirect UV detection) of a sample with high level of sulphate where nitrate and phosphate were not detected. In this instance elimination of sulphate was needed. In Fig. 4B the chromatogram obtained after elimination using the Ba^{2+} ion-exchange resin in the batch mode is shown.

CONCLUSIONS

The use of various eluents in ion chromatography with conductimetric or indirect UV detection for the determination of phosphate was tested. Low detection limits were obtained using indirect UV detection with phthalate or 1,5-naphthalenesulphonate eluents.

The results obtained for the recovery of phosphate using barium ion-exchange resins indicate that the procedure can be used for the determination of phosphate in samples with a large excess of sulphate. The elimination of the major interfering anions using anion-exchange resins and determination by ion chromatography is a precise and sensitive method for the determination of anions in saline samples and may therefore have advantages over conventional colorimetric methods.

TABLE V

RECOVERIES OF PHOSPHATE WITH A COMMERCIAL Ba^{2+} CARTRIDGES ($n = 5$)

SO_4^{2-}:PO_4^{3-} (mg/l)	Maxi-Clean Ba^{2+}				Maxi-Clean Ba^{2+} Plus			
	SO_4^{2-}		PO_4^{3-}		SO_4^{2-}		PO_4^{3-}	
	Average elimination (%)	R.S.D. (%)	Average recovery (%)	R.S.D. (%)	Average elimination (%)	R.S.D. (%)	Average recovery (%)	R.S.D. (%)
100:10	94.5	1.4	55.0	5.2	95.4	1.6	54.2	8.9
500:10	34.2	2.3	–	–	95.9	0.5	11.9	19.2
1000:10	–	–	–	–	94.4	1.1	3.9	20.7
5000:10	–	–	–	–	35.2	1.5	–	–

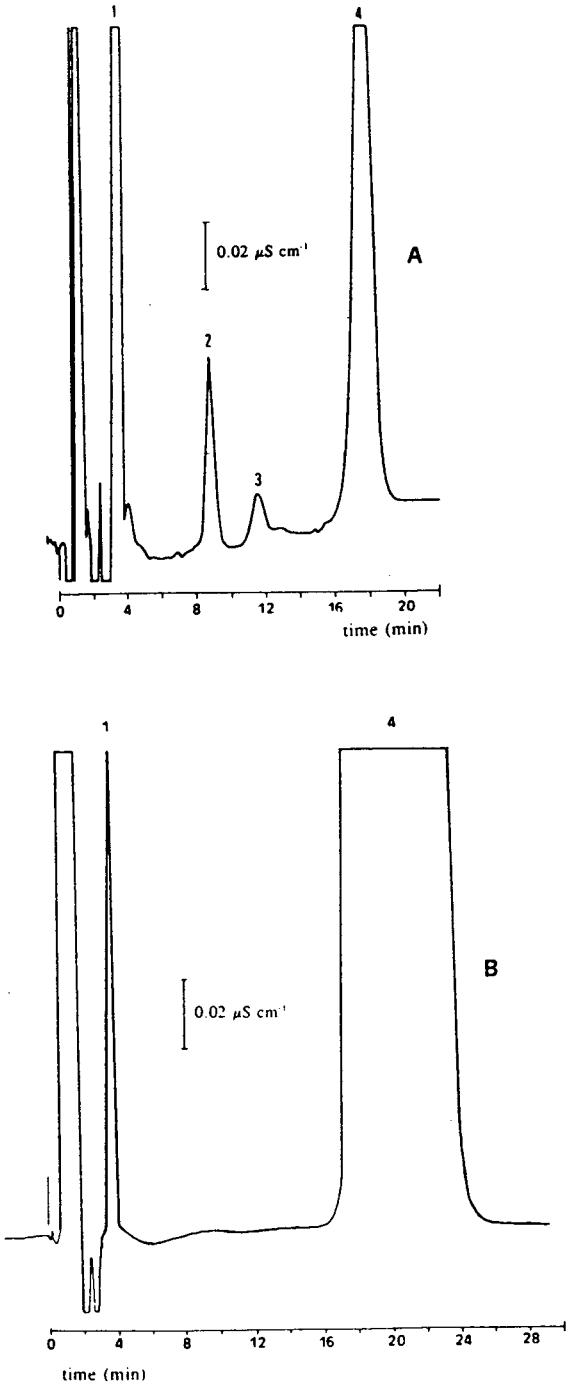

Fig. 3. Chromatograms of saline sediments. (A) Sample with a low level of sulphate (12.4 mg/g); (B) sample with a high level of sulphate (465.4 mg/g). Peaks: 1 = Cl^-; 2 = NO_3^-; 3 = HPO_4^{2-}; 4 = SO_4^{2-}. Column, Waters IC Pak A; eluent, 1.3 m*M* borate–gluconate (pH 8.5); flowrate, 1 ml/min; conductimetric detection.

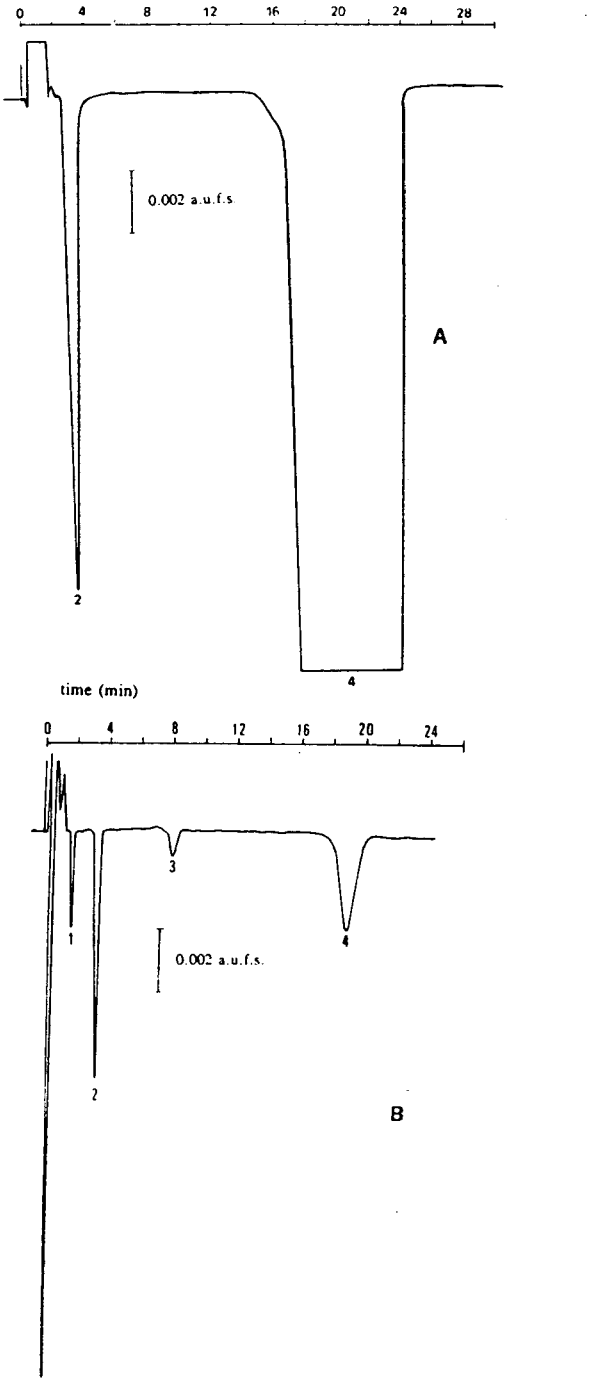

Fig. 4. Chromatograms of a saline sediment with a high level of sulphate (465.4 mg/g). (A) Without sulphate elimination; (B) after sulphate elimination. Peaks: 1 = $H_2PO_4^-$; 2 = Cl^-; 3 = NO_3^-; 4 = SO_4^{2-}. Column, Waters IC Pak A; mobile phase, 1 m*M* potassium hydrogenphthalate (pH 5.5); flowrate, 1 ml/min; indirect UV detection at 285 nm.

ACKNOWLEDGEMENT

This work was financially supported by the CIRIT (AR 91-61).

REFERENCES

1 P.R. Haddad, *J. Chromatogr.*, 482 (1989) 267.
2 S.Y. Tyree, Jr., and M.A.O. Bynum, *Limnol. Oceanogr.*, 29(6) (1984) 1337.
3 P.E. Jackson and W.R. Jones, *J. Chromatogr.*, 538 (1991) 497.
4 J.A. Cox and N. Tanaka, *Anal. Chem.*, 57 (1985) 383.
5 M. Murayama, M. Suzuki and S. Takitani, *J. Chromatogr.*, 466 (1989) 355.
6 S.R. Villaseñor, *Anal. Chem.*, 63 (1991) 1362.
7 Marheni, P.R. Haddad and A.R. Mutaggari, *J. Chromatogr.*, 546 (1991) 221.
8 P.F. Subosa, K. Kihara, S. Rokushika, H. Hatano, T. Murayama, T. Kubota and Y. Hanaoka, *J. Chromatogr. Sci.*, 27 (1989) 680.
9 P. Pastore, I. Lavagnini, A. Boaretto and F. Magno, *J. Chromatogr.*, 475 (1989) 331.
10 I.K. Henderson, R. Saari-Nordhaus and J.M. Anderson, Jr., *J. Chromatogr.*, 546 (1991) 61.
11 R. Saari-Nordhaus, J.M. Anderson, Jr., and I.K. Henderson, *Am. Lab.*, 22 (1990) 18.
12 G. Vanderfold, *J. Chromatogr.*, 602 (1991) 75.
13 P.E. Jackson and T. Bowser, *J. Chromatogr.*, 602 (1992) 33.
14 N. Chauret and J. Hubert, *J. Chromatogr.*, 469 (1989) 329.
15 Y. Miura and J.S. Fritz, *J. Chromatogr.*, 482 (1989) 155.
16 S.A. Maki and N.D. Danielson, *J. Chromatogr. Sci.*, 28 (1990) 537.
17 S.A. Maki and N.D. Danielson, *Anal. Chem.*, 63 (1991) 699.
18 S.A. Maki and N.D. Danielson, *J. Chromatogr.*, 542 (1991) 101.
19 S. Motomizu, M. Oshima and T. Hironaka, *Analyst*, 116 (1991) 695.
20 S.A. Maki and N.D. Danielson, *Chromatographia*, 33 (1992) 25.
21 M.T. Galceran and M. Diez, *An. Quim.*, 606 (1991) 605.
22 *Annual Book of ASTM Standards (11-02), D4183*, ASTM, Philadelphia, PA, 1989, p. 547.
23 A.D. Sosimenko and P.R. Haddad, *J. Chromatogr.*, 546 (1991) 37.
24 P.R. Haddad and C.E. Cowie, *J. Chromatogr.*, 303 (1984) 321.
25 P.E. Jackson and P.R. Haddad, *J. Chromatogr.*, 346 (1985) 125.
26 U. Karlson and W.T. Frankenberger, Jr., *Soil Sci. Soc. Am. J.*, 51 (1987) 72.

Journal of Chromatography A, 657 (1993) 87–93
Elsevier Science Publishers B.V., Amsterdam

CHROM. 25 524

Ion chromatography of alkaline earth and heavy metal ions by on-column derivatization with bisazochromotropic acid

Hiroko Wada*, Muneyoshi Matsushita, Takashi Yasui, Akio Yuchi, Hiromichi Yamada and Genkichi Nakagawa

Laboratory of Analytical Chemistry, Department of Applied Chemistry, Nagoya Institute of Technology, Showa-ku, Nagoya (Japan)

Chizuko Ohtsuka

Mizuho College, Mizuho-ku, Nagoya (Japan)

(First received June 21st, 1993; revised manuscript received August 25th, 1993)

ABSTRACT

Two columns (50 mm × 4.6 mm I.D.) packed with sulphonated styrene–divinylbenzene (PS–DVB) gel (particle size 10 μm) and sulphonated silica gel (particle size 5 μm) were used for the separation of alkaline earth metal and several transition metal ions. The mobile phase contained 3-morpholinopropanesulphonic acid (MOPS)–NaOH buffer and a colour-forming chelating agent, and on-column derivatization and spectrophotometric detection were employed. Arsenazo III, Chlorophosphonazo III, Carboxyarsenazo, Sulphonazo III and Dimethylsulphonazo were examined as mobile phase components for good separation and highly sensitive detection. The PS–DVB gel column and Chlorophosphonazo III gave the highest sensitivity. Ca^{2+}, Sr^{2+} and Ba^{2+} were separated in 5 min with a mobile phase containing $2 \cdot 10^{-4}$ *M* Chlorophosphonazo III and $2.5 \cdot 10^{-2}$ *M* MOPS–NaOH buffer (pH 7.0), whereas Mg^{2+} was eluted after 30 min. An irregular retention sequence was observed, *i.e.*, $Ca^{2+} < Sr^{2+} < Ba^{2+} \ll Mg^{2+}$; the capacity factors ($k'$) were 1.3, 3.3, 5.3 and 42.8, respectively. The separation of alkaline earth and several transition metal ions was also examined. Application to the determination of Ca^{2+} and Mg^{2+} in tap water is described.

INTRODUCTION

The separation and determination of alkaline earth metal and heavy metal ions have been carried out with ion-exchange columns mainly using conductimetric detection. On the other hand, reversed-phase high-performance liquid chromatography has been increasingly employed for the separation and determination of various metal ions with spectrophotometric detection. However, spectrophotometric detection in the visible absorption region has not often been employed in ion-exchange chromatography.

Fritz and co-workers [1,2] reported the separation of alkaline earth metal ions on a low-capacity cation-exchange resin with postcolumn derivatization and spectrophotometric detection. However, with post-column derivatization the analytical precision is sometimes influenced by the pumping delivery system. Zenki [3] and Toei [4–7] employed mobile phases containing a colour-forming agent, which reacts with metal ions to form coloured complexes, and applied

* Corresponding author.

0021-9673/93/$06.00

this method to the separation and determination of alkaline earth metal and some heavy metal ions. For higher sensitivity, better separation and better reproducibility, the selection of the column and chromogenic reagent and the eluent composition are important.

In this study, a sulphonated silica gel column and a sulphonated styrene–divinylbenzene (PS–DVB) gel column were examined for the separation of alkaline earth and some heavy metal ions. A mobile phase containing a chromogenic reagent and a buffer containing eluent cations, a double-plunger pump and a spectrophotometric detector were employed. The method was applied to the determination of Ca^{2+} and Mg^{2+} in tap waters. The separation of some heavy metal ions and alkaline earth metal ions was also studied.

EXPERIMENTAL

Apparatus

The chromatographic system consisted of an SRX-3600T double-plunger pump (Sanuki, Tokyo, Japan) or a CCPD double-plunger pump (Tosoh, Tokyo, Japan), a Model 860-CO column oven (JASCO, Tokyo, Japan), a JASCO Model 870 UV–Vis detector (wavelength range 190–700 nm; flow cell 8 μl; optical path length 5 mm) and a JASCO CC-11 recorder. A Sanuki SVM-6M2L metal-free sample injector (dead volume 2 μl) was used.

A TSKgel IC-Cation column (Tosoh) packed with sulphonated porous PS–DVB copolymer gel (particle diameter 10 μm; cation-exchange capacity 12 ± 2 μequiv./ml; pH range 1–12) and a TSK gel IC-Cation-SW column (Tosoh) packed with sulphonated silica gel (particle diameter 5 μm; cation-exchange capacity 0.3 ± 0.1 mequiv./g; pH range 2–8). Both columns were 50 mm × 4.6 mm I.D. and were made of plastics.

PTFE tubing of 0.5 mm I.D.was used throughout except between the column and sample injector (0.25 mm I.D.).

A UV-250 double-beam spectrophotometer (Shimazu, Kyoto, Japan) and an SAS-727 atomic absorption spectrophotometer (Seiko Denshi, Tokyo, Japan) were used.

Reagents

Five bisarylazochromotropic acids (Chlorophosphonazo III, Arsenazo III, Carboxyarsenazo, Sulphonazo III and Dimethylsulphonazo) were purchased from Dojindo (Kumamoto, Japan). Most of the Chlorophosphonazo III used in this work was kindly provided by Professor L. Sommer (Brno, Czech Republic). These reagents were used as received.

The solutions of alkaline earth metals were prepared by dissolving the analytical-reagent grade chlorides in water and were standardized against standard EDTA solution with the indicators. Calmagite for magnesium, Calcon carboxylic acid for calcium and magnesium Eriochrome Black T–EDTA for strontium and barium. Other metal ion solutions were prepared from the analytical-reagent grade nitrates or chlorides. These solutions were standardized against standard EDTA solution with the appropriate indicators.

Redistilled water or water purified by means of a Toray Pure LV-10T system (Toray, Tokyo, Japan) was used.

Mobile phases

Mobile phase A contained $2 \cdot 10^{-4}$ *M* Chlorophosphonazo III and $2.5 \cdot 10^{-2}$ *M* 3-morpholinopropanesulphonic acid (MOPS)–NaOH buffer. Mobile phase B contained $2 \cdot 10^{-4}$ *M* Chlorophosphonazo III, $2.5 \cdot 10^{-2}$ *M* MOPS–NaOH buffer and $6 \cdot 10^{-2}$ *M* KCl. Mobile phase C contained $2 \cdot 10^{-4}$ *M* Chlorophosphonazo III, $2.5 \cdot 10^{-2}$ *M* MOPS–NaOH buffer and $2 \cdot 10^{-2}$ *M* NaCl. The mobile phases, with the pH adjusted to 7.0, were filtered through a membrane filter (PTFE T050A047A; Toyoroshi, Tokyo, Japan).

Procedure

Mobile phase A was pumped at a flow-rate of 1.0 ml min^{-1}. After the column had been equilibriated with the mobile phase, an aliquot (10 μl) of sample solution was placed on the column via the injection valve. In order to prevent contamination with metal ions from a microsyringe, sample solution was introduced into the sample injector by suction. Elution of metal complexes was monitored at 655 nm. For

earlier elution of Mg^{2+}, mobile phase A was changed to mobile phase B after 10 min.

As city tap waters contained negligible concentrations of metal ions other than Ca^{2+} and Mg^{2+}, mobile phase C was employed for the determination of calcium and magnesium in tap water samples.

RESULTS AND DISCUSSION

Comparison of columns

Two kinds of columns, packed with sulphonated PS–DVB gel and sulphonated silica gel, were compared. With both columns the retention sequence of alkaline earth metal ions was the same, that is, $Ca^{2+} < Sr^{2+} < Ba^{2+} \ll Mg^{2+}$. The strong retention of Mg^{2+} was unusual. According to the catalogue from Tosoh, Mg^{2+} elutes faster than Ca^{2+} when using 0.5 m*M* ethylenediamine solution (pH 6.0) as the mobile phase with the same columns. The sensitivity of detection was higher with the PS–DVB gel than with the silica gel column (Fig. 1). Therefore, the PS–DVB gel column was mainly used in subsequent work.

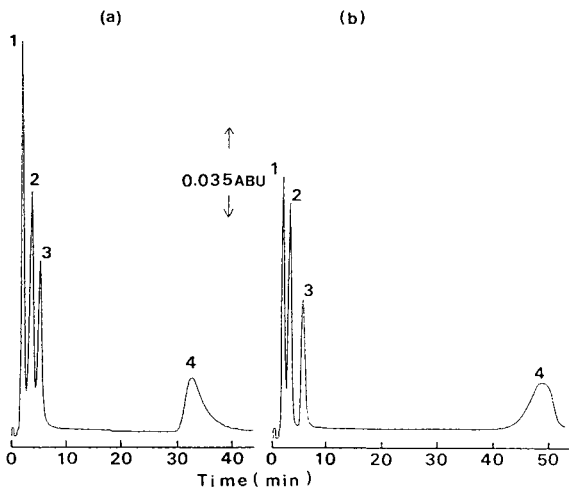

Fig. 1. Chromatograms of alkaline earth metal ions. (a) PS–DVB gel column (particle size 10 μm; 50 mm × 4.6 mm I.D.); (b) silica gel column (particle size 5 μm; 50 mm × 4.6 mm I.D.). Each metal ion concentration, $5 \cdot 10^{-4}$ *M*; injection volume, 10 μl; mobile phase A, $2.5 \cdot 10^{-2}$ *M* MOPS–NaOH buffer containing $2 \cdot 10^{-4}$ *M* Chlorophosphonazo III (pH 7.0); flow-rate 1.0 ml min^{-1}; detection wavelength 665 nm. Peaks: 1 = Ca; 2 = Sr; 3 = Ba; 4 = Mg.

Selection of chromogenic reagent

A chromogenic reagent as a component of the mobile phase may play the important role in the separation, elution and detection of metal ions. A chromogenic reagent that reacts with various metal ions to form stable and highly sensitive complexes must be selected. On the other hand, if the reagent forms inert complexes, good separations will not be obtained. Six water-soluble bisarylazo chromotropic acids, which are expected to form highly sensitive chelates with alkaline earth and heavy metal ions, were selected and examined. The structures of these reagents (Table I) are similar. Under almost identical conditions the absorption spectra of the reagents and the complexes with Mg^{2+}, Ca^{2+}, Sr^{2+} and Ba^{2+} were measured at *ca.* pH 7. Fairly large differences in absorbances between the free reagent and the complexes were observed with Chlorophosphonazo III and Arsenazo III. Chlorophosphonazo III was selected because the Mg^{2+}, Ca^{2+}, Sr^{2+} and Ba^{2+} complexes showed almost same absorbance at 665 nm. Chlorophosphonazo III, which gives the highest molar absorptivity of the complexes around pH 7, was employed as a component of mobile phase: $\varepsilon = 2.7 \cdot 10^4$ (Mg), $3.8 \cdot 10^4$ (Ca), $4.1 \cdot 10^4$ (Sr) and $4.2 \cdot 10^4$ (Ba) l mol^{-1} cm^{-1} at 660 nm. The absorption spectra are shown in Fig. 2. According to Budesinsky *et al.* [8], Chlorophosphonazo III forms complexes such as $Mg(H_4L)^{2-}$, $Ca(H_8L_2)^{6-}$, $Sr(H_8L_2)^{6-}$ and $Ba(H_6L_2)^{8-}$ and the conditional stability constants were reported to be $10^{5.3}$, $10^{10.0}$, $10^{11.5}$ and $10^{12.5}$, respectively,

TABLE I

BISAZOCHROMOTROPIC ACIDS EXAMINED

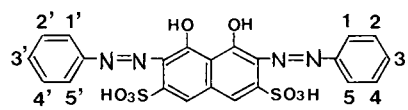

Compound	Substituents
Chlorophosphonazo III	1,1'-PO_3H_2, 3,3'-Cl
Arsenazo III	1,1'-AsO_3H_2
Carboxyarsenazo	1-COOH, 1'-AsO_3H_2
Sulphonazo III	1,1'-SO_3H
Dimethylsulphonazo	1,1'-SO_3H, 3,3'-CH_3

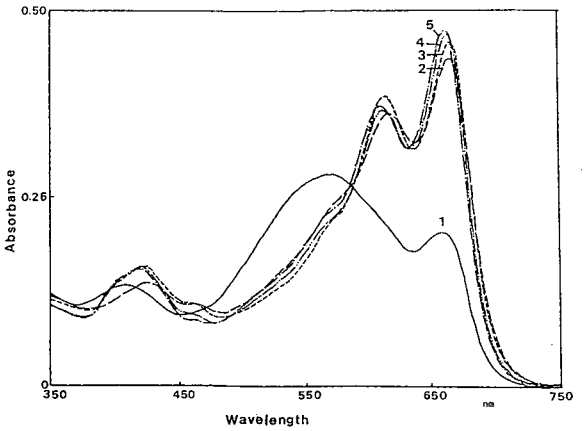

Fig. 2. Absorption spectra of Chlorophosphonazo III and its chelates at pH 7. 1 = Reagent; 2 = Mg; 3 = Ca; 4 = Sr; 5 = Ba. Reagent concentration, $1 \cdot 10^{-5}$ *M*; metal ion concentration, $8 \cdot 10^{-5}$ *M*.

at pH 7.5. The results of the continuous variation method in this work supported the ratio of metal to ligand in the complexes and the order of conditional stability constants estimated in the previous study [8].

Various heavy metal and rare earth metal ions also react with Chlorophosphonazo III to form similar coloured complexes.

Composition of mobile phase

MOPS–NaOH, CH_3COOH–CH_3COONa, ethylenediamine–HCl and trishydroxymethylaminomethane(Tris)–HCl were examined as components of the eluent. When ethylenediamine–HCl buffer was used the baseline was not stable and with Tris–HCl buffer Ba^{2+} and Mg^{2+} were not detected. When MOPS–NaOH buffer or CH_3COOH–CH_3COONa buffer was used, better chromatograms were obtained. When the pH of mobile phase was varied from 6 to 8, the best chromatogram was obtained at pH 7. The MOPS–NaOH buffer was selected owing to the larger buffer capacity around pH 7 (Fig. 3a). The concentration of NaCl in the buffer affected the retention times of the metal ions. The retention times at various concentrations of Na^+ in the mobile phase are shown in Fig. 3b. The best separation of Ca^{2+}, Sr^{2+} and Ba^{2+} was obtained with a mobile phase containing $2.5 \cdot 10^{-2}$ *M* MOPS–NaOH buffer (pH 7), whereas the retention of Mg^{2+} was still very strong.

Concentration of Chlorophosphonazo III

With increasing concentration of Chlorophosphonazo III the retention time decreased and the peak height increased, but on increasing the concentration to $3 \cdot 10^{-4}$ *M* the separation deteriorated (Fig. 3c). To achieve a smaller background and higher sensitivity, the concentration of Chlorophosphonazo III in the mobile phase was selected as $2 \cdot 10^{-4}$ *M*. The capacity factors (k') of Ca, Sr, Ba and Mg were 1.3, 3.3, 5.3 and 42.8, respectively, with the PS–DVB column and 0.8, 2.3, 5.3 and 59.5, respectively, with the silica gel column. The conditional stability constants of Chlorophosphonazo III complexes at pH 7.5 have been reported to be $10^{5.3}$ (MgH_4L), $10^{10.0}$ (CaH_8L_2), $10^{11.5}$ (SrH_8L_2) and $10^{12.5}$ (BaH_6L_2) [8]. The con-

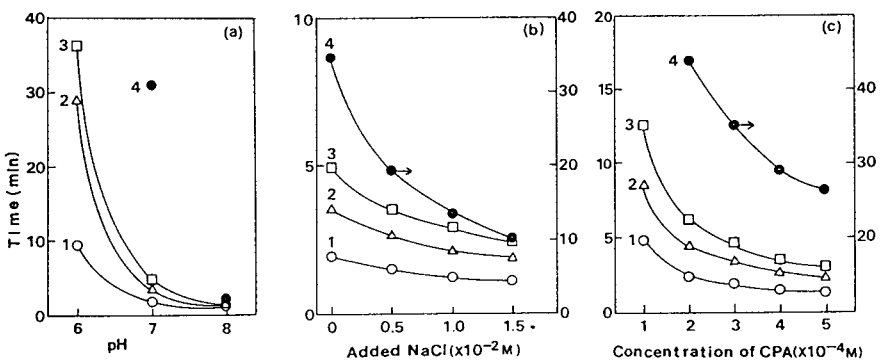

Fig. 3. Effects of (a) pH, (b) added NaCl concentration and (c) Chlorophosphonazo III concentration in the mobile phase on the retention time. 1 = Ca; 2 = Sr; 3 = Ba; 4 = Mg. The PS–DVB gel column was used.

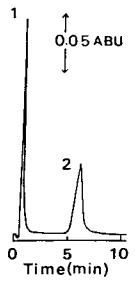

Fig. 4. Chromatogram of Ca and Mg. The PS–DVB gel column and mobile phase C were used. Peaks: 1 = Ca; 2 = Mg.

ditional stability constant of the magnesium complex is much smaller than those of the other complexes, whereas those of Ca, Sr and Ba complexes are almost same. The unusually strong retention of Mg^{2+} can be ascribed to the smaller interaction with Chlorophosphonazo III.

Effect of sodium ion concentration in mobile phase

The sodium ion concentration in the mobile phase was varied from $1.0 \cdot 10^{-2}$ to $2.0 \cdot 10^{-2}$ *M*. The retention of alkaline earth metals decreased with increasing Na^+ concentration. Using mobile phase A, Ca^{2+}, Sr^{2+}, Ba^{2+} and Mg^{2+} were separated, but the elution of Mg^{2+} was very slow (Fig. 1). For faster elution of Mg^{2+}, mobile phase A was changed to mobile phase B after 10 min. However, in this case the baseline raised and the reproducibility of Mg^{2+} determination deteriorated. When mobile phase C was used, Ca^{2+} and Mg^{2+} were clearly separated within 7 min. The chromatogram is shown in Fig. 4.

Effect of column temperature

The temperature of the column oven was varied from 25 to 50°C. The retention times of Ca^{2+}, Sr^{2+} and Ba^{2+} increased with increasing temperature but the peaks became broad. As the separation was not improved, a temperature of *ca.* 25°C was employed.

Calibration output

The calibration output was linear from $0.5 \cdot 10^{-4}$–$4.0 \cdot 10^{-4}$ *M* Ca^{2+}, Sr^{2+} and Ba^{2+} based on peak height (Fig. 5a) and from $0.5 \cdot 10^{-4}$ to $1.0 \cdot 10^{-3}$ *M* based on peak area (Fig. 5b). When only Ca^{2+} and Mg^{2+} were determined, the calibration outputs based on peak area were linear in the range $1.0 \cdot 10^{-5}$–$8 \cdot 10^{-5}$ *M* or $1.0 \cdot 10^{-4}$–$8 \cdot 10^{-4}$ *M*, as shown in Fig. 6.

Separation of alkaline earth metals and heavy metals

The retentions of Cr^{3+}, Mn^{2+}, Fe^{2+}, Co^{2+}, Ni^{2+}, Cu^{2+}, Zn^{2+}, Cd^{2+}, Pb^{2+}, Hg^{2+}, Al^{3+} and rare earth metal ions were examined. The peaks of Zn^{2+}, Cd^{2+}, Mn^{2+}, Co^{2+}, Ni^{2+} and Pb^{2+} were observed. Zn^{2+}, Cd^{2+} and Mn^{2+} were separated with mobile phase A (Fig. 7a), while Zn^{2+} and Cd^{2+} interfered with the determination of Ca^{2+}, Sr^{2+} and Ba^{2+}. By using an eluent containing $1.5 \cdot 10^{-2}$ *M* MOPS–NaOH buffer (pH 7) Ca^{2+}, Zn^{2+}, Sr^{2+} and Mn^{2+} were separated but Ba^{2+} and Cd^{2+} were not (Fig. 7b).

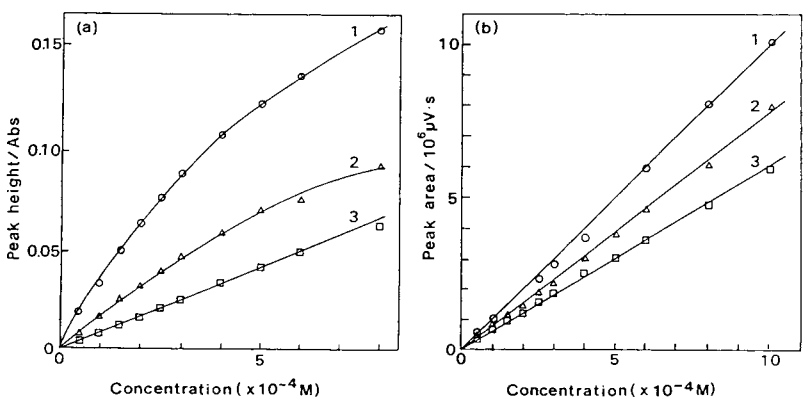

Fig. 5. Calibration outputs of Ca, Sr and Ba with mobile phase A. 1 = Ca; 2 = Sr; 3 = Ba. (a) Peak height; (b) peak area.

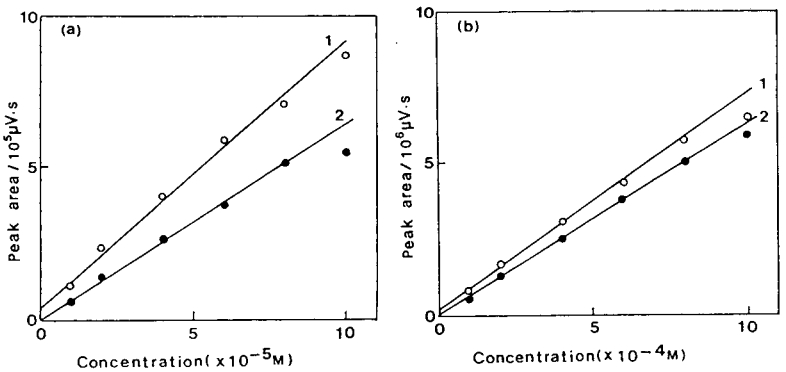

Fig. 6. Calibration outputs (peak area) of Ca and Mg with mobile phase C. 1 = Ca; 2 = Mg. Concentration range: (a) (1.0–10)·10^{-5} *M*; (b) (1.0–10)·10^{-4} *M*.

Co^{2+}, Ca^{2+}, Sr^{2+}, Ba^{2+} and Mn^{2+} at 45°C were separated but Zn^{2+} and Ca^{2+} were not, as shown in Fig. 7c.

Application

The method was applied to the determination of Ca^{2+} and Mg^{2+} in tap water samples. Using mobile phase A, Ca^{2+} was determined in several city tap waters. When strontium and barium ions ($2 \cdot 10^{-4}$ *M*) were added to the water sample, they did not interfere with the determination of calcium.

Using mobile phase C, Ca^{2+} and Mg^{2+} were determined in the several tap water samples from Nagoya and other cities near Nagoya. Sr^{2+}, Ba^{2+} and heavy metal ions were not detected in these sample waters. Selected results are given in Table II.

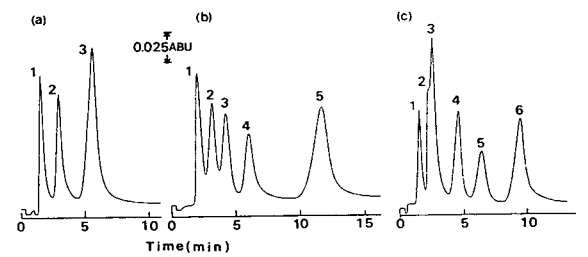

Fig. 7. Chromatograms of heavy metal and alkaline earth metal ions. Each metal ion concentration, $5 \cdot 10^{-4}$ *M*; injection volume, 10 μl. (a) Mobile phase A at room temperature; (b) mobile phase A containing $1.5 \cdot 10^{-2}$ *M* MOPS–NaOH buffer at room temperature; (c) mobile phase A at 45°C. Peaks: (a) 1 = Zn; 2 = Cd; 3 = Mn; (b) 1 = Ca; 2 = Zn; 3 = Sr; 4 = (Ba + Cd); 5 = Mn; (c) 1 = Co; 2 = Ca; 3 = Zn; 4 = Sr; 5 = Ba; 6 = Mn.

CONCLUSIONS

Sulphonated PS–DVB gel and sulphonated silica gel were compared for the separation of alkaline earth metal ions, and the former was found to be better with respect to separation and sensitivity. Chlorophosphonazo III was employed for on-column derivatization and detection. Metal ions in sample are exchanged with Na^{+} on the column and Chlorophosphonazo III in the mobile phase may accelerate the elution by forming the metal–Chlorophosphonazo III complexes. The larger retention of Mg^{2+} than those of other metal ions is considered to be due to the smaller stability constant of Mg–Chlorophosphonazo III complex.

TABLE II

DETERMINATION OF CALCIUM AND MAGNESIUM IN TAP WATER SAMPLES (mgl^{-1})

Ion	Method	Sample No.				
		1	2	3	4	5
Ca^{2+}	This work	6.60	6.40	7.20	15.6	6.12
	AAS	6.80	6.24	7.20	15.3	5.84
	EDTA titration	6.72	6.32	7.20	15.2	6.04
Mg^{2+}	This work	1.62	0.70	1.14	2.64	0.91
	AAS	1.65	0.72	1.20	2.76	0.90
	EDTA titration	1.67	0.73	1.11	2.93	0.87

ACKNOWLEDGEMENT

We thank Professor L. Sommer of Masaryk University (Brno, Czech Republic) for valuable discussions and for providing Chlorophosphonazo III.

REFERENCES

1 J.S. Fritz and J.N. Story, *Anal. Chem.*, 46 (1974) 825.
2 D.L. Smith and J.S. Fritz, *Anal. Chim. Acta*, 204 (1988) 87.
3 M. Zenki, *Anal. Chem.*, 53 (1981) 968.
4 J. Toei and N. Baba, *J. Chromatogr.*, 361 (1986) 368.
5 J. Toei, *Chromatographia*, 23 (1987) 355.
6 J. Toei, *Chromatographia*, 23 (1987) 583.
7 J. Toei, *Analyst*, 113 (1988) 247.
8 B. Budesinsky, K. Haas and A. Bezdekova, *Collect. Czech. Chem. Commun.*, 32 (1967) 1528.

Journal of Chromatography A, 657 (1993) 95–101
Elsevier Science Publishers B.V., Amsterdam

CHROM. 25 495

Simultaneous determination of inorganic anions and cations by ion chromatography with indirect photometric detection

Jinzhang Gao*, Huijie Bian, Jingguo Hou and Jingwan Kang

Department of Chemistry, Northwest Normal University, Lanzhou 730070 (China)

(First received May 11th, 1993; revised manuscript received August 11th, 1993)

ABSTRACT

Inorganic cations and anions were separated simultaneously on a silica-based Shim-pack WAX-1 column. The method is shown to provide efficient separation of Ca^{2+}, Mg^{2+}, Cl^- and NO_3^-. Using 1 m*M* phthalate–6 m*M* EDTA at pH 6.57 as the eluent, a mixture containing these ions was separated in less than 6 min with detection limits of 1.2–2 ng. The effects of the eluent pH, concentration and composition on the retention behaviour of the analytes were studied. Two practical applications are described.

INTRODUCTION

Ion chromatography coupled with indirect photometric detection (IPC), described by Small and Miller [1], is a simple but powerful technique for the separation and detection of many non-UV-absorbing inorganic and organic ions. A feature of this photometric approach is the use of UV-absorbing eluents that can displace the sample ions from the chromatographic column with detection in the effluent. Detection involves measuring the absorbance decrease (negative peak) as the analyte displaces a UV-active component in the mobile phase. This single-column method is at least as sensitive as the more conventional conductimetric detection method [2], and allows greater control over instrumental sensitivity. The method has been used for the separation of inorganic ions in a number of applications [3–7].

In general, anions are separated on an anion-exchange resin and cations on a cation-exchange resin. However, Fritz *et al.* [8] and Mou and Liu [9] reported that some transition metal ions could be separated with chloride or oxalic acid as eluent using a single anion-exchange column and a post-column derivatization detection method with 4-(2-pyridylazo)resorcinol. Matsushita [10] effected the chromatographic separation of inorganic anions and alkaline earth metal ions with EDTA as eluent, which converted metal cations into metal chelate anions using a single anion-exchange column and direct UV detection in series with a conductivity detector. The use of IPC in conjunction with anion- and cation-exchange columns in series for the simultaneous determination of anions and cations but independently of each other using a single chromatograph has been described [11]. Recently, IPC for the simultaneous determination of inorganic cations and anions on a mixed bed of anion and cation exchangers was reported by Pietrzyk *et al.* [12].

Most of the commonly used columns in IPC are low capacity ion-exchange resins or silica-based packing exchangers. In this work, a Shim-pack WAX-1 column (50 × 4 mm I.D.; 3 μm)

* Corresponding author.

0021-9673/93/$06.00

was selected. Surface silanol groups of the packings are chemically modified with a hydrophobic polymer to produce a neutral silica surface. A weakly basic stationary phase is chemically bonded to this silica support, producing a stable packing material for high-performance anion-exchange chromatography. The ion-exchange groups introduced on to the silica surface are tertiary amino groups. However, the column conditions for the simultaneous separation of cations and anions in a single anion-exchange column and using an indirect photometric detector must be modified. This paper describes a procedure by using 1 m*M* phthalate–6 m*M* EDTA as the eluent. The effects of the eluent composition, concentration, and pH value on the retention behaviour and detection sensitivity are discussed.

EXPERIMENTAL

Instrumentation and reagents

The liquid chromatograph used consisted of a Rheodyne Model 7125 valve injector (20-μl loop) and a Shimadzu (Kyoto, Japan) system including a solvent-delivery pump, an SPD-6AV UV–Vis spectrophotometric detector, a C-R3A Chromatopac and a Shim-pack WAX-1 column. UV spectral scans were produced with a U-3400 spectrophotometer (Hitachi).

All reagents were of analytical-reagent grade and aqueous solutions were prepared using doubly distilled water.

Chromatographic procedures

Mobile phases were prepared using analytical-reagent grade phthalic anhydride dissolved in water. The pH of each mobile phase was adjusted by dropwise addition of 1.0 *M* sodium hydroxide solution. All mobile phases were filtered through a 0.45-μm filter and degassed in an ultrasonic bath prior to use. Further chromatographic conditions are given in the figure captions.

RESULTS AND DISCUSSION

The UV spectrum from 250 to 330 nm of a phthalate solution (pH 3.72) shows an absorption maximum at 280 nm with a molar absorptivity of 1279 l/mol·cm. No other peaks are present in the spectrum. The UV spectrum from 200 to 330 nm of an EDTA solution (pH 5.56) shows no absorption. We chose 280 nm as the detection wavelength throughout this work.

The dissociation constants, pK_a, for phthalic acid (H_2P) are 2.95 and 5.41 [13]; the pK_a values for EDTA(H_4Y) are 0.9 (pK_{a_1}), 1.6 (pK_{a_2}), 2.0 (pK_{a_3}), 2.67 (pK_{a_4}), 6.16 (pK_{a_5}) and 10.26 (pK_{a_6}) [13]. It can be calculated that the solutions of phthalate and EDTA at pH 7.21 contain 98.44% P^{2-}, 91.74% HY^{3-} and 8.18% H_2Y^{2-}. It can be concluded from the above that P^{2-} and HY^{3-} are the predominant anions in the eluent if pH $\geq$ 6.2. Under these conditions, the reaction between an alkaline earth metal ion M^{2+} to form a chelate anion with HY^{3-} can be written as

$$M^{2+} + HEDTA^{3-} \rightleftharpoons MEDTA^{2-} + H^+$$

The separation of Ca^{2+}, Mg^{2+}, Cl^- and NO_3^- using a solution containing 1 m*M* H_2P and 6 m*M* EDTA at pH 6.57 as the eluent is shown in Fig. 1.

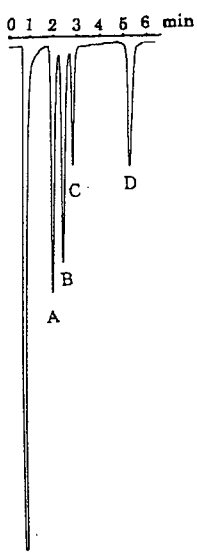

Fig. 1. Separation of a mixture of cations and anions by IPC. Eluent, 1 m*M* H_2P–6 m*M* EDTA (pH 6.57); flow-rate, 0.6 ml/min; column temperature, 25°C; detection wavelength, 280 nm; absorbance units full-scale, 0.04. Peaks; A = 0.9 μg Ca^{2+}; B = 0.5 μg Mg^{2+}; C = 0.8 μg Cl^-; D = 1.4 μg NO_3^-.

Effect of basicity on eluent strength

In this work, the acidity of the eluent over a wide range did not affect the capacity of the strong ion-exchange column, but mainly affected the dissociation of H_2P and EDTA in the eluent. Some details are as follows.

In the anion-exchange process A^{x-} as a counter ion undergoes an ion exchange with the chelate anion and inorganic anion. The exchange process is

$$yA^{x-}_{(S)} + xB^{y-}_{(M)} \rightleftharpoons yA^{x-}_{(M)} + xB^{y-}_{(S)}$$

where S and M represent the stationary and mobile phase, respectively, and A^{x-} and B^{y-} represent the counter ion and sample ion, respectively. Assuming activity coefficients to be equal to unity, we express the selectivity coefficient K_A^B as

$$K_A^B = \frac{[A^{x-}]^y_{(M)}[B^{y-}]^x_{(S)}}{[A^{x-}]^y_{(S)}[B^{y-}]^x_{(M)}} \quad (1)$$

The distribution coefficient for B^{y-} is

$$D_M = \frac{[B^{y-}]_{(S)}}{[B^{y-}]_{(M)}} = \left\{\frac{[A^{x-}]_{(S)}K_A^{B\,1/y}}{[A^{x-}]_{(M)}}\right\}^{y/x} \quad (2)$$

On the other hand, an ion-exchange equilibrium between OH^- and A^{x-} also exists:

$$A^{x-}_{(S)} + xOH^-_{(M)} \rightleftharpoons A^{x-}_{(M)} + xOH^-_{(S)}$$

Similarly, the selectivity coefficient K_A^{OH} is

$$K_A^{OH} = \frac{[A^{x-}]_{(M)}[OH^-]^x_{(S)}}{[A^{x-}]_{(S)}[OH^-]^x_{(M)}} \quad (3)$$

By combination of eqns. 2 and 3:

$$D_M = \frac{[B^{y-}]_{(S)}}{[B^{y-}]_{(M)}} = \frac{K_A^{B\,1/x}[OH^-]^y_{(S)}}{K_A^{OH\,y/x}[OH^-]^y_{(M)}} \quad (4)$$

From eqn. 4, we concluded that the higher the basicity of the eluent, the weaker is the retention of the sample ions. This is consistent with the experimental results shown in Fig. 2.

In Fig. 2, the peaks for the first three anions are completely overlapped at pH 5.30, the peaks for Mg^{2+} and Cl^- are completely overlapped in the pH range 5.30–5.94 and the peaks for Ca^{2+} and Cl^- are completely overlapped below pH

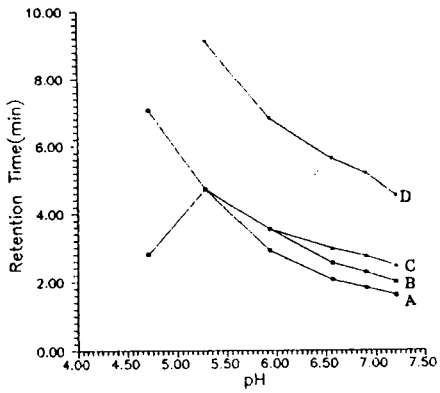

Fig. 2. Retention time *versus* the pH of the eluent. Eluent, 1 m*M* H_2P–6 m*M* EDTA. Other conditions as in Fig. 1.

5.30. However, NO_3^- was well resolved, but the retention time for NO_3^- was extremely long at pH <5.30. It was noticeable that the retention time for Mg^{2+} increased with increasing basicity of the eluent at pH <5.30. We presumed that MgY^{2-} was dissociated below pH 5.3. According to the conditional equilibrium constants [14], 4.1 for CaY^{2-} and 2.1 for MgY^{2-} at pH 5.0, the stability of CaY^{2-} is 100 times higher than that of MgY^{2-}, and the chelate MgY^{2-} cannot exist stably in this pH range.

The effects of pH on the retention behaviour of Cl^- and NO_3^- were expected to be dependent on the acid dissociation constants of H_2P and EDTA. However, the effects of pH on the retention behaviour of Ca^{2+} and Mg^{2+} were expected to be dependent on both the conditional stability constants of metal EDTA chelates and the acid dissociation constants of H_2P and EDTA.

Effect of basicity of eluent on detection sensitivity

Hydroxyl ions in a weakly acidic eluent can act as counter ions when the eluent pH is much greater than its pK_a value. Both A^{x-} and OH^-, which are retained by the anion exchanger, can be displaced by the sample ions. This makes the sensitivity of detection lower than the molar absorptivity of phthalate. Hence a pH of the eluent generally maintained in the acid range will produce a powerful separation and a more sensi-

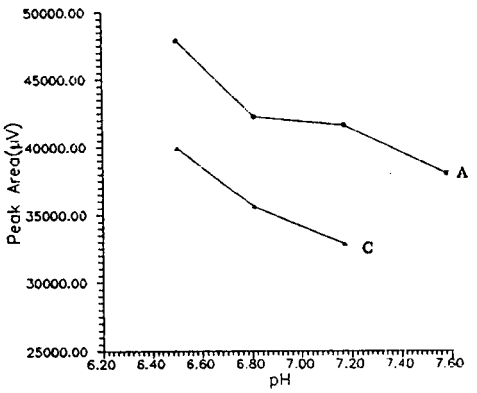

Fig. 3. Plot of sample peak area *versus* eluent pH. Conditions as in Fig. 1.

tive detection. The plot in Fig. 3 verified the point that the detection sensitivity decreases with increasing hydroxyl ion concentration using a weakly acidic mobile phase with $pH > pK_a$ with the IPC method described in this paper.

The result indicates that the ideal eluent pH for complete and optimum separation of the four analytes should be controlled in the range 6.2–7.0; this would eliminate the deleterious effect on detection caused by hydroxyl ions and could avoid damage to the chromatographic column.

Effect of eluent concentration on signal-to-noise ratio

The peak area or peak height for analytes depends on the concentration of the IPC eluent (Fig. 4). Low eluent concentrations are recommended for achieving low background absorbance and good detection limits [1]. This was also predicted by Yeung [15] using the equation

$$C_{lim} = C_m/(D_R T_R) \quad (5)$$

where C_{lim} is the concentration limit of detection, C_m is the concentration of the eluent, D_R is the dynamic reserve (ratio of background signal to background noise) and T_R is the transfer ratio, which is expressed as the number of eluent molecules displaced by one analyte molecule. Eqn. 5 shows a direct proportionality between C_{lim} and C_m. These trends are typical and consistent with all indirect detection techniques, because the relative change in the baseline absorbance is more pronounced at low than at high background absorbance levels. A low eluent concentration provides high sensitivity and powerful separation compared with more concentrated eluents. However, it is important to note that a too dilute eluent will result in overlong run times and a decrease in sensitivity due to band spreading.

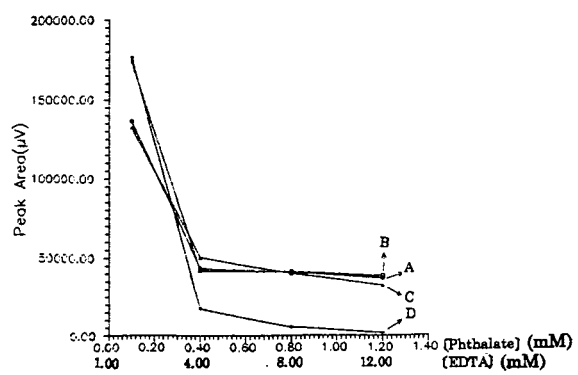

Fig. 4. Plot of sample peak area *versus* eluent concentration. Conditions as in Fig. 1.

Effect of eluent composition on retention behaviour

The elution mechanism of IPC using a mixed eluent as in this work is complicated. A series of mixed eluents containing various concentrations of H_2P and EDTA at pH 7.4 were studied, and also two single eluents, H_2P (1 m*M*, pH 6.95) and EDTA (6 m*M*, pH 7.02). Fig. 5 illustrates the chromatogram of Ca^{2+}, Mg^{2+}, Cl^- and NO_3^- using EDTA as eluent with detection at 230 nm. All the analytes were well resolved, but baseline noise cannot be deleted. In addition, no peaks appeared when the wavelength was set at 280 nm using the same eluent, because EDTA and the EDTA chelate do not absorb at this wavelength. Fig. 6 shows a chromatogram of the samples obtained using H_2P as eluent with detection at 280 nm. Only two negative peaks for Cl^- and NO_3^- were observed, and peaks for Ca^{2+} and Mg^{2+} were not found because Ca^{2+} and Mg^{2+} cations could not be retained by the anion-exchange column. The experiment was carried out by injecting MY^{2-} into the chromatographic column and two negative peaks were obtained.

From the above experiments, two theoretical

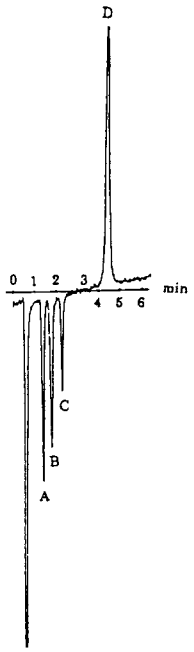

Fig. 5. Separation of a mixture of cations and anions. Eluent, 6 m*M* EDTA (pH 7.02); detection wavelength, 230 nm.

models were presumed. The separation of Ca^{2+} and Mg^{2+} was probably based on two factors: the competitive formation balance between metal cations and EDTA and the anion-exchange balance between EDTA anion chelate

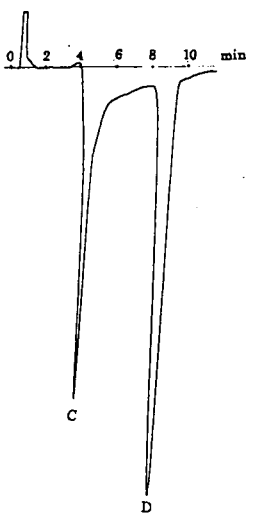

Fig. 6. Separation of chloride and nitrate. Eluent, 1 m*M* H_2P (pH 6.95); detection wavelength, 280 nm.

and counter ions. When HY^{3-} and P^{2-} displaced MY^{2-} from the column into the eluent, the H_2P concentration was changed, which resulted in a negative absorption at 280 nm, corresponding to an indirection detection mode. The mechanism can be explained as follows:

$$3MY^{2-}_{(M)} + 2HY^{3-}_{(S)} \rightleftharpoons 3MY^{2-}_{(S)} + 2HY^{3-}_{(M)} \quad (6)$$

$$MY^{2-}_{(M)} + P^{2-}_{(S)} \rightleftharpoons MY^{2-}_{(S)} + P^{2-}_{(M)} \quad (7)$$

By combining eqns. 6 and 7 we obtain

$$4MY^{2-}_{(M)} + 2HY^{3-}_{(S)} + P^{2-}_{(S)} \rightleftharpoons 4MH^{2-}_{(S)} + 2HY^{3-}_{(M)} + P^{2-}_{(M)} \quad (8)$$

The selectivity coefficient $K^{MY}_{Y,P}$ is

$$K^{MY}_{Y,P} = \frac{[MY^{2-}]^4_{(S)}[HY^{3-}]^2_{(M)}[P^{2-}]_{(M)}}{[MY^{2-}]^4_{(M)}[HY^{3-}]^2_{(S)}[P^{2-}]_{(S)}} \quad (9)$$

The molar fraction of MY^{2-} in solution is

$$\Phi = \frac{[MY^{2-}]}{[M^{2+}] + [MY^{2-}]} \quad (10)$$

The distribution coefficient for M^{2+} can be deduced by combining eqns. 9 and 10:

$$D_M = \frac{[MY^{2-}]_{(S)}}{[M^{2+}]_{(M)}} = K^{MY\ 1/4}_{Y,P} \frac{\Phi}{1-\Phi} [HY^{3-}]^{1/2}_{(S)}[P^{2-}]^{1/4}_{(S)} \times ([HY^{3-}]^2_{(M)}[P^{2-}]_{(M)})^{-1/4} \quad (11)$$

The logarithmic form of eqn. 11 is

$$\log D_M = \frac{1}{4}\log K^{MY}_{Y,P} + \log\left(\frac{\Phi}{1-\Phi}\right) + \frac{1}{2}\log [HY^{3-}]_{(S)} + \frac{1}{4}\log [P^{2-}]_{(S)} - \frac{1}{4}\log ([HY^{3-}]^2_{(M)}[P^{2-}]_{(M)}) \quad (12)$$

where $K^{MY}_{Y,P}$, $[HY^{2-}]_{(S)}$ and $[P^{2-}]_{(S)}$ are constants. However, Φ can also be a constant if the concentration of EDTA in each of the eluents is much higher than that of metal cations. In this event, a straight line should be obtained on

plotting log K' *vs.* log$\{[HY^{3-}]^2_{(M)}[P^{2-}]_{(M)}\}$, and the theoretical slope value should be −0.25.

Experiments showed that the correlation coefficients for Ca^{2+} and Mg^{2+} are −0.9994 and −0.9999, respectively, and the actual slope values for both are exactly the correct value, −0.25. Apparently the actual counter ions in the eluent for Ca^{2+} and Mg^{2+} are HY^{3-} and P^{2-}, which are compatible with the hypotheses described above.

The separation model for monovalent anions can be described as follows. It was assumed that Cl^- and NO_3^- were displaced from the column by the counter ions HY^{3-} and P^{2-}, which also resulted in a negative absorption at 280 nm, corresponding to an indirect detection mode:

$$HY^{3-}_{(S)} + 3L^-_{(M)} \rightleftharpoons HY^{3-}_{(M)} + 3L^-_{(S)} \quad (13)$$

$$P^{2-}_{(S)} + 2L^-_{(M)} \rightleftharpoons P^{2-}_{(M)} + 2L^-_{(S)} \quad (14)$$

By combining eqns. 13 and 14, we obtain

$$HY^{3-}_{(S)} + P^{2-}_{(S)} + 5L^-_{(M)} \rightleftharpoons HY^{3-}_{(M)} + P^{2-}_{(M)} + 5L^-_{(S)} \quad (15)$$

The logarithmic form of D_M for L^- can be deduced similarly:

$$\log D_M = \frac{1}{5}\log K^L_{Y,P} + \frac{1}{5}\log [P^{2-}]_{(S)} + \frac{1}{5}\log [HY^{3-}]_{(S)} - \frac{1}{5}\log([HY^{3-}]_{(M)}[P^{2-}]_{(M)}) \quad (16)$$

where $K^L_{Y,P}$, $[P^{2-}]_{(S)}$ and $[HY^{3-}]_{(S)}$ are constants. A linear relationship should exist between log D_M and log $\{[HY^{3-}]_{(M)}[P^{2-}]_{(M)}\}$, and the theoretical slope value should be −0.20.

Experiments indicated that the correlation coefficients for Cl^- and NO_3^- are −0.9952 and −0.9963, respectively, and the actual slope values are −0.22 and −0.20, respectively.

Six monovalent anions were separated under the same conditions and their slope values and correlation coefficients are given in Table I.

The binary eluent used is effective in separating some other common cations and anions, and the absolute retention times for these ions are given in Table II.

TABLE I

SLOPE VALUES AND CORRELATION COEFFICIENTS FOR ANIONS

Eluent, 1 m*M* H_2P–6 m*M* EDTA (pH 7.03); injection volume, 10 μl (1 m*M*). Other conditions as in Fig. 1.

Anion	Slope	Correlation coefficient
BrO_3^-	−0.20	−0.9960
Cl^-	−0.20	−0.9968
NO_2^-	−0.19	−0.9961
ClO_3^-	−0.19	−0.9951
Br^-	−0.19	−0.9937
NO_3^-	−0.24	−0.9793

Applications

The correlation coefficients of the calibration graphs for Ca^{2+}, Mg^{2+}, and Cl^- are excellent, varying from 0.9992 to 0.9995. The detection limits for Ca^{2+}, Mg^{2+} and Cl^- are 1.2, 1.4, and 2 ppm, respectively (signal-to-noise ratio = 2) when using the optimized mobile phase.

The IPC method described was used to determine alkaline earth metal ions and chloride in tap water and Yellow River water. The concentrations of these three ions determined by this technique are given in Table III.

TABLE II

ABSOLUTE RETENTION TIMES FOR CATIONS AND ANIONS

Ion	Absolute retention time (min)	Ion	Absolute retention time (min)
Ba^{2+}	3.08[a]	BrO_3^-	2.37[b]
Pb^{2+}	3.56[a]	Cl^-	3.02[b]
Ni^{2+}	7.05[a]	NO_2^-	3.67[b]
Mn^{2+}	4.81[a]	ClO_3^-	4.00[b]
Co^{2+}	6.48[a]	Br^-	5.12[b]
Zn^{2+}	6.65[a]	NO_3^-	5.65[b]
Cu^{2+}	14.86[a]		
Bi^{3+}	3.33[a]		
Rh^{3+}	3.34[a]		

[a] Eluent, 1.2 m*M* H_2P–1.2 m*M* EDTA (pH 5.54); injection volume, 10 μl (1 m*M*). Other conditions as in Fig. 1.

[b] Eluent, 1.2 m*M* H_2P–1.2 m*M* EDTA (pH 7.02); injection volume, 10 μl (1 m*M*). Other conditions as in Fig. 1.

TABLE III

ANALYTICAL RESULTS FOR TWO WATER SAMPLES

Eluent, 1 m*M* H_2P–6 m*M* EDTA (pH 7.25); injection volume, 20 μl.

Sample	Ca^{2+} (ppm)[a]	Mg^{2+} (ppm)[a]	Cl^- (ppm)[a]
Tap water	72.0	22.6	43.2
Yellow River water	50.5	16.7	35.0

[a] Values are (w/w).

REFERENCES

1 H. Small and T.E. Miller, Jr., *Anal. Chem.*, 54 (1982) 462.
2 D.R. Jenke, P.K. Mitchell and G.K. Pagenkopf, *Anal. Chim. Acta*, 55 (1983) 279.
3 P.J. Naish, *Analyst*, 109 (1984) 809.
4 T.E. Miller, *Am. Lab.*, 18 (1986) 49.
5 J.H. Sherman and N.D. Danielson, *Anal. Chem.*, 59 (1987) 490.
6 K.-Y. Jiang, M.-C. Liu, Z.-D. Hu and P.-L. Zhu, *Chromatographia*, 29 (1990) 131.
7 S.A. Maki and N.D. Danielson, *Anal. Chem.*, 63 (1991) 699.
8 J.S. Fritz, D.T. Gjerde and C. Pohlandt, *Ion Chromatography*, Hüthig, New York, 1982, Ch. 2.
9 S.-F. Mou and K.-L. Liu, *Li zi se pu*, Science, Beijing, 1986, p. 138.
10 S. Matsushita, *J. Chromatogr.*, 312 (1984) 327.
11 Th.E. Miller, Jr., *Anal. Chem.*, 57 (1985) 1591.
12 D.J. Pietrzyk, S.M. Senne and D.M. Brown, *J. Chromatogr.*, 546 (1991) 101.
13 Wuhan University, *Fen xi hua xue*, High Education, Beijing, p. 577.
14 Wuhan University, *Fen xi hua xue*, High Education, Beijing, p. 290.
15 E.S. Yeung, *Acc. Chem. Res.*, 22 (1989) 125.

Journal of Chromatography A, 657 (1993) 103–109
Elsevier Science Publishers B.V., Amsterdam

CHROM. 25 213

Characterization of capillary column stationary phases by statistical analysis of retention data☆

J. Sanz, M.I. Jiménez and I. Martínez-Castro*

Instituto de Química Orgánica General (CSIC), Juan de la Cierva 3, 28006 Madrid (Spain)

(First received December 10th, 1992; revised manuscript received April 14th, 1993)

ABSTRACT

Characterization of the stationary phases of gas chromatographic capillary columns was attempted by statistical analysis of retention data obtained from test mixtures regularly used in the laboratory. The method was applied to columns belonging to two groups: the first group included those coated with two methyl silicone-based stationary phases, SE-30 (OV-1) and SE-54, while columns in the second group contained FFAP, AT-1000 and Carbowax 20M, three polyethylene glycol-based phases. The relative retention of a single pair of components allowed a complete classification of the two phases of the non-polar group, whereas the polar columns were difficult to classify even using discriminant statistical techniques.

INTRODUCTION

The so-called "column test mixtures" allow a simple quality control method for capillary columns that is very useful for both GC users and manufacturers. They provide information about efficiency and deactivation, and can serve to measure the phase ratio [1,2]. Some attempts have been made to use these mixtures as an indicator of column polarity. The typical elution order of Grob's mixtures I and II [3–5] has been proposed as an aid to determining the type of stationary phase in a column; but since these mixtures are analysed in programmed temperature mode, parameters related to geometrical properties of columns can change the elution pattern. For similar phases, such as SE-30 and SE-54 columns, mixture II provides almost identical elution patterns.

McReynolds constants [6] are based on the determination of the retention indices of several probe compounds, and on the use of a squalane (reference) column. Since they were developed mainly for the characterization of the stationary phases in packed columns, the probe compounds are very volatile and their retention indices are often difficult to determine with accuracy in capillary columns, especially in those with a very high phase ratio. Other methods have been proposed for phase characterization, based on thermodynamic criteria [7,8], selectivity index [9], relative retentions [10] and other measures [11].

In the present work we applied statistical analysis to the characterization of the polarity of capillary columns, using test mixtures in the isothermal mode. Capacity ratio (k) values from several groups of both non-polar and polar columns were used as starting data. The quantitative values assigned in the column characterization are a general measure of the phase chromatographic behaviour and can also be used for phase identification. Our main objective was to assess the possibility of differentiation between columns coated with stationary phases of slightly different polarity, independently of their tube material, deactivation grade and phase ratio.

* Corresponding author.

☆ Presented at the *21st Scientific Meeting of the Spanish Group of Chromatography and Related Techniques*, Granada, October 21–23, 1992.

0021-9673/93/$06.00

MATERIALS AND METHODS

A total of 56 capillary columns, coated with non-polar silicone (SE-30, OV-1 and SE-54) or polyethylene glycol (PEG)-based (Carbowax 20M, FFAP and AT-1000) stationary phases, described in Table I, were tested. They were either prepared in our laboratory (using the static method) or purchased from different suppliers (Alltech, Deerfield, IL, USA; Varian, Walnut Creek, CA, USA; Teknokroma, Barcelona, Spain). These columns had been used in many analytical applications and their dimensions, phase ratios and deactivation grades were very different.

Test mixtures were prepared with reagents of analytical grade dissolved in dichloromethane (all from Merck, Darmstadt, Germany). The components in each mixture (Table II) were selected to include, in a close elution range for columns of each phase group, several chemically different compounds. Mixtures were injected into columns of the non-polar group at 100°C, and at 160°C into columns of the polar group.

Retention data from columns in Table I were collected over several years, when each column was tested. Different gas chromatographs [Hewlett-Packard (Palo Alto, CA, USA) Model 5890; Perkin-Elmer (Norwalk, CT, USA) Models 900 and 3920; Varian, Model 3300; Carlo Erba (Milan, Italy) Models 4130 and 5160] and recorders were used. Carrier gas was always nitrogen at a flow-rate near the Van Deemter optimum in every case. Injections were made in split mode, with split ratios varying between 30:1 and 150:1.

Capacity ratios (k) were obtained from retention time and dead time measures for the components in each test mixture (eight components for the non-polar mixture, five for the polar mixture). Relative retentions $r_{x,y}$ were calculated for all possible pairs of components x,y (28 pairs for the non-polar mixture, ten for the polar mixture). These relative values were used in the characterization in order to avoid possible errors in the determination of film thickness and column internal diameter.

Discriminant analysis was carried out by using the BMDP program package [16]. Stepwise discriminant analysis (program 7M in the BMDP package) calculates the combination of variables that best predicts the group to which a case belongs: in each step, the variable having the highest F value is added to the combination. Mean values, standard deviations and coefficients of variation for each variable were also calculated by the same program.

RESULTS AND DISCUSSION

Methyl silicones (OV-1, SE-30 and others) are very commonly used in capillary GC. Incorporation of a small proportion of phenyl groups (about 5% in SE-54) leads to improved properties at low temperatures [17], although the level of substitution is not enough to provide any worthwhile selectivity [18].

Seventeen columns prepared with SE-30 or OV-1 were considered to belong to a single group (group A1), since these phases are considered to be equivalent [17,18]; McReynolds constants (Table III) are almost identical for the two phases. Eight columns prepared with SE-54 were included in group A2.

When the $r_{x,y}$ non-polar data set from groups A1 and A2 was submitted to stepwise discriminant analysis, a 100% correct classification was obtained with the quotient between capacity ratio of dodecane and capacity ratio of naphthalene [k(C12)/k(N) variable], which showed the highest F value. Although a combination of more variables calculated by discriminant analysis provides an even better separation between SE-30 and SE-54 groups, the use of one or two variables is enough to show the difference between both groups. Fig. 1 plots the non-polar columns using as variables k(C13)/k(E10) and k(C12)/k(N).

The most common poly(ethylene oxide) or PEG-based phases are the Carbowax group. Carbowax 20M is the trade name of a PEG polymer with an average molecule mass between 15 000 and 20 000; although extensively used, it has the disadvantage of batch-to-batch variability [22]. The reaction product of Carbowax 20M with nitroterephthalic acid has better properties for the elution of free acids, and is usually called free fatty acid phase (FFAP) [23]. A purified

TABLE I

CHARACTERISTICS OF THE COLUMNS USED IN THIS STUDY

d_f = Film thickness; N = no; Y = yes.

Phase	Tubing	I.D. (mm)	Length (m)	d_f (μm)	Leaching[a]	Dehydration[b]	Deactivation[c]	Cross-linked
SE-30	Pyrex	0.2	22	0.17	Y	Y	N	N
SE-30	Pyrex	0.2	24	0.1	Y	Y	TMSI	N
SE-30	Pyrex	0.2	16	0.12	Y	Y	D4	N
SE-30	Pyrex	0.2	19	0.1	Y	Y	D4	Y
SE-30	Pyrex	0.2	12	1.4	Y	Y	D4	Y
OV-1	Pyrex	0.2	6.5	0.25	Y	Y	D4	Y
OV-1	Pyrex	0.2	24	0.1	Y	Y	D4	N
OV-1	Pyrex	0.35	22	0.3	N	N	N	N
OV-1	Silica	0.22	24	0.3	N	N	TMSI	Y
OV-1	Silica	0.22	22	0.14	N	N	TMSI	Y
OV-1	Silica	0.22	25	0.14	N	N	TMSI	N
OV-1	Silica	0.22	25	0.15	N	N	N	N
OV-1	Silica	0.33	22	0.08	N	N	N	N
OV-1	Silica	0.25	10	0.2	N	N	N	Y
OV-1	Silica	0.25	5	0.2	N	N	N	Y
OV-1	Silica	0.1	5	0.1	N	N	N	Y
Methylsilicone	Silica	0.2	10	–	(Supplier: Alltech)			
Methylsilicone	Silica	0.33	4.5	–	(Supplier: Varian)			
SE-54	Soda-lime glass	0.2	20	0.08	Y	Y	HMDS + DPTMDS	N
SE-54	Soda-lime glass	0.2	20	0.16	Y	Y	HMDS + DPTMDS	N
SE-54	Pyrex	0.2	43	–	Y	Y	HMDS + DPTMDS	Y
SE-54	Pyrex	0.2	18	0.05	Y	Y	TMSI	Y
SE-54	Silica	0.2	25	0.2	N	Y	N	N
SE-54	Silica	0.25	10	0.2	N	Y	N	Y
SE-54	Silica	0.2	23	0.15	N	Y	N	N
SE-54	Silica	0.32	37	0.32	(Supplier: Teknokroma)			
AT-1000	Pyrex	0.2	15	1.0	Y	Y	GPTMS	Y
AT-1000	Silica	0.22	18	1.1	Y	Y	GPTMS	Y
AT-1000	Silica	0.22	9.5	0.3	Y	Y	GPTMS	Y
AT-1000	Silica	0.22	9.5	0.3	Y	Y	GPTMS	Y
AT-1000	Silica	0.22	9.0	0.3	Y	Y	GPTMS	Y
AT-1000	Silica	0.22	10	0.3	Y	Y	GPTMS	Y
FFAP	Silica	0.25	10	0.37	Y	Y	GPTMS	Y
FFAP	Silica	0.25	9	0.37	Y	Y	GPTMS	Y
FFAP	Silica	0.25	10	0.37	Y	Y	GPTMS	Y
FFAP	Silica	0.25	10	0.37	Y	Y	GPTMS	Y
FFAP	Silica	0.25	8	0.37	Y	Y	GPTMS	Y
FFAP	Silica	0.25	9	0.37	Y	Y	GPTMS	Y
FFAP	Silica	0.32	11	1.6	Y	Y	GPTMS	Y
Carbowax 20M	Silica	0.22	20	0.17	N	N	N	N
Carbowax 20M	Silica	0.22	20	0.19	N	N	N	N
Carbowax 20M	Silica	0.2	23	0.2	N	N	GPTMS	Y
Carbowax 20M	Silica	0.25	22	0.3	Y	Y	GPTMS	Y
Carbowax 20M	Pyrex	0.2	–	0.4	Y	Y	N	Y
Carbowax 20M	Pyrex	0.2	18	0.2	Y	Y	GPTMS	Y
Carbowax 20M	Pyrex	0.2	21	0.2	Y	Y	GPTMS	Y
Carbowax 20M	Pyrex	0.25	–	1.0	Y	Y	N	Y
Carbowax 20M	Pyrex	0.2	10	0.5	Y	Y	N	Y

(Continued on p. 106)

TABLE I *(Continued)*

Phase	Tubing	I.D. (mm)	Length (m)	d_f (μm)	Leaching[a]	Dehydration[b]	Deactivation[c]	Cross-linked
Carbowax 20M	Pyrex	0.19	20	0.1	Y	Y	PEG	Y
Carbowax 20M	Pyrex	0.19	20	0.1	Y	Y	PEG	Y
Carbowax 20M	Pyrex	0.35	20	0.85	Y	N	N	N
Carbowax 20M	Pyrex	0.35	18	0.85	Y	Y	NaCl	N
Carbowax 20M	Pyrex	0.35	18	0.76	Y	Y	NaCl	N
Carbowax 20M	Pyrex	0.35	18	0.85	Y	Y	NaCl	N
Carbowax 20M	Pyrex	0.35	18	0.85	NH_4F	N	N	N
Carbowax 20M	Pyrex	0.2	20	0.1	NH_4F	N	PEG	Y
Carbowax 20M	Pyrex	0.2	11	0.35	NH_4F	N	PEG	Y

[a] Leaching according to Grob [5], NH_4F [12].
[b] Dehydration according to Grob [5].
[c] Treatments with: D4 (octamethylcyclotetrasiloxane) [13], TMSI (trimethylsilylimidazole), HMDS + DPTMDS (hexamethyldisilazane + diphenyltetramethyldisilazane) [5], GPTMS (glycidoxypropyltrimethoxysilane) [5], PEG [14], NaCl [15].

TABLE II

COMPONENTS OF TEST MIXTURES USED FOR POLARITY ASSESSMENT

Component	Code	Non-polar test	Polar test
Undecane	C11	+	−
2,4-Dimethylaniline	A	+	−
Dodecane	C12	+	−
Naphthalene	N	+	+
n-Decanol	ol	+	+
Tridecane	C13	+	−
Carvacrol	Cv	+	−
Methyldecanoate	E10	+	−
Dicyclohexylamine	am	−	+
Nonadecane	C19	−	+
o-Cresol	oCr	−	+

FFAP is distributed by Alltech under the name AT-1000 [20], whereas Supelco only distributes columns under the name SP-1000 [21]. The McReynolds constants for these phases are listed in Table III. While the Carbowax 20M and Carbowax-TPA constants given by McReynolds [6] are almost identical, those of FFAP are clearly different from the latter; other literature values [19,21] are very scattered.

The 31 columns tested with the polar mixture were coated with Carbowax 20M, AT-1000 and FFAP as stationary phases, and were submitted to different preparation treatments as summarized in Table I.

Columns prepared with FFAP and AT-1000 were considered in a first step to belong to the same group (group P1), since the manufacturer of AT-1000 [20] claims that they are equivalent. Columns prepared with Carbowax 20M were included in group P2. When groups P1 and P2 were submitted to stepwise discriminant analysis, the variable with the highest F value was k(N)/k(ol); however, 5 of the 31 columns were incorrectly classified using this single variable (see Fig. 2). The use of more variables somewhat improved the classification; a combination of variables k(ol)/k(am), k(N)/k(am), k(C19)/k(am) and k(N)/k(ol) (canonical variable 1 in Fig. 2) reduced to three the number of incorrect classifications.

In a second step, columns in group P1 were subclassified into groups P1A (FFAP) and P1B (AT-1000). Groups P1A, P1B and P2 were then submitted to discriminant analysis. The results of the best classification, achieved using variables k(ol)/k(am), k(c19)/k(am), k(N)/k(ol) and k(oCr)/k(ol), are shown graphically in Fig. 3; classification was incorrect in 4 of the 31 columns.

There was a clear difference between the results from the non-polar columns (Fig. 1) and

TABLE III

McREYNOLDS CONSTANTS OF THE STUDIED PHASES

Phase	ΔI Benzene	ΔI Butanol	ΔI 2-Pentanone	ΔI Nitropropane	ΔI Pyridine	Ref.
SE-30	15	53	44	64	41	6
OV-1	16	55	44	65	42	6
SE-30	10	53	39	65	58	19
SE-54	33	72	66	99	67	6
FFAP	340	580	397	602	627	6
AT-1000	–	–	–	–	–	20
SP-1000	332	555	393	583	543	21
Carbowax TPA	321	537	367	573	520	6
Carbowax 20M	322	536	368	572	510	6
Carbowax 20M	278	483	322	518	463	19
FFAP	325	541	370	577	511	This work
AT-1000	334	557	384	595	533	This work
Carbowax 20M	335	567	389	594	550	This work
Carbowax 20M	346	580	398	610	561	This work

the polar columns (Figs. 2 and 3). In the first case, the separation into groups was easy: the use of a single variable seems to be enough to classify an unknown column, and even to detect a mixture of phases, in spite of differences in dimensions, materials and preparation methods. However, for columns prepared with Carbowax 20M, FFAP or AT-1000, the separation was less clear. From the plots in Figs. 2 and 3, it can be seen that the dispersion among columns of the same group is close to the separation between groups. The use of discriminant functions including four or more variables was required for classification purposes, but even in this case some classifications were not correct.

A reason for these results could be the high variation in the $r_{x,y}$ values for the Carbowax 20M columns: the mean relative standard deviation was 4.98% for Carbowax 20M, 1.83% for FFAP, 1.29% for AT-1000, 2.35% for SE-30 and 2.54% for SE-54. More important, however, seems to be the difference between the chromatographic

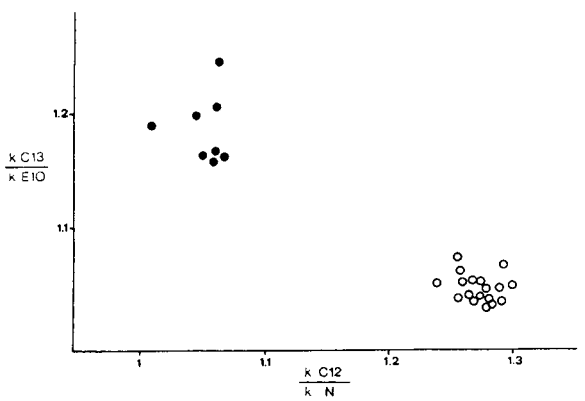

Fig. 1. Plot of non-polar columns using $r_{x,y}$ values. ○ = Group A1 (SE-30, OV-1); ● = group A2 (SE-54).

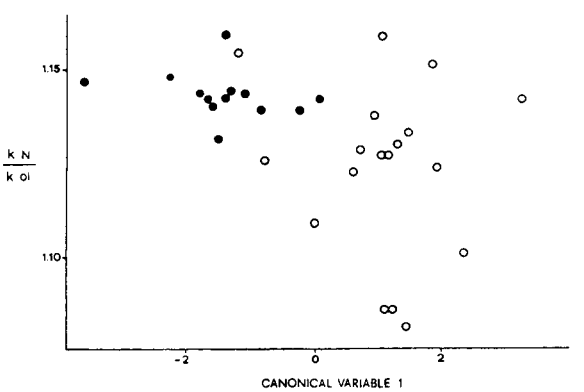

Fig. 2. Plot of polar columns using discriminant analysis. ● = Group P1 (FFAP, AT-1000); ○ = group P2 (Carbowax 20M).

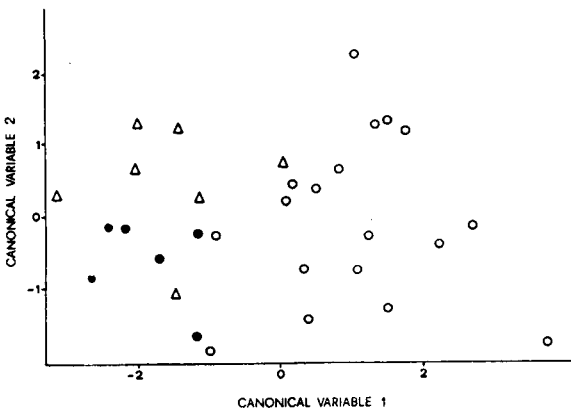

Fig. 3. Plot of polar columns using discriminant analysis. △ = Group P1A (FFAP); ● = group P1B (AT-1000); ○ = group P2 (Carbowax 20M).

properties of these phases. The mean value of the absolute differences between $r_{x,y}$ values for SE-30 and SE-54 columns was 0.214, while for Carbowax 20M and AT-1000 it was only 0.043.

From these results, Carbowax 20M, FFAP and AT-1000 are then difficult to distinguish using this set of variables. Other chromatographic differences, for example the better properties of FFAP in the elution of free acids, also depend on deactivation procedures and are difficult to quantify. However, these phases could probably be correctly classified using chromatographic retention data from other different compounds.

The use of McReynolds constants presents similar problems. Data from refs. 6 and 19–21 in Table III seem to indicate a high dispersion even for the two Carbowax 20M phases. We measured the retention indices of McReynolds probe compounds at 120°C on a FFAP, an AT-1000 and two Carbowax 20M capillary columns (Table III): the values also show a high scatter.

Although our results were calculated using data from capillary columns and could have an important error, they seem to confirm the high degree of chromatographic variation previously found [22] among the columns prepared with PEG-based phases. Since differences of deactivation and dimensions can be discounted (they did not impair the distinction of silicones) the reason for the broad variability of Carbowax 20M should be related to the phase properties. Besides its batch-to-batch variability, this phase seems to be very sensitive to oxidation and ageing [24]. The use of Superox 20M (which is supposed to present better properties than Carbowax) is now in progress in our laboratory; the new data could be used to indicate the extent of degradation of the phases used above.

The method presented here can be applied to other gas chromatographic stationary phases by selecting suitable probe compounds. It can be used in the identification of "unknown" capillary columns and also in the characterization of mixed-phase capillary columns whose phase composition cannot be determined from the coating procedure. The results could also be used to substitute a column for another with a different phase but with an equivalent behaviour: for instance, a column coated with FFAP can be more like a Carbowax one than two different Carbowax columns.

Although the work presented here has been a time-consuming process, it only has to be carried out once. Using the above results as a starting point, it is only necessary to prepare a solution and make a single injection in order to confirm that the chromatographic behaviour of a column corresponds or not to a given stationary phase. The columns are usually correctly identified in a laboratory, but a quality control is always necessary when a column is bought. In some cases, where identification tags are wrong (or lost), the use of a characterization sample affords an easy way to solve the problem.

ACKNOWLEDGEMENT

This work was supported by DGICYT (Projects PB88-034 and PB91-0077-C03-02).

REFERENCES

1 S.P. Cram, F.J. Yang and A.C. Brown III, *Chromatographia*, 10 (1977) 397.
2 R.R. Freeman, *Application Note AN 228-36*, Hewlett-Packard, Palo Alto, CA, 1983.
3 K. Grob Jr., G. Grob and K. Grob, *J. Chromatogr.*, 156 (1978) 1.
4 K. Grob, G. Grob and K. Grob Jr., *J. Chromatogr.*, 219 (1981) 13.

5 K. Grob, *Making and Manipulating Capillary Columns for Gas Chromatography*, Hüthig, Heidelberg, 1986.
6 W.O. McReynolds, *J. Chromatogr. Sci.*, 8 (1970) 685.
7 J. Novak, J. Ruzickova, S. Wicar and J. Janak, *Anal. Chem.*, 45 (1973) 1365.
8 R.V. Golovnya and D.R. Grigoryeva, *J. Chromatogr.*, 290 (1984) 275.
9 M.B. Evans, J.K. Haken and T. Toth, *J. Chromatogr.*, 351 (1986) 155.
10 W. Burns and S. Hawkes, *J. Chromatogr. Sci.*, 15 (1977) 185.
11 S.K. Poole, B.R. Kersten and C.F. Poole, *J. Chromatogr.*, 471 (1989) 91.
12 F.I. Onuska, M.E. Comba, T. Bistrichi and R.J. Wilkinson, *J. Chromatogr.*, 142 (1977) 117.
13 B.V. Wright, P.A. Peaden, M.L. Lee and T.J. Stark, *J. Chromatogr.*, 248 (1982) 17.
14 W.A. Aue, C.R. Hastings and S. Kapila, *Anal. Chem.*, 45 (1973) 725.
15 J.J. Franken, G.A.F.M. Rutten and J.A. Rijks, *J. Chromatogr.*, 126 (1976) 117.
16 *BMDP Statistical Software Manual*, University of California Press, Berkeley, CA, 1988.
17 L. Blomberg, *J. High Resolut. Chromatogr. Chromatogr. Commun.*, 5 (1982) 520.
18 J.K. Haken, *J. Chromatogr.*, 300 (1984) 1.
19 F. Vernon and P.L. Gopal, *J. Chromatogr.*, 150 (1978) 45.
20 *Chromatography Catalog 250*, Alltech Associates, Deerfield, IL, 1991.
21 *Chromatography Products Int. Catalog*, Supelco, Bellefonte, PA, 1991.
22 M. Verzele and P. Sandra, *J. Chromatogr.*, 158 (1978) 111.
23 K. Hammerstrand and D.R. Gere, *Varian Aerograph Previews and Reviews*, 10 (1967) 6; cited by M.K. Whiters, *J. Chromatogr.*, 66 (1972) 249.
24 J.A. Yancey, *J. Chromatogr. Sci.*, 23 (1985) 370.

Journal of Chromatography A, 657 (1993) 111–118
Elsevier Science Publishers B.V., Amsterdam

CHROM. 25 528

Determination of dissolved gases and furan-related compounds in transformer insulating oils in a single chromatographic run by headspace/capillary gas chromatography

Yves Leblanc

Département de Chimie, Université de Montréal, P.O. Box 6128, Montréal, Québec H3C 3J7 (Canada)

Roland Gilbert*, Jocelyn Jalbert and Michel Duval

Institut de Recherche d'Hydro-Québec, 1800 Montée Sainte-Julie, Varennes, Québec J3X 1S1 (Canada)

Joseph Hubert

Département de Chimie, Université de Montréal, P.O. Box 6128, Montréal, Québec H3C 3J7 (Canada)

(First received January 5th, 1993; revised manuscript received August 26th, 1993)

ABSTRACT

A static headspace/capillary gas chromatographic technique has been developed allowing dissolved gases and furan-related compounds in power transformer oils to be determined in a single chromatographic run. The simultaneous determination of these two classes of compounds from a single sample injection represents a definite advantage over current procedures for the detection of impending performance failure of the unit. The method uses gas chromatography with porous-layer open tubular (PLOT) columns and a valve operated in sequence for flowpath selection. Also, comparison with the current method using packed columns showed that dissolved-gas analysis with PLOT columns provides better peak shapes and lower detection limits ($S/N_b = 3$): 5, 3 and 1 ppm (v/v) for hydrogen, carbon oxides and light hydrocarbons respectively. Detection of 2-furaldehyde is possible down to 0.5 ppm (w/w).

INTRODUCTION

Analysis of dissolved gases in insulating oils is an efficient diagnostic tool for routine performance monitoring of power transformers. As a result of a malfunction, gases such as H_2, CH_4, C_2H_2, C_2H_4, C_2H_6, C_3H_8 and C_4H_{10} may evolve from thermal or electrical degradation of insulating oil [1]. When paper insulation is involved, CO and CO_2 are also produced. The concentrations and proportions of the dissolved gases can be related to the type of fault occurring in a transformer without taking the equipment out of service [2,3]. However, the production of carbon oxides cannot be specifically associated with cellulose degradation since they can also be formed as a result of long-term oxidation of the oil or introduced by equilibration of a limited surface of oil with air in the transformer expansion chamber. Also, it has been shown recently that the degradation of paper insulation results in the formation of furans, such as 2-furaldehyde, which dissolve in oil [4–7]. Thus, moni-

* Corresponding author.

0021-9673/93/$06.00

toring these compounds can give complementary information specifically related to the state of the solid insulation.

The analytical methods used for dissolved-gas analysis generally comprise vacuum extraction [8] or stripping [9] of the gases followed by gas chromatographic separation. Analysis of less volatile furan-related compounds requires a second technique involving liquid- or solid-phase extraction followed by high-performance liquid chromatography [4,5]. A headspace method allowing automated analysis has recently been reported [10] as an alternative to vacuum gas extraction. This procedure, coupled with gas chromatographic separation, offers a precision better than 5% with detection limits ($S/N_b = 3$, where S and N_b are the net signal and the background noise, respectively) for hydrogen, carbon monoxide and methane, carbon dioxide and hydrocarbons of 7, 10, 5 and 1 ppm (v/v) respectively. The analytical performance of this technique was shown to be similar to that of the ASTM D3612 vacuum method [8] currently used for routine dissolved-gas analysis, while allowing a larger number of oil samples to be analysed by the same operator as a result of automation.

Gas chromatographic separation for dissolved-gas analysis is generally achieved using dual-packed columns to separate permanent gases and light hydrocarbons: a molecular sieve column is connected at the outlet of a porous polymer column through a valve used for column isolation [10]. Recently commercialized porous-layer open tubular (PLOT) capillary columns have not yet found an application in this field [11–15]. Firor [16] has used PLOT columns for the analysis of natural gas, refinery gas and process stream and has found that these columns provide shorter retention times, better resolution and lower detection limits than packed columns. The shorter retention times obtained could allow heavier insulation breakdown products such as the furan-related compounds to be determined.

This paper reports on the application of PLOT columns for the analysis of dissolved gases and furan-related compounds in transfer oils by the headspace/gas chromatographic technique. The possibility of measuring dissolved gases and cellulose insulation breakdown products in a single chromatographic run could simplify routine monitoring procedure for public utilities. In addition, compared with the previous packed column system, greater sensitivities for the dissolved gases are expected.

EXPERIMENTAL

Instrumentation

The instrumentation used for this study is depicted schematically in Fig. 1. It is the same as that used in a previous work for packed columns [10]. An HP-19395A static headspace unit (Hewlett-Packard, Palo Alto, CA, USA) equipped with a six-port injection valve (V1) and a 1-ml sample loop is used to extract the dissolved gases from transformer oil. An HP-5890 gas chromatograph (also from Hewlett-Packard) equipped with a thermal conductivity detector, a nickel catalyst unit to convert CO and CO_2 into CH_4, and a flame ionization detector was used for all

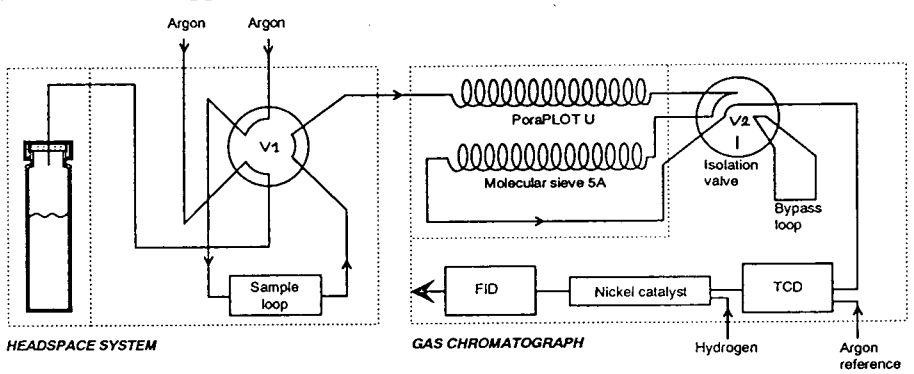

Fig. 1. Schematic diagram of the headspace/gas chromatographic instrumentation. FID = Flame ionization detector; TCD = thermal conductivity detector.

analyses. The methanizer was maintained at 350°C and fed with pure hydrogen serving both as reactant for the catalyst and fuel for the flame ionization detector. A ten-port pneumatic valve (V2) for column isolation (Valco, Houston, TX, USA) with 1/16-in. (1 in. = 2.54 cm) fittings was installed on the gas chromatograph and maintained at 150°C. A 10 m × 0.53 mm molecular sieve 5A capillary column with 50 μm adsorbant thickness (Chrompack, Raritan, NJ, USA) was connected at the outlet of a 35 m × 0.53 mm PoraPLOT U column with 20 μm adsorbant thickness (also from Chrompack) through the isolation valve to separate the lighter gases (H_2, O_2, N_2, CH_4 and CO) poorly resolved on the porous-polymer column. The event controller used for valve action (V2), thermal conductivity detection and flame ionization detection signal acquisition and the instrumental conditions for the headspace unit were identical to those previously described [10]. For packed columns, the system configuration was the same as in capillary mode with an HP molecular sieve column (0.8 m × 1/8 in., 45–60 mesh) connected at the outlet of an HP Porapak N column (4 m × 1/8 in., 80–100 mesh). The chromatographic conditions used for both systems are given in Table I. Positive identification of the furans was accomplished using an HP-5971 mass spectrometer that was connected to the outlet of the columns through a splitter. A tenth of the total flow was directed to the mass spectrometer used in chemical ionization mode. The peaks were identified using the mass spectral library NTIS/EPA/NIH obtained from Hewlett-Packard (G1033A).

Chemicals and standards

The capillary and packed chromatographic systems were evaluated for gas separation by headspace/gas chromatographic analysis of sealed vials purged with different standard gas mixtures of 100, 1000 and 5000 ppm of each gas (H_2, O_2, N_2, CH_4, CO, CO_2, C_2H_2, C_2H_4, C_2H_6, C_3H_8) in argon (Scott Specialty Gases, Plumsteadville, PA, USA). A special gas mixture was also used with concentrations specified in Fig. 2.

Dissolved-gas oil standards were used for the calibration and analytical performance evaluation of the method. The preparation of these standards was done according to Duval and Giguère [17]. Sub-standards were obtained by diluting the dissolved-gas oil standard with degassed oil in the headspace vials. The dilution factor was determined by weighing. Preparation of headspace vials for analysis was done as follows: after being sealed with PTFE-lined septa, the vials were purged with argon; 15 ml of oil sample were then introduced into the vial, releasing pressure build-up through a 0.5 mm

TABLE I

CHROMATOGRAPHIC CONDITIONS

	Packed columns	Capillary columns
Carrier gas	Argon, 40 ml/min	Argon, 15 ml/min
Catalytic gas	Hydrogen, 70 ml/min	Hydrogen, 40 ml/min
Valve operation	0–7 min, columns in series 7–18 min, molecular sieve bypassed	0–2.5 min, columns in series 2.5–10.5 min, molecular sieve bypassed 10.5–15.0 min, columns in series 15.0–20 min, molecular sieve bypassed
Oven programme	40°C for 4 min 40 to 180°C at 20°C/min 180°C for 7 min	40°C for 4 min 40 to 65°C at 8°C/min 65°C for 4.9 min 65 to 115°C at 10°C/min 115 to 190°C at 20°C/min 190°C for 3.75 min
Detection	Thermal conductivity at 250°C Flame ionization at 350°C	Thermal conductivity at 250°C Flame ionization at 350°C

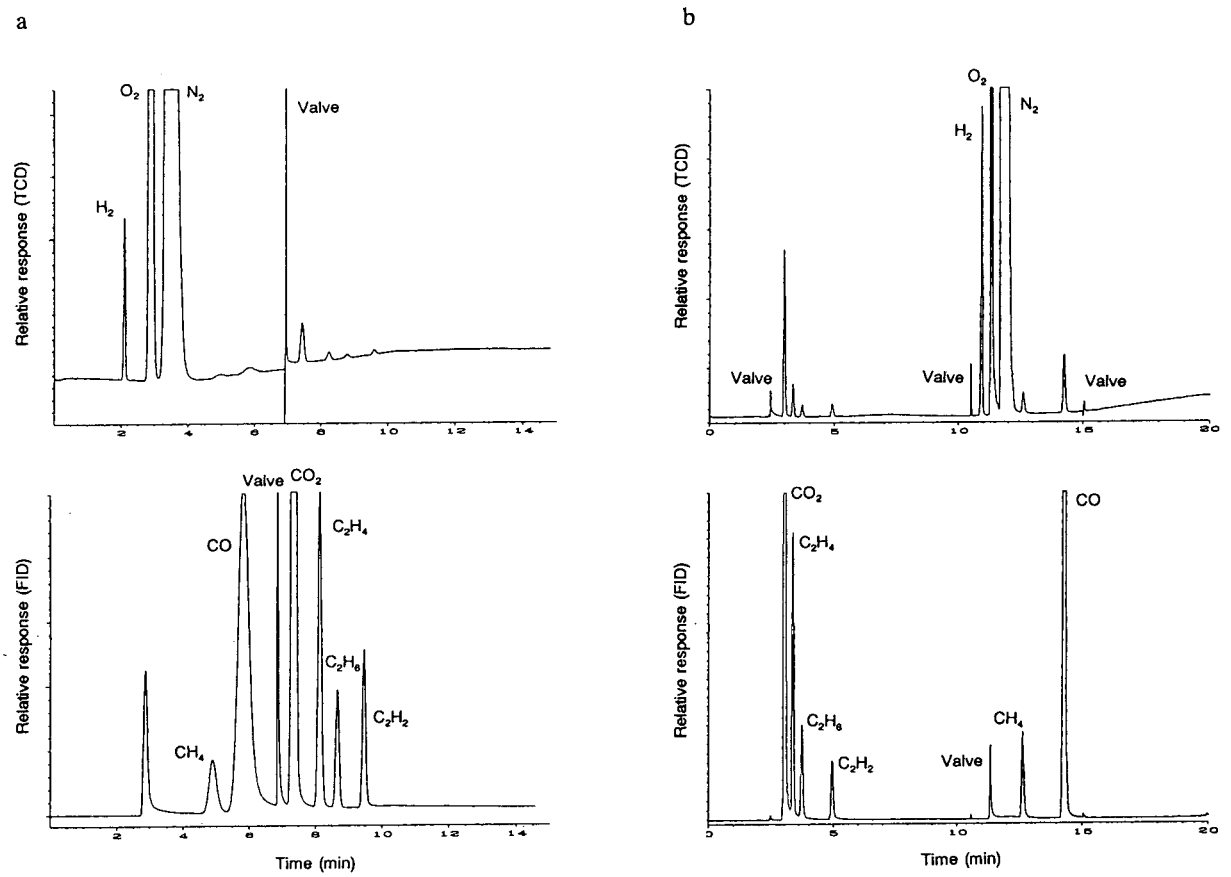

Fig. 2. Chromatograms of 1 ml gas standard injection. (a) Packed columns and (b) capillary columns. Certified gas mixture concentrations (ppm, v/v): 1485 H_2, 423 CH_4, 4365 CO, 7221 CO_2, 569 C_2H_4, 205 C_2H_6, 292 C_2H_2, in air (Matheson Gas Products, Secaucus, NJ, USA).

O.D. needle. The vials were weighed before and after filling to control the volume introduced. A 30-ml syringe (Perfectum, Thomas Scientific, Swedesboro, NJ, USA) with an 1.2 mm O.D. stainless-steel needle was used for this transfer. The 20-ml glass vials were purchased from Wheaton (Millville, NJ, USA).

The following procedure was used to prepare a solution of furans in oil: after purging 1 l of Voltesso 35 (Esso Imperial Oil Company, Sarnia, Ontario, Canada) transformer insulating oil with helium, a few microlitres each of 2-furaldehyde, 5-methylfurfural, 2-acetylfuran and furfuryl alcohol at 99% purity (Aldrich, Milwaukee, WI, USA) were added and homogenized by manually shaking the solution for a few seconds. This solution was introduced into vials as for dissolved-gas oil samples.

RESULTS AND DISCUSSION

Capillary columns for dissolved-gas analysis

Chromatograms from packed and capillary columns for a standard gas mixture injected from the headspace unit are compared in Fig. 2. The retention times for non-permanent gases obtained with capillary columns are shorter than those obtained with packed columns. The permanent gases appear at later retention times as a result of the valve operating sequence used for column isolation. When packed columns are used (Fig. 2a), the two columns are initially in

series and the permanent gases elute from the molecular sieve just before column isolation is achieved to ensure bypass of the hydrocarbons. When the capillary columns are used (Fig. 2b), the permanent gases do not elute from the molecular sieve as fast as the hydrocarbons from the PoraPLOT U with the result that column isolation is achieved while the permanent gases are still in the molecular sieve column. In order for these gases to elute, the time window in the hydrocarbon peak elution sequence must be long enough to allow the second column to be switched back in series. By adjusting the chromatographic conditions, this can be achieved between propane ($t_R \approx 9$ min) and butane ($t_R \approx 16$ min). Later, the molecular sieve is again isolated for the remainder of the chromatographic run to allow higher hydrocarbon elution. Dual-capillary column separation of dissolved gases requires three valve actions (V2) compared with only one with packed columns.

The peak widths and detection limits obtained with both column technologies are compared in Tables II and III. As expected, the peaks are sharper with capillary columns, especially for CH_4 and CO, resulting in slightly better sensitivity in the determination of dissolved gases in power transformer oils. In addition, the resolution of two adjacent peaks is higher with the capillary column system and is at least 2.3. This allows a more than adequate resolution for quantitative analysis of dissolved gases. The noise on the background signal was approximately the same for both systems. However, the background signal was more stable in capillary mode, allowing easier peak detection and better reproducibility. It is not possible to compensate for the sensitivity loss of the packed columns by increasing the injection volume: first, the methane and carbon monoxide peaks would start to overlap while, second, the higher vial pressurization required to fill the loop would result in dilution of the headspace, thus offsetting the volume increase.

The time required for complete chromatographic analysis is approximately the same for both systems; C_4H_{10} elutes at 17 min in packed mode compared with 16 min with capillary columns (species not present in the sample of Fig. 2).

TABLE II

COMPARISON OF PEAK WIDTHS AND RETENTION TIMES t_R FROM PACKED AND CAPILLARY COLUMNS[a]

Gas	Packed columns[b]		Capillary columns	
	Peak width (min)	t_R (min)	Peak width (min)	t_R (min)
H_2	0.06	2.13	0.06	10.91
O_2	0.10	2.92	0.05	11.32
N_2	0.25	3.45	0.18	11.79
CH_4	0.25	5.03	0.10	12.63
CO	0.38	5.98	0.10	14.30
CO_2	0.12	7.56	0.07	3.01
C_2H_4	0.12	8.37	0.08	3.40
C_2H_6	0.12	8.91	0.08	3.71
C_2H_2	0.11	9.74	0.10	4.92

[a] Peak widths measured at half-height.
[b] Results obtained under the conditions given in ref. 10.

TABLE III

COMPARISON OF DETECTION LIMITS ($S/N_b = 3$) FOR PACKED AND CAPILLARY COLUMNS

Gas	Concentration in ppm in oil (v/v)	
	Packed columns[a]	Capillary columns
H_2	7	5
CO, CH_4	10	3
CO_2	5	3
C_2H_2, C_2H_4, C_2H_6	1	1

[a] From ref. 10.

Extension of the analytical capabilities

Since capillary columns have a lower retention volume than packed columns, it could be possible to determine compounds otherwise retained on the porous-polymer packed column. Fig. 3 shows a headspace/gas chromatogram of an in-service transformer oil sample. On the flame ionization detector, peaks appearing after 19 min could not be observed with packed columns, even over an extended chromatographic run. It

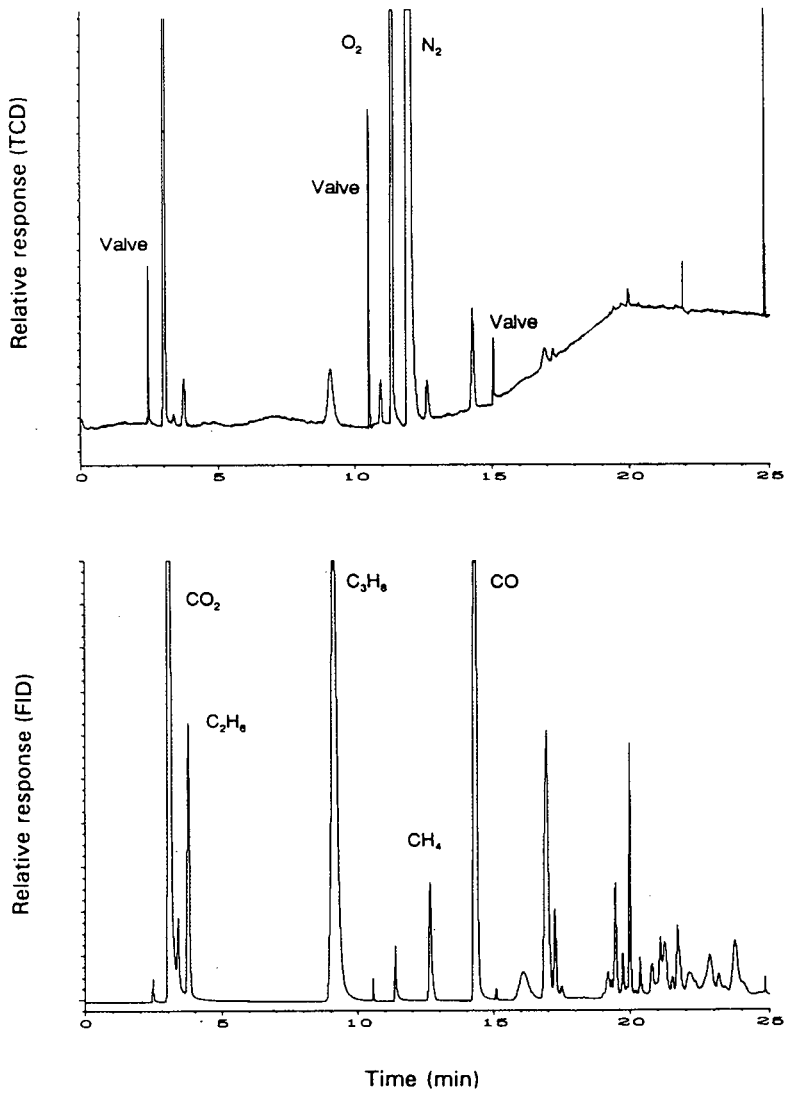

Fig. 3. Chromatograms of an in-service transformer oil sample by headspace/gas chromatography. Conditions as in Table I.

has been noted that this region of the chromatogram varies from one transformer oil sample to another and could possibly be representative of the internal condition of equipment. However, some of these peaks also noted in new Voltesso 35 might be attributed to volatile compounds normally present in this type of insulating oil.

An additional important benefit of replacing the packed columns by the capillary columns for dissolved-gas analysis is that furan-related compounds resulting from cellulose insulation breakdown can be analysed by the same chromatographic technique as dissolved gases by extending the run, as seen in Fig. 3. To demonstrate the potential of this approach, Fig. 4 shows a headspace/gas chromatogram from an oil standard containing 25 ppm (w/w) of each furan compound. Single furan oil standards provided the retention times observed. The identity of the chromatographic peaks labelled 1–4 in Fig. 4 was further confirmed by GC–MS: molecular ions and fragments were observed for each compound studied. For example, Fig. 4 shows the mass spectrum of the chromatographic peak labelled

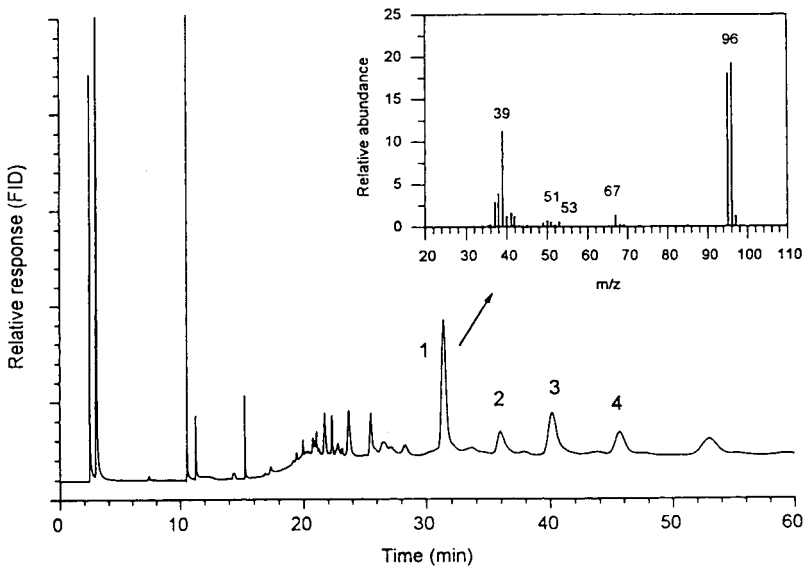

Fig. 4. Chromatogram of a Voltesso insulating oil standard containing 25 ppm (w/w) furans —FID channel only. Peaks: 1 = 2-furaldehyde; 2 = furfuryl alcohol; 3 = 2-acetylfuran; 4 = 5-methylfurfural.

"1". It was identified as 2-furaldehyde with a 97% match to the spectral database. Peaks 2, 3 and 4 were also identified by the same method with a minimum of 91% spectral match. Under the instrumental conditions given in Table I, the detection limits are 0.5 ppm (w/w) for 2-furaldehyde and 5 ppm (w/w) for 5-methylfurfural, 2-acetylfuran and furfuryl alcohol.

In order to validate this method on real samples, a series of analyses on in-service transformer oil samples were performed. 2-Furaldehyde was observed in a sample taken from a unit known to be defective. Fig. 5a shows the resulting chromatogram of selected ions specific for the furans investigated (m/z = 29, 37, 38, 39, 95, 96, 97, 98, 110 and 112). From the total ion chromatogram, we were able to focus on 2-furaldehyde by tracing the ion chromatogram for mass 96, which is the molecular ion (Fig. 5b).

On the basis of the results so far, it is obvious that the technique represents a useful means of pinpointing defaults in transformers, an aspect which requires further investigation. In this respect, the headspace/capillary gas chromatographic method presents a breakthrough over the techniques already available for routine dissolved-gas analysis.

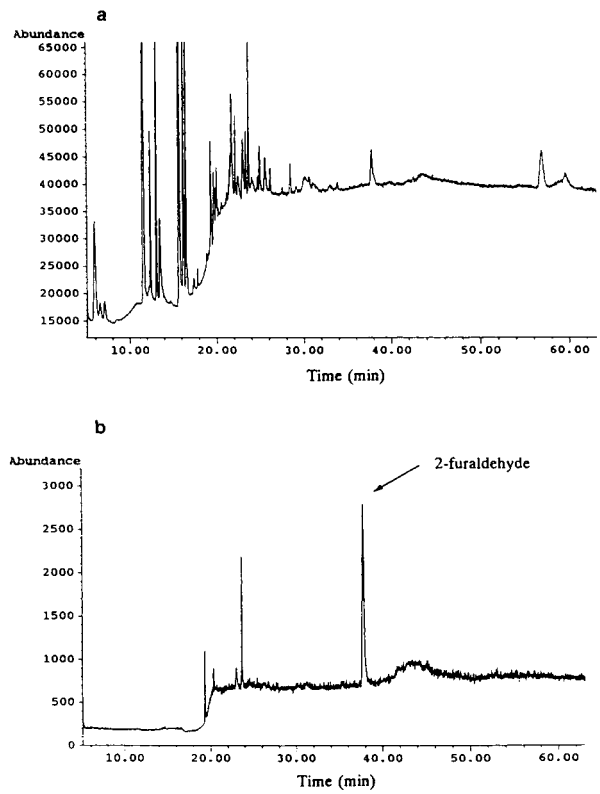

Fig. 5. Selected ions chromatograms of an in-service oil sample with 2-furaldehyde. (a) Total from selected-ion chromatograms (m/z = 29, 37, 38, 39, 95, 96, 97, 98, 110 and 112) and (b) ion chromatogram of m/z = 96.

ACKNOWLEDGMENTS

The authors would like to thank the Hydro-Québec's Direction Appareillage for funding this project. We are grateful to the Fonds FCAR of Québec for a Graduate Fellowship awarded to Y.L.

REFERENCES

1 J. Galand, M. Thibault, F. Viale, J. Samat and P. Vuarchex, *Rev. Gen. Elect.*, 81 (1972) 727–739.
2 M. Duval, F. Langdeau, G. Bélanger and P. Gervais, *Minutes of the 55th International Conference of Doble Clients*, Doble Engineering Co., Watertown, MA, 1988, Section 10, pp. 7.1–7.10.
3 M. Duval, *IEEE Electr. Insul. Mag.*, 5 (1989) 22–27.
4 P.J. Burton, M. Carballeira, M. Duval, C.W. Fuller, J. Graham, A. de Pablo, J. Samat and E. Spicar, presented at the *Conférence Internationale des Grands Réseaux Électriques, Paris, 1988*, paper 15-08.
5 F.P. DiSanzo, G.L. Johnson, V.J. Giarrocco and P. Sutton, *J. Chromatogr. Sci.*, 26 (1988) 77–79.
6 D.H. Shroff and A.W. Stannett, *Proc. IEEE*, 132 (1985) 312–319.
7 P.J. Burton, J. Graham, A.C. Hall, J.A. Laver and A.J. Oliver, presented at the *Conférence Internationale des Grands Réseaux Électriques, Paris, 1984*, paper 12-09.
8 *Annual Book of ASTM Standards*, American Society for Testing and Materials, Watertown, PA, 1988, method D3612.
9 *Publication 567*, International Electrotechnical Commission, Geneva, 1977.
10 Y. Leblanc, R. Gilbert, J. Hubert and M. Duval, *J. Chromatogr.*, 633 (1993) 185–193.
11 J. de Zeeuw, R.C.M. de Nijs and L.T. Henrich, *J. Chromatogr. Sci.*, 25 (1987) 71–83.
12 J. de Zeeuw, R.C.M. de Nijs, J.C. Buyten, J.A. Peene and M. Mohnke, *J. High Resolut. Chromatogr. Chromatogr. Cummun.*, 11 (1988) 162–167.
13 P. Fuchs, *Fresenius' Z. Anal. Chem.*, 333 (1989) 738.
14 J. Röper and W. Kochen, *Fresenius' Z. Anal. Chem.*, 333 (1989) 747.
15 H.-J. Schaeffer, *J. High Resolut. Chromatogr.*, 12 (1989) 69–81.
16 R.L. Firor, *Am. Lab.*, 22 (1989) 26–28.
17 M. Duval and Y. Giguère, *Minutes of the 51st International Conference of Doble Clients*, Doble Engineering Co., Watertown, MA, 1988, Section 10, pp. 1–6.

Journal of Chromatography A, 657 (1993) 119–122
Elsevier Science Publishers B.V., Amsterdam

CHROM. 25 252

Flash pyrolysis–gas chromatography of the kerogen and asphaltene fractions isolated from a sequence of oil shales ☆

J.C. del Río*, J. García-Mollá, F.J. González-Vila and F. Martín

Instituto de Recursos Naturales y Agrobiología de Sevilla, CSIC, P.O. Box 1052, 41080-Seville (Spain)

(First received December 10th, 1992; revised manuscript received April 24th, 1993)

ABSTRACT

Molecular characterization of the kerogen and asphaltene fractions isolated from three oil shales taken at increasing depth from the same deposit was carried out by means of flash pyrolysis–gas chromatography. Pyrolysis products were detected by simultaneous flame ionization detection and sulphur-selective flame photometric detection using a stream splitter at the end of the capillary column. *n*-Alkanes, *n*-alk-1-enes and sulphur compounds represent the major pyrolysis products of both kerogen and asphaltene fractions. Organosulphur compounds were only detected in the kerogen fractions and were completely absent from the asphaltene fractions. A sequential removal of thiophenes was observed in the set of kerogens. It is suggested that breakdown of sulphur–sulphur and carbon–sulphur bonds may occur preferentially in the kerogen macromolecule rather than the breakdown of carbon–carbon bonds to give rise to the asphaltenes.

INTRODUCTION

As is well known, knowledge of the chemical nature of asphaltenes and kerogens may help in a better understanding of the source of precursor materials, the environmental conditions of deposition and the type of diagenetic, catagenetic and maturation processes.

Flash pyrolysis–gas chromatography (Py–GC) is one of the most important analytical tools for the structural characterization of insoluble organic materials present in such samples. Hydrocarbons produced by pyrolysis of kerogens and their precursors have been investigated for many years [1–3].

Today, an important goal in fossil fuel geochemistry is the determination of the amounts and types of organically bound sulphur in sedimentary organic matter since sulphur moieties play a key role in polycondensation processes leading to macrostructures such as kerogens. Sulphur compounds are well known constituents of fossil macromolecules and occur in a variety of molecular structures, including aliphatic thiols, mono- and disulphides and aromatic structures such as alkylated thiophenes, benzothiophenes and dibenzothiophenes [4,5]. In this work we study the pyrolysis behaviour of kerogens, and their related asphaltenes, isolated from a set of Spanish oil shales, in order to get insight into the structure of these materials. We focused our interest on the nature of the sulphur compounds produced in the pyrolysis using simultaneous flame ionization detection (FID) and sulphur-selective flame photometric detection (FPD).

* Corresponding author.

☆ Presented at the *21st Scientific Meeting of the Spanish Group of Chromatography and Related Techniques*, Granada, October 21–23, 1992.

0021-9673/93/$06.00

EXPERIMENTAL

The oil shale samples were taken from the Puertollano (Ciudad Real, Spain) deposit. The geological setting of this oil shale, from the Stephanian B, has already been described [6]. Three samples were collected at the Emma Mine, at increasing depth (Emma A, B and C).

Raw oil shale samples were milled and extracted exhaustively with methylene chloride–methanol (1:1). Minerals were removed by successive treatments with 20% HCl (12 h, 60°C) and HCl–HF (1:1) (24 h, 60°C, twice). The leached material was extensively washed and extracted with water until it was free of chloride ions. The dried residues (kerogens) were then analysed by flash Py–GC. Alternatively, aliquots of the oil shale extracts were dissolved in a minimum amount of chloroform and the asphaltene fractions precipitated with *n*-pentane. Asphaltenes were separated by centrifugation, and the pentane subsequently removed by decanting. The precipitation process was repeated twice in order to purify the asphaltenes.

The samples (20–40 mg) were pyrolysed at a temperature setting of 800°C for 20 s, using a Chemical Data System (CDS) Pyroprobe 122 system. The pyrolysates were rapidly removed from heated interface (300°C) by a stream of helium onto a 30 m × 0.25 mm I.D. fused-silica capillary column coated with DB-5 (J & W Scientific) in a Varian 3300 gas chromatograph equipped with an effluent splitter and both flame ionization and flame photometric detectors. The column temperature was held at −25°C for 4 min and raised to 300°C at a rate of 4°C/min. Helium was used as carrier gas. Tentative identification of the FPD peaks was made by comparison with chromatograms already published. Differentiation of some isomer clusters was also accomplished by GC–MS analyses.

RESULTS AND DISCUSSION

The kerogen and asphaltene fractions isolated from the selected oil shale samples were pyrolysed and the thermal degradative products analysed on-line by GC with simultaneous FID and FPD. Fig. 1 shows the FID and FPD

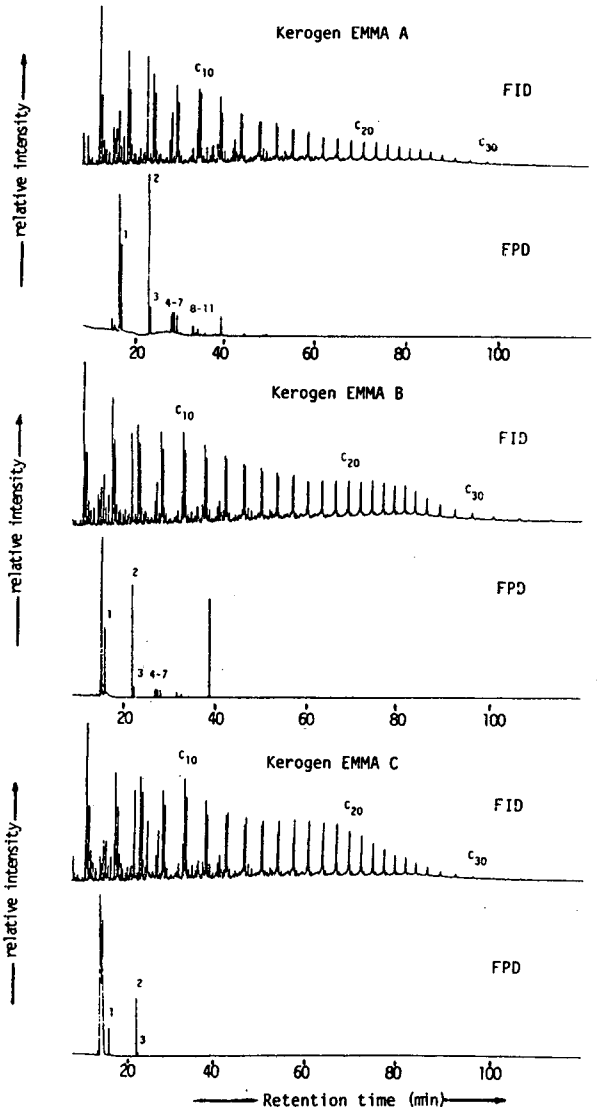

Fig. 1. Flash pyrolysis–gas chromatograms (FID and FPD traces) of the kerogen fractions isolated from the Puertollano oil shales Emma A, B and C (numbers in the FPD trace refer to the organosulphur compounds listed in Table I).

chromatograms of the kerogen pyrolysates. Peak identifications for the sulphur compounds in the FPD trace are reported in Table I. The pyrograms were dominated by a series of doublets consisting of *n*-alk-1-enes and *n*-alkanes ranging up to C_{31}. This fact confirms the high aliphatic character of the kerogen fraction isolated from the Puertollano oil shale. This character probably arises from a highly aliphatic and resistant

TABLE I

SULPHUR COMPOUNDS IDENTIFIED IN THE PYROLYSATES

1	Thiophene
2	2-Methylthiophene
3	3-Methylthiophene
4	2-Ethylthiophene
5	2,5-Dimethylthiophene
6	2,4-Dimethylthiophene
7	2,3-Dimethylthiophene
8	2-Ethyl-5-methylthiophene
9	2-Ethyl-4-methylthiophene
10	2,3,5-Trimethylthiophene
11	2-Methyl-5-vinylthiophene

biomacromolecule of present-day and extant organisms that has been selectively preserved during diagenesis [7]. These biomacromolecules can explain the high aliphatic character of the kerogen fractions studied here, and the series of *n*-alkanes and *n*-alk-1-enes produced in the pyrolysis. A slight trend towards the production of higher hydrocarbons was observed in going from sample A to B and C. The main aromatic compounds identified in the pyrolysates (benzene, toluene and xylenes) were only found in minor amounts. Prist-1-ene, thought to be derived from the thermal breakdown of macromolecularly bound tocopherols [8], was not found in any of the kerogen pyrolysates.

The FPD pyrograms of the kerogen fractions revealed that thiophene and C_1–C_3 alkylated thiophenes were the major sulphur-containing pyrolysis products. Hydrogen sulphide was not produced in the pyrolysis, indicating the absence of sulphide and/or polysulphide moieties in the kerogen fractions isolated from the Puertollano oil shales. It may be possible that these moieties are lost in preference to thiophenic structures.

Each alkylthiophene cluster presents a limited number of isomers. This is an indication that the thiophenic compounds present in the kerogen would be formed from breakdown of pre-existing thiophenic molecules in the kerogen and not from reaction of sulphur (or H_2S) with organic radicals during pyrolysis. The kerogen fractions isolated from the Puertollano oil shale showed a predominance of compounds derived from moieties with linear carbon skeletons (2-alkyl- and 2,5-dialkylthiophenes). Nevertheless, the contribution of branched/isoprenoid structures (2,3-dialkyl- and 2,3,5-trialkylthiophenes) is considerable, as they correspond to nearly 15% of the alkylthiophenes.

The organically bound sulphur is probably formed by incorporation of inorganic sulphur species into functionalized precursor lipids during early diagenesis. The sulphur compounds are incorporated into kerogens, which with increasing maturity become more aromatic and are released upon pyrolysis as aromatic thiophenes.

The FID pyrograms of the asphaltenes isolated from the same oil shales are shown in Fig. 2. They show a predominance of hydrocarbons extending up to C_{35}, further than in the kerogen pyrolysates. However, examination of the FPD pyrograms of the asphaltene fractions (not shown here) showed that no sulphur compounds were present. This would suggest that breakdown of the kerogen may occur preferentially at the sulphur bridges. It may be possible that the preferential breakdown of the thiophene bridges present in the macromolecular structure of the kerogen will release smaller fragments, giving rise to the formation of asphaltene moieties, in

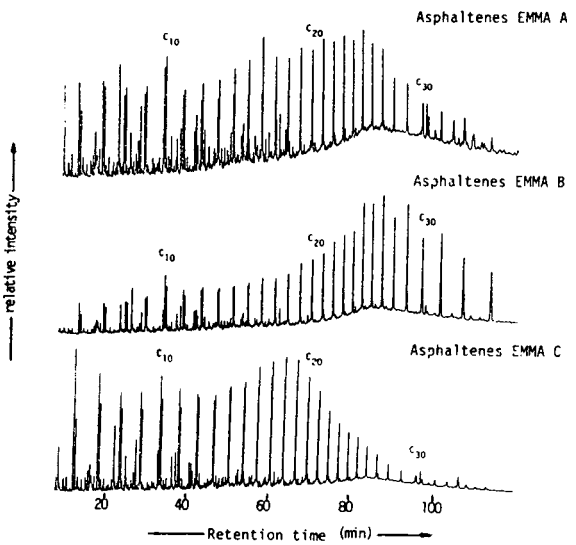

Fig. 2. Flash pyrolysis–gas chromatography (FID trace) of the asphaltene fractions isolated from the Puertollano oil shales Emma A, B and C.

agreement with the fact that asphaltenes are thought to be essentially small solubilized kerogen fragments [9]. In fact, sulphur–sulphur and sulphur–carbon bonds are weaker than carbon–carbon bonds [10,11]. This result would suggest that the S-containing moieties, as thiophenes, are mainly bound to the macromolecular matrix by C–S bonds. The presence of these weak bonds lowers the maximum of the activation energy distribution for the thermal degradation. Thus, it is well known that sulphur-rich kerogens exhibit a much lower Rock–Eval T_{max} than sulphur-poor kerogens of the same maturity [12,13]. These results would support the idea that the organic sulphur is, at least partially, responsible for the early petroleum generation from S-rich kerogens. Organically bound sulphur has been implicated in the formation of low-API-gravity[a], asphaltene-rich petroleums at a low level of thermal exposure [11].

CONCLUSIONS

The kerogen and asphaltene fractions isolated from a set of oil shales from the Puertollano deposit were analysed by flash pyrolysis–gas chromatography with simultaneous FID and FPD. This technique proved to be useful in getting insight into the macromolecular structure of the geopolymers (asphaltene and kerogen) isolated from the selected oil shales. The main compounds produced were series of *n*-alkanes and *n*-alkenes arising probably from the presence of a highly aliphatic and resistant biopolymer in their structure. Sulphur compounds were only detected in the pyrolysis of the kerogens, suggesting that sulphur–sulphur and sulphur–carbon bonds may be preferentially broken down rather than the carbon–carbon bonds in the kerogen macromolecule to give rise to the asphaltenes. A lack of H_2S has been observed in the kerogen pyrolysates, suggesting that (poly)sulphide moieties are removed preferentially during diagenesis and maturation, rather than thiophenic moieties.

[a] API = American Petroleum Institute. °API gravity is a measure of the specific gravity of a crude oil.

REFERENCES

1 D. van de Meent, S.C. Brown, R.P. Philp and B.R.T. Simoneit, *Geochim. Cosmochim. Acta*, 44 (1980) 999–1013.
2 S.R. Larter, in K.J. Voorhees (Editor), *Analytical Pyrolysis Techniques and Explorations*, Butterworths, London, 1984, 212–275.
3 R.P. Philp, A. Bakel, A. Galvez-Sinibaldi and L.H. Lin, *Org. Geochem.*, 15 (1988) 915–926.
4 W.L. Orr and C.M. White (Editors), *Geochemistry of Sulfur in Fossil Fuels* (*ACS Symposium Series*, No. 429), Americal Chemical Society, Washington, DC, 1990.
5 J.S. Sinninghe Damsté and J.W. de Leeuw, *Fuel Processing Technology*, 30 (1992) 109–178.
6 R.H. Wagner, *Ann. Fac. Cienc., Porto*, 64 (1985) 171–231.
7 E.W. Tegelaar, J.W. de Leeuw and C. Saiz-Jimenez, *Sci. Total Environm.*, 81/82 (1989) 1–17.
8 H. Goossens, J.W. de Leeuw, P.A. Schenck and S.C. Brassell, *Nature*, 312 (1984) 440–442.
9 B.P. Tissot and D.H. Welte, *Petroleum Formation and Occurrence*, Springer, Heidelberg, 2nd ed., 1984.
10 E. Tannenbaum and Z. Aizenshtat, *Org. Geochem.*, 8 (1985) 181–192.
11 W.L. Orr, *Org. Geochem.*, 10 (1986) 499–516.
12 T.I. Eglinton, J.S. Sinninghe Damsté, M.E.L. Kohnen, J.W. de Leeuw, S.R. Larter and R.L. Patience, in W.L. Orr and C.M. White (Editors), *Geochemistry of Sulfur in Fossil Fuels* (*ACS Symposium Series*, No. 429), American Chemical Soceity, Washington, DC, 1989, pp. 529–565.
13 T.I. Eglinton, J.J. Sinninghe Damsté, M.E.L. Khonen and J.W. de Leeuw, *Fuel*, 69 (1990) 1394–1404.

Journal of Chromatography A, 657 (1993) 123–129
Elsevier Science Publishers B.V., Amsterdam

CHROM. 25 570

Analysis of replacement chlorofluorocarbons using carboxen microtraps for isolation and preconcentration in gas chromatography–mass spectrometry

S.J. O'Doherty*, P.G. Simmonds and G. Nickless

Biogeochemistry Centre, University of Bristol, Cantocks Close, Bristol BS8 1TS (UK)

(Received July 12th, 1993)

ABSTRACT

A microtrap containing a mixture of Carboxen 1000/1003 has successfully been developed for trapping and preconcentrating the very volatile replacement chlorofluorocarbons (CFCs) (fluorinated hydrofluorocarbons and hydrochlorofluorocarbons) from sample volumes of several litres. We have shown that a mixture of replacement CFCs can be quantitatively adsorbed and desorbed when a Carboxen-filled microtrap is held at −50°C, thus negating the need for cryotrapping, or cryofocussing using liquid nitrogen. The adsorbed compounds are rapidly desorbed by the direct ballistic heating of the microtrap to a temperature of 260°C in about 4 s. The application of these microtraps in the automated GC–MS analysis of the replacement CFCs and other environmentally important trace gases is presently under development in our laboratories for eventual deployment in remote atmospheric monitoring stations.

INTRODUCTION

The replacement chlorofluorocarbons (CFCs) fall into two groups, the hydrochlorofluorocarbons (HCFCs) and the fluorinated hydrofluorocarbons (HFCs), this latter term will be used to describe all of the replacement CFCs in this paper. Introduction of hydrogen atoms into the CFC molecule reduces the molecular energy, and hence the stability resulting in oxidative destruction of the HFCs in the troposphere, primarily by OH radical attack. The ozone depleting potentials of the HFCs is typically zero to ten percent that of CFCs and from 10 to 100 times less in terms of atmospheric warming potential [1–3]. Industrial sources indicate that, at the present time, the following HFCs are the most likely to be used as replacements; HFC 125, 143a, 134a, 22, 124, 142b and 123. The chemical formulae, molecular masses, and boiling points are listed in Table I.

Methods for the analysis of atmospheric trace constituents include canister and cartridge sampling [4,5], and whole air cryotrapping with a post desorption cryofocussing step using liquid nitrogen [6–10]. There are logistic difficulties in supplying liquid nitrogen to remote locations on

TABLE I

PHYSICAL CHARACTERISTICS HFCs

Compound	Structure	Boiling point (°C)	M_r
HFC 125	CF_3CF_2H	−48.4	120
HFC 143a	CF_3CH_3	−47.6	84
HCFC 22	$CHClF_2$	−40.8	86
HFC 134a	CF_3CH_2F	−25.9	102
HCFC 124	CF_3CFHCl	−11.8	136
HCFC 142b	CH_3CF_2Cl	−9.8	101
HCFC 123	CF_3CHCl_2	28.0	152

* Corresponding author.

0021-9673/93/$06.00

a routine basis, and the cost can be over US $100/(day · system) [11]. An alternative approach employs microtraps filled with a suitable adsorbent which allows direct thermal desorption into a capillary column thereby bypassing the cryofocussing step [12–15]. We have followed and improved this approach using very small microtraps filled with carbon molecular sieve type adsorbents ("Carboxens"). However, to achieve adequate sensitivity for mass spectral detection of the HFCs at ppt (v/v) concentrations they must be quantitatively trapped from several litres of air. Clearly for compounds such as HFCs, which are not strongly retained by most of the commonly used adsorbents, the need to trap large sample volumes conflicts with the design of a microtrap containing a minimal amount of adsorbent. In an earlier paper [16] we described how this problem could be solved, using Carboxen-filled microtraps for the preconcentration of very volatile HFCs at sub ambient temperatures by maintaining the microtrap in a small dewar cooled to a temperature of −50°C using a Neslab Cryocool Immersion cooler (Portsmouth, UK), thus avoiding the use of liquid nitrogen. To achieve optimal chromatographic resolution and efficiency it is important to match the dimensions of the microtrap and the gas flows to those of the capillary column. It is also desirable to heat the trap as rapidly as possible to prevent band spreading during the desorption stage. We present here the means by which the trapped HFCs can be quantitatively desorbed from the Carboxen microtraps directly onto a capillary column connected to a Finnigan MAT ion trap mass spectrometer.

EXPERIMENTAL

Microtraps

The design of the microtraps used in the experiments can be used in Fig. 1. The length of the microtraps and the amount and type of Carboxen material used could be varied to suit the type of analysis being carried out. However, the small dimensions of the trap coupled with the small quantity of adsorbent used in these experiments is consistent with the objective of maintaining rapid desorption and efficient chromatographic resolution. The microtraps were maintained at −50°C by cooling the airspace in a sealed dewer, using a Cryocool Immersion cooler. The microtraps were heated in early experiments by applying 60 V a.c. from a variable transformer to an external heating wire wrapped round the trap, this raised the temperature to approximately 260°C in 10 s. A more rapid method of heating was subsequently adopted by the use of direct resistive heating of the microtrap itself.

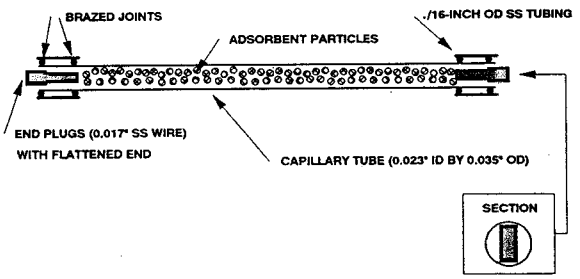

Fig. 1. Microtrap (overall length 18 cm). SS = Stainless steel; " = inch (1 inch = 2.54 cm).

Sample preconcentration

The major components of the sample preconcentration system are illustrated in Fig. 2. All tubing used was SS 306 (stainless steel) (1/16 or 1/8 in. O.D.), connections were made either by stainless steel Swagelok or Valco fittings. A

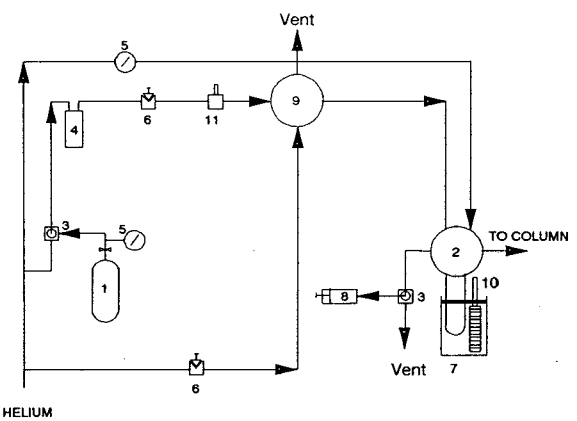

Fig. 2. Cryogenic preconcentration apparatus. 1 = Sample canister; 2 = 6-port valve; 3 = 3-way valve; 4 = Nafion drier; 5 = pressure regulator; 6 = needle valve; 7 = sample loop in a dewer; 8 = volume measurement; 9 = 4-port valve; 10 = cryoprobe; 11 = toggle valve.

standard HFC mixture was contained in a 30-l electropolished stainless steel canister. The canister was connected to a 3-way valve (Whitey ss-41xs2), which permitted either sample or helium to be passed through a drier, which consisted of nafion tubing in a container packed with molecular sieve 5A [17]. The flow-rate was controlled using a Nupro fine metering valve. Two Valco valves were used, the first 4-port valve enabled the system to this point be purged with helium or sample. The second valve, a 6-port switching valve, allowed sample or helium to be passed through the trap in one mode (sample or helium purge mode), in the other mode (desorption mode) helium column flow passed through the trap. The second 3-way valve (Hamilton, HVP 3-3) and syringe enabled determination of the volume of sample passed through the microtrap.

Gas chromatography–mass spectrometry (GC–MS) conditions

All experiments were carried out using a Finnigan ITS-40 GC–MS apparatus. Separation of the HFC mixture was carried out using two separate columns (a) CPSil-5 50 m, 0.32 mm I.D., 5-μm film thickness wall-coated open tubular (WCOT) capillary column, (b) Alumina Al_2O_3/KCl 50 m, 0.32 mm I.D., 5-μm film thickness porous-layer open tubular (PLOT) capillary column. The GC–MS conditions used in the experiments can be seen in Table II. Detailed chromatographic separations of a large number of HFCs and CFCs have been reported elsewhere [18].

TABLE II

GC–MS CONDITIONS

Conditions	CPSil-5 column	Al_2O_3/KCl column
GC conditions		
Carrier gas	Helium	Helium
Flow rate (ml/min)	1	1
Oven	30°C isothermal	30°C hold 3 min 15°C/min, 180°C hold 12 min
Transfer line (°C)	50	180
MS conditions		
Mass scan range	15–170	15–170
Acquire time (min)	10	30
Peak threshold	10	10
Mass defect	0	0
Ionization mode	Electron impact	Electron impact
Auto gain control	On	On

RESULTS AND DISCUSSION

Carboxen 1003 using CP Sil-5 column

A microtrap containing Carboxen 1003 (30 cm × 0.058 cm I.D., 22 mg, 60/80 mesh), previously tested for its adsorptive properties, using methods described in an earlier paper [16], appeared to have a similar capacity to that of Carboxen 1000 (the strongest HFC absorber) for a number of HFC compounds. Desorption tests with this adsorbent were carried out at room temperature followed by tests at −50°C. Initial observations indicates that complete desorption of the HFCs, especially the higher boiling ones, was not possible at the heating rate employed (60 V a.c. for 10 s), the trap was heated 4 times before complete desorption was effected. Using a digital thermometer with a thermocouple connected directly to the trap the heating rate and maximum temperature achieved was monitored for different Variac output voltages. The optimum heating rate was determined by replicate desorptions from the Carboxen 1003 trap, while noting each HFCs peak area, peak width at half height and retention time. Fig. 3 illustrates the effect of altering the desorption heating rates on peak shape, as expected, the faster heating rate produces more efficient and better resolved peaks.

Using the optimised desorption heating rate (140 V a.c. for 2 s), increasing amounts of HFC mixture were adsorbed/desorbed from the trap and the regression lines for each HFC plotted. As can be seen from Figs. 4 and 5, each HFC standard can be quantitatively adsorbed/desorbed from Carboxen 1003 at room temperature for volumes ranging from 1–25 ml. However, in practice, where it is necessary to quantitatively trap trace amounts of HFCs from several litres of air then the microtrap must be cooled. A num-

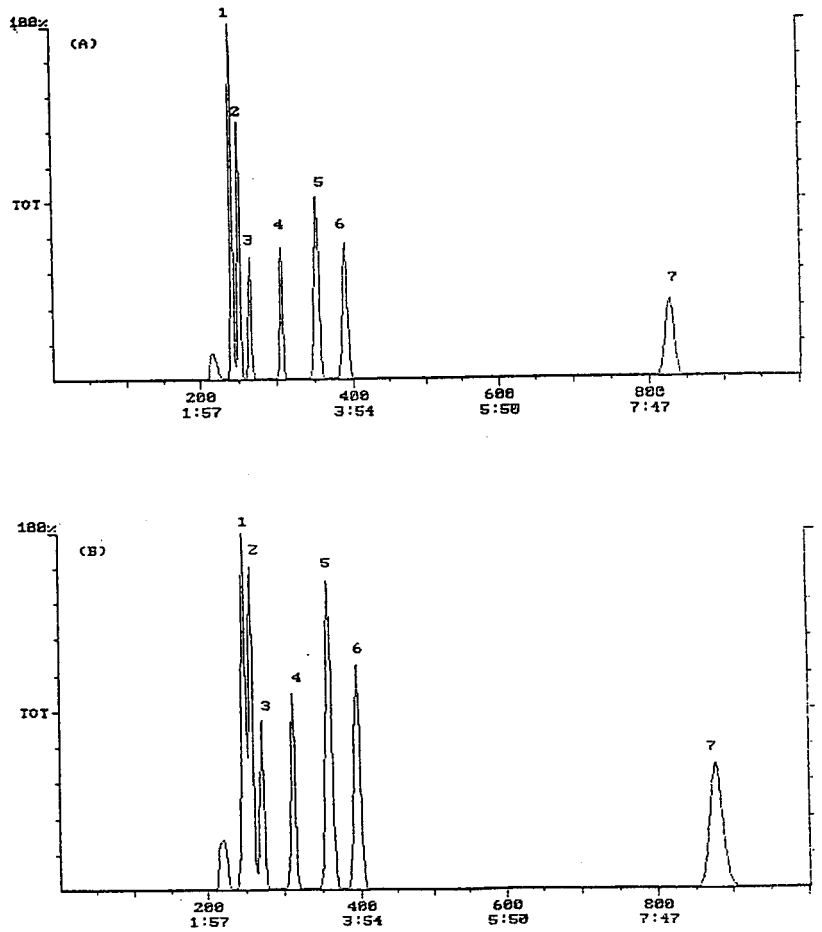

Fig. 3. Effect of different desorption heating rates on peak shape. (A) 140 V a.c. for 2 s; (B) 60 V a.c. for 10 s. Peaks; 1 = 125; 2 = 143a; 3 = 134a; 4 = 22; 5 = 124; 6 = 142b; 7 = 123. Scales on *x*-axis: (top) scan No.; (bottom) time in min:s.

ber of problems were encountered as soon as the trap was cooled using the Cryocool probe. Firstly the trap contained approximately twice the quantity of adsorbent necessary to quantitatively trap the least retained HFC at −50°C. This excess volume of adsorbent made it difficult to efficiently desorb the HFC standard at sub-ambient temperatures. Although, the trap heating rate was not affected significantly by the sub-ambient temperature, the post-desorption cooling rate was much more rapid resulting in possible readsorption of the HFCs before they have had a chance to leave the trap thereby compromising resolution and quantitation of the most volatile HFCs. Secondly, a problem of co-elution of residual contaminant compounds such as carbon dioxide, nitrogen, water and oxygen can induce ion-molecule reactions which adversely affects quantitation of the early eluting HFCs. It has been reported [19] that when a trap is heated, any exogenous water collected on the trap will be transferred onto the GC column along with the compounds of interest, the water coats the column this creates a negative solvent effect and disrupts the proper interaction of the analytes with the column stationary phase. This could result in broadened peaks, reduced sensitivity and unstable quantitative % R.S.D.s, especially for those compounds that elute before or with the water; in addition reconstructed ion chromatography (RIC) baseline drop off at the end of water peak elution causes unstable area

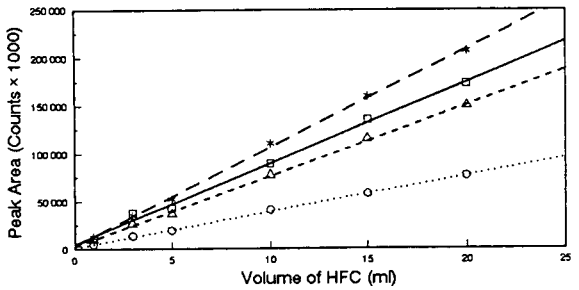

Fig. 4. Quantitation of Carboxen 1003 using total ion current (TIC) for HFC mixture at room temperature. Correlation coefficients: 125 (□) = 0.995; 143a (△) = 0.999; 134a (○) = 0.998; 142b (*) = 0.998.

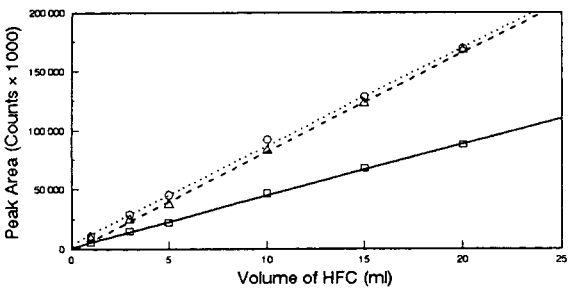

Fig. 5. Quantitation of Carboxen 1003 using TIC for HFC mixture at room temperature. Correlation coefficients: 22 (□) = 0.999; 124 (△) = 0.999; 123 (○) = 0.998.

peak counts for analytes that elute in the same region. Finally, background water can result in the loss of molecular ion intensity for some compounds due to a combination of charge exchange and proton transfer with water.

The preferred solution to these problems is to use the minimum amount of Carboxen adsorbent necessary for quantitative trapping of the least retained HFC, and to increase the retention time of the early eluting HFCs relative to the contaminant compounds.

Carboxen 1000 using alumina PLOT column

An alumina/KCl PLOT capillary column was used as an alternative to the CPSil-5 column since other studies carried out in our laboratory indicated that the HFCs and potential contaminants were better separated. However, it had also been previously reported from a number of separate sources [20–22] that owing to the basicity of alumina PLOT columns, they showed a

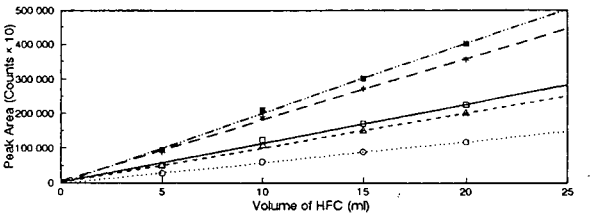

Fig. 6. Quantitation of Carboxen 1000 with HFC mixture using TIC results (alumina PLOT column). Trap at room temperature. Correlation coefficients: 143a (□) = 0.990; 125 (△) = 0.996; 134a (○) = 0.998; 142b (*) = 0.998; 124 (■) = 0.998.

tendency to cause dehydrohalogenation of some HFCs. Also from earlier adsorbent studies using both direct and indirect methods to test adsorbent performance [17] Carboxen 1000 was found to be the strongest adsorbent for the lowest boiling HFCs. Therefore, a microtrap containing Carboxen 1000 was tested to determine if the HFCs could also be efficiently desorbed. A microtrap containing only 11 mg of Carboxen 1000 (18 cm × 0.058 cm I.D., 10 cm active length, 45–60 mesh) was subjected to the same tests described above for the Carboxen 1003 adsorbent. Figs. 6–8 illustrate that all of the HFCs except HFC 22 and the highest boiling HFC 123 can be quantitatively trapped and

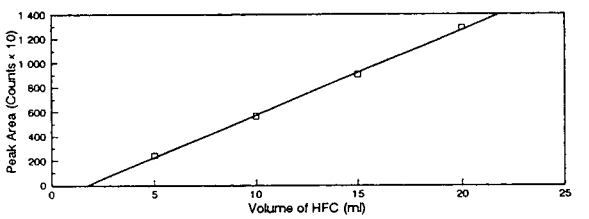

Fig. 7. Quantitation of Carboxen 1000 with HFC mixture using TIC results (alumina PLOT column): 22. Trap at room temperature. Correlation coefficient = 0.998.

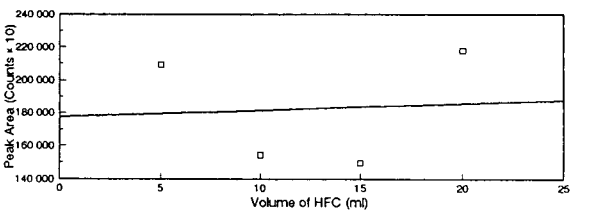

Fig. 8. Quantitation of Carboxen 1000 with HFC mixture using TIC results (alumina PLOT column): 123. Trap at room temperature. Correlation coefficient 0.005.

desorbed at room temperature, for standard sample volumes between 5 and 20 ml. Interestingly, Fig. 7 shows that HFC 22 is not only dehydrohalogenated but dehydrohalogenated quantitatively as indicated by a correlation coefficient close to the value of 1 and a negative intercept. Fig. 8 shows that no correlation exists between the amount of HFC 123 trapped and the amount desorbed, suggesting that Carboxen 1000 traps HFC 123 so strongly that it cannot be efficiently desorbed at the temperatures currently employed (*ca.* 260°C). Subsequent experiments revealed that CFC 123 is strongly retained and possibly dehydrohalogenated by the Alumina PLOT column which adversely affects its quantitation. It is clear from the above results that Carboxen 1000 is the adsorbent of choice for the low boiling HFCs, but perhaps too strong an adsorbent for the higher boiling HFCs. It was not necessary to continue further tests, at sub-ambient temperatures, since this would only accentuate the problem by increasing the adsorbents capacity. The logical progression from this point is to use a combination microtrap with a weaker adsorbent material in front of Carboxen 1000, so that the higher boiling HFCs would be trapped before reaching the Carboxen 1000. Any lower boiling HFCs, which break through the first adsorbent would be retained by the Carboxen 1000, thus enabling all HFCs to be quantitatively trapped and desorbed.

Carboxen 1003 and Carboxen 1000 dual adsorbent microtrap

A dual adsorbent microtrap containing Carboxen 1003 (6 mg) and Carboxen 1000 (5 mg) (24 cm × 0.058 cm I.D., 14 cm active length, 60–80 mesh) was tested using the same procedure as previously described. Since the CPSil-5 column was currently installed in the ITS-40, it was decided that quantitation of the less volatile HFCs (22, 142b, 124 and 123) would be carried out using this column, and quantitation of the most volatile HFCs (143a, 125 and 134a) would be carried out using the alumina PLOT column. This procedure for quantitation was also necessary since it has been previously demonstrated that the alumina PLOT column dehydrohalogenates HFC 22, and other CFCs and halocarbons.

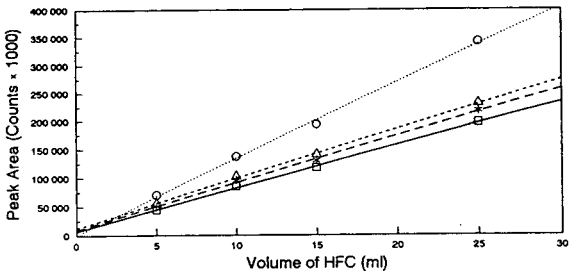

Fig. 9. Quantitation of a mixed Carboxen trap used to trap increasing volumes of HFC mixture (CPSil-5). Correlation coefficients; 22 (□) = 0.999; 124 (△) = 0.999; 142b (○) = 0.997; 123 (*) = 0.998. Trap at −50°C.

The results shown in Fig. 9 indicate that the less volatile HFCs can be quantitatively trapped and desorbed from a mixed Carboxen trap maintained at a sub ambient temperature of −50°C, in addition to this Fig. 10 shows that each of the HFCs (with the exception of HFC 124), can be trapped and will not be displaced even after passing 2 l of helium through the trap before the compounds are desorbed. Interestingly, if quantitation using peak heights is carried out it appears that HFC 124 is not displaced. It should be noted that HFC 123 behaves normally when desorbed onto the CPSil capillary, thereby confirming that earlier problems associated with this compound were related to losses on the alumina PLOT column and not the adsorbent.

These tests were then repeated using the alumina PLOT column. The results shown in Figs. 11 and 12 confirm the above results in addition to showing that the lower boiling HFCs can also be quantitatively trapped and desorbed at sub-ambient temperatures.

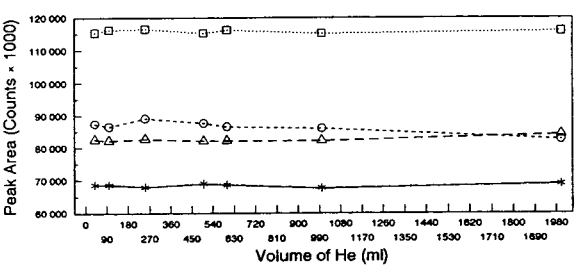

Fig. 10. Peak area *vs.* desorption of 10 ml of HFC sample after passing increasing volumes of helium through mixed Carboxen trap. CPSil-5 column; trap at −50°C. * = 22; ○ = 124; □ = 142b; △ = 123.

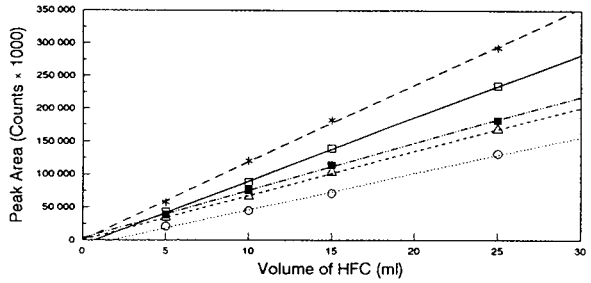

Fig. 11. Quantitation of a mixed Carboxen trap used to trap increasing volumes of HFC mixture (alumina PLOT column). Trap at −50°C. Correlation coefficients: 143a (□) = 0.999; 125 (△) = 0.999; 134a (○) = 0.997; 142b (*) = 0.999; 124 (■) = 0.999.

CONCLUSIONS

It has been shown that the very volatile HFCs can be quantitatively trapped and desorbed from a mixed Carboxen microtrap without the use of liquid cryogens. In order to determine the HFCs in ambient air we have assumed a basic detection threshold to be 1 ppt (v/v). For a compound such as HFC 142b with a molecular mass of 101 this is equivalent to $4.5 \cdot 10^{-15}$ g. Hence, with a mass spectrometer sensitivity of 10 picograms this would necessitate concentration of the compound from about 2.2 litres of ambient air. The results presented here indicate that it would be possible to trap and preconcentrate the HFCs from a 2–3 l air sample. In addition, a main concern was that by desorbing from a microtrap at a flow-rate of 1 ml/min (governed by the maximum flow-rate into the ion trap), the peak shape and resolution of the HFCs might not be preserved, this concern was proved to be unfounded. It is clear that the design of the microtrap with its near capillary dimensions, the small amount of Carboxen material needed to trap the HFCs at −50°C and the rapid and efficient heating system provide a simple, efficient and cost effective alternative to the usual method of cryogenic trapping and cryofocussing of very volatile compounds.

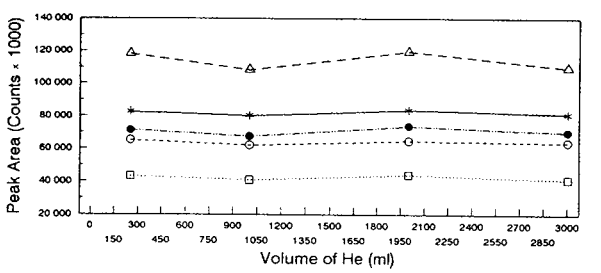

Fig. 12. Peak area *vs.* desorption of 10 ml of HFC sample after passing increasing volumes of helium through mixed Carboxen trap. Alumina PLOT column; trap at −50°C. * = 143a; ○ = 125; □ = 134a; △ = 142b; ● = 124.

REFERENCES

1 *Scientific Assessment of Stratospheric Ozone, Vol. II, Appendix: AFEAS Report, Sec. IX; Report No. 20*, World Meteorological Organization Global Ozone Research and Monitoring Project, 1989, 380–401.
2 D.A. Fisher, C.H. Hales, D.L. Filkin, M.K.W. Ko, N. Dak Sze, P.S. Connell, D.J. Wuebbles, I.S.A. Isaken and F. Stordal, *Nature*, 344 (1990) 508–516.
3 *Alternatives to Chlorofluorocarbons, Bulletin AG-1*, Freon Production Laboratory, DuPont Chemicals, Wilmington, DE, 1991.
4 F.J. Reineke and K. Bachmann, *J. Chromatogr.*, 323 (1985) 323–329.
5 S. Muller and M. Oehme, *J. High Resolut. Chromatogr.*, 13 (1990) 34–39.
6 M. Teronia and G. Alaerts, *J. Chromatogr.*, 328 (1985) 367.
7 N. Schmidbauer and M. Oehme, *J. High Resolut. Chromatogr.*, 8 (1985) 404–406.
8 T. Kohno and K. Kuwata, *J. Chromatogr.*, 587 (1991) 338–342.
9 P.V. Doskey, *J. High Resolut. Chromatogr.*, 14 (1991) 724–728.
10 N. Kirshen and E. Almasi, *J. High Resolut. Chromatogr.*, 14 (1991) 484–489.
11 E.A. Woolfenden and G.M. Broadway, *LC-GC Int.*, 5(12) (1992) 28–35.
12 J.B. Phillips, J.R. Valentin and G.C. Carle, *ASTM Spec. Tech. Publ.*, 13 (1982) 135–141.
13 W. Frank and H. Frank, *Chromatographia*, 29 (1990) 571–574.
14 K. Grob, A. Artho, C. Frauenfelder and I. Roth, *J. High Resolut. Chromatogr.*, 13 (1990) 257–260.
15 H. Frank, W. Frank, H.J.C. Neves and R. Englert, *Fresenius' J. Anal. Chem.*, 340 (1991) 678–683.
16 S.J. O'Doherty, P.J. Simmonds and G. Nickless, *J. Chromatogr.*, 630 (1993) 265–274.
17 B.E. Foulger and P.G. Simmonds, *Anal. Chem.*, 51 (1979) 1089–1090.
18 G.A. Sturrock, P.G. Simmonds and G. Nickless, *J. Chromatogr.*, 648 (1993) 423–431.
19 E. Johnson and A. Madden, *Technical Report No. 616*, Finnigan MAT, Hemel Hempstead, UK.
20 T. Noij, J.A. Rijks and C.A. Cramers, *Chromatographia*, 26 (1988) 139–141.
21 T. Noij, P. Fabian, R. Borchers, C.A. Cramers and J.A. Rijks, *Chromatographia*, 26 (1988) 149–156.
22 L. Burgess and D.M. Kavanagh, *New Fluorochemicals Team: Technical Note No. 12*, ICI Chemicals & Polymers Ltd., September 1989.

Journal of Chromatography A, 657 (1993) 131–137
Elsevier Science Publishers B.V., Amsterdam

CHROM. 25 253

Evaluation of isoflurane in air by thermal desorption–gas chromatography☆

C. Prado*, F. Periago and I. Ibarra

Instituto Nacional de Seguridad e Higiene en el Trabajo, E-30120 Murcia (Spain)

J. Tortosa

Servicio de Anestesiología, Hospital Virgen de Arrixaca, E-30120 Murcia (Spain)

(First received December 10th, 1992; revised manuscript received April 24th, 1993)

ABSTRACT

A method to quantify the exposure of operating room personnel to isoflurane has been developed. Thermally desorbable passive samplers were used to adsorb isoflurane. The anaesthetic concentration was then determined by gas chromatography. Several adsorbents were evaluated, Chromosorb 106 being the most adequate for isoflurane adsorption and thermal desorption. Additionally, a suitable calibration method for thermal desorption–GC was developed. Finally, a laboratory evaluation was carried out to determine the isoflurane sampling rate for the chosen sorbent. The effects of humidity and storage time on both the system response and reproducibility were also checked.

INTRODUCTION

There is growing evidence that occupational exposure to anaesthetic gases represents a health hazard. In general, the numerous epidemiological investigations agree fairly well that there is an excess risk of spontaneous abortion, but no agreement exists on carcinogenic and teratogenic effects [1]. It has been reported that one of the most serious shortcomings of these studies is the lack of quantitative information on the nature, degree and length of exposure to anaesthetic agents that could allow any cause–effect relationship between exposure and adverse effect to be found [2].

Isoflurane (Forane, 1-chloro-2,2,2 trifluoroethyl-difluoromethyl-ether), either alone or with nitrous oxide, has become one of the most widely used inhalation anaesthetics in operating theatres [3]. Therefore, it is important to develop simple methodologies for the determination of the exposure to isoflurane of personnel working in these environments.

The most common method for the determination of personnel exposure to gases and organic vapours is to draw air, by means of a portable pump, through a tube containing a solid sorbent able to retain the specific compound of interest. This way of sampling, called active, is not useful for the operating theatre staff, since it is undoubtedly uncomfortable. Alternatively, passive sampling does not require air-taking devices, so it offers a good and unobstrusive way of sampling.

In passive sampling, the environmental pollutant diffuses across a convection-free air zone within the sampler to a collection medium, where it is adsorbed. In most passive samplers, the adsorbed vapour is desorbed with a solvent

* Corresponding author.

☆ Presented at the *21st Scientific Meeting of the Spanish Group of Chromatography and Related Techniques*, Granada, October 21–23, 1992.

0021-9673/93/$06.00

and quantitatively measured by gas chromatography. Owing to the relatively low concentrations of isoflurane in operating theatres, solvent desorption techniques are insufficiently sensitive, since only a small amount of the collected isoflurane would be analysed. Thus, thermal desorption methods can offer some advantages, the most important being their higher sensitivity, since the whole sample is available for analysis.

The aim of this study was to develop a method to quantify the exposure of operating room personnel to isoflurane by means of thermally desorbable passive samplers. A suitable sorbent was selected, the performance of diffusive samplers for isoflurane was evaluated and the effects of humidity and storage time on sorbent capacity were checked under controlled laboratory conditions.

Finally, the use of a controlled atmosphere device for the calibration of the thermal desorption–gas chromatography system is also described.

EXPERIMENTAL

Passive samplers

The passive samplers used were the standard stainless-steel tubes for an ATD50 thermal desorption system (Perkin-Elmer, Beaconsfield, UK) (89 mm × 6.4 mm O.D.). The tubes were packed with 150 mg of a solid sorbent. Prior to use, and during storage, the tubes were protected with storage caps; when used, a diffusion cap was fitted to allow controlled exposure to the environment.

Thermal desorption–gas chromatography system

All passive samplers were desorbed by means of the ATD50 system, directly connected to a Perkin-Elmer Model 8700 gas chromatograph by a heated transfer line. Thermal desorption was done in two stages: first, the tube was heated with the carrier gas flowing through it, transferring the desorbed vapours from the sample tube to a cooled trap (packed with Tenax TA, SKC, Valley View, PA, USA). Afterwards, when the entire sample had been collected, the trap was rapidly heated to desorb the volatile materials, which were rapidly injected into the GC column via the heated transfer line.

Adsorbent selection

The solid sorbents studied were packed in the standard sample tubes and placed between the injector and the flame ionization detector of the gas chromatograph, like a column, and a given flow of carrier gas (dry nitrogen) was passed through it. A known amount of isoflurane (Forane, Abbot Laboratory, Madrid, Spain) was injected, and the volume of carrier gas required up to the beginning of the elution peak of isoflurane was calculated. Measurements were made in the 40–180°C temperature range.

Three sorbents were considered, Tenax TA, Chromosorb 102 and Chromosorb 106 (SKC).

Calibration method for the thermal desorption–gas chromatography system

Calibration standard tubes were prepared by generating an isoflurane standard atmosphere, and injecting known volumes of this through the sampling tube. Standard atmospheres of isoflurane vapour in air were dynamically generated using the syringe injection technique, as previously described [4], and were checked by active samplers consisting of activated charcoal tubes connected to the atmosphere by means of a sampling pump. In all cases the concentration measured by the activated charcoal tubes agreed to the theoretical concentration calculated from airflow and syringe speed within 10% [5], so this value of the theoretical concentration can be considered as the true concentration of isoflurane in the test atmosphere (X_{ref}). The coefficient of variation, as determined by on-line chromatography, was 4%.

Fig. 1 illustrates the system used to generate the controlled atmosphere as well as to obtain calibration standards. To do the latter, a servomotor-driven gas syringe of 50 ml capacity alternately draws from the standard atmosphere and expels the sample through the adsorbent tube, by means of both an inversion of the polarity of the motor that powers the syringe and automatic changes in the position of a three-way valve. Different volumes of air were drawn through the adsorbent tubes to obtain different calibration standards over the range required.

Determination of sampling rate and performance of diffusive samplers for isoflurane

Diffusive sampling was carried out with the

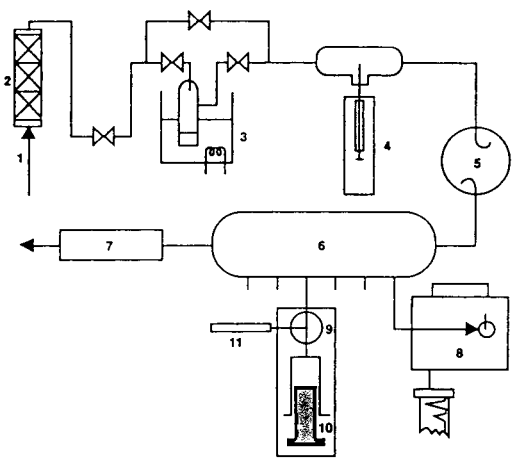

Fig. 1. Scheme of the system used to generate the controlled atmosphere and to obtain calibration standards. 1 = Air intake; 2 = filter; 3 = humidifier; 4 = automatic injector; 5 = mixing chamber; 6 = sampling chamber; 7 = humidity sensor; 8 = gas chromatograph; 9 = three-way PTFE valve; 10 = servomotor-driven syringe; 11 = adsorbent tube.

ATD50 sampling tubes packed with Chromosorb 106 having diffusive caps without membranes.

The experiments with isoflurane were performed according to the scheme shown in Table I, which is a concise version of the Instituto Nacional de Seguridad e Higiene en el Trabajo (INSHT) protocol [5]. This requires the generation of controlled atmospheres having three different concentrations of the pollutant (for isoflurane 1.3, 13 and 26 ppm were used) and the simultaneous exposure of six samplers for each one of the five experiments. The humidity of the final atmosphere could be adjusted by introducing water bubblers into the incoming airflow. A temperature of 20–25°C, a relative humidity (RH) of 40–45% and a relative air speed on the surface of the diffusive monitors of 0.7–1 m/s were used.

TABLE I

CONCISE VERSION OF THE INSHT PROTOCOL TO EVALUATE THE PERFORMANCE OF THE PASSIVE SAMPLER FOR ISOFLURANE

Concentration (ppm)	Sampling time		
	0.5 h	2 h	8 h
1.33	X		X
13.25		X	
26.50	X		X

Thermal desorption of the isoflurane collected was carried out in two stages with nitrogen as a carrier gas (68.95 kPa), an oven temperature of 240°C, 6 min of desorption time, trap lower and upper temperatures of −30 and 240°C, respectively, and a transfer line temperature of 100°C. The GC analyses were performed with a fused-silica capillary column (25 m × 0.2 mm I.D., free fatty acid phase 0.3 μm film thickness) (Hewlett-Packard, Palo Alto, CA, USA), using nitrogen at 68.95 kPa as carrier gas. The oven and detector temperatures were 90 and 200°C, respectively.

Sampling rates (diffusive uptake rates, *SR*) were calculated for each of the samplers, according to the following equation derived from Fick's law

$$SR = \frac{m}{c \cdot t} \quad (1)$$

where m is the amount of isoflurane adsorbed (ng), c is the atmosphere concentration (ppm, v/v) and t is the exposure time (min).

A set of four experiments was carried out at two different isoflurane concentrations (1.33 and 26.5 ppm) and two exposure times (90 and 480 min), to determine the effect of humidity on the uptake capacity of the adsorbent solid. In addition, samplers containing different amounts of isoflurane were stored for 2 weeks at room temperature to test storage stability.

A set of four experiments was carried out at two different isoflurane concentrations (1.33 and 26.5 ppm) and two exposure times (90 and 480 min), to determine the effect of humidity on the uptake capacity of the adsorbent solid. In addition, samplers containing different amounts of isoflurane were stored for 2 weeks at room temperature to test storage stability.

RESULTS AND DISCUSSION

Adsorbent selection

It has been reported that non-constant sampling rates are a serious drawback of the use of passive samplers for thermal desorption [6]. Some papers claim that the observed variations are functions of time solely, so that the effective

sampling rate during an actual exposure can be calculated from calibration graphs of uptake rate *versus* time [7,8]. Other studies predict reduced sampling efficiency as a function of both concentration and time [6,9,10]. In general, it is accepted that the phenomenon of decreasing uptake rates is associated with the relative strength of the adsorbent.

Adsorbents for thermal desorption should show, on the one hand, high adsorptivity to ensure that the rate of sample concentration is constant over the period of exposure and, on the other hand, sufficiently low adsorptivity to allow complete thermal desorption. So, it is very important to select the more adequate adsorbent to each pollutant, especially in this case because isoflurane is a very volatile compound.

Three adsorbents were checked: Tenax TA, Chromosorb 102 and Chromosorb 106. The plots of the logarithm of the "initial specific retention volume" *versus* reciprocal absolute temperature for the three adsorbents are shown in Fig. 2. From this plot the specific retention volumes at 20°C can be calculated, being 45.2, 7.3 and 0.2 l/g for Chromosorb 106, Chromosorb 102 and Tenax TA, respectively.

These calculated values seem to be low, since it has been reported that to ensure the adsorbent is strong enough the retention volume should exceed 60 l per g of adsorbent at room temperature. However, in special cases, weaker adsorbents may be used [7], and it is to be considered that the values reported here are for initial, not overall, specific retention volumes.

The values obtained indicated that Chromosorb 106 was the strongest adsorbent of the three evaluated, while Tenax had the lowest adsorption capacity, under the experimental conditions used in the present work. However, the use of Tenax for isoflurane collection has been described previously [11].

Based on the above-mentioned results, Chromosorb 106 was initially chosen as the adsorbent. Its strength was then tested in order to ensure that it would be able to give a constant sampling rate. Thus, sampling rates were calculated for a wide range of concentrations (between 1.3 and 27.2 ppm) and times (between 30 and 480 min) for a set of six samplers for each of the experiments.

Fig. 3 shows the average values of sampling rates for all six samplers under the different conditions tested. There were no significant changes in sampling rate even at high exposure dose, when it has been claimed that sampling rate should decrease for a non-ideal adsorbent [12]. So, Chromosorb 106 was definitively selected for isoflurane uptake.

Calibration methods for the thermal desorption–gas chromatography system

The ATD50 was used with an on-line gas chromatograph, and the relationships between sample amount on the tube and integrated peak

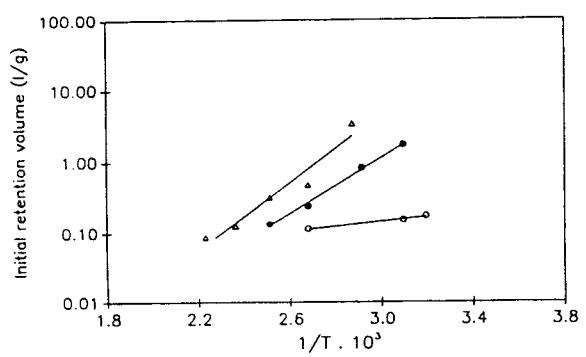

Fig. 2. Determination of adsorbent strength for isoflurane on (○) Tenax TA, (●) Chromosorb 102 and (△) Chromosorb 106.

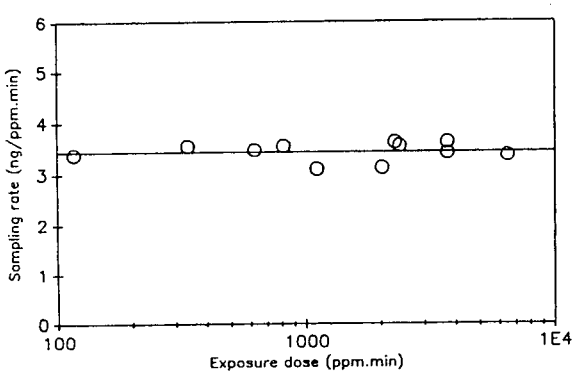

Fig. 3. Variation of sampling rate with time and concentration of isoflurane.

area had to be established. One of the main difficulties with such a system is achieving an appropriate calibration, since it cannot be carried out in a straightforward way as for normal chromatography. This is because measured concentrations are very low, of the order of a few micrograms and internal standards cannot be used, so injections have to be very precise; standards used for calibration should follow the same treatment protocol as ambient samples. Additionally, in this study, the compound to be analysed is very volatile, so a better wide-application method for calibration would be desirable. Thus, the commonly suggested methods for obtaining calibration curves cannot be used. This is because isoflurane is so volatile that it cannot be injected alone, using the ATD injector, since it evaporates from the needle, resulting in wrong injection volumes [13] and, alternatively, any solvent to be used must elute after isoflurane. This latter condition results in long analysis time and, additionally, the solvent accumulates in the cold trap, thus requiring several cleaning desorptions.

Taking into account the above-mentioned facts, the use of an isoflurane-controlled atmosphere for the generation of calibration standard tubes is proposed, according to the details described in the Experimental section and Fig. 1. This system allows for a reproducible and reliable way to transfer known amounts of sample to the GC system through the ATD apparatus. Additionally, it allows the most appropriate calibration range to be chosen, using the same isoflurane atmosphere. No solvent is required, so analysis times are shortened. This shortening is even improved by the fact that standard calibration tubes are easily prepared, thus facilitating the calibration curve checking. As no internal standard can be used, the proposed method helps to carry out the full analysis with the highest precision and reproducibility possible (as Fig. 4 shows), thus overcoming the disadvantages associated with the presently available methods for volatile compounds.

Performance of the sampler for isoflurane

For a passive sampler to be appropriate, *SR* must be constant for any combination of exposure time and concentration, since it is this parameter that allows the amount of contaminant collected by the sampler to be correlated with its ambient concentration. Therefore, the sampler behaviour towards environmental isoflurane under controlled laboratory conditions has to be determined and the effect of changes in variables such as concentration of isoflurane in air, sampling time and moisture content of air require to be established. The INSHT diffusive sampler validation protocol [5] has been used to evaluate the performance of the sampler for isoflurane. This protocol is a reliable and well-established one, whose requisites match those of the well-known Health and Safety Executive (HSE) protocol [14].

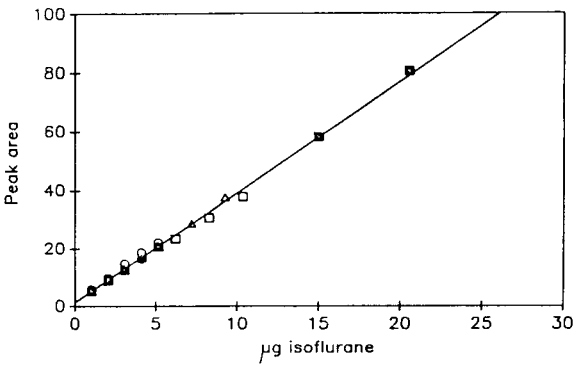

Fig. 4. Calibration curve for isoflurane using standard tubes obtained by controlled atmospheres. Different symbols correspond to different days the calibration was carried out.

The *SR* values were calculated according to eqn. 1, and the results are summarized in Table II. For 30 min and low-level concentration the peak area was indistinguishable from background. From the results, the experimental *SR*, as a mean of all the values obtained, was calculated, resulting in a value of 3.43 ng/ppm · min. Using this experimental *SR* value, the concentration for each sampler was recalculated; its mean value, X, and the standard deviation (R.S.D.) were determined for each of the experiments carried out, as shown in Table III. The obtained results fulfil the protocol requirements, as the precision was less than 7% and the bias less than 10% for all cases. Thus, the above-

TABLE II

SR VALUES FOR DIFFERENT COMBINATION OF EXPOSURE TIME AND ISOFLURANE CONCENTRATION

Concentration of isoflurane	Sampling rates (*SR*) (ng/ppm · min)		
	90 min	290 min	480 min
X_{ref} = 1.27 ppm	3.27		
	3.29		
	3.16		
	3.66		
	3.37		
	3.53		
X_{ref} = 1.28 ppm			3.44
			3.47
			3.42
			3.66
			3.39
			3.45
X_{ref} = 12.82 ppm		3.47	
		3.54	
		3.84	
		3.82	
		3.50	
		3.54	
X_{ref} = 26.52 ppm	3.62		
	3.41		
	3.79		
	3.47		
	3.47		
	3.55		
X_{ref} = 23.13 ppm			3.02
			3.10
			3.08
			3.08
			3.34
			3.20

mentioned value for the sampling rate is valid and suitable and can be considered as the standard sampling rate of the sampler.

Humidity can influence the performance of the adsorbent, altering its adsorption capacity. The results of the experiments to check the effect of humidity on Chromosorb 106 are shown in Table IV, where it can be seen that high humidity values affected neither the collection nor the recovery of isoflurane.

TABLE III

ANALYSIS OF EXPERIMENTAL DATA TO DETERMINE THE PROTOCOL COMPLIANCE

X = Mean value of the measured concentration; X_{ref} = true concentration of the vapour in the test atmosphere; bias = $(X - X_{ref})/X_{ref} \times 100$ ($\leq$10% [5]); R.S.D. = relative standard deviation ($\leq$7% [5]).

90 min	290 min	480 min
X = 1.26 ppm X_{ref} = 1.27 ppm Bias = 0.8% R.S.D. = 6.3%		
		X = 1.28 ppm X_{ref} = 1.28 ppm Bias = 0.0% R.S.D. = 2.8%
	X = 13.53 ppm X_{ref} = 12.82 ppm Bias = 5.5% R.S.D. = 4.6%	
X = 27.46 ppm X_{ref} = 26.52 ppm Bias = 3.5% R.S.D. = 3.9%		
		X = 21.16 ppm X_{ref} = 23.13 ppm Bias = 8.5% R.S.D. = 3.6%

When dealing with automatic sampling, it is interesting to know how long samples can be stored prior to analysis without loss or alteration of the collected pollutants. Thus, it is recom-

TABLE IV

EFFECT OF HUMIDITY ON ISOFLURANE RECOVERY

Concentration (ppm)	Relative humidity (%)	Exposure time (min)	Recovery[a]
1.27	40	90	0.992 ± 0.062 (6)
1.31	98	90	0.999 ± 0.024 (6)
23.13	40	480	1.001 ± 0.036 (6)
26.27	98	480	0.999 ± 0.033 (6)

[a] Mean ± standard deviation; number of samples in brackets.

TABLE V

EFFECT OF STORAGE ON ISOFLURANE RECOVERY

Concentration (ppm)	Exposure time (min)	Recovery
2.02	90	1.001 (6) 0.998 (4)[a]
26.29	480	1.001 (6) 1.091 (2)[a]

[a] Samples analysed 2 weeks after exposure; number of samples in brackets.

mended that the effects of a period of storage, under standard and controlled conditions, after exposure to a pollutant vapour should be investigated. The results of the storage experiments, which are shown in Table V, indicate that samples can be stored for periods of 2 weeks at room temperature without loss of recovery.

CONCLUSIONS

Chromosorb 106 is a suitable adsorbent for isoflurane as it allows a constant sampling rate independent of both time and concentration. The experiments carried out to study the performance of the passive sampler —a standard ATD sampling tube containing Chromosorb 106— indicated that this sampler can be used for the determination of isoflurane in operating room ambient. Its standard sampling rate was 3.43 ng/ppm · min. Samplers can be stored, at room temperature, for periods up to 2 weeks without affecting the recovery, and there was no observable effect of humidity.

The generation of calibration standard tubes by using a controlled atmosphere and injecting known volumes of it through the sampling tube eliminates many of the problems encountered with other calibration methods and gives a good reproducibility.

REFERENCES

1 M. Imbriani, S. Ghittori, P. Zadra and R. Imberti, *Am. J. Ind. Med.*, 20 (1991) 103.
2 A.M. Sass-Kortsak, J.T. Purdham, P.R. Bozek and H. Murphy, *Am. Ind. Hyg. Assoc. J.*, 53 (1992) 203.
3 M. Imbriani, S. Ghittori, G. Pezzagno and E. Capodaglio, *J. Toxicol. Environ. Health*, 25 (1988) 393.
4 J.F. Periago, A. Luna, A. Morente and A. Zambudio, *J. Appl. Toxicol.*, 12 (1992) 91.
5 Instituto Nacional de Seguridad e Higiene en el Trabajo (INSHT), *Diffusive Samplers Validation Protocol for Vapour Organic Compounds*, MTA/PV-II/90.
6 N. Van Den Hoed and M.T.H. Halmans, in A. Berlin, R.H. Brown and K.J. Saunders (Editors), *Diffusive Sampling*, Royal Society of Chemistry, London, 1987, p. 131.
7 Perkin-Elmer, in J.H. Glover (Editor), *Thermal Desorption in Industrial Hygiene and Environmental Analysis*, Spantech, 1991, p. 61.
8 R.W. Coutant, R.G. Lewis and J. Mulic, *Anal. Chem.*, 57 (1985) 219.
9 P. Rosmanith, in A. Berlin, R.H. Brown and K.J. Saunders (Editors), *Diffusive Sampling*, Royal Society of Chemistry, London, 1987, p. 161.
10 D.W. Underhill, *Am. Ind. Hyg. Assoc. J.*, 45 (1984) 306.
11 W.M. Gray, J. O'Sullivan, H.B. Houldsworth and N. Musgrave, in A. Berlin, R.H. Brown and K.J. Saunders (Editors), *Diffusive Sampling*, Royal Society of Chemistry, London, 1987, p. 89.
12 N. Van Den Hoed and O.L.J. Van Asselen, *Ann. Occup. Hyg.*, 35 (1991) 273.
13 Perkin-Elmer, in J.H. Glover (Editor), *Thermal Desorption in Industrial Hygiene and Environmental Analysis*, Spantech, 1991, p. 58.
14 Health and Safety Executive, *Methods for the Determination of Hazardous Substances. Protocol for Assessing the Performance of Air Diffusive Sampling*, MDHS 27, London, 1983.

Journal of Chromatography A, 657 (1993) 139–145
Elsevier Science Publishers B.V., Amsterdam

CHROM. 25 532

Optimization of ion trap parameters for the analysis of dilute samples in the presence of an interfering matrix

Analysis of polychlorinated biphenyls in transformer oil

K. Salomon* and S.E. Buttrill, Jr.

The Edward L. Ginzton Research Center, Varian Associates, 3075 Hansen Way, Palo Alto, CA 94304-1025 (USA)

(First received May 5th, 1993; revised manuscript received August 26th, 1993)

ABSTRACT

The analysis of dilute samples in the presence of an interfering matrix was improved by optimizing the operating parameters of an ion trap in a GC–ion trap system. For a mixture of nine polychlorinated biphenyls (PCBs) in 1% transformer oil, two strategies were successfully employed to increase signal-to-noise (S/N) ratios. By limiting the mass range scanned to those m/z values that include most of the ion fragments due to PCBs and increasing the number of microscans per scan in this regime, S/N values were increased by a factor of 1.5. Further improvements in S/N by up to a factor of ten are achieved by raising the radio frequency (rf) storage level so that low molecular weight ions due to the transformer oil are not stored. An upper limit on how high the rf storage level can be adjusted is determined by the storage efficiency of the ion trap which decreases at high rf storage levels. Ion dissociation is also a limiting factor at high rf storage levels. Best detection limits for five of the nine PCBs studied were obtained when the rf storage level was tuned to $m/z = 74$, a regime where most of the transformer oil ions are no longer stored.

INTRODUCTION

Techniques for environmental analysis often depend on the ability to identify and quantitate trace amounts of analyte in the midst of the interfering matrix. Often the properties of the matrix are such that signals from the matrix overlap with those of the analyte and the inherent sensitivity of a particular technique toward the compound of interest is diminished. Because most analytical techniques are geared toward samples with interferences, it is often necessary to perform sample cleanup procedures prior to analysis. The process is time consuming and extra handling may result in some sample loss. Consequently, there is much interest in developing techniques where analytes in complicated matrices can be analyzed without prior sample manipulation.

Another complication of environmental analyses is that not all components of a mixture are of regulatory interest or highly toxic. Usually only a few components of a mixture pose an environmental hazard and it is important to have some way of quickly and reliably determining if these species are present. Mass spectrometers are useful detectors in this regard, and GC–mass spectrometry systems have become popular anlytical techniques because of their sensitivity, dependability, and universal response toward organic compounds. Tandem mass spectrometry (MS–MS) detectors are useful for increased sensitivity towards analytes in interfering matrices [1], although the overall sensitivity is reduced.

* Corresponding author.

0021-9673/93/$06.00

The application of an ion trap mass spectrometer to environmental analyses is very promising. Among the attractive features are the low detection limits that result from trapping ions in a confined space and the population build-up that results. Mixture analysis capabilities are possible with an ion trap using it in a MS–MS mode [2]. In addition, some work has been done to determine if the ion trap can be optimized for trace analyte detection without resorting to MS–MS [3–5], which would be desirable because of the higher sensitivity of the analysis as well as the library searchability of the resulting electron impact mass spectra.

We were interested in studying the operating conditions of the ion trap mass spectrometer to elucidate which parameters could be adjusted to increase the analyte response in a background of an interfering matrix. The number of ions stored in an ion trap is a complicated function of the ionization time, the applied d.c. voltage ($V_{d.c.}$), the rf drive frequency (Ω) and the amplitude (V_{rf}) of the radio frequency (rf) voltage and the geometry of the ion trap (usually characterized in terms of the trap radius r). There is also great flexibility in setting the range of masses scanned in the ion trap so that only selected mass ranges or even selected ions can be scanned. Unfortunately many of these parameters are interrelated, so that they can not be optimized independently. In addition, there are limits as to how far from normal operating conditions some parameters can be tuned before good mass spectra are no longer obtained. For example, simply increasing the ionization time so that more analyte ions are created can fill the trap with too many ions so that space–charge effects are a problem [6]. Clearly a systematic approach, based on the limits of stable operating conditions in an ion trap, needs to be developed to guide one in choosing which parameters to adjust so that the signal of a selected analyte ion in the midst of undesired background ions is enhanced.

We have chosen to investigate the detection and quantitation of polychlorinated biphenyls (PCBs) in transformer oil as an example of the analysis of trace components in a complex matrix. PCBs are present in the environment as mixtures of many of the 209 theoretically possible congeners and were widely used in electrical transformers, condensers and paints because of their thermal and chemical stability. However, it is the stability of PCBs combined with the toxic properties of some congeners that makes them so dangerous and their identification and quantitation critical. Mass spectrometers are useful for identifying which isomers are present but can be limited by the interferences from the matrix [7–9]. Extensive cleanup methods have been developed but are time consuming [10–12]. An optimized protocol for the analysis of dilute analytes in complex matrices using the ion trap without prior cleanup can be useful for PCB analysis.

EXPERIMENTAL

Sample preparation

The nine PCBs used are: 2,6-dichlorobiphenyl and 4,4′-dichlorobiphenyl (parent ion m/z 222); 2,2′,6,6′-tetrachlorobiphenyl and 3,3′,4,4′-tetrachlorobiphenyl (parent ion m/z 292); 2,2′,4,4′,6,6′-hexachlorobiphenyl and 3,3′,4,4′,5,5′-hexachlorobiphenyl (parent ion m/z 360); 2,2′,3′3′,5,5′,6,6′-octachlorobiphenyl and 2,3,3′,4,4′,5,5′,6-octachlorobiphenyl (parent ion m/z 430); and decachlorobiphenyl (parent ion m/z 500). All were obtained from Ultra Scientific (North Kingstown, RI, USA) as was the transformer oil. The nine PCB mixture was prepared in HPLC-grade hexane obtained from Aldrich (Milwaukee, WI, USA) and spiked with 1% (v/v) transfer oil. For the narrow mass range studies, the concentration of each PCB was 200 pg/μl; a more dilute solution of 50 pg/μl in each PCB was used for the studies in which the rf storage level was optimized. Octachloronaphthalene obtained from Ultra Scientific was used as an internal standard.

Ion trap conditions

All experiments were performed on a Saturn II GC–ion trap system using a septum-equipped programmable injector (SPI) manufactured by Varian Associates (Walnut Creek, CA, USA). No modifications were made to the instrument.

Electron impact ionization was used. Rf storage amplitudes were adjusted using the Saturn software; voltages corresponding to mass-to-charge ratios of 20, 46, 74, 102, 145, 153 and 160 were used. The range of masses scanned was adjusted in the acquisition method editor; individual settings are detailed in the section on narrow mass range scanning.

The automatic gain control (AGC) level was set to 30 000 and kept constant from run-to-run. The ionization time for each microscan is directly proportional to the AGC level setting and inversely proportional to the total number of ions detected in the trap during a 200 μs prescan. A computer algorithm is used to automatically adjust the ionization time of the microscan based on the number of ions detected in the trap during the prescan. If too many ions are present in the trap the ionization time for the microscan is reduced to keep the population of ions below a level where space charge effects would degrade resolution. Conversely, if very few ions are detected during the prescan, the ionization time is increased so that the population of ions is increased and sensitivity is improved. The maximum ionization time is 25 ms.

GC conditions

GC conditions for a DB-5 column with helium as the carrier gas were taken from ref. 13. The column was purchased from Varian (Sunnyvale, CA, USA) and was 30 m × 0.25 mm I.D. with a film thickness of 0.25 μm. The oven program used was as follows: 1 min at 80°C; 80–150°C at 4°C/min; 150–280°C at 2°C/min; and 6.5 min at 280°C. The injector program was 120–200°C at 120°C/min and then at 200°C for the duration of the analysis. The elution order of the PCBs along with their retention times were as follows: 2,6-dichlorobiphenyl (23.11 min); 4,4′-dichlorobiphenyl (29.43 min); 2,2′,6,6′-tetrachlorobiphenyl (32.10 min); 2,2′,4,4′,6,6′-hexachlorobiphenyl (43.09 min); 3,3′,4,4′-tetrachlorobiphenyl (47.09 min); 2,2′,3,3′,5,5′,6,6′-octachlorobiphenyl (58.15 min); 3,3′,4,4′,5,5′-hexachlorobiphenyl (61.45 min); 2,3,3′,4,4′,5,5′,6-octachlorobiphenyl (68.24 min) and decachlorobiphenyl (73.43 min).

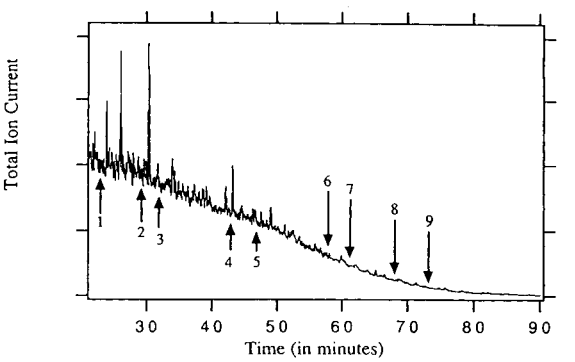

Fig. 1. Plot of total ion intensity as a function of time. Arrows point to the time at which the indicated PCB isomer elutes. Spikes in the chromatogram are due to column bleed.

RESULTS AND DISCUSSION

The difficulty of analyzing PCBs in transformer oil is demonstrated by the chromatogram shown in Fig. 1, where it can be seen that the PCB peaks are completely obscured by the coeluting transformer oil. Transformer oil is a mixture of aliphatic, alicyclic and polynuclear aromatic hydrocarbons with alkyl substituents [11] and some transformer oil components will have the same masses and boiling ranges as the PCBs. A mass spectrum of the transformer oil used in our studies is shown in Fig. 2. Very large signals from a typical hydrocarbon fragmentation pattern are seen for m/z values less than 130. At masses of interest for PCB analysis (m/z values

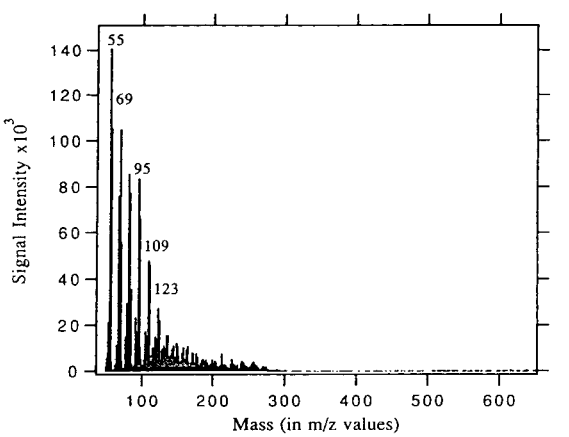

Fig. 2. Mass spectrum of a 1% transformer oil in hexane solution.

greater than 200), the signal intensities of the transformer oil fragments are considerably smaller than at low masses.

Because most of the transformer oil mass fragments are grouped in a low mass regime, two strategies for optimizing the PCB signal can be investigated. In one, the mass range scanned by the instrument is limited to the mass range of the parent PCB ion; most of the transformer oil ions will not be included in the scan. This technique will be referred to as narrow mass range scanning. The other strategy will be to raise the rf storage level so that low mass ions due to transformer oil are not stored in the ion trap and then filling the ion trap with more PCB ions by increasing the ionization time.

Narrow mass range scanning

A full mass range scan in the Saturn ion trap typically has the endpoints of m/z 50 and 650. When acquiring data at the rate of 1 s/scan, the instrument is actually performing three microscans per scan. The three microscans are averaged to produce the final scan recorded at that time in the chromatographic analysis.

In a narrow mass range scan, only a limited range of masses is scanned. For the analysis of PCBs in transformer oil, the range of mass scanned includes the parent PCB peak as well as some of the major fragments. For 2,6-dichlorobiphenyl, the mass range scanned was m/z 145–265; the number of microscans per scan rose to eight. A chromatogram run using full mass range scanning and displayed in the single ion monitoring mode of m/z 222 produces a peak for 2,6-dichlorobiphenyl with $S/N = 6.5$. The same sample run under narrow mass range conditions results in a peak with $S/N = 9.5$. A library search identified the peak as a dichlorobiphenyl even though only m/z values between 145 and 265 were available. The Saturn software allows for different mass ranges in different segments of a chromatogram and it was possible to do customized narrow mass range scans for each of the nine PCBs. Scans included the parent ion as well as fragments up to 70 m/z values less. Improvements in S/N were seen for all PCBs using narrow mass range scanning and matches were made to library mass spectra.

Increasing the number of microscans per scan increases the number of signal measurements that are averaged for the recorded scan. Based on a statistical analysis, the increase in the S/N value should be proportional to the square root of the ratio of the number of microscans per scan using narrow mass range scanning to the number of microscans per scan using full mass range scanning. In the example described above, the expected increase was a factor of 1.6 which is fairly close to the observed improvement of 1.45. It seems reasonable to assume that by limiting the mass range scan to an even more narrow mass range that further improvements in S/N should occur. A very narrow mass range scan of m/z 210 to 230 was run on the dichlorobiphenyl sample. The number of microscans per scan jumped to 20 and the expected improvement was a factor of 2.6. However, the observed improvement was only 1.7 which is not much better than using a narrow mass range scan. The observed deviation from the predicted behavior may be due to the non-random nature of the noise source; the major contribution to the background is from transformer oil ions at the same m/z as the PCB ion of interest.

Raising the rf storage level

The amplitude of the rf storage voltage (V_{rf}) determines the lower mass limit of which ions are stored in the ion trap. The relationship between V_{rf} and the stability parameter q_z is a complicated function based on the solutions to the Mathieu equation of ion motion in an oscillating electric field. For a conventional ion trap with the endcaps grounded, a radius of 1 cm and operating at 1 MHz, q_z is related to the ion mass (m), the charge on the ion (z) and V_{rf} as follows [14].

$$q_z = \frac{0.0978 V_{rf}}{m/z} \quad (1)$$

Ions with q_z values greater than 0.908 do not have stable trajectories and exit from the ion trap. Under normal operating conditions, the amplitude of the storage voltage is chosen so that all ions with m/z values greater than 20 are stored in the ion trap. By increasing the amplitude of V_{rf}, the q_z value for an ion of a given

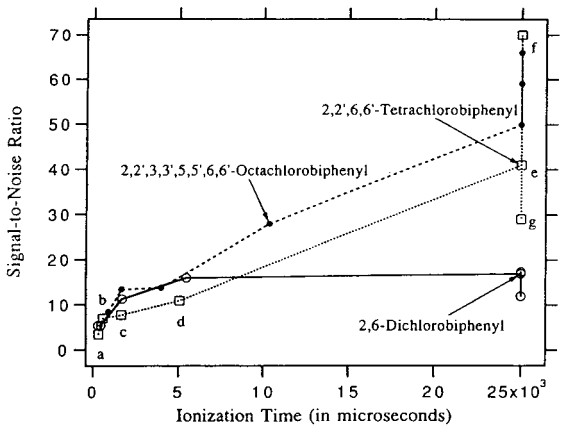

Fig. 3. *S/N* values as a function of ionization time. The lower case letters at each point correspond to the storage level used to generate the recorded ionization time. Mass-to-charge ratios are: (a) 20, (b) 46, (c) 74, (d) 102, (e) 145, (f) 153 and (g) 160.

mass increases and when q_z becomes greater than 0.908, the ion assumes an unstable trajectory and is not stored. Lower mass ions reach the point of instability before higher mass ions as V_{rf} is increased.

For the PCB sample in transformer oil, raising the rf storage level eliminates many of the lower molecular weight transformer oil ions from the trap. Since the ion trap has a fixed capacity for the total number of ions that can be stored before space-charge repulsion is a problem, a decrease in the number of low-molecular-mass ions trapped allows for the storage of more higher-molecular-mass PCB ions. The ionization time is increased so that more ions are created. Since the transformer oil fragments are the major background source, the increase in the number of PCB ions relative to transformer oil ions trapped should lead to an increase in *S/N*.

To demonstrate the benefit of the increased ionization time made possible by raising the rf storage level, the PCB in transformer oil sample was analyzed with the rf storage level set to one of the following *m/z* values: 20, 46, 74, 102, 145, 153 or 160. Narrow mass range scanning of at least 70 *m/z* values was used for each PCB. *S/N* ratios for the parent PCB ions and ionization times were measured for each PCB at each rf storage level. As shown in Fig. 3, a substantial improvement in the *S/N* values for each of the PCBs is observed as the ionization time increases. For octachlorobiphenyl, the increase in *S/N* was from 9 (measured when the ionization time was less than one thousand microseconds) to 70 (measured when the ionization time was at 25 ms). (There is some variation in *S/N* values at 25 ms because *N* is very small, often only 2, 3 or 4 counts.) *S/N* values measured at the default storage level of *m/z* 20 and best *S/N* values for all nine PCBs are included in Table I.

S/N values may have been even greater at high rf storage levels had there not been loss of PCB parent ions due to fragmentation. It was

TABLE I

DETECTION LIMITS AND *S/N* VALUES FOR NINE PCBs AT DEFAULT AND OPTIMUM SETTINGS

Compound	Detection limit at *m/z* 20 (in pg/μl)	Best detection limit (in pg/μl)	Storage level	*S/N* at *m/z* 20	Best *S/N*	Storage level
2,6-Dichlorobiphenyl	48	8	74	5	17	102
4,4'-Dichlorobiphenyl	79	10	74	2	8	153
2,2',6,6'-Tetrachlorobiphenyl	10	5	145	3	60	153
3,3',4,4'-Tetrachlorobiphenyl	10	7	74	3	17	153
2,2',4,4',6,6'-Hexachlorobiphenyl	34	3	74	6	150	160
3,3',4,4',5,5'-Hexachlorobiphenyl	25	6	102	4	32	153
2,2',3,3',5,5',6,6'-Octachlorobiphenyl	50	1	74	9	70	160
2,3,3',4,4',5,5',6-Octachlorobiphenyl	41	4	46	10	43	145
Decachlorobiphenyl	40	6	46	30	140	102

possible to monitor the extent of PCB fragmentation as the rf storage level was increased by analyzing a PCB sample without transformer oil (so that interferences at similar m/z values are reduced) under full mass range scanning conditions. The observed dissociation pathway is the loss of two chlorine atoms. By monitoring the ratio of the PCB parent ion signal to the signal of the peak at an m/z value 70 lower, it was possible to record the extent of fragmentation at high rf levels. Results for five of the PCBs are shown in Fig. 4.

All of the PCBs show decreases in the ratio of parent ion to fragment; for some it is expecially significant. 2,3-Dichlorobiphenyl, 2,2′,6,6′-tetrachlorobiphenyl, 2,2′,4,4′,6,6′-hexachlorobiphenyl and 2,2′,3,3′,5,5′,6,6′-octachlorobiphenyl have fragmentation ratios that decline by more than 40% at high rf storage levels. The behavior of the dichlorobiphenyl fragmentation ratio is somewhat bizarre; it increases as the rf storage level is increased from m/z 102 to 145. More than likely this behavior is due to the instability of the m/z 152 fragment at a storage level corresponding to m/z 145. The other five PCBs do not have such extensive fragmentation.

An important and more universal factor leading to the loss of ion signal at high rf storage levels is the decrease in storage efficiency of the ion trap at high rf storage levels. While the proportion of sample ion relative to matrix ions increases at higher rf levels, the total number of ions stored in the trap declines. The variations in trapping efficiency are demonstrated by monitoring the signal intensities of five fragment ions from perfluorotributyl amine as the rf storage level is increased. (Perfluorotributylamine is used for mass calibration and is introduced into the ion trap at a constant pressure through a separate inlet system.) The ionization time was held constant so that the same number of ions were created at each of the different rf storage levels studied. The results are shown in Fig. 5.

The number of perfluorotributylamine ions stored decreases once the rf storage level is increased beyond m/z 50 or 60. For the perfluorotributylamine fragments at m/z 69 and 131, the signal intensity drops to zero at the rf storage levels above the corresponding m/z value. The ion fragments at m/z 264, 414 and 614 all show a monotonic decrease from m/z 60 to 160. For a PCB analysis, the decrease in storage efficiency at higher rf storage levels counteracts the benefits obtained by the concomitant increase in ionization time. At some rf storage level, there will be an optimum regime for the analysis of the PCBs in transformer oil matrix.

The detection limits for all PCBs were measured at each of seven different rf storage levels.

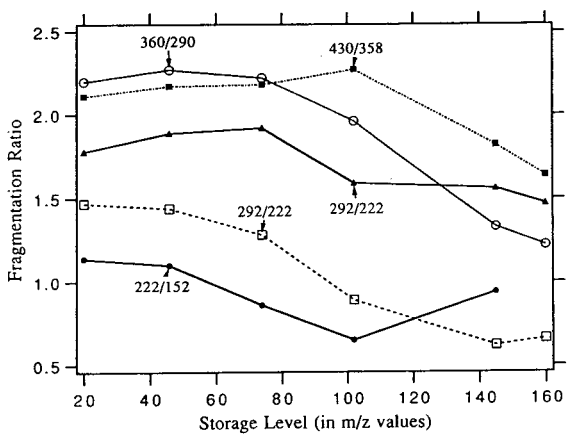

Fig. 4. Fragmentation ratio of five PCBs plotted as a function of rf storage level setting. ● = 2,6-Dichlorobiphenyl; □ = 2,2′,6,6′-tetrachlorobiphenyl; ▲ = 3,3′,4,4′-tetrachlorobiphenyl; ○ = 2,2′,4,4′,6,6′-hexachlorobiphenyl; ■ = 2,3,3′,4,4′,5,5′,6-octachlorobiphenyl.

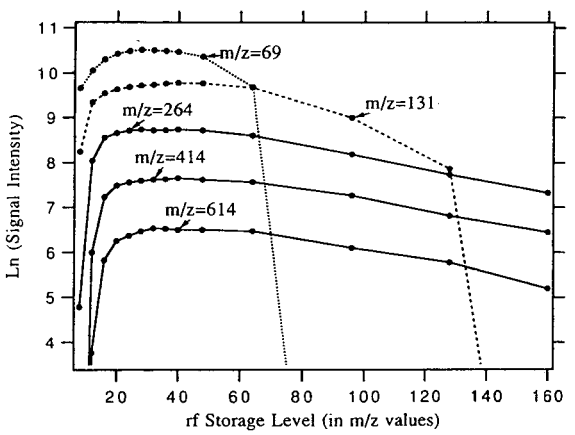

Fig. 5. Signal intensities of perfluorotributyl amine fragment ions as a function of rf storage level. The ionization time was held constant at 1.2 ms.

The calculation of detection limits is based on an EPA-suggested method [13]. The detection limits were determined by analyzing the PCB mixture at each rf setting three times, calculating the standard deviation for each compound from the three runs and then multiplying the standard deviation by 4.3. Optimum detection limits for each of the nine PCBs are included in Table I as well as the detection limits obtained at the default storage level of m/z 20. Best detection limits were measured at a storage level setting of m/z 74 for both dichlorobiphenyl isomers, 3,3′,4,4′-tetrachlorobiphenyl, 2,2′,4,4′,6,6′-hexachlorobiphenyl and 2,2′3,3′,5,5′6,6′-octachlorobiphenyl. For eight PCBs, optimum settings were between m/z values of 46 and 102, storage levels where a significant number of transformer oil ions were excluded from the trap and where the storage efficiency of the trap was still high. The optimum detection limits obtained using our protocol are comparable with those reported using a GC–electron-capture detection system [13].

CONCLUSIONS

We have outlined two strategies for improving the analysis of dilute samples in a transformer oil matrix. Narrow mass range scanning can be used to improve S/N ratios by a factor of 1.5 as compared to a full mass range scan. Raising the rf storage level so that low molecular weight matrix ions are not stored leads to an increase in S/N by nearly a factor of 10. Optimum detection limits were measured in a regime where the increase in signal intensity resulting from increased ionization times dominated over the loss in trapping efficiency at high rf storage levels.

REFERENCES

1 R.W. Konrat and R.G. Cooks, *Anal. Chem.*, 50 (1978) 91A–92A.
2 R.G. Cooks and R.E. Kaiser, *Acc. Chem. Res.*, 23 (1990) 213–219.
3 M.L. Alexander, P.H. Hemberger, M.E. Crisper and N.S. Nogar, *Anal. Chem.*, 65 (1993) 1609–1614.
4 C.K. Huston, *J. Chromatogr.*, 606 (1992) 203–209.
5 C.S. Creaser, D.S. Mitchell and K.E. O'Neill, *Int. J. Mass Spectrom. Ion Phys.*, 106 (1991) 21–31.
6 J.F.J. Todd, R.M. Waldren, R.E. Mather and G. Lawson, *Int. J. Mass Spectrom. Ion Phys.*, 28 (1978) 141–151.
7 R.H. Liu, S. Ramesh, J.Y. Liu and S. Kim, *Anal. Chem.*, 56 (1984) 1808–1812.
8 R.D. Voyksner, J.R. Hass, G.W. Sovocool and M. Bursey, *Anal. Chem.*, 55 (1983) 744–749.
9 T. Cairns and E.G. Sigmund, *Anal. Chem.*, 53 (1981) 1599–160.
10 A.L. Alford-Stevens and W.L. Budde, *Anal. Chem.*, 57 (1985) 2452–2457.
11 V.P. Nero and R.D. Hudson, *Anal. Chem.*, 56 (1984) 1041–1043.
12 H.M. Klimisch and D.N. Ingebrigtson, *Anal. Chem.*, 52 (1980) 1675–1678.
13 G.S. Durell and T.C. Sauer, *Anal. Chem.*, 62 (1990) 1867–1871.
14 R.E. March and R.J. Hughes, *Quadruple Storage Mass Spectrometry*, Wiley, New York, 1989, p. 198.

Journal of Chromatography A, 657 (1993) 147–153
Elsevier Science Publishers B.V., Amsterdam

CHROM. 25 212

Application of thermal desorption to the biological monitoring of organic compounds in exhaled breath ☆

J.F. Periago*, C. Prado and I. Ibarra

Instituto Nacional de Seguridad e Higiene en el Trabajo, E-30120 Murcia (Spain)

J. Tortosa

Servicio de Anestesiología del Hospital Virgen de la Arrixaca, E-30120 Murcia (Spain)

(First received December 10th, 1992; revised manuscript received April 14th, 1993)

ABSTRACT

We have developed a thermal desorption–gas chromatographic method for the analysis of organic compounds in exhaled breath air, to be used in the biological monitoring of environmental exposure. The exhaled breath sampler is based on the concentration of compounds present in alveolar air in a solid sorbent material. Isoflurane (1-chloro-2,2,2-trifluoroethyl-difluoromethyl-ether), an inhaled anaesthetic used widely in surgery, and styrene, used in boat construction and the manufacture of fibreglass-reinforced plastics, are partially eliminated from the body in exhaled breath, samples of which can therefore be used to monitor biological exposure to these two organic compounds. Recoveries were tested in controlled atmospheres of isoflurane or styrene, with Chromosorb 106 or Tenax, respectively, as the adsorbent. We also investigated the influence of relative humidity, an important factor in breath sampling, on adsorption.

INTRODUCTION

The development of industrial hygiene programme as a complement to environmental assessment of chemical contaminants with biological monitoring has awakened enormous interest in the search for biological indices of occupational exposure. Among the methods available for biological monitoring, exhaled breath offers certain advantages, because it is non-invasive in nature, and hence well accepted by workers. Moreover, the compounds of interest are analysed directly, thus minimizing the chances of spurious results caused by factors from outside the atmosphere in the workplace [1,2].

Several types of exhaled breath samplers have been used for breath analysis. Mixed expired air comprises alveolar air diluted by atmospheric air retained in the dead space of the respiratory tract (mouth, nose, pharynx, trachea and bronchi), whereas alveolar air (end-exhaled air) normally makes up two-thirds of the tidal volume.

Alveolar air sampling permits valid estimates of partial solvent pressure in arterial blood, particularly in the case of non-polar solvents, given the equilibrium between alveolar gas and arterial blood [3–5]. A number of methods have been developed to sample alveolar air from a single exhalation for chromatographic analysis [6–9], however these may be affected by water vapour condensation and excessive sample dilution. Instrumental methods have also been used for the direct analysis of exhaled air by gas chromatography [10], photoionization detection [11] or mass spectrometry [12,13]. These proce-

* Corresponding author.

☆ Presented at the *21st Scientific Meeting of the Spanish Group of Chromatography and Related Techniques*, Granada, October 21–23, 1992.

0021-9673/93/$06.00

dures may be cumbersome and are usually costly.

The aim of this work was to apply the thermal desorption technique to a portable system for end-exhaled breath sampling [14], based on the concentration of solvents in alveolar air captured in a solid adsorbent for chromatographic analysis. The advantages of thermal desorption prior to gas chromatography are considerable in samples collected 16 h post exposure, on the following morning before occupational re-exposure. The system was validated for isoflurane (1-chloro-2,2,2-trifluoroethyl-difluoromethyl-ether), a surgical anaesthetic, and for styrene, a basic component used in the manufacture of reinforced fibreglass plastics, in controlled atmospheres and in human exposures in the field.

EXPERIMENTAL

Sampler design

The prototype of the exhaled breath sampler designed and built in our laboratory consists of a Haldane–Priestley tube modified to concentrate aliquots of exhaled air from one or more exhalations. The system (Fig. 1) is based on an inversion of the polarity of the motor that powers the syringe, so that the plunger alternately draws in exhaled air and expels the sample through the adsorbent cartridge, a mechanism controlled by automatic changes in the position of the three-way valve. The aluminium tube, 1 m long by 26 mm in diameter, is fitted with a disposable mouthpiece, and equipped with a valve that is opened when air is exhaled through the system, and which closes at the end of exhalation. The tube is insulated with a 15-mm-thick electrically heated jacket that maintains the internal temperature at 40–45°C. The three-way PTFE valve is connected to (I) the end of the Haldane–Priestley tube at a point approximately 5 cm from the mouthpiece with a copper connector, (II) the 50-ml capacity gas syringe, which is filled and emptied by a rack system, and (III) the adsorbent tube. In the first step of the procedure, the three-way valve control mechanism (Fig. 1) opens channels I and II while exhaled air is being aspirated from the aluminium tube, and closes channel III. In the second step, channels II and III are open to pass the exhaled air through the adsorbent tube, while channel I is kept closed. The servomotor-driven syringe draws in air from the aluminium tube and expels it through the adsorbent. The direction of the motor is reversed automatically by a pair of end-of-run switches, which also control the position of the three-way valve. A counter records the number of complete runs of the aspiration/expulsion cycle, and the sequence can be repeated automatically or step by step. The prototype, which weighs approximately 5 kg, is built so that the 1-m-long aluminium tube can be separated into two sections for transport. The sampler requires an external electrical power source.

Adsorbent cartridges

The adsorbent cartridge consists of a standard metallic tube for an ATD 50 thermal desorption system (Perkin-Elmer, Beaconsfield, UK) measuring 89 mm long by 6.4 mm in diameter. The cartridge was packed with 200 mg of 20–40-

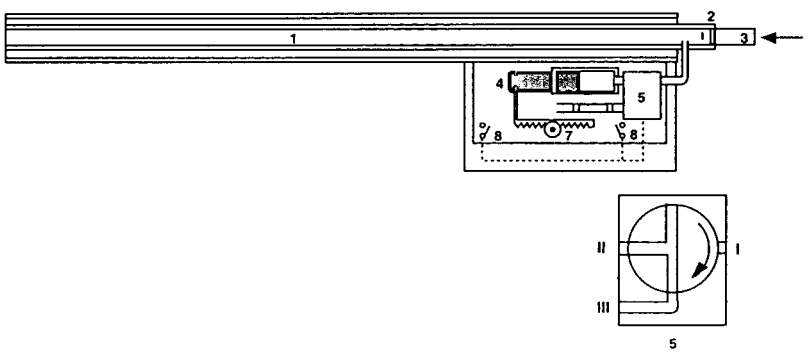

Fig. 1. Schematic diagram of the exhaled breath sampler system. 1 = Insulated aluminium tube; 2 = back-flow valve; 3 = disposable mouthpiece; 4 = syringe; 5 = three-way valve; 6 = adsorbent cartridge; 7 = servomotor; 8 = end-of-run switches.

mesh Chromosorb 106 (SKC, PA, USA) for isoflurane, or with 150 mg of 20–40-mesh (0.84–0.42 mm) Tenax TA (SKC) for styrene, and was sealed at the end of the procedure for transport and storage.

Instrumental analysis

All samples of exhaled breath air were desorbed with a Perkin-Elmer Model ATD 50 automatic thermal desorption system, directly connected to a Perkin-Elmer Model 8700 gas chromatograph by a heated transfer line. Thermal desorption was done in two stages. First, the tube was heated with the flowing carrier gas, which transfers the desorbed vapours from the sample tube to a cooled trap. When the entire sample had been collected, the trap was rapidly heated to desorb the volatile materials and to rapidly inject the sample into the GC column via a heated transfer line. The cooled trap was packed with Tenax. The operating conditions are summarized in Table I.

Validation in controlled atmosphere

The system was validated in controlled atmospheres containing isoflurane (Abbot Laboratories, Madrid, Spain) and styrene (Merck, Darmstadt, Germany) and designed to simulate the concentrations of these compounds in human breath. Fig. 2 illustrates the system used to generate the controlled atmosphere. The coefficient of variation, as determined by on-line chromatography, was less than 4%. Validation assays were performed under varying conditions of relative humidity and concentration. Six sam-

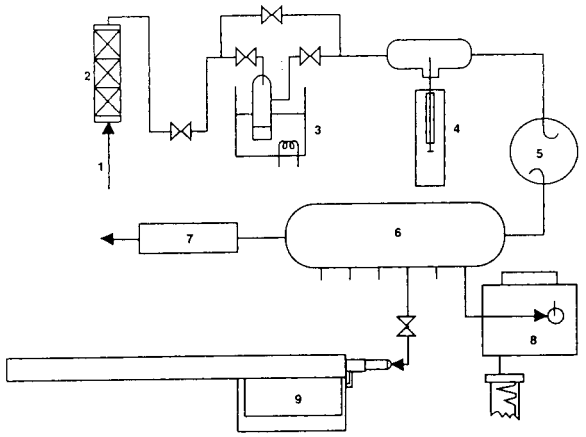

Fig. 2. Scheme of the system used to generate the controlled atmosphere. 1 = Air intake; 2 = filter; 3 = humidifier; 4 = automatic injector; 5 = mixing chamber; 6 = sampling chamber; 7 = humidity sensor; 8 = gas chromatograph; 9 = exhaled air sampler system.

TABLE I

EXPERIMENTAL CONDITIONS FOR THERMAL DESORPTION AND GAS CHROMATOGRAPHY

FID = Flame ionization detection.

	Isoflurane	Styrene
Thermal desorption parameters		
Carrier gas	N_2 (68.95 kPa, 10 p.s.i.)	N_2 (68.95 kPa, 10 p.s.i)
Desorption	Two stages	Two stages
Oven temperature	240°C	200°C
Cold trap		
Lower temperature	−30°C	−30°C
Upper temperature	240°C	300°C
Heated transfer line temperature	100°C	120°C
Gas chromatographic parameters		
Stationary phase	FFAP[a]	FFAP[a]
Film thickness	0.3 μm	0.3 μm
Column length	25 m	25 m
Column inside diameter	0.2 mm	0.2 mm
Detector temperature	70°C	120°C
Detection	FID	FID

[a] Hewlett-Packard, Palo Alto, CA, USA.

TABLE II

EXPERIMENTAL CONDITIONS USED TO VALIDATE THE EXHALED BREATH SAMPLER IN A CONTROLLED ATMOSPHERE OF ISOFLURANE

Uptake volume: 0.6 l.

Relative humidity (%)	Concentration (mg/m^3)	Recovery (C_c/C_a)[a]
98	24.8	0.986 ± 0.033 (6)
98	5.0	1.023 ± 0.013 (6)
40	24.8	1.007 ± 0.022 (6)
40	5.0	1.009 ± 0.029 (6)
50	15.2	0.998 ($n = 2$)[b]

[a] Mean ± standard deviation, with number of samples in parentheses.
[b] Samples analysed 15 days after collection.

ples were collected under each of the conditions tested, which are summarized in Tables II and III. The total sample volume was always 0.6 l, divided into three aliquots of 0.2 l each. An air stream was passed through the tube at a rate of 4 l/min for 2 min before each sample run. In an additional control assay, clean air was passed through the tube and a blank sample collected under each of the experimental conditions. Two additional samples taken at concentrations near the higher end of the concentration range were stored for 15 days at room temperature before analysis to compare these results with those from other samples at high concentrations, which were analysed immediately.

TABLE III

EXPERIMENTAL CONDITIONS USED TO VALIDATE THE EXHALED BREATH SAMPLER IN A CONTROLLED ATMOSPHERE OF STYRENE

Uptake volume: 0.6 l.

Relative humidity (%)	Concentration (mg/m^3)	Recovery (C_c/C_a)[a]
98	26.6	1.019 ± 0.047 (6)
98	3.8	0.995 ± 0.026 (6)
40	26.6	1.004 ± 0.033 (6)
40	3.8	0.975 ± 0.033 (6)
50	21.0	0.989 ($n = 2$)[b]

[a] Mean ± standard deviation, with number of samples in parentheses.
[b] Samples analysed 15 days after collection.

Experimental studies in human exposures

The system was assayed in subjects habitually exposed to these compounds in the workplace. In both cases we measured the exposure concentrations with personal diffusive samplers attached to three exposed subjects. For isoflurane, Perkin-Elmer-type diffusive tubes packed with Chromosorb 106 were used; for styrene, 3M-3500 diffusive samplers (3M, MN, USA) were used.

For isoflurane, the same subject was exposed on two consecutive days to levels of 55 mg/m^3 for 2.8 h (day 1) and 70 mg/m^3 for 6 h (day 2). Exposures took place during the subjects' habitual occupation in an operating room of a large medical centre.

For styrene, two factory workers were exposed to 360 or 243 mg/m^3 for 6 h on the same day.

In all subjects, exhaled breath samples were collected immediately after the end of the shift, every 15 min for the next 1.5 h and 16 h later, before beginning the next shift. The uptake volume collected in all cases was 1 l of exhaled air from five exhalations (0.2 l each).

RESULTS

Table II summarizes the experimental conditions of the validation tests in controlled atmospheres containing isoflurane and styrene. The influence of the humidity, concentration and storage were analysed from the recoveries obtained under each condition, calculated as $r = C_c/C_a$, where C_c represents the concentration in the adsorbent cartridge and C_a the mean concentration in the controlled atmosphere. The recovery values obtained with isoflurane and styrene approached unity, with relative standard deviation less than 12%. In blank samples taken after clean air was passed through the uptake system, no isoflurane or styrene was detected under any of the conditions tested, suggesting that no adsorption–desorption phenomena occurred in any of the components.

Profiles of isoflurane and styrene in exhaled breath samples collected after occupational exposures are shown in Figs. 3 and 4. Both

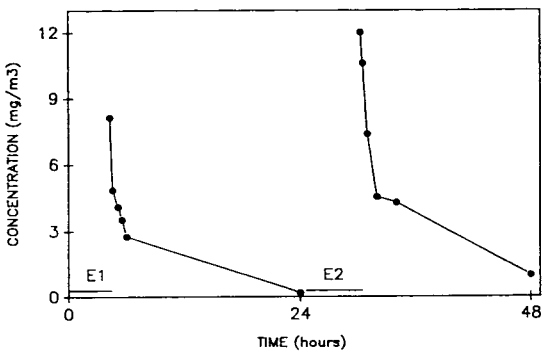

Fig. 3. Profiles of isoflurane in exhaled breath air after two consecutive daily exposures in the workplace. E1 = Environmental concentration = 58 mg/m^3, exposure time = 2.8 h. E2 = Environmental concentration = 70 mg/m^3, exposure time = 6 h.

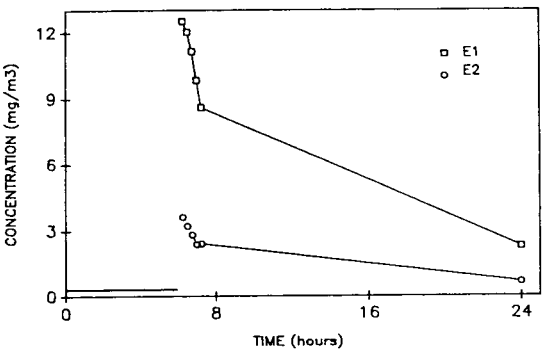

Fig. 4. Profiles of styrene in exhaled breath air of two workers after exposure in the workplace. E1 = Environmental concentration = 360 mg/m^3, exposure time = 6 h. E2 = Environmental concentration = 243 mg/m^3, exposure time = 6 h.

compounds were detectable in samples taken 16 h after exposure (0.19 and 0.98 mg/m^3 for isoflurane; 0.65 and 2.27 mg/m^3 for styrene).

DISCUSSION

The results of two-way analysis of variance (ANOVA) tests of the recoveries obtained in validation experiments in controlled atmospheres (Table IV) show no significant variations between the different conditions of humidity and concentration, thus the determinations were not affected by the elevated relative humidity of sampled air. These findings make our system similar in terms of reliability to those based on direct sampling of breath exhaled into glass tubes, as the fraction collected with our system is that which most closely represents the alveolar fraction. However, our sample system, in contrast to most of those described up to now, offers the further advantage of adsorption onto a solid substrate, which concentrates the sample and facilitates its transport and storage with minimal loss over a period of 15 days without requiring special measures of preservation (Tables II and III).

TABLE IV

RESULTS OF ANALYSIS OF VARIANCE OF THE RECOVERIES OBTAINED IN VALIDATION EXPERIMENTS IN CONTROLLED ATMOSPHERES

NS = Not significant at 5% level.

Source of variation	Degrees of freedom	Sum of squares	Mean square	F Calculated	F Test
Isoflurane					
Relative humidity	1	$7.7042 \cdot 10^{-5}$	$7.7042 \cdot 10^{-5}$	0.107	NS
Concentration	1	$2.3404 \cdot 10^{-3}$	$2.3404 \cdot 10^{-3}$	3.257	NS
Interaction	1	$1.9260 \cdot 10^{-3}$	$1.9260 \cdot 10^{-3}$	2.680	NS
Error	20	0.0140	$7.1858 \cdot 10^{-4}$		
Styrene					
Relative humidity	1	$1.7340 \cdot 10^{-3}$	$1.7340 \cdot 10^{-3}$	1.321	NS
Concentration	1	$4.3202 \cdot 10^{-3}$	$4.3202 \cdot 10^{-3}$	3.292	NS
Interaction	1	$4.2667 \cdot 10^{-5}$	$4.2667 \cdot 10^{-5}$	0.032	NS
Error	20	0.0260	$1.3123 \cdot 10^{-3}$		

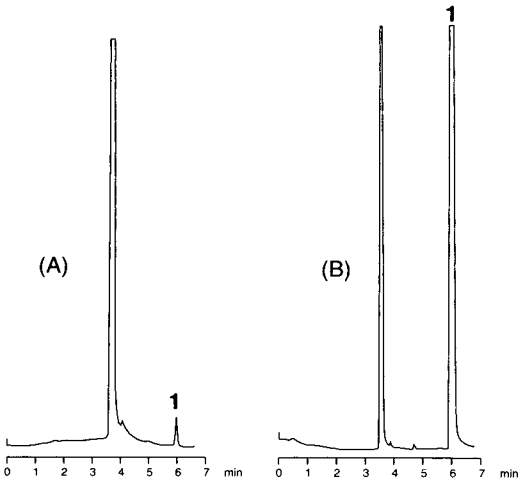

Fig. 5. Capillary gas chromatogram of samples taken from controlled atmospheres of styrene (1), using different desorption techniques. (A) Uptake volume of air: 500 ml. Adsorbent: activated charcoal. Desorption volume: 250 μl carbon disulphide. Injection volume: 2 μl. (B) Uptake volume of air: 50 ml. Adsorbent: Tenax TA. Thermal desorption.

The system designed by us permits repeated sampling of a single or of multiple successive exhalations with a single adsorbent cartridge, which provides concentrated samples.

Although the system enriches the sample on the adsorbent to concentrations appropriate for the analytical method proposed here, the use of adsorbents susceptible to thermal desorption can markedly improve the results, as the entire, undiluted sample is analysed. This contrasts with the need to dilute the sample when solvent desorption is used, as depicted in Fig. 5. This feature is of particular interest for measuring the very low concentration of organic compounds in exhaled breath some time after exposure has occurred, but before the next working day is begun. The value of such determinations in occupational toxicology lies in their ability to detect the accumulation of substances in fatty tissues [15]. Thermal desorption of samples collected in a solid adsorbent may therefore make it possible to detect and quantify low levels of compounds a considerable time after exposure has occurred, as shown in Figs. 6 and 7, which illustrate the findings in samples of exhaled breath collected 16 h after exposure to isoflurane and styrene, respectively.

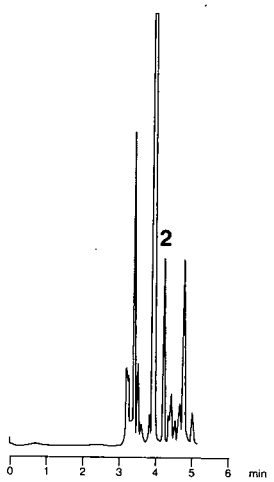

Fig. 6. Capillary gas chromatogram of an exhaled breath sample taken 16 h after exposure to 58 mg/m^3 isoflurane (2) for 2.8 h.

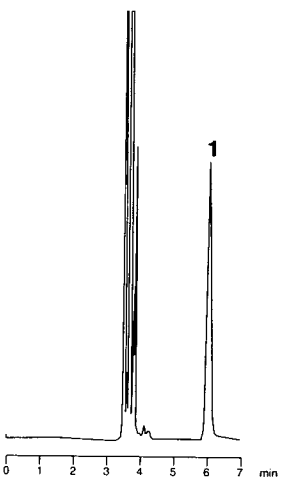

Fig. 7. Capillary gas chromatogram of an exhaled breath sample taken 16 h after exposure to 243 mg/m^3 styrene (1) for 6 h.

ACKNOWLEDGEMENT

We thank Ms. Karen Shashok for translating the original manuscript into English.

REFERENCES

1 R.S. Waritz, in L.J. Cralley and L.V. Cralley (Editors), *Patty's Industrial Hygiene and Toxicology*, Wiley–Interscience, New York, 2nd ed., 1985, pp. 116–124.

2 B. Krotoszynski, G. Gabiel and H. O'Neill, *J. Chromatogr. Sci.*, 15 (1977) 232.
3 H.K. Wilson, *Scand. J. Work. Environ. Health*, 12 (1986) 174.
4 A. Manolis, *Clin. Chem.*, 29 (1983) 5.
5 G.R. Kelman, *Br. J. Ind. Med.*, 39 (1982) 259.
6 B.M. Wright, *J. Physiol.*, 184 (1966) 66.
7 M. Imbriani, S. Ghittori, G. Pezzagno and E. Capodaglio, *G. Ital. Med. Lav.*, 4 (1982) 271.
8 F. Brugnone, L. Perbellini, E. Gaffuri and P. Apostoli, *Int. Arch. Occup. Environ. Health*, 47 (1980) 245.
9 G. von Machata, *Arbeitsmed. Sozialmed. Praeventivmed.*, 21 (1986) 5.
10 J. Fernández, E. Guberan and J. Caperos, *Am. Ind. Hyg. Assoc. J.*, 37 (1976) 143.
11 L. Molhave and O.F. Penderson, *Int. Arch. Occup. Environ. Health*, 54 (1984) 65.
12 A.M. Lovett, N.M. Reid, J.A. Buckley, J.B. French and D. Cameron, *Biomed. Mass. Spectrom.*, 6 (1979) 91.
13 F.M. Benolt, W.R. Davidson and A.M. Lovett, *Anal. Chem.*, 55 (1983) 805.
14 J.F. Periago, A. Luna, A. Morente and A. Zambudio, *J. Appl. Toxicol.*, 12 (1992) 91.
15 P.O. Droz, M.M. Wu, W.G. Cumberland and M. Berode, *Br. J. Ind. Med.*, 46 (1989) 447.

Journal of Chromatography A, 657 (1993) 155–164
Elsevier Science Publishers B.V., Amsterdam

CHROM. 25 214

Evaluation and optimization of the automatic thermal desorption method in the gas chromatographic determination of plant volatile compounds ☆

Joaquín L. Esteban, Isabel Martínez-Castro and Jesús Sanz*

Instituto de Química Orgánica General (CSIC), Juan de la Cierva 3, 28006 Madrid (Spain)

(First received December 10th, 1992; revised manuscript received April 14th, 1993)

ABSTRACT

The automatic thermal desorption (ATD) method was used in the gas chromatographic determination of the volatile components of plants. The reproducibility of the method was evaluated for several operating conditions; the results were better than those obtained with other sample preparation methods (simultaneous distillation–extraction and solvent extraction). Some applications of the ATD method in the gas chromatographic determination of volatile components of Umbelliferae seeds are also presented, including the determination of the enantiomeric forms of limonene.

INTRODUCTION

Gas chromatography (GC) is the method of choice for the analysis of the complex mixtures of volatile compounds usually present in plants; however, it requires as a preliminary step the elimination of the non-volatile material. Many methods have been used in the isolation of volatile compounds, the most important being headspace trapping, solvent extraction, steam distillation and supercritical fluid extraction.

Thermal desorption from the sample has also been widely used, as both the sample size and the time required for its preparation are greatly reduced. Many laboratory-made systems [1–3] have been developed; some suppliers of gas chromatographs include the thermal desorption system as a sophisticated method of sample introduction [4]. However, few studies evaluating the quantitative results of the methods based on thermal desorption of volatile compounds in plants have been carried out.

An absolute evaluation of any sample preparation system would require an accurate previous knowledge of the sample composition. This is very difficult for real samples, however, as any analytical method including a fractionation step can introduce a discriminating factor in the results. We present in this paper an evaluation of the quantitative performance of an automatic thermal desorption (ATD) system, focusing on a study of the reproducibility of the method under different operating conditions. The results are compared with those obtained by using other sample preparation techniques (solvent extraction and steam distillation), and the possibility of artifact formation caused by thermal decomposition in different samples is discussed.

EXPERIMENTAL

Plant samples

Chamaecyparis lawsoniana Parl. (Lawson cypress) was selected for the evaluation of the method, as a previous study using steam distilla-

* Corresponding author.

☆ Presented at the *21st Scientific Meeting of the Spanish Group of Chromatography and Related Techniques*, Granada, October 21–23, 1992.

0021-9673/93/$06.00

tion had shown that its leaves (readily available) contain a very complex mixture of mono-, sesqui- and diterpenes with molecular mass in the range 136–280. This range of volatile components could be considered to cover those of many aromatic plants, whose more usual components are mono- and sesquiterpenes. After drying, the leaves were ground and homogenized using a mechanical blender. Ground samples were kept refrigerated in closed vials until analysis.

Seeds of several Umbelliferae plants were also collected (*Thapsia villosa*, *Heracleum sphondylium*) or purchased (*Petroselinum crispum*).

Steam distillation

Samples (2–4 g) were distilled using the micro simultaneous distillation–extraction (SDE) method (Chrompack, Middelburg, Netherlands) described by Godefroot *et al.* [5]. Pentane was used as a non-polar solvent.

Extraction

Plant samples (10 g) were shaken with 100 ml of diethyl ether. The process was repeated and the extracts were washed, concentrated by evaporation to a volume of 100 ml, dried over sodium sulphate and filtered.

Gas chromatography

The gas chromatographic equipment included an AutoSystem Gas chromatograph, a Model 400 automatic thermal desorption system (ATD-400) (described in detail later) and a Nelson Model 1020 data processor, all supplied by Perkin-Elmer (Norwalk, CT, USA). Nitrogen was used as the carrier gas and flame ionization detection was used. A laboratory-made fused-silica capillary column (column A; 25 m × 0.22 mm I.D.) coated with methylsilicone OV-1 was programmed from 70 to 220°C at 4°C/min. For chiral separations, a laboratory-made fused-silica capillary column (column B; 20 m × 0.22 mm I.D.) coated with 10% permethylated β-cyclodextrin in OV-1701 as stationary phase was kept at 72°C for 15 min and then programmed to 220°C at 4°C/min.

Automatic thermal desorption

The ATD-400 is an automatic thermal desorption system developed by Perkin-Elmer for the introduction of samples into a GC system. Although basically designed for the determination of volatile contaminants in the atmosphere, it can also be applied to other analytical problems. A summary of its operating mode and of the instrumental settings used in this study are as follows.

The sample to be analysed has to be contained in a small capped tube (desorption cartridge). In our case, the plant sample (1–40 mg) is placed in the desorption cartridge, between two glass-wool plugs. After a leak test, the cartridge is heated (50–400°C) in a flow of inert gas (nitrogen) for a selected time (desorption time, 1–30 min). The volatiles are adsorbed on Tenax GC in a cold trap (−30°C), which can then be heated to 400°C in a few seconds, allowing rapid transfer to the GC capillary column through a heated (50–225°C) fused-silica line.

The flow rates through the system and the amount of volatiles transferred to the column can be controlled by means of two flow splitters; the first (inlet split) is placed between the sample cartridge and the cold trap and the second (outlet split) after the cold trap.

Gas chromatography–mass spectrometry (GC–MS)

GC–MS was carried out using an HP-5890 gas chromatograph coupled to an HP-5971A mass detector (Hewlett-Packard, Palo Alto, CA, USA). A fused-silica capillary column (column C; 12 m × 0.22 mm I.D.) with OV-1 as stationary phase, supplied by Hewlett-Packard, was kept at 70°C for 5 min and then programmed from 70 to 220°C at 6°C/min. Helium was used as the carrier gas.

Methodology

Sample components were characterized from their retention times; when possible, they were identified by comparing their mass spectra and chromatographic retentions with published data [6–9] and, in some instances, with analytical data from standard compounds. Determinations (percentage relative composition) were made directly from integrator peak areas.

Several analyses were also carried out in order to check the importance of incomplete transfer

of volatile components through the ATD system, thermal decomposition or artifact formation. Each series included a run with the sample cartridge, one or several runs with empty cartridges (blanks) and a final run at a high oven temperature with the first cartridge.

The reproducibility of the method was evaluated from the relative standard deviation (R.S.D.) determined for each component from quantitative data from a series of analyses.

Calculations were carried out on a PC microcomputer.

RESULTS

Preliminary experiments

The SDE method [5] and liquid solvent extraction, which are the most widely used methods in the fractionation of plant volatile components, were selected for comparison with the ATD method. Special attention was given first to the qualitative and quantitative differences found among them.

A volatile fraction of *Chamaecyparis lawsoniana* obtained by the SDE method was analysed by GC–MS using column C under the chromatographic conditions previously described. The volatile components of this plant had been already studied [10–12]; limonene was reported to be the main component in all instances (15–65%). Our results were significantly different, as oplopanonyl acetate was present at a 37.5% concentration (calculated from the total ion current trace). Table I lists the components identified or characterized from their retentions and mass spectra and their retention times under the GC–MS conditions mentioned earlier.

Fig. 1 shows the GC results (column A) with the (a) SDE, (b) diethyl ether extraction and (c and d) ATD methods.

The ATD trace (c) includes some peaks (marked with black spots in Fig. 1c) which do not appear in the other chromatograms. Most of these peaks were identified as furyl derivatives, and seem to arise from the thermal decomposition of the carbohydrates present in the plants. This was confirmed by some ATD–GC runs (using the same conditions) on plant samples containing no volatile compounds, as they presented the same peaks. When the oven temperature was decreased from 300°C (Fig. 1c) to 180°C (Fig. 1d), these peaks disappeared.

The size of peaks 28 and 29 in trace (c) decreased when the oven temperature was decreased to 180°C. These peaks were clearly present in the chromatograms of the SDE extracts (see Fig. 1a), but these were very small in

TABLE I

VOLATILE COMPOUNDS OF AN SDE EXTRACT OF *CHAMECYPARIS LAWSONNIANA* IDENTIFIED OR CHARACTERIZED FROM THEIR RETENTION TIMES AND MASS SPECTRA

Compounds marked with asterisks were used in the reproducibility studies. See text for GC–MS column and conditions.

No.	Compound	Retention time (min)
1*	α-Pinene	3.01
2	α-Fenchene	3.24
3*	Sabinene	3.73
4	β-Myrcene	4.17
5*	δ-3-Carene	4.76
6	*p*-Cymene	5.00
7*	(*R*)-(+)Limonene	5.31
8	γ-Terpinene	6.28
9	Terpinen-4-ol	10.28
10	*p*-Cymen-8-ol	13.22
11	Bornyl acetate	14.20
12*	Mol. mass 180	14.39
13	γ-Terpenyl acetate	16.10
14*	α-Terpenyl acetate	16.48
15*	Mol. mass 180	17.12
16*	*trans*-Caryophyllene	19.01
17	Mol. mass 204	19.22
18*	Thujopsene	19.36
19	α-Humulene	20.09
20*	Bicyclosesquiphellandrene	20.38
21*	Mol. mass 204	20.91
22	Mol. mass 204	21.39
23*	γ-Cadinene	21.54
24	Mol. mass 204	21.72
25*	Calamenene	22.06
26*	δ-Cadinene	22.29
27	Mol. mass 222	22.39
28*	β-Oplopenone	24.40
29*	β-Oplopenone isomer	25.17
30*	Oplopenonyl acetate	31.92
31*	Mol. mass 262	32.97
32*	Kaurene derivative	33.30
33*	Mol. mass 272	35.03

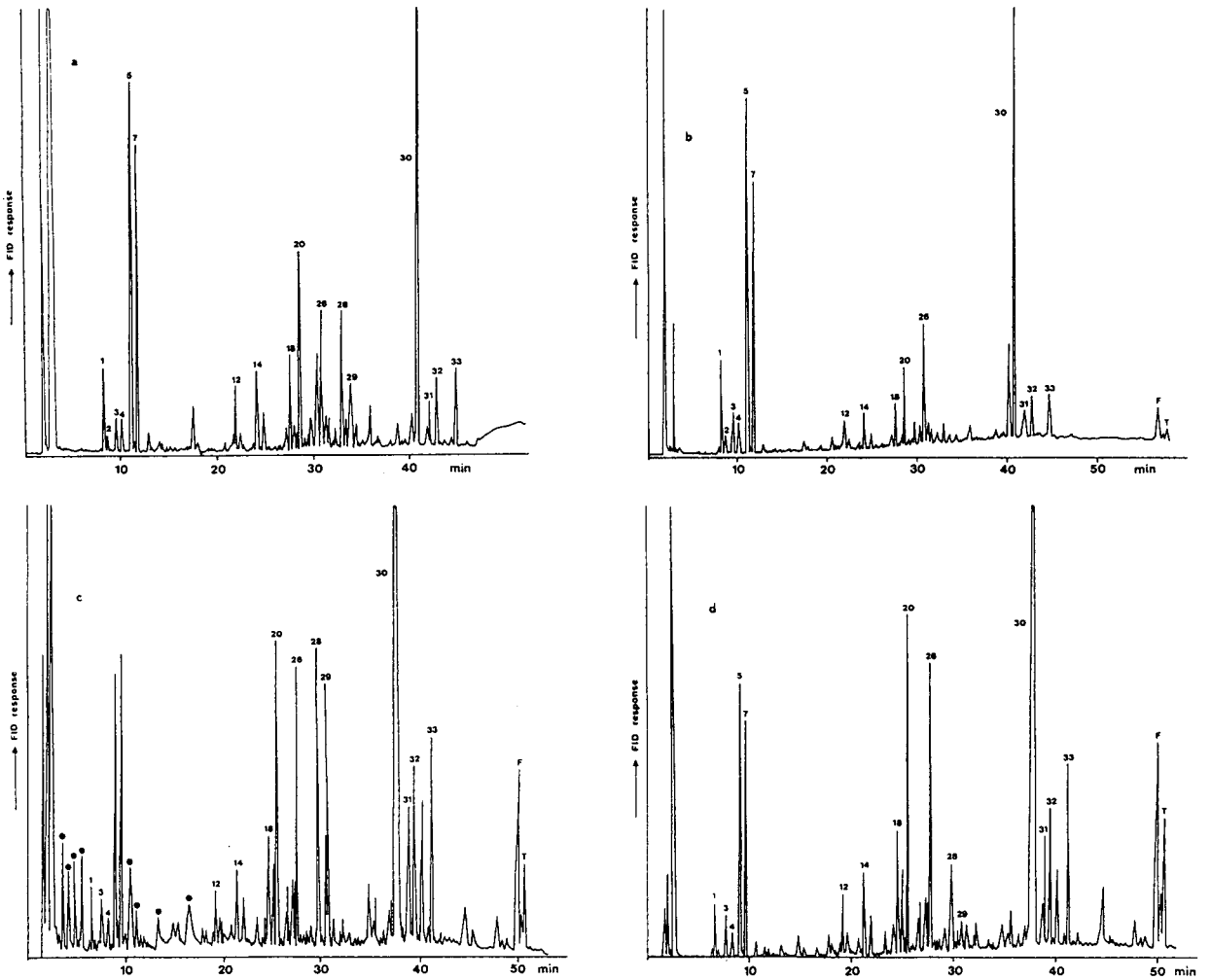

Fig. 1. GC traces of *Chamecyparis lawsonniana* volatile components obtained by different techniques: (a) SDE; (b) solvent extraction; (c) ATD (oven temperature 300°C); (d) ATD (oven temperature 180°C). See text for chromatographic conditions. Peak numbers as in Table I. F = ferruginol; T = totarol. Peaks marked with black spots correspond to thermal degradation compounds.

the solvent extract trace (b), thus seeming to be related to sample heating. Component 28 was identified as β-oplopenone by comparison of its mass spectrum with published data [13], while the mass spectrum of peak 29 seems to indicate a similar structure. In order to confirm that both components result from the thermal decomposition of the main component, oplopanonyl acetate, this compound was isolated by column chromatography as an almost pure compound and then submitted to an SDE extraction. When the resulting fraction was analysed by GC–MS, 4.5% of component 28 and 5.7% of component 29 appeared, showing that oplopanonyl acetate is partially decomposed by the SDE procedure; the ATD at low temperatures seems to decompose this compound to a lesser extent.

Peaks F (ferruginol) and T (totarol) appeared in both the diethyl ether extract and in the ATD traces, but not in that corresponding to the SDE fraction. Nevertheless, after an ATD run, they also appeared as small peaks in subsequent blank

TABLE II

EFFECT OF OPERATING PARAMETERS ON ATD RELATIVE CONCENTRATION (%) VALUES FOR DIFFERENT COMPOUNDS

(A) Oven temperature; (B) desorb flow-rate; (C) desorb time. Nr = Normal elution; Bl = blank; Cr = blank using the first cartridge. See text for details.

Compound No.	(A) Oven temperature (°C)											
	150			180			200			300		
	Nr	Bl	Cr	Nr	Bl	Cr	Nr	Bl	Cr	Nr	Bl	Cr
5	100	0	0	100	0	0	100	0	0	100	0	0
14	86.1	0	13.9	100	0	0	100	0	0	100	0	0
20	79.8	0	20.2	100	0	0	100	0	0	100	0	0
30	80.1	1.1	8.8	98.9	0.5	0.6	99.2	0.4	0.4	99.5	0.4	0.1
	(B) Desorb flow-rate (ml/min)											
	50			20			10			5		
	Nr	Bl	Cr	Nr	Bl	Cr	Nr	Bl	Cr	Nr	Bl	Cr
5	100	0	0	75.2	0	24.8	43.6	0	56.4	28.5	0	71.5
14	100	0	0	78.5	0	21.5	43.1	0	56.9	41.0	0	59.0
20	100	0	0	83	0	17.0	51.8	0	48.2	41.1	0	58.9
30	98.9	0.5	0.6	56.8	4.6	42.6	47.3	7.7	45.0	12.9	28.4	58.7
	(C) Desorb time (min)											
	15			11			8			4			2		
	Nr	Bl	Cr	Nr	Bl	Cr	Nr	Bl	Cr	Nr	Bl	Cr	Nr	Bl	Cr
5	100	0	0	96.3	0	3.7	91.5	0	8.5	92.9	0	7.1	91.4	0	8.6
14	100	0	0	99.9	0	0.1	99.9	0	0.1	95.0	0	5.0	94.6	0	5.4
20	100	0	0	97.8	0	2.2	96.0	0	4.0	94.4	0	5.6	92.9	0	7.1
30	98.9	0.5	0.6	97.7	1.0	1.3	95.3	2.3	2.4	76.3	9.6	4.1	26	43.2	30.8

runs, indicating contamination of the system. Several blank runs were required to eliminate their peaks.

Selection of desorption conditions

As high temperatures seem to produce sample and matrix artifacts, but low temperatures can give rise to incomplete elution of less volatile compounds, several ATD–GC series were run at different over temperatures, desorb flow-rates and desorb times in order to evaluate the effects of these parameters on the ATD elution. Each series included a run using the sample cartridge as usual, a blank run using an empty cartridge and a blank run using the original cartridge and a higher oven temperature (300°C). Several blank runs were included between series when necessary. The results are summarized in Table II; values for each component are expressed as its relative amount (%) in each run of the series.

TABLE III

MEAN RELATIVE VALUES (NORMALIZED TO $\Sigma = 100\%$) AND R.S.D. (EIGHT SERIES OF MEASUREMENTS, 20 SELECTED VOLATILE COMPONENTS)

See Table I for identification. Series A–E, ATD–GC. Common operating conditions: oven temperature, 180°C, desorb flow-rate, 50 ml/min; desorb time, 15 min. (A) Inlet split, 75 ml/min; outlet split, 50 ml/min; higher trap temperature, 320°C, sample size, 10 mg. (B) Inlet split, 75 ml/min; outlet split, 50 ml/min; higher trap temperature, 250°C; sample size, 10 mg. (C) Inlet split, 200 ml/min; outlet split, 100 ml/min; higher trap temperature, 320°C; sample size, 65 mg. (D) Inlet split, 100 ml/min; outlet split, 100 ml/min; higher trap temperature, 320°C; sample size, 40 mg. (E) Inlet split, 0 ml/min; outlet split, 50 ml/min; higher trap temperature, 320°C; sample size, 5 mg. Series F, SDE extract (same extract, four injections). Series G, SDE extracts (five extractions). Series H, solvent extracts (three extracts).

Component	Mean relative value							
	A	B	C	D	E	F	G	H
1	0.7	0.9	1.0	0.9	0.5	1.9	2.1	3.5
3	0.7	0.6	0.6	0.8	0.6	0.9	1.1	1.7
5	4.0	4.5	4.8	4.2	3.0	9.4	10.5	14.2
7	3.4	3.7	3.8	3.7	2.6	7.4	8.1	11.0
12	1.0	1.0	1.0	1.0	1.0	1.7	1.4	1.4
14	1.3	1.4	1.4	1.3	1.3	2.1	2.1	1.7
15	0.7	0.7	0.7	0.7	0.7	0.9	1.0	0.7
16	0.5	0.5	0.5	0.4	0.4	0.8	1.1	0.8
18	1.6	1.6	1.6	1.4	1.4	2.6	2.9	2.3
20	5.9	6.1	6.2	5.8	5.7	5.0	5.9	3.9
21	0.9	1.1	1.1	1.0	1.0	1.5	0.9	0.9
23	1.1	1.1	1.1	1.0	1.1	1.1	1.2	1.0
25	0.8	0.9	1.0	0.8	0.9	2.4	3.0	0.0
26	5.5	5.0	4.5	5.0	4.9	5.9	5.5	8.0
28	2.1	2.0	2.0	2.4	2.8	4.4	4.7	1.3
29	0.4	0.5	0.5	0.6	0.8	2.4	2.4	0.5
30	62.2	61.6	61.4	61.7	64.2	43.8	40.1	40.8
31	1.8	1.8	1.8	1.8	2.1	1.3	1.1	1.6
32	2.5	2.3	2.3	2.7	2.6	1.8	2.1	2.1
33	2.8	2.8	2.8	2.9	2.7	2.3	2.5	2.4
	R.S.D. (%)							
	A	B	C	D	E	F	G	H
1	9.4	21.2	7.8	14.9	20.9	5.7	19.6	12.7
3	2.0	17.6	13.0	13.7	10.0	9.0	17.9	12.2
5	7.4	13.7	5.2	12.4	10.1	4.4	15.6	10.6
7	7.7	10.8	4.6	16.0	12.8	5.3	14.3	10.2
12	5.0	6.8	1.5	6.0	8.5	21.7	10.6	17.9
14	2.3	6.1	2.1	6.2	6.5	3.0	7.3	3.1
15	8.1	8.7	8.9	12.2	8.7	9.6	6.8	4.7
16	2.0	7.6	1.5	13.4	6.5	22.7	20.9	24.5
18	3.3	3.9	2.7	7.5	10.1	5.0	6.4	1.5
20	1.0	1.9	3.2	3.0	5.8	0.5	7.9	3.6
21	5.2	3.3	5.5	5.2	8.5	17.0	15.0	20.1
23	3.0	4.6	6.6	4.8	5.7	10.1	4.8	26.2
25	6.6	7.2	9.7	11.3	16.0	1.3	12.4	0.0
26	2.5	5.9	4.3	8.8	9.2	2.3	13.0	4.6
28	6.8	17.6	17.7	10.2	8.2	5.5	4.1	2.7
29	19.4	11.7	10.8	24.7	17.0	21.9	26.0	13.0
30	0.9	2.0	1.2	1.8	2.3	3.2	11.8	5.6
31	2.7	2.9	3.9	4.5	21.1	18.2	15.5	26.6
32	3.8	3.4	3.4	5.5	4.8	2.4	7.8	8.1
33	2.7	3.2	1.8	7.9	5.0	4.4	7.3	3.9

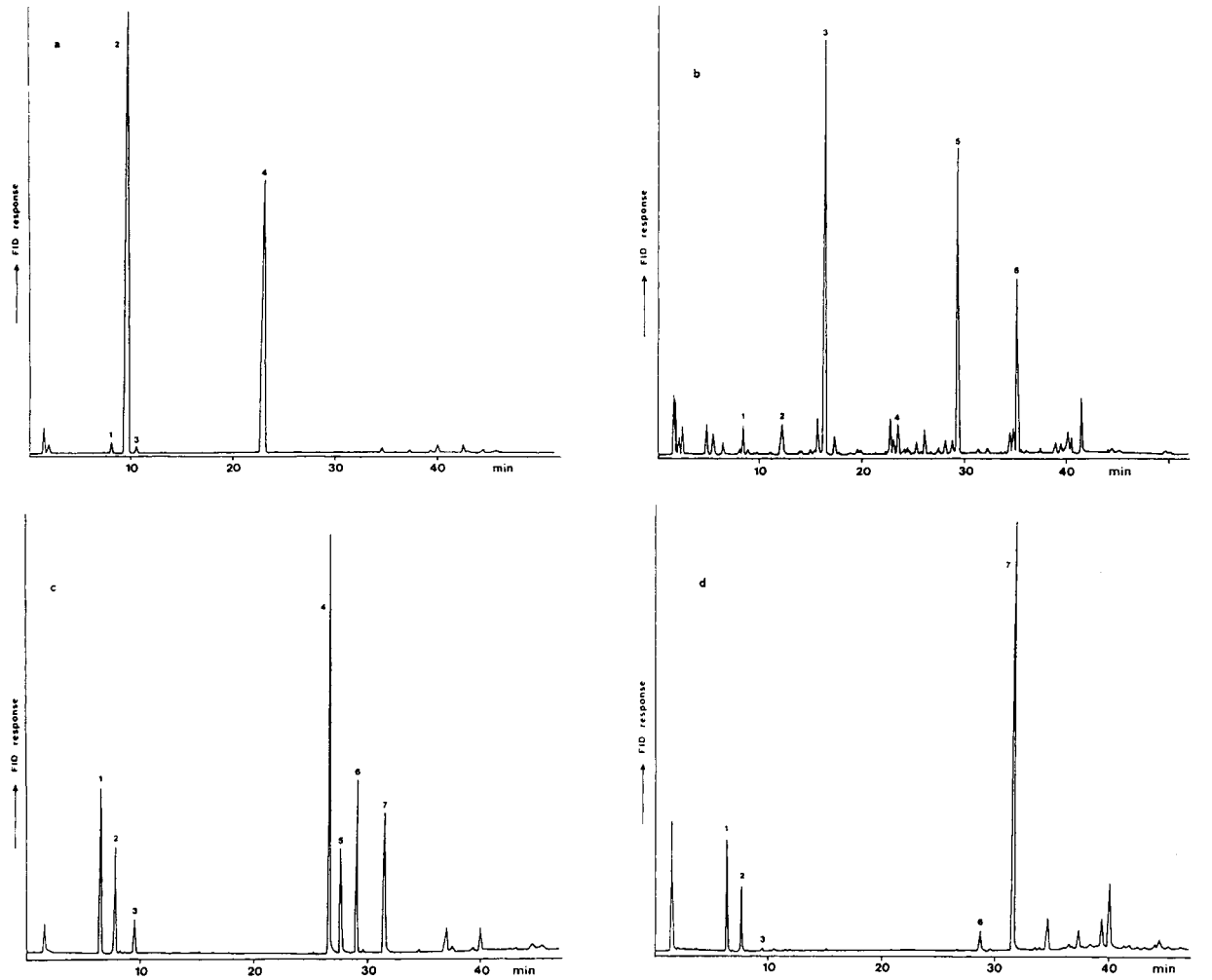

Fig. 2. ATD–GC traces of volatile components of Umbelliferae seeds. (a) *Thapsia villosa*: 1 = β-myrcene; 2 = limonene; 3 = α-terpinene; 4 = methylisoeugenol. (b) *Heracleum sphondylium*: 1 = isopropyl isobutyrate; 2 = isobutyl isopentanoate; 3 = *n*-octyl acetate; 4 = *n*-octyl butyrate; 5 = *n*-octyl hexanoate; 6 = *n*-octyl octanoate. (c) and (d) *Petroselinum crispum* (parsley): 1 = α-pinene; 2 = β-pinene; 3 = β-phellandrene; 4 = myristicine; 5 = trimethoxyallylbenzene; 6 = tetramethoxyallylbenzene; 7 = apiole. See text for chromatographic conditions.

The results of the first series (A, desorb flow-rate = 50 ml/min, desorb time = 15 min) indicate that components of medium and low volatility can be incompletely eluted at an oven temperature of 150°C. Taking into account the possibility of artifact formation at high oven temperatures, 180°C seem to be advisable for components of a broad volatility range. A lower oven temperature could be used with samples containing high-volatility compounds.

Series B in Table II (oven temperature = 180°C, desorb time = 15 min) show the importance of a high desorb flow-rate for complete elution from the sample cartridge of compounds of both high and low volatility. Flow-rates ≥50 ml/min seem to be advisable.

In series C (oven temperature = 180°C, desorb flow-rate = 50 ml/min), the negative effect of a short desorb time seems similar to, although less marked than, that of the desorb flow-rate. A

desorb time of 15 min seems to be advisable, as longer times at high temperatures could increase the danger of artifact formation.

Reproducibility

In order to evaluate the reproducibility of the ATD procedure, five series (A–E, each consisting of ten samples) of ATD–GC analyses were run. The values of the basic operating parameters were those recommended in the previous series: oven temperature 180°C, desorb flow-rate 15 ml/min and desorb time 15 min. The inlet split, outlet split and sample size were varied in order to determine the influence of possible sampling errors caused by plant sample heterogeneity on the reproducibility. Series F (SDE extract, four injections), series G (five SDE extracts) and series H (three solvent extracts) were also run for comparison purposes. For each series, mean values and R.S.D.s were calculated for the twenty selected compounds marked with asterisks in Table I; the results are given in Table III.

Although the quantitative elution pattern was similar for ATD, solvent extraction and SDE, the mean values for high-volatility compounds are in general higher for SDE and solvent extraction, whereas those of low-volatility compounds are higher for the ATD method. The best reproducibility was shown by series A and C (mean R.S.D.s 5.1% and 5.8%). The lower performance of the other ATD series was mainly caused by the high R.S.D.s for the most volatile components; since the mean R.S.D. was 9.9% for series E it seems that the use of too small amounts of plant material can introduce a sampling error. Hence the use of relatively high sample amounts with high splitting ratios seems to allow a satisfactory reproducibility.

Although the number of runs in the solvent extraction and SDE series is too small to draw statistical conclusions, it is clear that their reproducibility was lower (the R.S.D. was 8.7% for series F, 12.3% for series G and 10.6% for series H).

Example of application

The ATD–GC method was applied to the determination of the volatile components of seeds of the Umbelliferae family. The ATD operating conditions were those of series A in Table III. GC was carried out with column A using the previously described ATD and chromatographic conditions.

Seeds of *Thapsia villosa*, *Heracleum sphondylium* and parsley (*Petroselinum crispum*) were analysed. Approximately one quarter of a seed (1.5 mg) was introduced into the ATD cartridge for *T. villosa* and a single seed (6–7 mg) for *H. sphondylium*. Two different commercial samples of parlsey were analysed: 2–3 seeds (2–3 mg) were used.

The ATD composition (Fig. 2) was very similar in all instances to that found by SDE. No artifacts related to thermal decomposition were observed. The elution of volatile compounds was checked by running empty cartridges after each sample and was found to be complete.

The presence of different chemotypes and intermediate forms in parsley has been discussed recently [14]. Fig. 2c and d indicate that even using single seeds, chemical differences could be clearly shown by the ATD–GC method.

ATD also allowed the determination of chiral volatile compounds. One of the main volatile components of *Thapsia villosa* seeds is limonene (Fig. 2a). As this compound can be present in (*R*)-(+)- and (*S*)-(−)-forms, an ATD–GC analysis was carried out using column B, coated with a chiral phase. Fig. 3a shows the limonene peak obtained when about one quarter of a *Thapsia villosa* seed was analysed by ATD–GC. When the seed was spiked with (*R*)-(+)-limonene, a single limonene peak was also obtained. However, when the seed was spiked with (*S*)-(−)-limonene, a double peak appeared as shown in Fig. 3b. The retention times of both peaks corresponded to those found when injecting through the ATD a mixture of (*R*)-(+)- and (*S*)-(−)-limonene.

DISCUSSION

All sample fractionation procedures present advantages and drawbacks, which depend on the compounds to be analysed, their concentration in the sample and the possible effects of the matrix. In the case of plant volatile compounds, the main advantages of the ATD procedure are the possibility of carrying out a volatile frac-

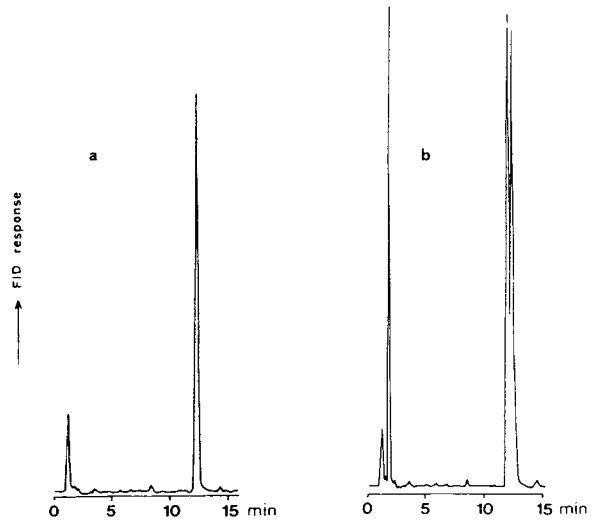

Fig. 3. ATD–GC determination of limonene in *Thapsia villosa* seeds using a chiral column. See text for chromatographic conditions. (a) *Thapsia villosa* seed; main peak is limonene. (b) *Thapsia villosa* seed spiked with (*S*)-(−)-limonene.

tionation on-line with the GC analysis, eliminating the need for a time-consuming extraction or fractionation step, and the small amount (1–20 mg, depending on volatile concentration) of plant required.

An additional advantage of the ATD method is its flexibility of use. Many operational parameters such as temperatures, flow-rates and splitting ratio can be changed, selecting their optimum values for a given application. Many possibilities of method implementation were not studied in this work, such as the introduction of plant solvent extracts into the ATD cartridge in order to avoid the artifacts produced from thermal decomposition of the insoluble compounds and the use of different adsorbents in the cold trap and of different packing materials for the plant in the sample cartridge.

When compared with other well established methods of plant volatile analysis, such as steam distillation and extraction, the ATD method, according to our results, presents better reproducibility probably because sample fractionation and introduction are carried out automatically.

Thermal decomposition of labile volatile compounds, which also occurs when using the SDE method, can be reduced in the ATD method while maintaining a high volatile recovery by selecting an oven temperature between 150 and 200°C. Thermal production of artifacts from the matrix is also very low at these temperatures.

Although liquid solvent extraction does not produce thermal decomposition, it is a slow technique that usually requires a concentration step; component recoveries can depend on the solvent used.

The method of choice when the sample contains thermally labile components seems to be supercritical fluid extraction, although in some instances extractable matrix components can interfere with GC analysis [15].

The possibility of system contamination is a drawback of the ATD method when compounds in the molecular mass range 300–400 are present in high concentrations in the sample. These compounds can be desorbed from the sample cartridge at 150–180°C, but they can partially remain in the system and appear in subsequent runs. The use of a lower oven temperature would result in incomplete desorption of compounds in the molecular mass range 200–300, which can have interesting flavour properties. A high desorb flow-rate would perhaps be necessary in the analysis of these samples.

We have applied the ATD method successfully to samples of different plant species. From our results, it seems to be useful when very large numbers of GC analyses are required in order to obtain results of statistical value and it is necessary to use only a small amount of plant. Possible applications include analytical studies on the distribution of volatile compounds in plants or chemotaxonomic studies based on their volatile composition. Once the instrument parameters have been optimized and the problems related to the specific application have been minimized, single plants (for chemotaxonomic studies) or parts of plants, flowers or leaves (for distribution studies) can be automatically analysed; when necessary, the use of chiral GC columns can allow the determination of enantiomeric composition.

ACKNOWLEDGEMENTS

This work was supported by the Comunidad Autónoma de Madrid (project No. C150/91)

and by the DGICYT (projects PB88-034 and PB91-0077-C03-02). We thank Dr. R. Morales (Jardín Botánico, CSIC, Madrid) for the botanical analysis of the plant samples used in this study and Dr. M.C. de la Torre (Instituto de Química Orgánica General, CSIC, Madrid) for the isolation and identification of oplopanonyl acetate. We also thank M.I. Jiménez for column preparation.

REFERENCES

1 Y. Chen, Z. Li, D. Xue and L. Qi, *Anal. Chem.*, 59 (1987) 744.
2 P. Werkhoff and W. Bretschneider, *J. Chromatogr.*, 405 (1987) 87.
3 G. Reglero, M. Herraiz, T. Herraiz and J. Sanz, *J. Chromatogr.*, 483 (1989) 43.
4 J. Barberio and J. Twibell, *J. High Resolut. Chromatogr.*, 14 (1991) 637.
5 M. Godefroot, P. Sandra and M. Verzele, *J. Chromatogr.*, 203 (1981) 325.
6 F.W. McLafferty and D.B. Stauffer, *Wiley/NBS Registry of Mass Spectral Data*, Wiley, New York, 1989.
7 W. Jennings and T. Shibamoto, *Qualitative Analysis of Flavor and Fragrance Volatiles by Glass Capillary Gas Chromatography*, Academic Press, New York, 1980.
8 N.W. Davies, *J. Chromatogr.*, 503 (1990) 1.
9 R.P. Adams, *Identification of Essential Oils by Ion Trap Mass Spectroscopy*, Academic Press, New York, 1989.
10 M. Yatagai, T. Sato and T. Takahashi, *Biochem. Syst. Ecol.*, 13 (1985) 377.
11 M.S. Karawya, F.M. Soliman, E.A. Aboutabl and T.A. El-Kersh, *Egypt. J. Pharm. Sci.*, 27 (1986) 341.
12 H.L. De Pooter, J.R. Vermeesch, L.F. De Buyck, Q.L. Huang, N.M. Schamp and A. De Bruyn, *J. Essential Oil Res.*, 3 (1991) 1.
13 G. Vernin, J. Metzger, K.N. Suon, D. Fraisse, C. Ghiglione, A. Hamond and C. Parkanyi, *Lebensm. Wiss. Technol.*, 23 (1990) 25.
14 A. Lamarti, A. Badoc and R. Bouriquet, *J. Essential Oil Res.*, 3 (1991) 425.
15 S.B. Hawthorne, D.J. Miller and M.S. Krieger, *J. High Resolut. Chromatogr.*, 12 (1989) 714.

Journal of Chromatography A, 657 (1993) 165–173
Elsevier Science Publishers B.V., Amsterdam

CHROM. 25 530

Concept of effective mass and hidden mass for calculation of mobility of organic anions and peptides

Mieczysław Wroński

Department of Chemical Technology and Environmental Protection, University of Łódź, Pomorska 18, Łódź (Poland)

(First received October 19th, 1992; revised manuscript received August 27th, 1993)

ABSTRACT

The concept presented for the calculation of electrophoretic mobility is based on three assumptions: (1) the molecular mass M can be treated as composed of effective mass E and hidden mass H, $M = E + H$; (2) the mobility u is proportional to the charge Z and inversely proportional to the effective mass to the power 2/3; and (3) both E and H are additive functions of composition. Butyric acid was chosen as a standard fulfilling the condition $M = E$, $H = 0$, resulting in the equation $u = 668ZE^{-2/3} \cdot 10^{-5}$ cm^2 s^{-1} V^{-1}. The suggested approach involves the summation of all special contributions to the hidden mass and calculation of the mobility from the effective mass $E = M - \Sigma H$. The total hidden mass involves values dependent on hydrocarbon structure, H_α, dependent on functional groups, H_β, and contributions of certain subunits such as amino acids in peptides, H_t. The H_α contributions for aliphatic compounds can be expressed as a function of the methylene (together with CH_3 and CH but with the exception of CHOH chains) group content in the molecule. H_α for aromatic compounds depends on the nature of the aromatic ring. The special contributions were derived from the mobilities of about 200 compounds. Mobilities calculated by the suggested approach indicate an average relative error of ±1.5% for organic acids and ±0.8% for peptides.

INTRODUCTION

A knowledge of the relationship between ionic mobility, molecular mass and molecular structure is of prime importance for electrophoretic separation, determination and identification. It has been established experimentally that the electrophoretic mobility u is proportional to the charge Z and inversely proportional to the molecular mass M to the power $-b$:

$$u = aZM^{-b}$$

where a and b are constants. Jokl [1] and Blasius and Preetz [2], using paper electrophoresis, found $b = 1/2$, whereas Offord [3], on basis of an extensive study of peptides determined, $b = 2/3$. The electrophoresis of mercapto acids in cellulose gel [4] resulted in $b = 1/2$, while the mobilities extrapolated to zero concentration of cellulose gel [5] are best represented by $b = 2/3$. The mobilities measured by means of paper or gel electrophoresis are influenced by adsorption and sieving effects, whereas capillary isotachophoresis offers the results without additional disturbances [6,7].

THEORETICAL

It has been assumed that the molecular mass M can be considered as being composed of two parts, an effective mass E and a hidden mass H, $M = E + H$, and that the mobility u is proportional to the effective mass to the power $-2/3$ and to the charge Z

$$u = kZE^{-2/3} \quad (1)$$

where k is a constant. By introducing butyric acid as a standard fulfilling the condition $M = E$, $H = 0$, with $M = 88.11$ and $u = 33.7 \cdot 10^{-5}$ cm^2 s^{-1} V^{-1} and charge $Z = 1$ (in the calculation M of acids and a positive charge are used), the constant k will be given by $k = 33.7 \cdot 88 \cdot 11^{2/3} =$

0021-9673/93/$06.00

$668 \cdot 10^{-5}$ cm^2 s^{-1} V^{-1}. The mobility will be then expressed by

$$u = 668ZE^{-2/3}$$

$$= 668Z(M - H)^{-2/3} \cdot 10^{-5} \text{ cm}^2 \text{ s}^{-1} \text{ V}^{-1} \quad (2)$$

where Z is relative charge. The effective mass is defined by the expression

$$E = (668Zu^{-1})^{1.5} \quad (3)$$

When two identical ions combine to form a new one, then in accord with the rule of additivity $M_2 = 2M_1$, $E_2 = 2E_1$ and $H_2 = H_1$, and as follows from eqn. 2, the ratio of mobilities will be given by

$$u_2 u_1^{-1} = Z_2 Z_1^{-1} \cdot 2^{-2/3} \quad (4)$$

When ionization remains unchanged, $Z_2 = 2Z_1$, and $u_2 u_1^{-1} = 1.26$. In the case of an exchange of subunits, $M_{1,2} + M_{3,4} = M_{1,3} + M_{2,4}$, the additivity of effective masses and hidden masses will be expressed by

$$E_{1,2} + E_{3,4} = E_{1,3} + E_{2,4}$$

$$H_{1,2} + H_{3,4} = H_{2,4} + H_{12,3}$$

EXPERIMENTAL

Most of the mobilities considered were taken from papers by Hirokawa and co-workers [8–13]. The others, involving mercapto acids, disulphides, sulphonic acids and N-acetyl derivatives of amino acids, were calculated from relative step heights, determined in this laboratory, using the equation [7]

$$u = \frac{u_S u_L}{u_S + h(u_L - u_S)} \quad (5)$$

where u_S is the mobility of the standard ion, perchlorate = $66.7 \cdot 10^{-5}$ cm^2 s^{-1} V^{-1} or trichloroacetate = $36.2 \cdot 10^{-5}$ cm^2 s^{-1} V^{-1}, and u_L is the mobility of the leading ion, chloride = $79.0 \cdot 10^{-5}$ cm^2 s^{-1} V^{-1}.

Measurements of relative step heights were performed using an isotachophoretic analyser produced by Labeco (Slovakia), retaining a concentration of leading chloride ion of 0.01 *M*. Sulphonic acids were examined at pH 3.5 and mercapto acids and N-acetylamino acids at pH 6.0, using β-alanine and histidine buffers. The terminating electrolytes used were either isocapronic acid or 2-(N-morpholino)ethanesulphonic acid (MES) or sodium tetraphenylborate.

RESULTS AND DISCUSSION

The results of the measurements and calculations are presented in Tables I–VI and Fig. 1. The mobility always corresponds to full ionization of carboxylic or sulphonic groups. The hidden mass can be in general expressed as the sum $H = H_\alpha + H_\beta$, where H_α depends on the basic hydrocarbon structure and H_β is the contribution of the functional group. The relationship between hidden mass $H_\alpha = M - E - H_\beta$ and the number of methylene groups (CH_3 and CH groups are included, with the exception of CHOH chains) in the molecule is demonstrated in Fig. 1 and Table I. The established relationship can be expressed by the following equations:

Aliphatic carboxylic acids in methanol:

$$H_\alpha = 12(n - 1) \quad n \geq 1 \quad (6)$$

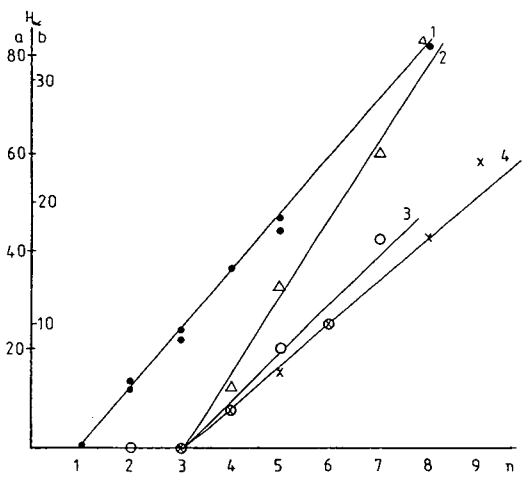

Fig. 1. Relationship between hidden mass, $H_\alpha = M - EM - H_\beta$, and the number of the methylene groups in a molecule. (1) (Scale a): ● = carboxylic acids in methanol, $H_\beta = 0$; full line, $H_\alpha = 12\ (n - 1)$. (2) (Scale b): △ = carboxylic acids in water, $H_\beta = 0$; full line, $H_\alpha = 6\ (n - 3)$. (3) (scale b): ○ = divalent carboxylic acids in water, $H_\beta = 14$; full line, $H_\alpha = 4\ (n - 3)$. (4) (scale b): × = sulphonic acids in water, $H_\beta = 48$; full line, $H_\alpha = 3.5\ (n - 3)$.

TABLE I

MOBILITIES, u (10^{-5} cm^2 s^{-1} V^{-1}), OF CARBOXYLIC AND SULPHONIC ACIDS, MOLECULAR MASSES, M, EFFECTIVE MASSES, E, AND HIDDEN MASSES, H

No.	Acid	u	M	E	H
1	Acetic	42.4	60	62	−2
2	Propionic	36.9	74	77	−3
3	Butyric	33.7	88	88	0
4	Valeric	31.6	102	97	5
5	Hexanoic	30.2	116	104	12
6	Heptanoic	28.4	130	114	16
7	Octanoic	27.4	144	120	24
8	Nonanoic	26.7	158	125	33
9	Oxalic	74.6	90	76	14
10	Malonic	66.0	104	91	13
11	Succinic	60.3	118	104	14
12	Glutaric	55.6	132	118	14
13	Adipic	52.4	146	129	17
14	Pimelic	49.9	160	138	22
15	Suberic	47.2	174	150	24
16	Azelaic	45.9	188	157	31
17	Sebacic	44.9	202	162	40
18	Methanesulphonic	50.5	96	48	48
19	Ethanesulphonic	42.7	110	62	48
20	Propanesulphonic	37.5	124	75	49
21	Butanesulphonic	33.9	138	87	51
22	Pentanesulphonic	31.4	152	98	54
23	Hexanesulphonic	29.4	166	108	58
24	Octanesulphonic	26.2	194	129	65
25	Nonanesulphonic	25.1	208	137	71
26	Dodecanesulphonic	22.3	250	164	86
In methanol as solvent					
27	Acetic	43.8	60	60	0
28	Propionic	43.4	74	60	14
29	Butyric	41.6	88	64	22
30	Valeric	40.8	102	66	36
31	Hexanoic	39.6	116	69	47
32	Nonanoic	37.1	158	76	82
33	Decanoic	38.4	172	73	99
34	Palmitic	32.6	256	93	163

Aliphatic carboxylic acids in water:

$$H_\alpha = 6(n-3)\ n \geq 3 \quad (7)$$

Divalent aliphatic carboxylic acids in water:

$$H_\alpha = 4(n-3)\ n \geq 3 \quad (8)$$

Aliphatic sulphonic acids in water:

$$H_\alpha = 3.5(n-3)\ n \geq 3 \quad (9)$$

In order to explain the above relationships, the formation of a loop containing at lease four methylene groups was assumed, resulting in a decrease in the outward surface of the molecule. The change in H_α per methylene group is, up to a certain n in water, constant for a given group of acids and differences between the groups of acids may be explained by the different compactness of the loops.

As can be derived from Table I and Fig. 1 from $n = 7$ for carboxylic acids in water and from $n = 8$ for sulphonic acids in water there is an additional increase in hidden mass, indicating the

TABLE II

MOBILITIES, u (10^{-5} cm^2 s^{-1} V^{-1}), OF MERCAPTO ACIDS AND DISULPHIDES, EFFECTIVE MASSES, E, HIDDEN MASSES, H, AND RATIOS OF MOBILITIES

No.	Mercapto acid	Thiol			Disulphide	
		u_1	E	H	u_2	u_2/u_1
1	Mercaptoacetic	40.3	67	25	50.0	1.24
2	2-Mercaptopropionic	36.3	79	27	45.8	1.26
3	3-Mercaptopropionic	35.5	81	25	44.2	1.25
4	Acetylcysteine	30.0	105	58	37.5	1.25
5	Acetylhomocysteine	29.0	110	67	37.0	1.28
6	Acetylpenicillamine	27.8	118	73	34.7	1.25
7	Captopril	24.8	139	78	30.7	1.24
8	N-(2-Mercaptopropionyl)glycine	30.3	104	59	37.8	1.25
9	Glutathione	22.2	165	142	27.3	1.23
10	2-Mercaptoethanesulphonic	39.7	69	73	49.2	1.24

additional decrease in the outward surface. This phenomenon can be explained by association or micellization in water. No loops and no association are found in methanol as solvent.

The results for thiols and disulphides are summarized in Table II. The contribution of a mercapto group to the hidden mass can be found directly from results Nos. 1–3 as 25, 27 and 25, and indirectly by subtraction of the value of 48 (H_β of sulphonic group) from result No. 10, $73 - 48 = 25$. Assuming the hidden mass for the NH–CO group to be 32, as derived from peptides, the hidden mass for the SH group in N-(2-mercaptopropionyl)glycine will be $59 - 32 = 27$. This contribution for the SH group in captopril can be found by subtracting the contributions of proline, 20, and NHCO: $78 - 20 - 32 = 26$.

The average ratio of mobilities of disulphides to thiols amounts to 1.25, in good agreement with eqn. 4 for $Z_2 = 2Z_1$.

Table III gives the special contribution to the hidden mass of the acid derived from the results in Tables I, II and IV. The values can be utilized for the calculation of mobility from composition using eqn. 2. The sum of the special contributions is subtracted from the molecular mass and the effective mass thus found is inserted in eqn. 2.

The effective mass of fluorine and chlorine substituents in methanol as solvent is negative, which means that the substitution of hydrogen results in an increase in mobility. The contribu-

TABLE III

CONTRIBUTIONS OF FUNCTIONAL GROUPS TO HIDDEN MASS

Functional group	Hidden mass	
	Water	Methanol
Fluorine	18	22
Chlorine	30	38
Bromine	69	80
Iodine	120	126
Hydroxyl	14	19[a]
Carbonyl	21	–
Nitro	38	–
Second aliphatic carboxylic	14[b]	–
Sulphydryl	26	–
Sulphonic	48	–
Amino, methoxy, ethoxy in benzene ring	3	–
Benzene ring in carboxylic or sulphonic acids	36	57
Benzene ring with alkyl substituents	25	–
Benzene ring in phenol	9	–
Pyridine ring in nicotinic acid	38	56
Naphthalene ring	61	–
Methylene groups in monocarboxylic acids	$6(n-3)$	$12(n-1)$
Methylene groups in divalent carboxylic acids	$4(n-3)$	–
Methylene groups in sulphonic acids	$3.5(n-3)$	

[a] Aromatic OH 24.
[b] Second aromatic COOH 3.

TABLE IV

DETERMINED, u, AND CALCULATED, u_{calc}, MOBILITIES (10^{-5} cm^2 s^{-1} V^{-1}), MOLECULAR MASSES, M, AND CONTRIBUTIONS OF FUNCTIONAL GROUPS TO HIDDEN MASS, H_{contr}

No.	Acid	u	M	H_{contr}	u_{calc}
1	Fluoroacetic	43.9	78	18	43.5
2	Trifluoroacetic	42.5	114	3 × 18	43.5
3	Chloroacetic	41.9	95	31	41.9
4	Dichloroacetic	39.4	129	2 × 31	40.4
5	Trichloroacetic	36.2	164	3 × 31	38.9
6	3-Chloropropionic	36.8	109	31	36.5
7	2-Chlorobutyric	32.8	123	31	32.8
8	5-Chlorovaleric	30.8	137	31 + 6	31.0
9	Bromoacetic	38.8	139	69	39.3
10	2-Bromopropionic	33.4	153	69	34.8
11	2-Bromobutyric	30.8	167	69	31.4
12	4-Bromobutyric	32.8	167	69	31.4
13	5-Bromovaleric	30.8	181	6 + 69	29.8
14	2,3-Dibromopropionic	32.3	232	2 × 69	32.3
15	Tribromoacetic	34.9	297	3 × 69	33.2
16	Iodoacetic	40.2	186	120	40.8
17	3-Iodopropionic	34.9	200	120	35.9
18	4-Iodobutyric	32.9	214	120	32.3
19	5-Iodovaleric	30.8	228	6 + 120	30.6
20	3,4-Dibromofluoroacetic	36.9	236	2 × 69 + 18	35.9
21	Chlorodibromoacetic	34.9	252	2 × 69 + 31	35.1
22	Glycolic	42.3	76	14	42.4
23	Lactic	36.5	90	14	37.2
24	2-Hydroxybutyric	34.2	104	14	34.2
25	Glyceric	36.3	106	2 × 14	36.5
26	Glucuronic	26.6	194	5 × 14	26.8
27	Gluconic	27.2	196	5 × 14	26.6
28	2-Chloro-3-hydroxybutyric	32.9	139	31 + 14	32.3
29	Glyoxalic	37.8	92	21	38.9
30	Pyruvic	40.4	88	21	40.4
31	Trichlorolactic	34.2	193	3 × 31 + 14	34.2
32	Maleic	62.0	116	14	61.1
33	Fumaric	61.2	116	14	61.1
34	Tartaric	60.5	150	3 × 14	58.9
35	Citric	70.8	192	3 × 14	70.8
36	2-Ketoglutaric	59.0	146	14 + 21	57.8
37	Malic	59.0	134	2 × 14	59.6
38	Thiomalic	58.5	150	14 + 26	58.2
39	2,3-Dimercaptopropanesulphonic	34.4	188	2 × 26 + 48	33.7
40	2-Hydroxyethanesulphonic	39.6	126	14 + 48	41.7
41	Cyclobutane-1,1-dicarboxylic	51.1	144	14	52.0
42	Cyclopentane-1,1-dicarboxylic	50.0	158	14 + 4	49.5
43	Cyclohexane-1,1-dicarboxylic	48.0	172	2 × 4 + 14	47.2
44	Methylmalonic	58.5	118	14	60.3
45	Methylethylmalonic	50.0	146	14	51.5
46	Propylmalonic	52.0	146	14	51.5
47	Diethylmalonic	49.5	160	4 + 14	49.0
48	Ethylpropylmalonic	47.0	174	2 × 4 + 14	47.0
49	Dipropylmalonic	46.0	188	3 × 4 + 14	44.9
50	Oxaloacetic	56.0	132	14	55.4
51	3-Propylglutaric	47.0	174	3 × 4 + 14	47.7
52	Benzoic	34.4	122	36	34.4
53	Benzenesulphonic	38.7	158	36 + 48	37.8
54	*p*-Toluenesulphonic	31.1	172	25 + 48	31.2
55	*o*-Aminobenzoic	31.6	136	36 + 3	31.6
56	Sulphanilic	33.7	173	36 + 3 + 48	34.2
57	*p*-Fluorobenzoic	33.4	140	36 + 18	34.2

(Continued on p. 170)

TABLE IV *(continued)*

No.	Acid	u	M	H_{contr}	u_{calc}
58	*p*-Chlorobenzoic	33.4	157	36 + 31	33.2
59	*m*-Iodobenzoic	33.4	248	36 + 120	32.7
60	*p*-Bromobenzoic	31.5	201	36 + 69	31.8
61	*p*-Nitrobenzoic	32.1	167	36 + 38	32.5
62	3,5-Dinitrobenzoic	29.5	212	2 × 38 + 36	31.0
63	*p*-Toluic	29.1	136	25	28.9
64	*p*-Ethylbenzoic	26.5	150	25	26.7
65	2,3-Dimethylbenzoic	27.1	150	25	26.7
66	*o*-Isopropylbenzoic	24.7	164	25	24.9
67	2,4,6-Trimethylbenzoic	24.7	164	25	24.9
68	*p-tert.*-Butylbenzoic	23.2	178	25	23.3
69	*p*-Hydroxybenzoic	34.0	138	14 + 36	33.7
70	Salicylic	35.4	138	14 + 36	33.7
71	2,4-Dihydroxybenzoic	32.0	154	2 × 14 + 36	33.2
72	3,4-Dihydroxybenzoic	34.4	154	2 × 14 + 36	33.2
73	Gallic	34.4	170	3 × 14 + 36	32.7
74	*p*-Methoxybenzoic	28.3	152	36 + 3	28.5
75	*p*-Ethoxybenzoic	26.6	166	36 + 3	26.6
76	2-Nitro-3-bromobenzoic	28.2	246	38 + 36 + 69	30.4
77	2-Nitro-3-chlorobenzoic	31.3	201	38 + 31 + 36	31.8
78	Phenol	34.4	94	9	34.4
79	*p*-Nitrophenol	33.4	139	9 + 38	32.7
80	2,4-Dinitrophenol	31.3	184	2 × 38 + 9	31.2
81	Picric	31.5	229	3 × 38 + 9	29.8
82	*p*-Chlorophenol	33.4	129	9 + 31	33.5
83	2,4-Dichlorophenol	31.3	163	2 × 31 + 9	32.7
84	Vanillic	27.1	168	14 + 3 + 36	28.2
85	Cinnamic	28.3	148	36	28.7
86	Phenylacetic	31.7	136	36	31.0
87	Phenoxyacetic	27.8	152	36	28.0
88	Nicotinic	34.6	123	38	34.6
89	2-Naphthalenesulphonic	31.3	208	61 + 48	31.3
In methanol as solvent					
90	Acrylic	43.5	72	12	43.5
91	methacrylic	42.8	86	24	42.6
92	Crotonic	41.7	86	24	42.6
93	2,4-Hexadienoic	40.2	112	48	41.7
94	Fluoroacetic	45.7	78	23	46.1
95	Trifluoroacetic	52.9	114	3 × 23	52.9
96	Chloroacetic	45.6	95	38	45.0
97	Dichloroacetic	47.1	129	2 × 38	47.3
98	Trichloroacetic	47.3	164	3 × 38	49.2
99	2-Chloropropionic	43.9	109	12 + 38	44.0
100	Bromoacetic	45.3	139	80	44.0
101	2-Bromopropionic	43.1	153	12 + 80	43.1
102	2,3-Dibromopropionic	41.1	246	2 × 80 + 24	42.6
103	Iodoacetic	43.6	186	126	43.6
104	Glycolic	45.0	76	19	45.0
105	Lactic	43.8	90	12 + 19	44.0
106	2-Hydroxyisobutyric	43.2	104	24 + 19	43.2
107	3-Hydroxybutyric	41.4	104	24 + 19	43.2
108	Glyceric	41.0	106	2 × 19	40.0
109	Glucuronic	32.6	194	5 × 19	31.2
110	Benzoic	41.4	122	57	41.4
111	Salicylic	45.1	138	24 + 57	45.0
112	5-Bromosalicylic	44.4	218	80 + 24 + 57	45.0
113	*m*-Chlorobenzoic	41.3	157	57 + 38	42.6
114	Mandelic	40.2	152	57 + 24	38.9
115	Nicotinic	40.3	123	56	40.4

tion of the benzene ring may amount, depending on the substituents, to 36, 25 or 9. The hidden mass of phthalic acid is 39, which can be calculated as 36 + 3, taking a value of 3 for the second aromatic carboxylic group, or 25 + 14, assuming the decrease in the hidden mass of the benzene ring to be 25. It may be noted that the ratio 36:61 is in good agreement with the ratio 6:10 for the number of carbon atoms in benzene and naphthalene rings. The hidden mass of the pyridine ring is almost the same as that of benzene.

The results summarized in Table IV involve the contributions to the hidden mass of functional groups taken from Table III. The contributions of methylene groups are as follows: 6, Nos. 13 and 19, $n = 4$; 4, Nos. 42 and 47, $n = 4$; 8, Nos. 43 and 48, $n = 5$; 12, Nos. 49 and 51, $n = 6$. Obviously the methylene groups in cycloalkanes and in alkyl substituents should be taken into account.

The contributions of aliphatic hydroxyl groups are satisfactorily constant, but aromatic hydroxyl groups show some deviations, as can be seen from results Nos. 69–72. Possibly the dependence on the structure should be taken into account. The average relative error in the calculation of mobility from special contributions amounts to ±1.6%.

Table V demonstrates the hidden masses of some amino acids calculated from the mobilities of peptides ($H_{r,pep}$) summarized in Table VI by the following procedure. The mobility of glycine as determined by Hirokawa *et al.* [11] is $37.4 \cdot 10^{-5}$ cm^2 s^{-1} V^{-1}. The calculated effective mass of 75.5 is in good agreement with the molecular mass $M = 75.1$. It has been assumed that the hidden mass for free and combined glycine is zero. With this assumption, the contribution of the NH–CO peptide bond can be derived from values listed in Table VI, Nos. 1–5, as the ratio H/p, where $H = M - E$ and p is the number of peptide bonds. The results are 35, 30, 32, 32, 32 and 31, mean 32. It is now possible to calculate step by step the contributions of amino acids in peptides, as follows: No. 6, Ala–Gly, $H_{Ala} = 35 - 32 = 3$; No. 16, Ala–Gly–Gly, $H_{Ala} = 65 - 64 = 1$, Ala–Ala, $H_{Ala} = 0.5\ (37 - 32)$.

The second part of Table V (columns 4–7) contains the results concerning N-acetyl derivatives of amino acids. The hidden mass of N-acetylglycine represents the NH–CO bond in N-acetyl derivatives. The contributions of amino acids, $H_{r,ac}$, were calculated by subtraction of 29 from the values listed in the last column. The satisfactory agreement between $H_{r,pep}$ and $H_{r,ac}$ gives a strong support for the suggested calculations.

TABLE V

HIDDEN MASSES OF COMBINED AMINO ACIDS, H_r, DERIVED FROM MOBILITIES OF PEPTIDES, $H_{r,pep}$, AND FROM MOBILITIES OF N-ACETYLAMINO ACIDS, $H_{r,ac}$, MOBILITIES, u (10^{-5} cm^2 s^{-1} V^{-1}), MOLECULAR MASSES, M, AND HIDDEN MASSES, H, OF N-ACETYLAMINO ACIDS

No.	Amino acid	$H_{r,pep}$	$H_{r,ac}$	u	M	H
1	Gly	0	0	33.7	117	29
2	Ala	2	2	31.0	131	31
3	α-Amin	8	–	–	–	–
4	Val	13	13	27.9	159	42
5	Ser	15	–	–	–	–
6	Thr	16	–	–	–	–
7	Pro	16	20	29.5	157	49
8	Leu	20	19	26.7	173	48
9	Ileu	20	–	–	–	–
10	met	41	42	27.5	191	71
11	Asn	35	–	–	–	–
12	His	44	–	–	–	–
13	Phe	49	49	26.1	207	78
14	Trp	79	–	–	–	–
15	Tyr	88	–	–	–	–
16	Cys-SH	–	29	30.0	163	58

TABLE VI

DETERMINED, u, AND CALCULATED, u_{calc}, MOBILITIES OF PEPTIDES (10^{-5} cm^2 s^{-1} V^{-1}), MOLECULAR MASSES, M, HIDDEN MASSES, H, AND CONTRIBUTIONS OF COMBINED AMINO ACIDS TO HIDDEN MASS, H_{contr}

No.	Peptide	u	M	H	H_{contr}	u_{calc}
1	Gly–Gly	31.5	132	35	32	31.0
2	$(Gly)_3$	26.1	189	60	2×32	26.7
3	$(Gly)_4$	23.6	246	96	3×32	23.6
4	$(Gly)_5$	21.2	303	127	4×32	21.3
5	$(Gly)_6$	19.3	360	157	5×32	19.5
6	Ala–Gly	28.8	146	35	$32 + 2$	28.7
7	Gly–α-Amin	27.2	160	39	$32 + 8$	27.4
8	Gly–Val	26.0	174	44	$32 + 13$	26.1
9	Gly–Ileu	25.2	188	52	$32 + 20$	25.2
10	Gly–Leu	25.1	188	51	$32 + 20$	25.2
11	Gly–Thr	26.3	176	48	$32 + 16$	26.3
12	Gly–Ser	28.1	162	46	$32 + 15$	28.2
13	Gly–Asn	27.5	189	70	$32 + 35$	27.1
14	Gly–Phe	24.8	222	83	$32 + 49$	25.0
15	Gly–Trp	23.6	261	111	$32 + 79$	23.6
16	Ala–Gly–Gly	25.0	203	65	$2 \times 32 + 2$	25.1
17	Gly–Gly–Ileu	21.9	245	77	$2 \times 32 + 20$	22.5
18	Gly–Gly–Phe	21.9	279	111	$2 \times 32 + 49$	22.3
19	Gly–His–Gly	22.5	269	108	$2 \times 32 + 44$	22.5
20	Gly–Gly–Val	22.6	231	71	$2 \times 32 + 13$	23.2
21	Ala–Ala	27.0	160	37	$32 + 2 \times 2$	26.8
22	Ala–α-Amin	25.8	174	43	$2 \times 32 + 2 + 8$	25.7
23	$(Ala)_3$	22.2	231	64	$2 \times 32 + 3 \times 2$	22.5
24	Ala–Leu	23.9	202	55	$32 + 2 + 20$	23.8
25	Ala–Val	25.2	188	52	$32 + 2 + 13$	24.6
26	Ala–Ser	26.2	176	48	$32 + 2 + 15$	26.4
27	Ala–Asn	25.5	203	69	$32 + 2 + 35$	25.5
28	Ala–Met	24.2	220	75	$32 + 2 + 41$	24.2
29	Ala–Phe	23.9	236	89	$32 + 2 + 49$	23.6
30	Ala–Leu–Gly	21.3	259	84	$2 \times 32 + 2 + 20$	21.5
31	Gly–Leu–Ala	21.1	259	81	$2 \times 32 + 20 + 2$	21.5
32	Leu–Leu	21.6	244	72	$32 + 2 \times 20$	21.6
33	$(Leu)_3$	17.6	357	124	$2 \times 32 + 3 \times 20$	17.6
34	Leu–Val	22.3	230	66	$32 + 20 + 13$	22.2
35	Leu–Phe	21.8	278	109	$32 + 20 + 49$	21.4
36	Gly–Leu–Try	21.0	251	172	$2 \times 32 + 20 + 88$	21.0
37	Gly–Pro–Ala	22.5	243	82	$2 \times 32 + 16 + 2$	22.5
38	Gly–Phe–Phe	19.7	369	172	$2 \times 32 + 2 \times 49$	19.4
39	Leu–Gly–Phe	19.3	335	132	$2 \times 32 + 20 + 49$	19.7
40	$(Ser)_3$	22.0	279	112	$2 \times 32 + 3 \times 15$	21.7

The hidden mass of a peptide can be calculated from the composition by means of the equation

$$H = M - E = \sum_{r=1}^{m} rH_r + 32p \qquad (10)$$

where r, H_r and m are the number (index) of a given amino acid, its hidden mass and number of species in the molecule, respectively, *e.g.*, for a peptide $(Ala)_3(Gly)_5$, r for Ala = 3, for Gly = 5 and $m = 2$. As can be derived from eqns. 2 and 10, the mobility of a peptide can be calculated from the amino acid composition by the equation

$$u = Z \cdot 668\left(M - 32p - \sum_{r=1}^{m} rH_r\right)^{-2/3} \qquad (11)$$

The average relative error of calculated mobilities of peptides listed in Table VI amounts to ±0.8%.

The additivity of hidden masses can be demonstrated for peptides by the following examples:

Ala–ALa + Gly–Gly = 2 Ala–Gly; 37 + 35 = 72,

35 + 35 = 70 ;

Ala–Leu + Gly–Leu = Ala–Gly + Leu–Leu;

55 + 51 = 106, 35 + 72 = 107 ;

Ala–Ala + Gly–Ser = Ala–Gly + Ala–Ser;

37 + 46 = 83, 35 + 48 = 83 .

CONCLUSIONS

The demonstrated approach may be utilized for the calculation of mobilities from the known compositions and contributions of functional groups. The mobilities of asymmetric compounds can be calculated from those of symmetrical compounds. The method seems to be applicable to the examination of peptides and detergents and to follow the course of any change in the outward surface of a molecule.

REFERENCES

1 V. Jokl, *J. Chromatogr.*, 13 (1964) 451.
2 E. Blasius and W. Preetz, *Z. Anorg. Allg. Chem.*, 335 (1965) 16.
3 R.E. Offord, *Nature*, 211 (1966) 591.
4 M. Wroński, *J. Chromatogr.*, 288 (1984) 206.
5 M. Wroński, *J. Chromatogr.*, 469 (1989) 378.
6 F.M. Everaerts, J.L. Beckers and Th.P.E.M. Verheggen, *Isotachophoresis —Theory, Instrumentation and Application*, Elsevier, Amsterdam, 1976.
7 P. Boček, M. Deml, P. Gebauer and V. Dolnik, *Analytical Isotachophoresis*, VCH, Weinheim, 1988.
8 T. Hirokawa, M. Nishino, N. Aoki, Y. Koso, Y. Sawamoto, T. Yagi and J. Akiyama, *J. Chromatogr.*, 271 (1983) D1.
9 T. Hirokawa, M. Nishino and Y. Kiso, *J. Chromatogr.*, 252 (1982) 49.
10 T. Hirokawa, T. Tsuyoshi and Y. Kiso, *J. Chromatogr.*, 408 (1987) 27.
11 T. Hirokawa, T. Gojo and Y. Kiso, *J. Chromatogr.*, 369 (1986) 59.
12 T. Hirokawa, T. Gojo and Y. Kiso, *J. Chromatogr.*, 390 (1987) 201.
13 T. Hirokawa, R. Sugino and Y. Kiso, *J. Chromatogr.*, 585 (1991) 364.

Journal of Chromatography A, 657 (1993) 175–183
Elsevier Science Publishers B.V., Amsterdam

CHROM. 25 522

Improved capillary zone electrophoretic separation of basic proteins in uncoated fused-silica capillary by using ethylene diamine as a buffer additive

Liguo Song*, Qingyu Ou and Weile Yu

Lanzhou Institute of Chemical Physics, Chinese Academy of Sciences, Lanzhou, Ganshu 730000 (China)

(First received June 2nd, 1993; revised manuscript received August 23rd, 1993)

ABSTRACT

Ethylene diamine was used as a buffer additive to improve capillary zone electrophoretic separation of basic proteins in an uncoated fused-silica capillary and theoretical plate numbers of the order of a hundred thousand were obtained for all five standard proteins at pH 6.5, 8.0 and 9.5. The critical factors that affected the separation efficiency were the ethylene diamine concentration and the applied voltage at each pH value. Adsorption of ethylene diamine ions to the capillary inner wall significantly reduced the charge density of the wall, and therefore reduced the adsorption of basic proteins. Increasing the concentration of ethylene diamine increased this reduction, and caused an increase in the theoretical plate numbers of all proteins. Increasing the applied voltage caused an increase in the theoretical plate numbers of all proteins in the low-voltage region and a decrease in high-voltage region, which maybe attributed to excessive Joule heat.

INTRODUCTION

Since Jorgenson and Lukacs [1,2] established the theoretical basis of capillary zone electrophoresis (CZE) in the early 1980s, analysts have made great efforts to make it a routine method of separating macromolecules such as polypeptides, proteins and DNA bases. In theory, because these macromolecules have very low diffusion coefficients, separation efficiency can reach theoretical plate numbers of the order of millions [1,3,4]. However, adsorption of the macromolecules onto the capillary inner wall causes serious problems, including tailing peaks, resulting in low efficiency and low resolution. Sometimes it can even result in the absence of signal response after an injection [5]. Adsorption also continuously changes the property of the capillary inner wall, resulting in continuous change in the electroosmotic flow and therefore non-reproducible elution time [6].

The reason for adsorption is the opposite charge of the capillary inner wall and basic proteins. Fused silica always carries a negative charge in aqueous solution ($pI < 2$), while basic proteins carry a significant net positive charge when operating in the typical pH range used for CZE, resulting in strong coulombic attraction. Three main techniques have been designed to prevent the capillary wall–protein attraction: (1) by directly controlling charge density on the capillary inner wall through an additional electric field applied from the outside of the capillary; (2) by changing the composition of the carrier electrolyte; and (3) by modifying the capillary inner wall. Though all these techniques succeed in reducing adsorption to some extent, we still think that changing the composition of the carrier electrolyte is a simpler and more acceptable technique; it can also be combined with other techniques for even greater success.

* Corresponding author.

0021-9673/93/$06.00

In the technique of changing the composition of carrier electrolyte, Lauer and McManigill [3] raised the pH of the carrier electrolyte above the p*I* of basic proteins, so that coulombic repulsion suppressed adsorption. However, pH 11.0 solutions could decompose basic proteins. McCormick [7] demonstrated successful separation of peptides and proteins at low pH values at which the charge on the capillary inner wall approaches zero, but protonization of proteins caused low mass to charge ratios and prohibited high-resolution separation. Green and Jorgenson [8] added a high concentration of alkali metal salts to the carrier electrolyte to suppress the adsorption, but although they were successful Joule heat remained a problem. Bushey and Jorgenson [9] partly solved this problem by using a combination of a high concentration of zwitterionic buffer and alkali metal salts. Recently, Chen *et al.* [10] also demonstrated the value of using a high concentration of alkali metal salts in suppressing adsorption of basic proteins. Waters Chromatography Division of Millipore produced a zwitterionic modifier, AccuPure Z1-Methyl (a registered trademark), and Chen *et al.* [10] used a proprietary zwitterionic additive ZB-4; both improved the separation of basic proteins. Emmer *et al.* [11] improved capillary zone electrophoretic separation of basic proteins by using a fluorosurfactant buffer additive, FC134.

In this report, the use of ethylene diamine as a buffer additive is proposed for the first time, and high separation efficiency of basic proteins was obtained. Although amines such as spermine [12], morpholine [13], 1,3-diaminopropane [14], 1,4-diaminobutane [3,15] and 1,5-diaminopentane [16] have been used as buffer additives, we have found that a series of relatively simple buffers in uncoated fused-silica capillaries at pH values below the isoelectric points of basic proteins can give excellent separation. We also found that electroosmotic mobility varies with the concentration of ethylene diamine and the applied voltage, and that there is a linear relationship between electroosmotic flow and current. Since ethylene diamine is a common reagent in the laboratory, it is a more acceptable additive than some proprietary ones.

EXPERIMENTAL

Apparatus

The capillary electrophoresis apparatus used in this study resembles that reported earlier by Jorgenson and Lukacs [1,2]. It was constructed by the Peking Institute of New Technology Application (Peking, China). It consists of a high-voltage d.c. power supply delivering up to ±30 kV, a UV detector which has several optional wavelengths with fixed and removable devices for on-column detection, a Plexiglass box with a safety interlock and a syringe installation used to flush the capillary. The electrophoregrams were recorded with an HP3390A integrator (Hewlett-Packard, Avondale, PA, USA).

Reagents and materials

Lysozyme from egg white (p*I* 11.0) was purchased from Fluka Buchs, Switzerland). Ribonuclease from bovine pancreas (p*I* 9.45) was purchased from Merck (Darmstadt, Germany). Cytochrome *c* (p*I* 10.5) from horse heart, trypsinogen from bovine pancreas (p*I* 9.3) and α-chymotrypsinogen A from bovine pancreas (p*I* 9.1) were purchased from Sigma (St. Louis, MO, USA). Ethylene diamine anhydrous, sodium sulphate anhydrous, dimethyl sulphoxide and all other reagents were analytical grade and purchased in China. In all experiments, deionized water was used.

Stock protein solutions with individual concentrations of about 2.0 mg/ml were prepared and stored in a freezer. Sometimes 1% dimethyl sulphoxide (DMSO) was added to protein solutions as a neutral marker. Carrier electrolytes were prepared using the corresponding amounts of anhydrous ethylene diamine and anhydrous sodium sulphate, and adjusting the pH with phosphoric acid. Sample injection was accomplished by siphoning for 10 s at 8 cm.

Electrophoresis

A polyimide-coated fused-silica capillary (Yongnian Photoconductive Fibre Factory, Hebei, China) of 50 μm I.D. and 375 μm O.D. was used with a total length 75 cm, in which the detector was placed 55 cm from the capillary

inlet. Detection was monitored at 214 nm for all proteins and DMSO. Before using, a new capillary was flushed with 1 *M* KOH for 1 h and then equilibrated with carrier electrolyte overnight by using a syringe to force the solution through it. When a change of carrier electrolyte was needed, the same procedure was followed. Between two runs, the capillary was first flushed with one capillary volume of 1 *M* KOH, then with carrier electrolyte for 5 min. All analyses were run at ambient temperature between 16 and 18°C without temperature control.

RESULTS AND DISCUSSION

Effect of pH value and ethylene diamine concentration on the separation of basic proteins

When ethylene diamine was added to the carrier electrolytes, excellent separation of basic proteins could be obtained. Three pH values, 6.5, 8.0 and 9.5, were arbitrarily chosen to examine the effect of ethylene diamine, and at each pH value four concentrations of ethylene diamine between 20 m*M* and 80 m*M* were selected. In all experiments, 35 m*M* sodium sulphate was added to every carrier electrolyte, aiding in increasing the overall ionic strength and reducing attractions between proteins and capillary inner wall. The applied voltage was 12 kV for each run. Separations of five standard basic proteins at pH 8.0 are demonstrated in Fig. 1.

The results showed that raising the concentration of ethylene diamine could effectively reduce attraction between proteins and the capillary inner wall and improve the separation of basic proteins. When the concentration of ethylene diamine was low, noticeable peak tailing and low resolution were observed. But when the concentration of ethylene diamine was high enough, several unresolved peaks were baseline separated. Ribonuclease, trypsinogen and α-chymotrypsinogen A had very similar electrophoretic mobility, but at any pH value three peaks could be obtained with enough ethylene diamine in the carrier electrolytes. Impurity in lysozyme could also be successfully separated from lysozyme at pH 6.5 and pH 8.0 with enough ethylene diamine. Raising the concentration of ethylene diamine was not always beneficial; too high a concentration can result in low electoosmotic flow and long elution times.

Theoretical plate numbers calculated for individual proteins at different pH values and different concentrations of ethylene diamine are summarized in Table I. It is observed that theoretical plate numbers higher than a hundred thousand were obtained for all proteins, of which the highest was 740 000 for α-chymotrypsinogen A at pH 8.0/60 m*M* ethylene diamine. Because retention time increased with increasing concentration of ethylene diamine, the theoretical plate number of the neutral marker DMSO decreased in accordance with the theory of Jorgenson and Lukacs [1,2], expressed as follows:

$$N = \frac{(\mu_e + \mu_{osm})Vl}{2DL} \quad (1)$$

where N is the theoretical plate number, μ_e is the electrophoretic mobility of the analyte, μ_{osm} is the electroosmotic mobility, V is the applied voltage, l is the distance between the capillary inlet and the detector window, D is the diffusion coefficient of the analyte and L is the total length of the capillary. But, in contrast, the theoretical plate numbers of all proteins showed an obvious tendency to increase with increasing concentration of ethylene diamine, although the theoretical plate numbers of some proteins decrease at too high a concentration of ethylene diamine.

Raising the pH from 6.5 to 8.0 to 9.5 speeded up electroosmotic flow and caused short elution times for all proteins, but low resolution. Impurity in lysozyme could not be separated from lysozyme at pH 9.5. Changing the pH also caused changes in the elution sequence, especially for DMSO. At pH 6.5, its peak was far behind all the proteins; at pH 8.0, its peak overlapped with the three near peaks of ribonuclease, trypsinogen and α-chymotrypsinogen A, except that at up to 80 m*M* ethylene diamine it was separated from them; at pH 9.5, its peak was ahead of the three peaks, which indicated that ribonuclease, trypsinogen and α-chymotrypsinogen A were negatively charged.

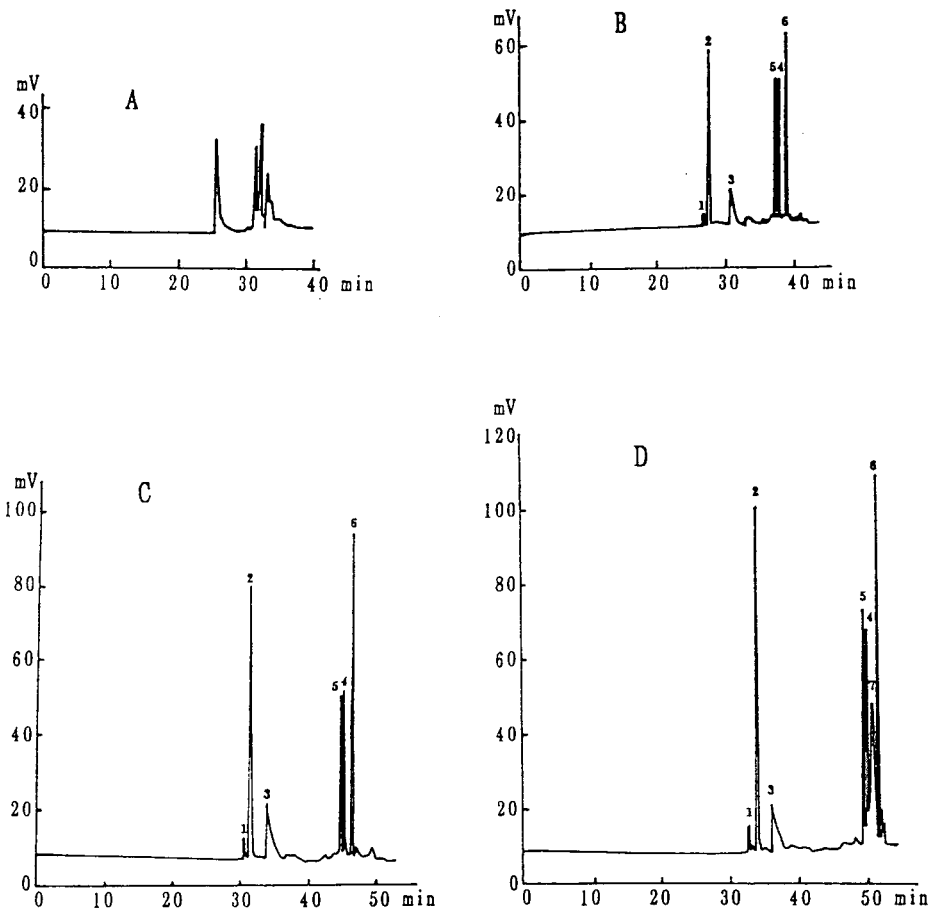

Fig. 1. Effect of ethylene diamine concentration on the separation of basic proteins at pH 8.0. Peaks: 1 = impurity of lysozyme; 2 = lysozyme; 3 = cytochrome *c*; 4 = ribonuclease; 5 = trypsinogen; 6 = α-chymotrypsinogen A; 7 = DMSO. Conditions: (A) 20 m*M* ethylene diamine, 27 μA; (B) 40 m*M* ethylene diamine, 31 μA; (C) 60 m*M* ethylene diamine, 34 μA; (D) 80 m*M* ethylene diamine, 38 μA.

Effect of applied voltage on the separation of basic proteins

Another factor which significantly affected the separation efficiency and separation resolution was the applied voltage. Three buffers, pH 6.5/60 m*M* ethylene diamine, pH 8.0/60 m*M* ethylene diamine and pH 9.5/80 m*M* ethylene diamine, were chosen to examine this effect. The results are demonstrated in Figs. 2 (pH 6.5) and 3 (pH 9.5). As was anticipated, increasing the applied voltage resulted in short elution times and low resolution at pH 6.5 and pH 8.0. In contrast, at pH 9.5 short elution times but high resolution of ribonuclease, trypsinogen and α-chymotrypsinogen A were obtained, which maybe attributed to the negative charge on the three proteins at pH 9.5. Theoretical plate numbers calculated for individual proteins at different pH values and different applied voltages are summarized in Table II. It is observed that the theoretical plate number of DMSO and all proteins showed a tendency to increase with increasing applied voltage in the low-voltage region, which conformed to the theory of Jorgenson and Lukacs [1,2] as expressed in eqn. 1. It is also observed that their efficiency decreased in the high-voltage region.

It is shown above that as a buffer additive

TABLE I

THEORETICAL PLATE NUMBER FOR BASIC PROTEINS AT DIFFERENT pH VALUES AND DIFFERENT CONCENTRATIONS OF ETHYLENE DIAMINE

Operation pH	Concentration of ethylene diamine (m*M*)	Current (μA)	Theoretical plate numbers $\cdot 10^{-4}$ [a]						
			Lysozyme[b]	Lysozyme	Cytochrome	Ribonuclease	Trypsinogen	Chymotrypsinogen	DMSO
6.5	20	27	[c]	1.1	[c]	[c]	6.8	[c]	5.1
	40	31	12.0	7.0	2.0	26.6	24.7	23.7	4.4
	60	34	17.8	9.1	2.4	30.1	35.5	30.7	3.6
	80	38	35.6	20.4	12.4	29.8	30.1	24.6	3.1
8.0	20	27	[c]	[c]	[c]	[c]	[c]	[c]	[d]
	40	31	17.1	11.0	1.2	30.9	35.3	51.5	[d]
	60	34	22.6	13.2	1.5	20.1	20.4	74.0	[d]
	80	38	31.8	23.5	7.5	25.3	34.2	43.2	[d]
9.5	30	30	[c]	4.8	3.5	5.1	[c]	[c]	8.1
	50	32	[c]	10.7	13.8	6.3	[c]	[c]	8.0
	60	34	[c]	12.1	14.9	12.2	[c]	[c]	7.8
	80	38	[c]	18.8	4.2	25.7	24.6	23.8	7.1

[a] $N = 5.54(RT/WI)^2$, where RT is the retention time and WI is the peak width at half-height.
[b] Impurity in lysozyme.
[c] Unresolved peaks.
[d] Did not measure theoretical plate numbers.

ethylene diamine is suitable over a wide pH range to improve the capillary zone electrophoretic separation of basic proteins. The critical factors that affect the separation efficiency and separation resolution are its concentration, the pH of the carrier electrolyte and the applied voltage. Because the pH values were arbitrarily chosen, it is anticipated that intermediate pH values between 6.5 and 9.5 can also be successfully used. pH values below 6.5 were also tried, but were unsuccessful. At pH 5.0 (adjusting pH with acetic acid), although four peaks were detected for five proteins, the separation efficiencies were low and elution times were very long. At pH 3.5, no signal was observed at the detector for a long time, though the electrode polarity was ever exchanged. The separations depicted in this preliminary work were all obtained on mixtures of proteins standards; no separation of complex matrices such as biological fluids was accomplished. But it is anticipated that, by choosing an appropriate pH value of the carrier electrolyte, concentration of ethylene diamine and applied voltage, an efficient and rapid separation of complex matrices will be obtained.

Reasons for the effect on separation efficiency of proteins

In order to study the effect on separation efficiency of proteins, the electroosmotic mobilities of the capillary at different pH values and different concentrations of ethylene diamine as well as at different pH values and different applied voltages were measured and are illustrated in Figs. 4 and 5.

It is observed from Fig. 4 that the electroosmotic mobilites of the capillary with ethylene diamine buffer at each pH value were much lower than those with metal salts buffer described in ref. 5. Unlike metal ions, positively charged ethylene diamine ions adsorbed tightly to the capillary wall, dramatically reducing the charge density of the wall and causing a dramatic reduction in electroosmotic mobility and adsorption of basic proteins to the capillary inner wall. Increasing the concentration of ethylene diamine enhanced these effects, and hence caused a dynamic decrease in electroosmotic mobility but an increase in the separation efficiency of all basic proteins.

It is not thought that increasing the applied voltage caused the increase in electroosmotic

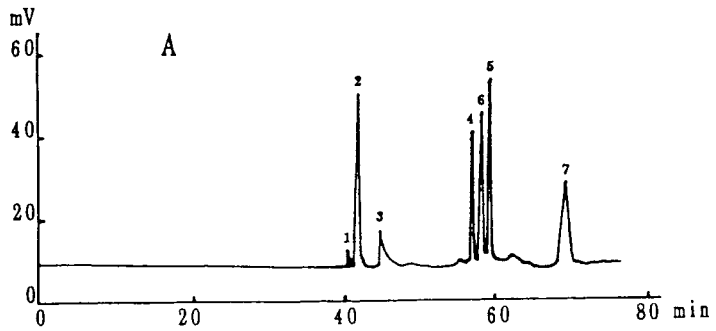

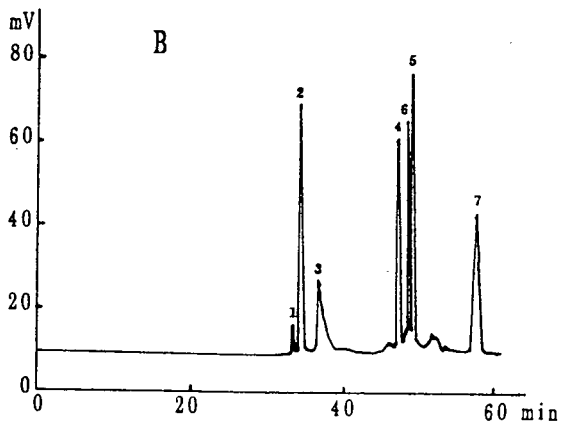

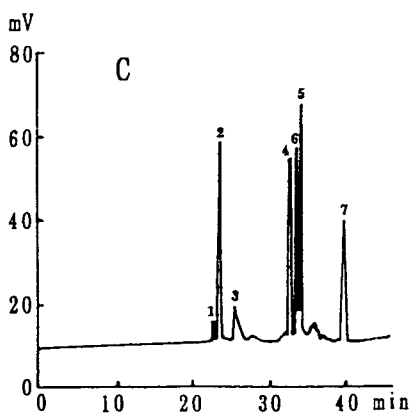

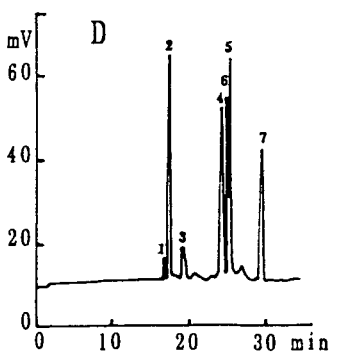

Fig. 2. Effect of applied voltage on the separation of basic proteins at pH 6.5. Peaks: 1 = impurity of lysozyme; 2 = lysozyme; 3 = cytochrome *c*; 4 = ribonuclease; 5 = trypsinogen; 6 = α-chymotrypsinogen A; 7 = DMSO. Conditions: (A) 9 kV, 27 μA; (B) 12 kV, 34 μA; (C) 15 kV, 50 μA; (D) 18 kV, 64 μA.

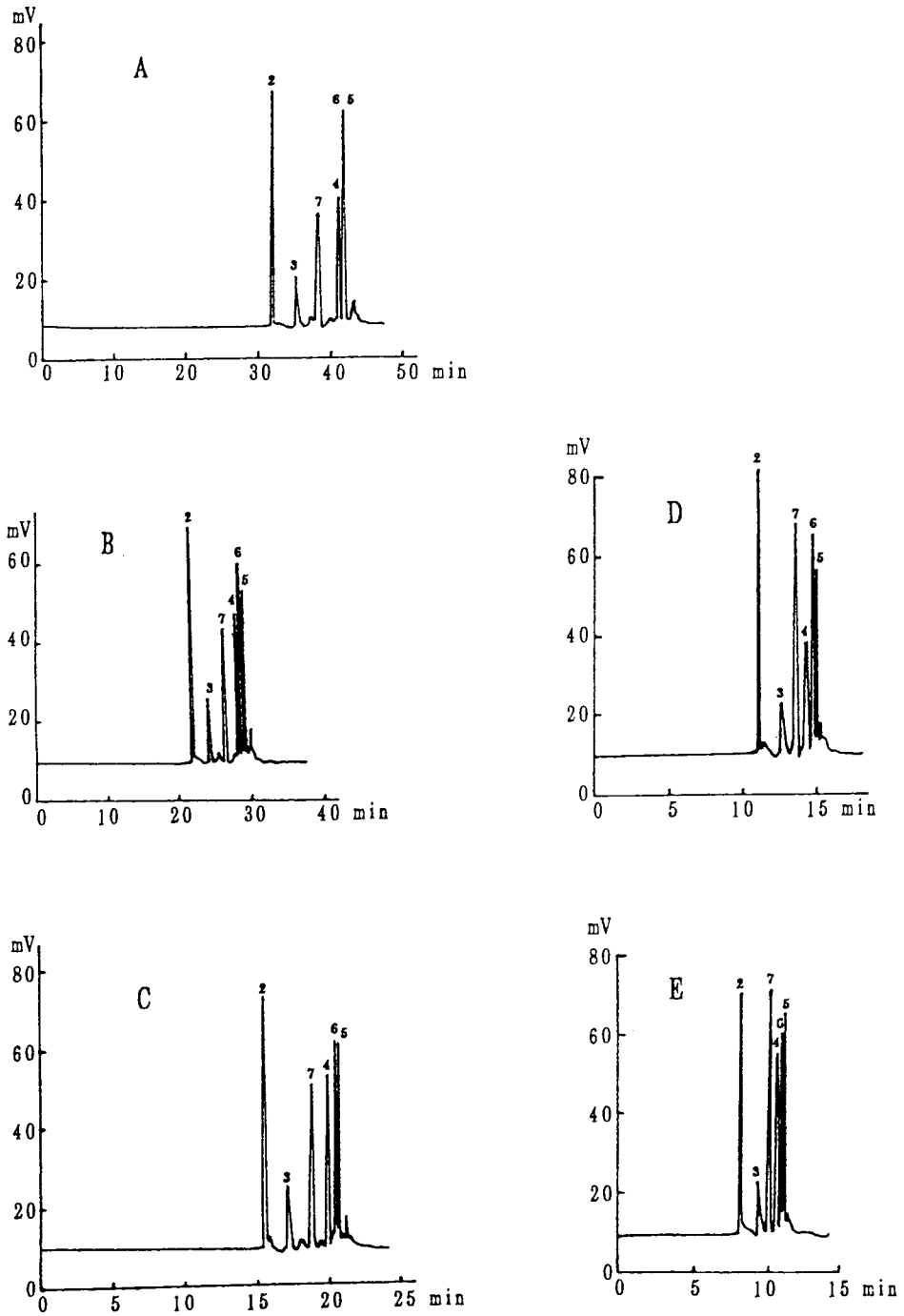

Fig. 3. Effect of applied voltage on the separation of basic proteins at pH 9.5. Peaks: 2 = lysozyme; 3 = cytochrome *c*; 4 = ribonuclease; 5 = trypsinogen; 6 = α-chymotrypsinogen A; 7 = DMSO. Conditions: (A) 9 kV, 25 μA; (B) 12 kV, 37 μA; (C) 15 kV, 52.5 μA; (D) 18 kV, 71.5 μA; (E) 21 kV, 94 μA.

TABLE II

THEORETICAL PLATE NUMBER FOR BASIC PROTEINS AT DIFFERENT pH VALUES AND DIFFERENT APPLIED VOLTAGES

Operation pH	Applied voltage (kV)	Current (μA)	Theoretical plate numbers $\cdot 10^{-4}$ [a]						
			Lysozyme[b]	Lysozyme	Cytochrome	Ribonuclease	Trypsinogen	Chymotrypsinogen	DMSO
6.5	9	27	14.4	11.6	1.6	26.5	24.6	23.2	2.8
	12	34	17.8	9.1	2.4	30.1	35.4	30.7	3.6
	15	50	12.0	10.1	5.4	25.9	21.5	20.3	4.9
	18	64	15.6	8.2	1.7	11.3	[c]	[c]	4.9
	21	87–91	[c]	7.3	1.2	12.4	[c]	[c]	[c]
8.0	9	23	15.0	8.3	0.7	5.8	4.4	61.7	[d]
	10.5	29	28.4	14.0	0.9	29.5	32.0	70.6	[d]
	12	34	22.6	13.2	1.5	20.1	20.4	74.0	[d]
	13.5	40	9.2	8.1	1.1	[c]	[c]	65.2	[d]
9.5	7.5	20	[c]	18.7	3.2	19.6	[c]	[c]	4.5
	9	25	[c]	18.1	3.3	27.8	[c]	[c]	5.1
	10.5	31	[c]	19.1	3.7	27.0	[c]	[c]	6.4
	12	37	[c]	18.8	4.2	24.8	24.6	23.8	7.1
	15	52–53	[c]	15.1	3.1	25.7	23.7	19.3	7.7
	18	70–73	[c]	12.7	2.3	18.5	16.1	19.5	6.5
	21	92–96	[c]	6.8	1.3	14.5	17.0	13.5	6.6

[a] $N = 5.54(RT/WI)^2$, where RT is the retention time and WI is the peak width at half-height.
[b] Impurity in lysozyme.
[c] Unresolved peaks.
[d] Did not measure theoretical plate numbers.

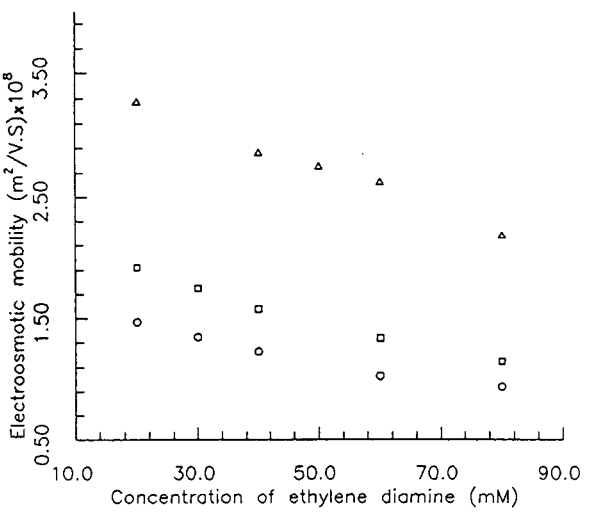

Fig. 4. Effect of the concentration of ethylene diamine on the electroosmotic mobility. The applied voltages were all 12 kV. ○ = pH 6.5; □ = pH 8.5, △ = pH 9.5.

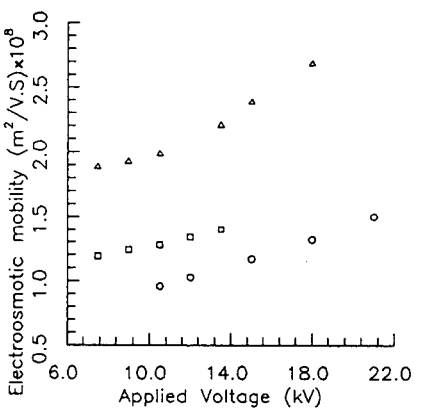

Fig. 5. Effect of the applied voltage on the electroosmotic mobility. ○ = pH 6.5/60 m*M* ethylene diamine; □ = pH 8.5/60 m*M* ethylene diamine; △ = pH 9.5/80 m*M* ethylene diamine.

mobility which is observed in Fig. 5. It was considered that Joule heat caused by high applied voltages across the capillary perhaps contributed to this increase, but it was also considered that Joule heat caused by low voltages such as 7.5, 9 kV, etc. may be efficiently dissipated by

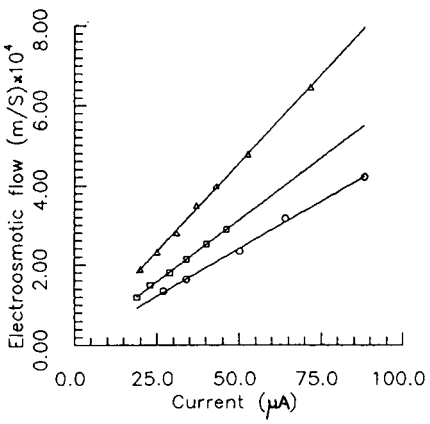

Fig. 6. Linear relationship between the electroosmotic flow and the current through the capillary. ○ = pH 6.5/60 m*M* ethylene diamine; □ = pH 8.5/60 m*M* ethylene diamine; △ = pH 9.5/80 m*M* ethylene diamine.

the capillary wall. According to ref. 17, although Joule heat can cause a non-linear relationship between electroosmotic flow and applied voltage, a linear relationship between electroosmotic flow and the current through the capillary did exist. In this study, a similar linear relationship also existed, as demonstrated in Fig. 6, so it is considered that Joule heat caused by applied voltages contributed to the increased electroosmotic mobility, and also caused the decreased efficiency of all basic proteins, even though the applied voltages were not very high.

ACKNOWLEDGEMENT

This work is financially supported by the National Natural Science Foundation of China.

REFERENCES

1 J.W. Jorgenson and K.D. Lukacs, *Anal. Chem.*, 53 (1981) 1298.
2 J.W. Jorgenson, in J.W. Jorgenson and M. Phillips (Editors), *New Directions in Electrophoretic Methods*, (*ACS Symposium Series*, No. 335), American Chemical Society, Washington, DC, 1987, p. 182.
3 H.H. Lauer and D. McManigill, *Anal. Chem.*, 58 (1986) 166.
4 G.J.M. Bruin, J.P. Chang, R.M. Kuhlman and K. Zegers, *J. Chromatogr.*, 471 (1989) 429.
5 J.K. Towns and F.E. Regnier, *Anal. Chem.*, 63 (1991) 1126.
6 M. Zhu, R. Rodriguez, D. Hansen and T. Wehr, *J. Chromatogr.*, 516 (1990) 123.
7 R.M. McCormick, *Anal. Chem.*, 60 (1988) 2322.
8 J.S. Green and J.W. Jorgenson, *J. Chromatogr.*, 478 (1989) 63.
9 M. Bushey and J.W. Jorgenson, *J. Chromatogr.*, 480 (1989) 301.
10 F.A. Chen, L. Kelly, R. Palmieri, R. Biehler and H. Schwartz, *J. Liq. Chromatogr.*, 15 (1992) 1143.
11 A. Emmer, M. Janssor and J. Roeraade, *J. Chromatogr.*, 547 (1991) 544.
12 V. Dolnik, J. Liu, J.F. Banks, Jr., M.V. Novotny and P. Boček, *J. Chromatogr.*, 480 (1989) 321.
13 R.G. Nielsen and E.C. Rickard, *J. Chromatogr.*, 470 (1989) 241.
14 J.A. Bullock and L.C. Yuan, *J. Microcol. Sep.*, 3 (1990) 241.
15 F.S. Stover, B.L. Haymore and R.J. McBeath, *J. Chromatogr.*, 470 (1989) 241.
16 V. Rohlicek and Z. Deyl, *J. Chromatogr.*, 494 (1989) 87.
17 T. Tsuda, K. Nomura and G. Nakagawa, *J. Chromatogr.*, 264 (1983) 385.

Journal of Chromatography A, 657 (1993) 185–191
Elsevier Science Publishers B.V., Amsterdam

CHROMSYMP. 2914

Capillary electrophoresis methods for the trace cation analysis of semiconductor grades of hydrogen peroxide ☆

Ronald A. Carpio*
SEMATECH, 2706 Montopolis Drive, Austin, TX 78741 (USA)

Petr Jandik and Edward Fallon
Waters Chromatography Division of Millipore Corporation, 34 Maple Street, Milford, MA 01757 (USA)

(First received October 31st, 1992; revised manuscript received August 2nd, 1993)

ABSTRACT

Method development and applications of capillary electrophoresis to the analysis of cations in highest purity grades of hydrogen peroxide which are used for semiconductor processing are discussed. Indirect UV detection in conjunction with electromigration sampling provides a sufficient sensitivity for measurements of low ppb (v/v) levels of contaminants. In contrast to hydrostatic sample introduction, the range of signal *vs.* concentration proportionality is limited with electromigration sampling. However, meaningful calibration plots can be obtained over the range of 1 to 35 ppb. Examples of electropherograms are presented for two different samples of semiconductor grade hydrogen peroxide. Also given are estimates of detection limits for cations found in analyzed samples.

INTRODUCTION

Purity requirements for semiconductor processing have increased to a level, typically the low or sub-ppb range, where only the most sensitive analytical tools available can be utilized. Inductively coupled plasma mass spectrometry (ICP-MS), graphite furnace atomic absorption spectroscopy (GFAAS), and ion chromatography (IC) are currently the most frequently employed methods. Unfortunately, the monitoring of hydrogen peroxide and other process chemicals under manufacturing conditions is frequently impossible by the current methods. Safety, clean room requirements and cost effectiveness are among the most important impediments to utilization of, for example, ICP-MS directly in the manufacturing environment.

Optimized capillary electrophoresis (CE) methodology for ion analysis [1] is emerging as an alternative to ICP-MS and GFAAS for trace metal analysis. With CE, frequent monitoring of multiple ions appears to be more feasible, even under the conditions encountered in semiconductor manufacturing.

Hydrogen peroxide was chosen for our study because it is utilized widely in critical wafer processing steps [2]. It also has a history of metallic contamination problems. Many of the contaminants can be traced to the measures which are used for stabilization of hydrogen peroxide against decomposition. Additionally, the presence of high levels of organic contami-

* Corresponding author.
☆ Presented at the *International Ion Chromatography Symposium 1992, Linz, September 21–24, 1992.* The majority of the papers presented at this symposium were published in *J. Chromatogr.*, Vol. 640 (1993).

0021-9673/93/$06.00

nants have been detected by total organic carbon (TOC) measurements, as well as by IC and HPLC procedures [3]. According to recent results by one of the authors [4], even the newly introduced stabilizer-free grades of hydrogen peroxide contain a large number of carboxylic impurities. Based on that observation, our study focused entirely on the evaluation of the usefulness of CE for the analyses of unstabilized samples of hydrogen peroxide.

EXPERIMENTAL

Instrumentation

All assays of hydrogen peroxide samples as well as of standard solutions were carried out with the Quanta 4000 capillary electropherograph (Waters). A positive power supply was utilized for all analyses of cations reported here. Data were analyzed with the help of Waters Millennium Data Station. The rate for data sampling was at 20 Hz. The capillary of standard dimensions (60 × 52 cm, 75 μm I.D.) was also from Waters. Indirect UV detection was carried out at 185 nm in all separations. Polypropylene vials (4 ml) from Sun Brokers (Wilmington, NC, USA) were used for both sample and carrier electrolyte solutions. Electromigrative sampling of cations was performed for 30 s at 10 kV. Additional and more specific separation and sampling conditions are given in figure captions.

Chemicals

Only deionized, 18.2 MΩ water generated by the Milli-Q Laboratory Water Purification System (Millipore, Bedford, MA, USA) was used in all experiments. The UV Cat 1 [5] carrier electrolytes were prepared following the previously described procedures. The UV Cat 2 carrier electrolyte was made up by dissolving 11.5 mg of UV Cat 2 (Waters) and 36.6 mg of 2-hydroxy-2,4,6-cycloheptatrienone, which is known as tropolone (Aldrich, Milwaukee, WI, USA), in 50 ml Milli-Q water. The resulting electrolyte solution of pH 4.25 was filtered and degassed prior to use. Whereas the UV Cat 2 electrolyte gave better results after a preconditioning of fused-silica capillary with 10% KOH, the UV Cat 1 electrolyte was employed without any preconditioning of capillaries. Ultrex grade 30% hydrogen peroxide was from Baker (Phillipsburg, NJ, USA). The unstabilized, semiconductor grade, 30% hydrogen peroxide was purchased from two different suppliers.

All standard solutions were prepared from analytical grade salts (Aldrich) rather than by dilution of 1000 ppm (v/v) AAS standard concentrates. AAS standards were not used since they are generally acidic solutions, and it was desired to avoid introducing any species, particularly protons, which could affect the metal complexing equilibria and which are not present in the samples being analyzed. Moreover, protons in the sample can give rise to an unwanted peak.

Catalytic decomposition of hydrogen peroxide

An aliquot of 30% hydrogen peroxide was placed into a precleaned (24 h in 0.1 *M* nitric acid, 24 h in 18.2 MΩ water) and prechecked PMP (polymethylpentene) beaker (blank electropherograms of cations in a volume of deionized after 30 min residence in a precleaned beaker). The PMP beakers were obtained from VWR Scientific (Westwood, MA, USA). After immersion of precleaned platinum gauze (Aldrich, 525 mg + 25 × 25 mm), the sample began to boil vigorously as the decomposition progressed. The completeness of peroxide destruction was verified by titrations, carried out after addition of iodide, using thiosulfate as volumetric solution and starch as indicator. The reduction of peroxide was usually complete after *ca.* 2 min.

RESULTS AND DISCUSSION

Selection of carrier electrolytes

Two carrier electrolytes were evaluated for application to hydrogen peroxide samples. The separation and detection results with these electrolytes had been reported previously for aqueous samples. The UV Cat 1 electrolyte [5] makes possible separations of up to 28 different cations. The UV Cat 1 electrolyte includes 4-methyl-2-benzylamine which serves as the chromophore to make indirect UV detection possible and HIBA (α-hydroxyisobutyric acid) for metal complexation. The range of cations that can be separated by the UV Cat 2 electrolyte is narrower and is

limited to the following analytes: potassium, barium, strontium, calcium, sodium, magnesium, manganese, zinc and nickel [6]. The reported detection limits in aqueous standards are in the range of 18 to 388 ppb [5] and 31 to 267 ppt [6] by hydrostatic and electromigration sampling, respectively. The UV Cat 2 electrolyte consists of a proprietary organic basic cation which absorbs strongly in the UV and tropolone to serve as the chelating agent.

The comparison of cation separations with the two different carrier electrolytes is shown in Fig. 1A and B. Hydrogen peroxide in both samples was destroyed prior to the analysis using the catalytic procedure described earlier. Previously, the UV Cat 2 electrolyte was shown to yield 2.5 to 5 times higher sensitivity relative to that observed for the same cations and by similar sampling procedure in the UV Cat 1 electrolyte [6]. Improved sensitivity between the two electrolytes is recognizable also in Fig. 1 for the peaks belonging to calcium, magnesium and manganese. The enhancement in sensitivity of the UV Cat 2 electrolyte relative to the UV Cat 1 electrolyte is probably attributable to the differences in the metal complexing properties that exists been tropolone and HIBA; however, a detailed explanation for the differences in sensitivity is beyond the scope of this paper. The peaks belonging to sodium and potassium, on the other hand, show comparable peak areas by both methods. The authors attribute this to their inability to control trace levels of sodium and ammonium under the experimental conditions chosen for this report. Ammonium comigrates with potassium in both electrolytes but a separation of ammonium and potassium can be achieved by inclusion of a suitable crown ether in the electrolyte [7]. Higher levels of inadvertent contamination of the sample analyzed with the UV Cat 1 electrolyte is assumed to be a possible explanation for comparable peak areas obtained for potassium/ammonium and sodium peaks.

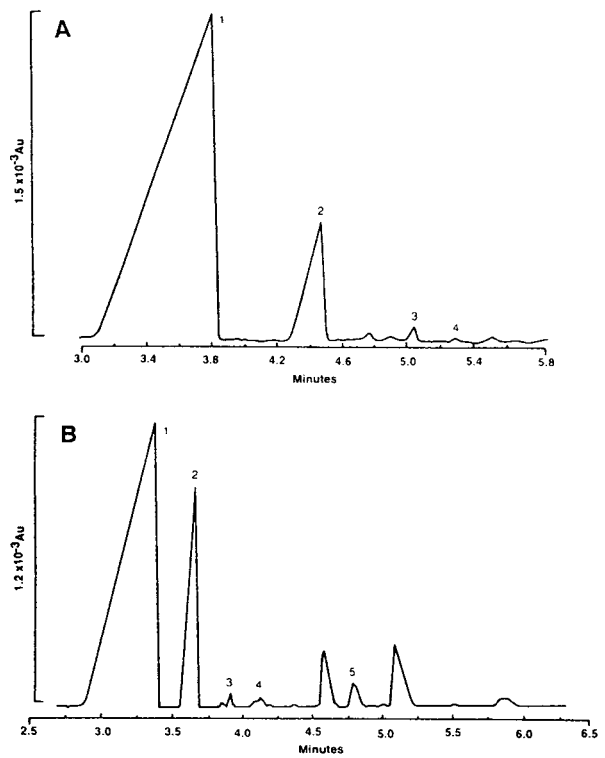

Fig. 1. (A) Electropherogram of Ultrex grade hydrogen peroxide, after catalytic decomposition, using 5 m*M* UV Cat 1–6.5 m*M* HIBA (pH 4.4). Fused-silica capillary dimensions 60 × 52 cm, 75 μm I.D.; separation voltage +20 kV; sampling for 30 s at 10 kV; indirect UV detection at 185 nm. (B) Electropherogram of identical sample and identical conditions used for Fig. 1A except the electrolyte was 1.2 m*M* UV Cat 2–3.0 m*M* tropolone. Peaks: 1 = potassium/ammonium, 2 = calcium, 3 = sodium, 4 = manganese (A) or magnesium (B), 5 = manganese.

We did not attempt to quantitate the impurities in the laboratory grade hydrogen peroxide. Yet, by comparison with subsequent separations in this report, it is clear that the levels of analytes shown in Fig. 1A and B are in the range of 0.1 to 1 ppm. These concentrations are at least an order of magnitude higher than those investigated in our calibration study (see the *Calibration Plots* paragraph below) and also much higher than the concentrations usually encountered in any semiconductor grade hydrogen peroxide. The additional, unknown peaks in Fig. 1A and B are attributable to the sample and not the carrier electrolyte.

Sample preparation

Hydrogen peroxide matrix can interfere with capillary electrophoretic analysis due to its redox ($E_o = +0.8$ V, [8]), complexing (log K_{FeL} *ca.* 9.3, [9]) and weakly acidic (pK *ca.* 11.6, [10]) properties.

Separations of cations with the help of the UV

Cat 1 carrier electrolyte are not possible in the 30% hydrogen peroxide. The quality of separation is strongly affected by excessive peak broadening and baseline noise. The highest analyzable concentration of hydrogen peroxide with the UV Cat 1 electrolyte is *ca.* 3%. This observation makes it preferable to employ catalytic reduction as a sample preparation for this method in order to avoid loss of sensitivity by dilution.

In contrast, the UV Cat 2 electrolyte can be used for analysis of cations even at 30% hydrogen peroxide. Neither a dilution nor catalytic reduction of peroxide matrix is required for separations with that electrolyte. An example of a direct cation analysis of concentrated hydrogen peroxide sample is shown in Fig. 2. The ability of UV Cat 2 electrolyte to separate cations without any interference from hydrogen peroxide is probably due to a more constant complexing behavior of tropolonate ligand contained in that electrolyte. Complexing ligands are used in CE electrolytes to increase selectivity. Due to the very close values of electrophoretic mobilities of most cations, CE separations would otherwise be difficult or impossible [1,5]. Whereas the complexing ability of most ligands (including α-hydroxyisobutyric acid in the UV Cat 1 electrolyte), decreases with increasing acidity, the values of stability constants of the tropolonate complexes are to a large degree independent of pH [8]. Based on this and on the quality of the separation shown in Fig. 2, UV Cat 2 appears to be the electrolyte of choice for the analysis of

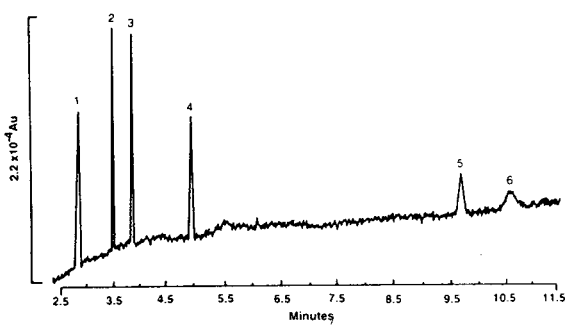

Fig. 2. Electropherogram of semiconductor grade 30% hydrogen peroxide spiked with 15 ppb of cations using same CE conditions as in Fig. 1B. Peak identification: 1 = potassium; 2 = calcium; 3 = sodium; 4 = manganese; 5 = nickel; 6 = zinc.

cations in concentrated hydrogen peroxide samples.

Calibration plots

Electromigration is a preferred mode of sample introduction from hydrogen peroxide samples. Due to the relatively low degree of dissociation, even at highest concentrations, hydrogen peroxide samples exhibit a lower conductivity than any of the carrier electrolytes under discussion. The preconcentration effect caused by electrostacking [1] can thus be expected not only for the catalytically reduced, but for concentrated hydrogen peroxide samples as well.

Feasibility of quantitation was evaluated by calibration plots for the concentration range of cations between 1 and approximately 35 ppb. Working conditions were such that it was not possible to prepare samples below 1 ppb without the danger of environmental contamination. It was found that above these levels (*i.e.* at 50–100 ppb and higher), slopes of calibration curves obtained by electromigration decreased almost to zero, making any quantitation difficult. These effects were observed with and without catalytic destruction of peroxide and can not thus be attributed to sample matrix. Linearity of electromigration sampling was investigated by one of the authors and conditions for reliable quantitation with that sampling mode were outlined in a recent report [11].

Fig. 3 shows representative calibration results for some of the cations analyzed directly in undecomposed 30% peroxide with the help of the UV Cat 2 electrolyte. Table I summarizes the linear regression results which cover the range of 1 to approximately 35 ppb. The slopes are given for both ppb and micromolar units. The former unit is in common use in the semiconductor industry, while the latter is of greater utility in making comparisons of CE behavior. Regarding the regression coefficients, we note that the value of the regression slope for sodium (2624) is approximately one half of that for all divalent cations in the same plot (Ca 4359, Mn 5393, Ni 4977 and Zn 5120). This shows the expected better sensitivity for divalent cations [12] on one hand and the compensating effect of sampling recoveries on peak areas on the other

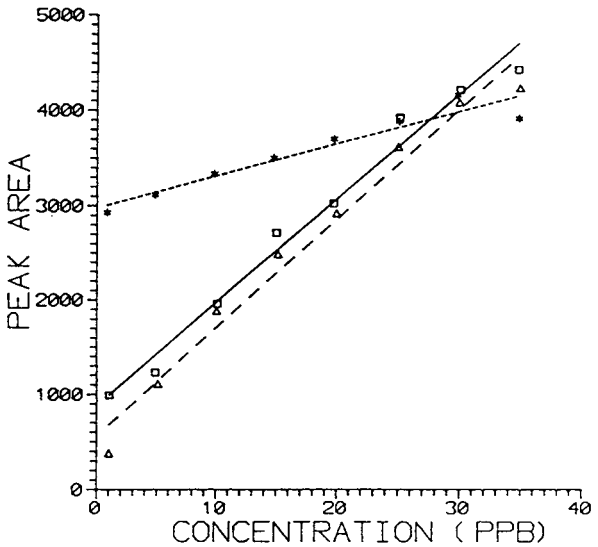

Fig. 3. Representative calibration plots shown for selected cations obtained using UV Cat 2 procedure. * = Potassium; △ = sodium; □ = calcium.

hand. If hydrostatic sampling were used, slowly migrating zinc ions would yield a larger area than, for example, the same amount of manganese ions. In electromigration, however, this effect is compensated for by a lower sampling recovery of less mobile ions, such as zinc, relative to that of more mobile ions, such as manganese. This also means that an approximate quantitation for multiple peaks is feasible after a calibration with just one standard. Because of the discussed compensation of increasing areas by decreasing recoveries, such "universal calibration" is probably possible only with electromigrative sampling. Of note in Fig. 3 is the regression line for the potassium peak. This can be explained by a large contamination of blank peroxide standard by either potassium or ammonium (see the discussion of the K/NH_4 peak in one of the preceding paragraphs). The nonzero intercepts reveal that the purest available semiconductor hydrogen peroxide which was selected for this work contained calcium, sodium, manganese, nickel, and potassium, but nondetectable levels of zinc.

TABLE I

LINEAR REGRESSION SUMMARY FOR CALIBRATION CURVES

Cation	Slope[a]		Intercept	R^{2} [b]
	m_1	m_2		
Potassium	1310	33.5	2958	0.921
Calcium	4359	108.8	870	0.980
Sodium	2624	114.1	564	0.977
Manganese	5393	98.2	442	0.966
Nickel	4977	84.8	569	0.997
Zinc	5120	78.3	−33	0.960

[a] m_1 slope for micromolar concentration, m_2 slope for ppb concentration.
[b] Correlation coefficient.

Analysis of samples

The two electropherograms in Fig. 4A and B illustrate the ability of the discussed technique to detect a group of cationic impurities even in the highest purity samples of hydrogen peroxide. Concentrated peroxide samples can be analyzed directly without the catalytic decomposition step usually employed prior to the CE analysis of anions. The detection limits at 2 × the signal-to-noise ratio are summarized in Table II. The detection limit for potassium is not reported, since, as discussed previously, potassium comigrates with ammonium under the conditions of analysis.

Copper was found to be an exception. The most reproducible results for this cation were obtained using the peroxide decomposition step and the UV Cat 1 electrolyte. Using this procedure, a detection limit of 1.3 ppb was established.

The ability to analyze directly the undiluted hydrogen peroxide samples is essential for the reliable determination of alkali and alkaline earth cations. If sample handling is reduced to a minimum, the possibility of sample contamination by these analytes is also minimized. In actual practice, it is necessary to work in a clean room environment or under prefiltered laminar flow conditions to keep the environmental contamination to an absolute minimum. Moreover, an accurate quantitation of all the detected cations in the semiconductor grades of hydrogen peroxide, which was not pursued in this particular study due to the inability to control airborne contamination, would require the use of

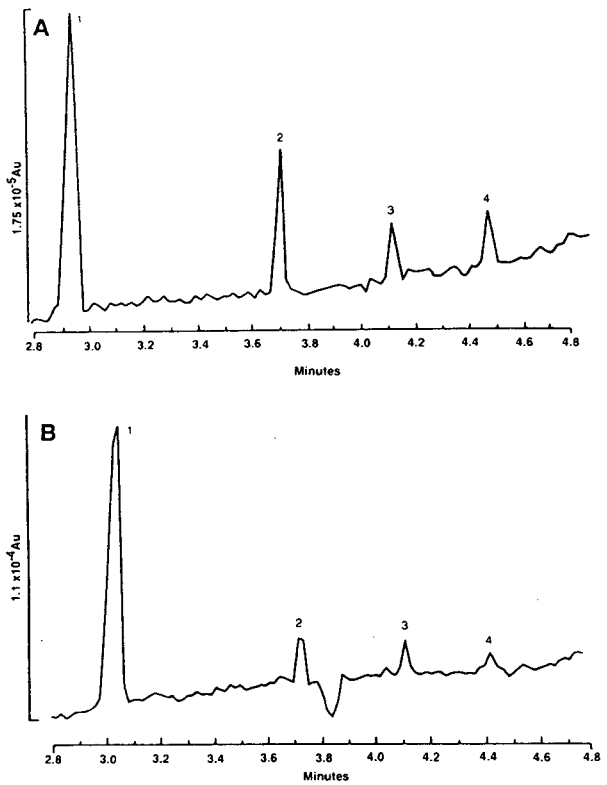

Fig. 4. (A) Electropherogram of source A semiconductor grade hydrogen peroxide (30% undecomposed, unstabilized) obtained using UV Cat 2 procedure listed in Fig. 1B. Detected species: 1 = potassium/ammonium; 2 = calcium; 3 = sodium; 4 = magnesium. (B) Electropherogram of source B semiconductor grade hydrogen peroxide obtained using same conditions as Fig. 4A. Detected species: 1 = potassium/ammonium; 2 = calcium; 3 = sodium; 4 = magnesium.

standard additions or the use of the calibration curve determined with a grade of hydrogen peroxide having lower trace metal contaminant levels that was available for this study. For example, using the standard additions approach, the Ca level for sample B was determined to be 6.2 ppb and Na was found to be 3.8 ppb.

The group IA cations have to be monitored and controlled carefully during semiconductor processing due to the deleterious effects of these ions upon semiconductor device properties, which can be attributed to the high diffusional mobility of these cations. From the alkaline earths, calcium is found most frequently in hydrogen peroxide samples of otherwise highest purity and the levels of that cation have to be also followed closely. Because of its lower cost and less extensive time requirements, the discussed method offers itself as an interesting alternative to GFAAS, which is exclusively utilized for IA and IIA cations at the present time [4].

TABLE II

LIMITS OF DETECTION IN 30% HYDROGEN PEROXIDE ANALYZED DIRECTLY WITH UV CAT2-TROPOLONE

Cation	Detection limit (ppb)
Potassium	–
Barium	2.8
Strontium	1.8
Calcium	0.7
Sodium	0.7
Magnesium	0.5
Manganese	1.3
Lithium	0.6
Nickel	3.3
Zinc	3.0

It is reasonable to assume that this CE approach can be further optimized to reduce the detection limits to the ppt levels which has already been achieved for water [6]. This study has illustrated the importance of the carrier electrolyte. There is a remaining need to not only enhance sensitivity but also to increase the number of metal ions which can be simultaneously determined. In fact, purity specifications for semiconductor processing chemicals continue to become more demanding. Soon the maximum allowable concentration of each metal ion will be 1 ppb, and an upper limit of 0.1 ppb is projected for the near future. Therefore, this work illustrates the enormous potential of CE for quality control testing of ultrapure chemicals.

REFERENCES

1 P. Jandik, W.R. Jones, A. Weston and P.R. Brown, *LC·GC*, 9 (1991) 634.
2 W. Kern, *Semicond. Int.*, 7 (1984) 94.
3 S. Sato *et al.*, *Technical Papers on Ultra Clean Technology*, Vol. 2, May 1988.

4 R. Carpio, J. Baylis, A. Diebold, R. Mariscal, T. Pinkston, D. Powell and E. Rosenfeld, in D.N. Schmidt (Editor), *Proceedings of the Symposium on Contamination Control and Defect Reduction in Semiconductor Manufacturing I*, Vol. 92-21, The Electrochemical Society, Pennington, NJ, 1992.
5 A. Weston, P.R. Brown, P. Jandik, W.R. Jones and A.L. Heckenberg, *J. Chromatogr.*, 593 (1992) 289.
6 A. Weston, P.R. Brown, P. Jandik and A.L. Heckenberg, *Anal. Chem.*, in press.
8 R.C. Weast (Editor), *Handbook of Chemistry and Physics*, CRC Press, Boca Raton, FL, 74th ed., 1993, pp. 8–24.
9 J. Evans, N. Uri and E.P. George, *Trans. Faraday Soc.*, 45 (1949) 230.
10 A.E. Martell, Texas A&M University, personal communication.
11 P. Jandik, M. Fuchs and W.R. Jones, *Electrophoresis*, submitted for publication.
12 E.S. Yeung, *Acc. Chem. Res.*, 22 (1989) 125.

Journal of Chromatography A, 657 (1993) 192–198
Elsevier Science Publishers B.V., Amsterdam

CHROM. 25 563

Short Communication

Comparison of the effects of extra-column aerosol and liquid-phase volumes on high-performance liquid chromatographic separations with inductively coupled plasma detection

Lori B. Allen and John A. Koropchak*

Department of Chemistry and Biochemistry, Southern Illinois University, Carbondale, IL 62901 (USA)

(First received April 1st, 1993; revised manuscript received September 7th, 1993)

ABSTRACT

This communication demonstrates that the extra-column, laminar-flow, aerosol volume for HPLC detection methods employing typical aerosol interfaces has a small effect on peak variance compared to extra-column volume in the liquid phase. The higher velocities used with aerosol systems accommodate larger extra-column volumes before band broadening becomes significant. The reported results are limited to situations where a laminar flow profile is established at atmospheric pressure.

INTRODUCTION

Liquid chromatography is often coupled via an aerosol interface to detectors such as mass spectrometry (LC–MS), inductively coupled plasma atomic emission or mass spectrometry (ICP-AES or ICP-MS), or light scattering [1–4]. With the large surface-area-to-volume ratio of aerosols, relatively non-volatile analytes are readily enriched in the droplet phase by the evaporation of the typically more volatile solvents. However, the use of an aerosol interface results in the addition of hundreds of milliliters of extra-column volume which is often used to condition the aerosol (evaporate and remove solvent vapors, modify the particle size distribution, etc.) prior to the detector. Commonly, this volume is in the laminar flow regime where band broadening as a result of convection and axial dispersion is expected to occur.

One report concerning the effects of extra-column aerosol-phase volume on chromatography detection by ICP-AES was published in 1982 [5]. This report compared internal *versus* external placement of the aerosol spray chamber with respect to the torch box. Internal placement resulted in additional liquid-phase extra-column volume while external placement added to the aerosol volume and minimized the extra-column liquid-phase volume. External placement resulted in lower peak broadening and demonstrated a lower sensitivity dependence on the mobile phase flow-rate as compared to internal

* Corresponding author.

0021-9673/93/$06.00

placement. This hinted that dispersion effects in the liquid volume are more significant than in the aerosol phase on a direct volume-to-volume basis and to minimize the loss of chromatographic resolution, placement of the spray chamber as close as possible to the column is preferred.

Perhaps more impressive was the interfacing of LC to MS with the counter-flow gas diffusion cell (CFGDC) by Vestec Corporation [6]. The CFGDC is one part of the universal interface and is used to remove solvent vapors from analyte transport system while at atmospheric pressure. As vapor removal is accomplished through evaporation and subsequent diffusion through a permeable membrane, the required processing volume is quite large. Nonetheless, Vestec has demonstrated that dispersion and particle losses are negligible.

More recently, we have published a report describing the influence of the aerosol volume on discrete signals with an ICP detector [7]. In brief, the aerosol-based laminar-flow volume between the spray chamber and the torch box was varied. The most dramatic condition tested for desolvated particles was the addition of 308 ml of aerosol volume (10 m of tubing with an internal diameter of 6.4 mm) which required a transport time of 37 s. This caused the peak width at half-maximum to increase by only 35%. Through computer simulation, band broadening for the conditions tested was shown to be the result of convective dispersion. An important parameter affecting convective dispersion is the peak residence time within the flow system [7]; lower residence times reduce band-broadening and minimize the loss in peak intensity. As aerosol interface systems generally operate at relatively high volumetric flows (l/min), peak residence time within hundreds of ml of flow volume can be relatively short. An additional factor, unique to aerosols that reduces the apparent band-broadening, is the irreversible nature of aerosol particle-transport wall collisions that occur because of either dispersion, centripetal or gravitational forces. Particles that are lost in this fashion may have otherwise caused the signal shape to broaden.

The influence of flame atomic absorption spectrometry (FAAS) on flow injection analysis signals has been reported by Fang *et al.* [8]. As with ICP-AES, FAAS utilizes a nebulizer and spray chamber to modify the aerosol prior to the flame. Unlike ICP-AES, the gas and liquid introduction velocities are higher. At a typical sample uptake flow-rate of 4.2 ml/min, dispersion was reported to be negligible with sample volumes as-low-as 50 μl. By analogy, they concluded that their detection system including readout was comparable to a 10 cm liquid-phase capillary tube with an internal diameter of 0.5 mm. For extremely small sample volumes (<10 μl), dispersion was independent of the liquid uptake flow-rate over a range of 1 to 6 ml/min because the analyte pulse is instantaneously distributed within the spray chamber.

The effects of liquid-phase flow volume on dispersion are well-known from the liquid chromatography and flow injection analysis literature [9,10]. In general as either the length or internal diameter of extraneous liquid-phase tubing increases, dispersion increases. This results from the convective flow profile. Coiling or knotting the transport path acts to minimize convective dispersion by improving radial mixing through the development of secondary flow streamlines.

The aim of this communication is to demonstrate the relative effects of the aerosol-phase extra-column volume *versus* liquid-phase volume for liquid chromatographic separations coupled with ICP-AES detection, although these effects should hold true with most other detectors using aerosol interfacing. To do this, we will compare liquid chromatograms for the separation of chromium species obtained with ICP-AES detection where: (a) aerosol and liquid-phase volumes are minimized, (b) liquid-phase volume is increased dramatically, and (c) aerosol-phase volume is increased dramatically. This is intended to show that with aerosol interfaces relatively large extra-column aerosol volumes can be tolerated without serious degradation of chromatographic profiles, unlike the situation with liquid-phase extra-column volumes.

EXPERIMENTAL

Instrumental

Fig. 1 represents an overview of the experimental system. The dual piston pump util-

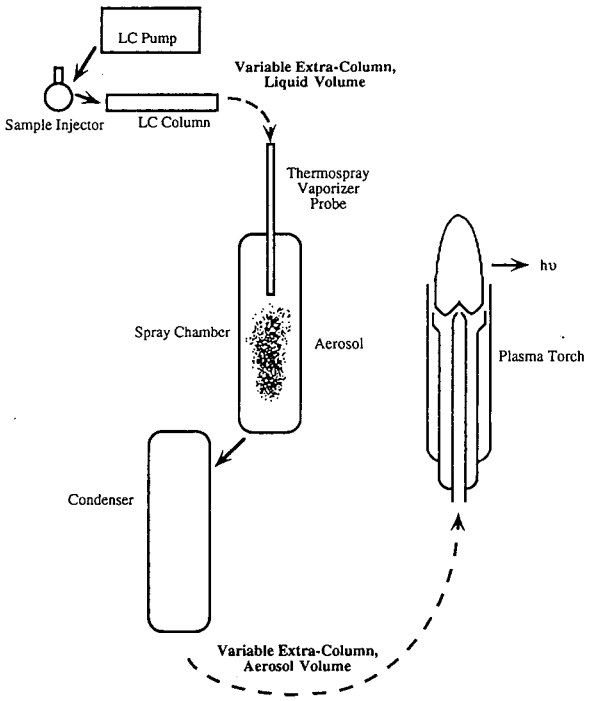

Fig. 1. Overview of experimental design. The dashed lines represent the location for the extra-column volumes.

ized in the separation was an Autochrom (Milford, MA, USA) Model 111. The flow-rate was 1.0 ml/min. The injector was a Rheodyne Model 7125 (Cotati, CA, USA) and was equipped with a 50-μl sample loop. The aerosol was generated by an aperture-based thermospray system. Thermospray sample introduction was chosen over pneumatic-based sample introduction because the particles produced are desolvated and hence of smaller size. This enriches the analyte concentration and results in improved mass transport efficiency for these experiments by reducing gravitational loss. Details surrounding the construction of the thermospray varporizer probe and optimization can be found elsewhere [11]. The exit aperture was 50 μm in diameter and the tip temperature was maintained at 176°C. The power to the probe was supplied by a Vestec (Houston, TX, USA) temperature controller. The spray chamber was heated to approximately 140°C and the condenser used to remove the solvent vapors was at 0°C. The combined spray chamber and condenser volume was 649 ml.

The ICP system was a Perkin-Elmer (Norwalk, CT, USA) Model 5500 operating at a forward power of 1.25 kW. The plasma gas flow-rate was 16 l/min with an auxiliary rate of 1.4 l/min. The carrier gas rate was 0.70 l/min and metered by a Tylan (Torrance, CA, USA) Model FC 260 mass flow controller. The chromium line used for detection was 205.5 nm. Wavelength modulation for background correction was accomplished by the oscillation of a quartz refractor plate positioned in front of the exit slit of the monochromator. The function generator used to drive the oscillation was a Wavetek (San Diego, CA, USA) Model 114 and the signal was tracked by a Stanford Research Systems (Sunnyvale, CA, USA) Model SR510 Lock-in-Amplifier. The viewing height was 7 mm above the load coil.

The signal was processed with Asystant + software (Macmillan Software, New York, NY, USA) via a MetraByte DAS-8 A/D (Keithley, Taunton, MA, USA) board and stored on an Epson Equity 1+ (Torrance, CA, USA) computer. Further signal processing was completed by converting the signal to an ASCII file and importing as a KaleidaGraph 2.0 (Synergy Software, Reading, PA, USA) file on a Macintosh Classic computer (Apple Computer, Cupertino, CA, USA).

Chromatographic separation

The separation chosen was the mobile-phase ion pairing speciation of chromium(VI) and chromium(III) which has been employed by this laboratory for thermospray sample introduction to ICP-AES [11]. The mobile phase composition was 5 m*M* sodium pentanesulfonic acid, 0.01 *M* magnesium acetate, 1% (v/v) acetic acid and 10% (v/v) methanol. The final pH was adjusted to approximately 3.5 with acetic acid. An Adsorbosphere HS C_{18} (Alltech, Deerfield, IL, USA) column was used. The size of the column packing was 7 μm and the column dimensions were 250 mm × 4.6 mm I.D. The Cr(III) concentration was 10 μg/ml and was prepared fresh from chromium nitrate to minimize the formation of additional complexes. The Cr(VI) concentration was 2 μg/ml and was prepared from potassium dichromate.

Equations

The following equations were used throughout this paper. The liquid-phase and aerosol-phase Reynold's flow numbers, R_e, were calculated as:

$$R_e = \frac{\rho v d}{\eta}$$

where ρ is the fluid density, v is the fluid velocity, d is the tube diameter and η represents the fluid viscosity [12]. The values chosen for both the fluid density and viscosity for the liquid flow number were that of water at room temperature.

The equation used for the calculation of resolution, R_s, was:

$$R_s = \frac{2\Delta Z}{W_x + W_y}$$

where ΔZ represents the difference in the retention times of the two species and W_x, W_y represents the baseline widths for the two components [12]. The baseline widths were estimated by assuming a Gaussian profile and hence, that the baseline width is 1.7 times greater than the full-width at half-maximum (FWHM). In a similar fashion, peak area was calculated as 1.25 times the product of the baseline width and peak height.

The reduced time constant (τ) was calculated as:

$$\tau = \frac{Dt}{a^2}$$

where D is the diffusion coefficient, t is time and a is the tube radius [13]. For the aerosol phase, a diffusion coefficient of $5.3 \cdot 10^{-6}$ cm^2 s^{-1} was used and 10^{-5} cm^2 s^{-1} for the liquid phase. A reduced constant of less than 0.01 indicates that convective dispersion is dominating whereas a value greater than 0.1 indicates diffusion controlled band-broadening.

Extra-column volumes

The goal of this study was to demonstrate the relative effects of liquid-phase and aerosol-phase volume by comparing three extremes: (a) a case where both liquid-phase and aerosol-phase volumes are minimized, (b) a case where the aerosol volume was kept the same as in (a), but the liquid-phase volume was increased dramatically, and (c) a case where the liquid-phase volume was minimized as in (a) but the aerosol volume was increased dramatically.

The dashed lines in Fig. 1 illustrate the experimental location for the added extra-column volumes. A chromatogram minimizing both the liquid- and aerosol-phase extra-column volume was acquired and will subsequently be called the *reference chromatogram*. In this case, the liquid volume between the column outlet and the thermospray probe was 2.74 μl [5.4 cm of polyether ether ketone (PEEK) tubing with an internal diameter of 254 μm]. The aerosol volume, excluding the spray chamber and condenser, was 31.7 ml (98.5 cm of tygon tubing with an internal diameter of 6.4 mm) and connected the condenser to the ICP torch.

In a second chromatogram, the liquid-phase volume between the end of the column and the thermospray vaporizer was increased to approximately 2.0 ml, using 2.2 m of PTFE tubing with an internal diameter of 1.09 mm for connection. This tubing was substituted for the PEEK tubing and coiled with a circumference of approximately 30 cm. The calculated Reynold's flow number was 84 which indicates laminar flow. The aerosol volume was the same as the reference chromatogram.

In the third chromatogram, the liquid volume was the same as the reference chromatogram. However, the aerosol volume between the exit of the aerosol condenser and the plasma torch was increased to 240 ml using 7.45 m of Tygon tubing with an internal diameter of 6.4 mm. This tubing was joined to the existing transport tube resulting in a final aerosol volume of 272 ml. The Tygon transport tubing was horizontal and straight except for four 90° bends. In this instance, the Reynold's number was 187 which is also in the laminar regime.

Reagents

All chemicals used were either HPLC or reagent grade. All solution containing glassware was scrupulously cleaned, acid soaked and rinsed with deionized/distilled water prior to use.

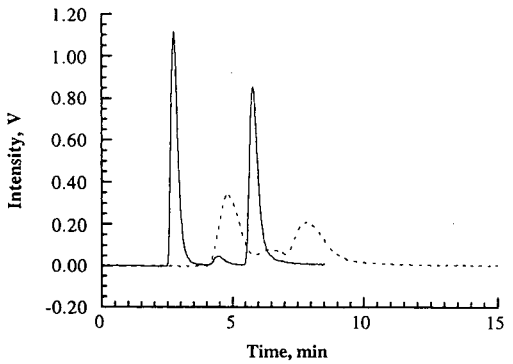

Fig. 2. Chromatogram (dashed line) demonstrating the influence of 2.0 ml of extra-column liquid-phase volume *versus* the reference chromatogram (solid line).

RESULTS AND DISCUSSION

Figs. 2 and 3, respectively, indicate the addition of extra-column liquid and aerosol volume on the chromatographic separation. The reference chromatogram represented by the solid line is the same in both figures. Each chromatogram consists of three peaks, the first of these is for Cr(VI) and the latter eluting component is for Cr(III). Although the exact identity of the interim peak is not known, it may be the result of Cr(III) complex formation with water [11]. The peak shapes are non-Gaussian which may reflect a slight over-loading of the column. Table I summarizes the figures-of-merit for each chromatogram. The values indicated in the data table correspond directly with the chromatograms in Figs. 2 and 3. The numbers indicated in parentheses express the percent relative standard deviation as calculated from two trials. With the exception of the residence time for the additional aerosol, the relative standard deviation is less than 10%. The higher deviation with the added aerosol is the result of using a manual trigger for the data acquisition process. Residence time was measured as the difference in elution times, determined at peak maximum intensity, for each respective component in the chromatograms. In this report, the differences between the reference and each of the other chromatograms are of interest.

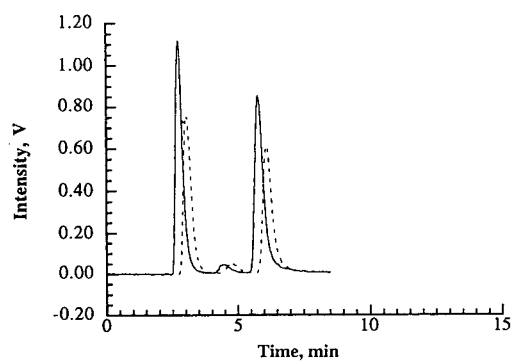

Fig. 3. Influence of 240 ml of extra-column aerosol volume on the chromatographic separation (dashed line). The solid line represents the reference chromatogram.

Table I shows that resolution was diminished substantially by the addition of 2.0 ml of liquid-phase, extra-column volume. In contrast, little change in resolution occurred with the addition of 240 ml of aerosol-phase volume. From the data table, the residence time for the Cr(VI) peak was only 17 s within the added aerosol volume, but was 125 s within the added liquid volume. Likewise for the added aerosol and liquid volumes, the residence times for the Cr(III) peak were 20 and 125 s, respectively. This is in good agreement with the anticipated times based on the added volume and the volumetric flow-rate. Hence, the integrity of the separation is better maintained in the larger volume of the aerosol-phase because of the lower residence time. The reduced time constant for the aerosol phase was 0.009 whereas the value was 0.42 for the liquid phase. This indicates that the aerosol phase was under the influence of convective dispersion but that the liquid-phase band-broadening was diffusion controlled. To realize a 125 s residence time in the aerosol phase with a tube of 6.4 mm I.D. at a volumetric rate of 0.7 l/min (as used in this work) would require a length of 45.3 m which has a reduced time constant of 0.006 which is still indicative of convective dispersion.

Also evident from the data table and Figs. 2 and 3, the peak heights are reduced to a greater extent by the addition of liquid-phase volume; this effect results from the differences in dispersion for the two cases, as outlined above. In contrast, the peak areas are influenced more by the added aerosol volume. For the added liquid-

TABLE I

COMPARISON OF THE FIGURES-OF-MERIT

FWHM represents the full-width at half-maximum intensity. Values in parentheses represent the percent relative standard deviation.

	Reference	Added liquid volume	Added aerosol volume
Intensity (V)			
Cr(VI)	1.12 (4.56%)	0.346 (8.22%)	0.758 (0.09%)
Cr(III)	0.85 (1.31%)	0.211 (6.27%)	0.614 (2.10%)
FWHM (s)			
Cr(VI)	16 (0.0%)	53 (6.4%)	18 (0.0%)
Cr(III)	20 (3.6%)	77 (0.9%)	22 (0.0%)
Residence time (s)			
Cr(VI)		125 (7.0%)	17 (16%)
Cr(III)		125 (6.9%)	20 (14%)
Area (V s)			
Cr(VI)	19.1	19.5	14.5
Cr(III)	18.1	17.3	14.4
Resolution	5.98	1.65	5.47

phase volume, one would anticipate a loss in signal intensity but that the area would remain constant. This trend is supported by the areas corresponding to the Cr(VI) and Cr(III) signals differing by only 2 and 4%, respectively.

In considering the added aerosol volume, a reduction in peak area results due to particle collisions and loss at the transport wall. Such collisions generally result in the irreversible adherence of the particle to the wall, and therefore loss of part of the total signal contained within the peak. However, particles most likely to be lost are those in the slow-velocity lamina closest to the wall. These particles represent the signal within the peak tail [7]. Therefore, loss of these particles leads to a reduction in peak tailing, counteracting dispersion effects on peak width and resolution to some extent.

CONCLUSIONS

This report compared dispersion and the loss of chromatographic resolution resulting from the addition of 2.0 ml of extra-column liquid volume to that resulting from the addition of 240 ml of aerosol volume. The effect of the aerosol volume on resolution was lower because the peak residence time within the added aerosol volume was significantly lower. In contrast, signal areas were reduced with the added aerosol volume because of particle losses at the wall. This latter effect also acts to counteract the detrimental effects of dispersion on band widths. These results demonstrate that relatively large extra-column aerosol-phase volumes can be tolerated when aerosol techniques are employed to interface liquid chromatography with aerosol-based detectors, compared to the effects of extra-column liquid-phase volume. Of course, the level of band-broadening and the absolute value of aerosol-phase volume that can be tolerated will depend on the bandwidths provided by the separation technique. Although these results are only demonstrated with ICP-AES detection, it is likely that these observations are also applicable to ICP-MS detection, to LC–MS with particle beam interfacing and to other neutral particle atmospheric pressure aerosol-based detectors.

REFERENCES

1 E.S. Yeung, *Detectors for Liquid Chromatography*, Wiley, New York, 1986.
2 S. Ahuja, *Trace and Ultratrace Analysis by HPLC*, Wiley, New York, 1992.
3 M. Brown, *Liquid Chromatography/Mass Spectrometry —Applications in Agricultural, Pharmaceutical, and Environmental Chemistry*, American Chemical Society, Washington, DC, 1990.
4 A. Al-Rashdan, D. Heitkemper and J.A. Caruso, *J. Chromatogr. Sci.*, 29 (1991) 98.
5 B.S. Whaley, K.R. Snable and R.F. Browner, *Anal. Chem.*, 54 (1982) 162.
6 J.G. Wilkes, C.H. Vestal and M.L. Vestal, in R.M. Caprioli (Editor), *Proceedings 38th ASMS Conference on Mass Spectrometry and Allied Topics, Tucson, A2, June 3–8, 1990*, p. 31.
7 J.A. Koropchak, L. Allen and J.M. Davis, *Appl. Spectrosc.*, 46 (1992) 682.
8 Z. Fang, B. Weiz and M. Sperling, *J. Anal. Atomic Spectrom.*, 6 (1991) 179.
9 J. Ruzicka and E.H. Hansen, *Flow Injection Analysis*, Wiley, New York, 1988.
10 L.R. Snyder and J.J. Kirkland, *Introduction to Modern Liquid Chromatography*, Wiley, New York, 1979.
11 S.B. Roychowdhury and J.A. Koropchak, *Anal. Chem.*, 62 (1990) 484.
12 B.L. Karger, L.R. Snyder and Cs. Horváth, *An Introduction to Separation Science*, Wiley, New York, 1973.
13 J.T. Vanderslice, A.G. Rosenfeld and G.R. Beecher, *Anal. Chim. Acta*, 179 (1986) 119.

Journal of Chromatography A, 657 (1993) 199–203
Elsevier Science Publishers B.V., Amsterdam

CHROM. 25 601

Short Communication

Ion-exchange chromatography with a soft sorbent operating in a pressurized column

M.B. Baru and I.V. Kozlovsky-Vagenina*

Branch of Shemyakin Institute of Bioorganic Chemistry, Russian Academy of Sciences, Puschino, Moscow Region 142292 (Russian Federation)

(First received January 13th, 1993; revised manuscript received September 28th, 1993)

ABSTRACT

A standard Pharmacia column was modified to enable pressurization with inert gas. The column moveable adaptor can follow the gel as the volume changes under pressure; thus, "dead volume-free" operation is achieved. A trial separation of natural bee venom components was carried out on the modified column with CM-Sephadex C_{25} in a pH and ionic strength gradient. It was found that, at 54 kPa pressure, the elution times of the bee venom constituents phospholipase a_2, apamin and melittin are reduced and the resolution is improved.

INTRODUCTION

Pressurization, widely used with rigid sorbents to improve packing [1,2] and optimize separation, is considered inapplicable to soft gels, though dextran gels, for instance, are known to be able to withstand pressures up to 1700 kPa [3]. In order to provide dead volume-free operation and optimize soft gel packing we made a minor improvement to the standard Pharmacia column by applying inert gas pressure to the gel bed via the moveable adaptor. Pressure can be adjusted to make the adaptor follow the gel volume variation during gel shrinking or swelling; additional pressurizing can also be accomplished. Such dead volume elimination at the column head is important when concentrated protein mixtures are applied to soft gel columns during gel filtration and in gradient elution from soft ion exchangers. Usually the ion exchange process is thought to depend least of all chromatographic methods on the packing quality. It was of interest to see if the zero dead volume column operation with additional pressure influences the pH and ionic strength gradient elution efficiency.

MATERIALS AND METHODS

A continuous-flow reaction system for biopolymer solid-phase synthesis served as a prototype of our device [4]. The moving piston is pressed close to the sorbent with preset force. Fig. 1 shows the modified $C_{16/20}$ column (Cat. No. 19-5101-01, Pharmacia, Sweden) with moveable adaptor AC 16 (1) (Cat. No. 19-5109-01), thermostat jacket JC 16/20 (2) (Cat. No. 19-5105-

* Corresponding author.
E-mail: Biochem@sovamsu.sovusa.com.

0021-9673/93/$06.00

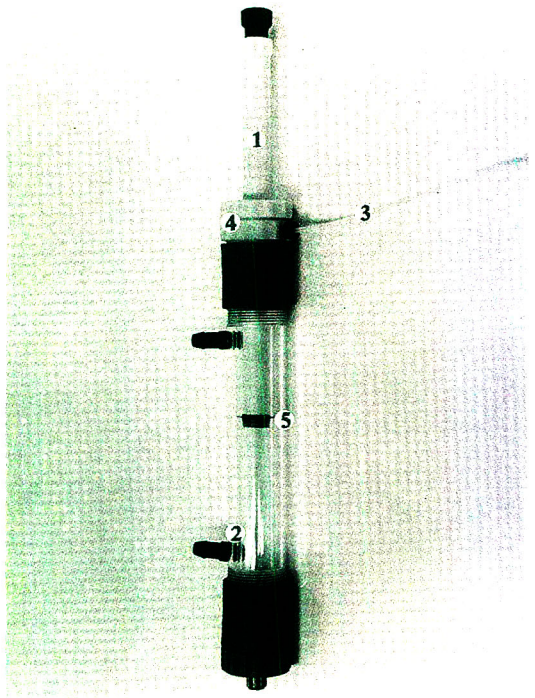

Fig. 1. General layout of the modified Pharmacia "dead volume-free" operated column: 1 = moveable adaptor; 2 = thermostat jacket; 3 = tubing for gas inlet; 4 = modified unit with fluoroplastic collar.

01) and a PTFE tube for inert gas feeding (3). The modified unit (4) was made from Caprolon (poly-ϵ-caproamid). The net gas pressure moving the adaptor was calculated by adding the pressure applied directly to the sorbent to the pressure component due to friction of the standard O-ring rubber seal (5) on the glass wall. The friction value determined experimentally depends on the wear of the O-ring seal and its retention against the column glass walls. In order to reduce friction the column glass walls were thoroughly silanized, as described by Stewart and Young [5]. The adaptor surface was polished in order to minimize the adaptor friction on the fluoroplastic collar edge. The fluoroplastic collar was inserted into the modified unit (4) in order to prevent the gas from leaking from the cavity. The moving adaptor gas pressure was chosen to overcome friction, thus minimizing the dead volume and also applying to the sorbent a pressure of 50–100 kPa.

The pressurized column was tested by separating crude natural bee venom into its basic components [6]: phospholipase a_2, melittin and apamin. The crude bee venom was a gift from Apis (Moscow, Russia). It was dissolved in 0.05 *M* triethylammonium acetate, pH 6.7 or 5.6 (25 mg in 3 ml), filtered through cotton and applied to the CM-Sephadex C_{25} column (Pharmacia, Sweden) equilibrated with the appropriate buffer. The starting gel volume was about 12 ml.

The non-adsorbed components of the sample were isocratically eluted. Then the chromatogram was developed at room temperature for 540 min with a pH and ionic strength linear gradient to 0.1 *M* triethylammonium acetate, pH 10, with 1.5 *M* NaCl. The flow-rate was 60 ml/h. The effluent was collected in 2-ml fractions. Detection at 226 nm was carried out with a Uvicord SII (LKB, Sweden). In experiments with pressure the column was packed and the chromatography was carried out under nitrogen pressure of 54 or 93 kPa.

The resulting bee venom constituents were identified by their HPLC retention time values and amino acid analysis data. Fractions corresponding to the eluting peak maxima were analysed by RP-HPLC with a Gilson analytical gradient system (Gilson Medical Electronics, Villiers-le-Bel, France) on a Synchropack C_4 column (250 × 4.1 mm I.D., 6.5 μm particle size; Alltech, USA). The linear gradient from 0.1% trifluoroacetic acid (TFA) to 70% acetonitrile (plus 0.1% TFA) in 35 min was used. The solvent flow-rate was 1.0 ml/min. The samples were analysed for amino acid composition with a Pico-Tag instrument (Waters, Milford, MA, USA).

RESULTS AND DISCUSSION

Figs. 2 and 3 depict the chromatographic separation of the bee venom components at initial pH values of 5.6 and 6.7, under pressure and without it. Phospholipase a_2, apamin and melittin are adsorbed at both pH values (p*I* 10.5,

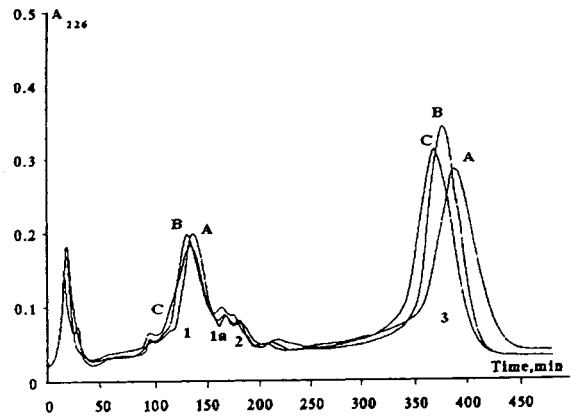

Fig. 2. Elution profile of bee venom at initial pH 5.6: (A) without external pressure; (B) with external pressure 54 kPa; (C) with external pressure 93 kPa. See text for chromatographic conditions.

7.9 and 12.1, respectively [6]); the front peak of non-adsorbed components was not analysed. According to amino acid analysis the first, second and the third peaks correspond to phospholipase a_2, apamin and melittin, respectively (see Table I).

The overall chromatogram character with pressure application remains practically the same, but the retention times and resolution values differ at both pH values (see Table II). It is seen that separation efficiency at the initial pH 5.6 rises slightly at 54 kPa, but at further pressure increase to 93 kPa the resolution becomes lower while the retention times remain practically the same as at 54 kPa. The initial pH 5.6 seems not to be favourable for separation of the bee venom components because basic peptides and protein are too strongly adsorbed, and elute slowly with the gradient; besides, phospholipase a_2 emerges as two peaks (peaks 1 and 1a, Fig. 2).

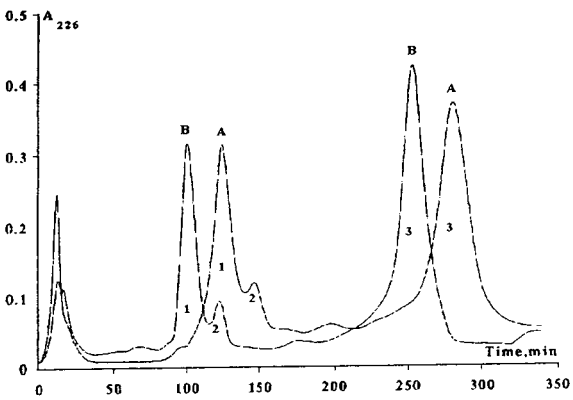

Fig. 3. Elution profile of bee venom at initial pH 6.7: (A) without external pressure; (B) with external pressure 54 kPa. See text for chromatographic conditions.

The separation appears to improve significantly when the initial pH is 6.7. The three substances emerge as three separate peaks and also elute more quickly than at the initial pH 5.6 (see Table II). The positive influence of 54 kPa pressure is also more pronounced. Resolution for peaks 1 and 2 rises under pressure approximately two-fold (see Table II), and the concentration of peak maximum fractions increases 1.7-fold for the first two peaks and 1.2-fold for the third one according to HPLC analysis.

The separation improvement under 54 kPa pressure is probably caused by facilitation of ion diffusion to the sites of reaction and increase in the available pore volume, resulting in more uniform eluent distribution in the bed volume. Diffusion facilitation is of critical importance, as the rate of ion exchange on weak acid gels is controlled by the rate of cation diffusion through the exchanger particles to the sites of reaction and diffusion of the displaced ions out of the interior of the exchanger [7]. Also, pressure application prevents channelling, which is most pronounced upon gel contraction [8].

The determination of pressure optimum for a chromatographic separation and the elucidation of the exact mechanism of the observed phenomena need further studies.

ACKNOWLEDGEMENTS

We are grateful to V. Abakumov and A. Danilov for their help, valuable advice and the bee venom sample. We thank M. Kozlovsky and A. Polyakova for technical assistance.

TABLE I

AMINO ACID ANALYSIS DATA OF THE BEE VENOM CONSTITUENTS

a = Analytical and t = theoretical numbers of amino acids.

	Apamin		Phospholipase a_2		Melittin	
	a	t	a	t	a	t
Asp/Asn	1.04	1	12.5	16	0.14	–
Glu/Gln	3.48	3	4.7	6	2.27	2
Ser	0.03	–	7.8	10	1.15	1
Gly	0.09	–	9.4	12	3.56	3
His	0.95	1	4.7	6	–	–
Arg/Thr	3.21	2 + 1	11.7	15	3.92	4
Ala	3/ref[a]	3	3.1	4	2/ref[a]	2
Pro	1.14	1	3.9	5	1.10	1
Tyr	0.03	–	6.3	8	0.06	–
Val	0.06	–	3.9	5	1.70	2
Met	–	–	2.3	3	–	–
Cys	2.08	4	6.3	8	–	–
Ile	–	–	3.1	4	2.58	3
Leu	0.78	1	7.0	9	3.50	4
Phe	–	–	3.9	5	–	–
Lys	0.84	1	8.6	11	2.49	3

[a] Reference values used for calculation of amino acid quantity.

TABLE II

CHARACTERISTICS OF SEPARATION EFFICIENCY

Separation conditions	Peak No.	Retention time (min)	Resolution	Total resolution
Initial pH 5.6				
Without pressure	1	134		
t_0 = 13 min	2	183	1.14	
	3	405	3.01	4.15
54 kPa	1	128		
t_0 = 8 min	2	174	1.28	
	3	366	4.57	5.85
93 kPa	1	128		
t_0 = 9 min	2	171	1.02	
	3	362	4.15	5.17
Initial pH 6.7				
Without pressure	1	125		
t_0 = 12 min	2	145	0.83	
	3	286	3.71	4.54
54 kPa	1	98		
t_0 = 10 min	2	120	1.57	
	3	250	4.33	5.90

REFERENCES

1 *Description of a preparative liquid chromatograph: Performances and Applications*, Jobin Yvon, Longjumeau, France, February 5, 1976.
2 *Preparative Columns*, Biotech Products International, Brussels, Belgium, March/April 1992, p. 12.
3 W.W. You, J.J. Kirkland and D.D. Bly, *Modern Size-Exclusion Liquid Chromatography —Practice of Gel Permeation and Gel Filtration Chromatography*, Wiley, New York, 1979, p. 2.
4 M.B. Baru, I.L. Rodionov, L.Ya. Shestakovsky and V.T. Larin, *Int. Pat. WO 88:89900366. 9*, July 29, 1988.
5 J.M. Stewart and J.D. Young, *Solid Phase Peptide Synthesis*, Pierce, Rockford, IL, 2nd ed., 1984, p. 53.
6 J. Gauldie, J.M. Hanson, F.D. Rumjanek, R.A. Shipolini and C.A. Vernon, *Eur. J. Biochem.*, 61 (1976) 369–376.
7 D. Reichenberg, in C. Calmon and T.R.E. Kressman (Editors), *Ion Exchangers in Organic and Biochemistry*, Interscience, New York, 1957, p. 72.
8 F. Helfferich, *Ionenaustauscher, Band 1, Grundlagen. Struktur, Herstellung, Theorie*, Verlag Chemie, Weinheim, 1959, Ch. 9.

Journal of Chromatography A, 657 (1993) 204–207
Elsevier Science Publishers B.V., Amsterdam

CHROM. 25 594

Short Communication

High-performance liquid chromatographic separation of phenylthiocarbamyl derivatives of amino acids from protein hydrolysates using a Partisphere C_{18} column

E.Y. Suzuki and R.J. Early*

Department of Animal Sciences, University of Hawaii at Manoa, 1800 East–West Road, Honolulu, HI 96822 (USA)

(First received June 7th, 1993; revised manuscript received September 27th, 1993)

ABSTRACT

The conditions for the rapid analysis of amino acids in protein hydrolysates are given for the Whatman Partisphere C_{18} cartridge column. Amino acids from protein hydrolysates are derivatized to phenylthiocarbamyl (PTC) derivatives and separated within 22 min. The Partisphere column is generally less expensive than specialty columns designed for the PTC derivative. The "void sealing" capability of this column, in addition to its guard column attachment, increases the life span of the column.

INTRODUCTION

Analyzing amino acids as phenylthiocarbamyl (PTC) derivatives has gained increased popularity over the past several years due to the fact that the derivatization is simple and stable (one-step derivatization at room temperature); does not require special detection apparatus (uses a standard UV detector at 254 nm); and is very adaptable to most HPLC systems [1]. Specialty columns are available on market for PTC-amino acid analysis [1]. But, generally these specialty columns are among the most expensive columns available. It would be more convenient and less expensive to use more common, multipurpose columns for these analyses. In this respect, the conditions for several of these columns have been reported [2–5]. However, unique separation conditions must be generated for each new column and these conditions take considerable time to develop. In this report, separation conditions are presented for the analyses of PTC derivatives of amino acids from protein hydrolyses using a 125×4.6 mm Partisphere C_{18} cartridge columns available from Whatman (Clifton, NJ, USA).

EXPERIMENTAL

Amino acid hydrolysis

A 10-mg sample of oven-dried (59°C) mixed fish feed (65% crude protein) was placed in a 10-ml hydrolysis tube (Pierce, Rockford, IL, USA). Norleucine and α-aminobutyric acid internal standard (10 μmol each in 100 μl distilled water) were added to the tube; 900 μl of 6 *M* HCl was then added; the tube was flushed three times with nitrogen followed by evacuation; and the sample was hydrolyzed for 24 h at 105°C

* Corresponding author.

0021-9673/93/$06.00

under vacuum. A 50-μl aliquot of hydrolyzate was removed and dried under nitrogen; 50 μl of 50% triethylamine in methanol was added to neutralize the acid; and the sample was again dried under vacuum. Norleucine, α-amino-butyric acid and amino standards (AA-S-18) were purchased from Sigma (St. Louis, MO, USA).

Derivatization

Samples were derivatized according to Bidlingmeyer *et al.* [1]. Briefly, 20 μl of methanol–phenylisothiocyanate–triethylamine–water (7:1:1:1) were added and left for 20 min at room temperature. Phenylisothiocyanate was purchased from Pierce. Methanol and triethylamine was purchased from Fisher Scientific (Santa Clara, CA, USA). Solvents were removed under vacuum and the sample was reconstituted in 2 ml of solvent A (below) and filtered through a nylon-66 0.45-μm filter (Fisher Scientific) before injection.

Chromatography

Chromatography was performed using a Shimadzu HPLC system (Kyoto, Japan) consisting of two LC-6A pumps, column oven (CTO-6A), pump controller (SCL-6A), auto injector (SIL-6A) and variable-wavelength UV detector (SPD-6AV). Data were collected and processed with an Axxiom (Model 727) chromatography data system (Calbasas, CA, USA). UV detection was at 254 nm and 20 μl were injected. The HPLC solvents were similar to that described by Ebert [3]. Solvent A was composed of 50 m*M* sodium acetate and triethylamine (4 ml/l) adjusted to pH 6.4 with phosphoric acid. Solvent B was composed of 50% solvent A, 40% acetonitrile and 10% methanol. All solvents were purchased from Fisher Scientific. All solvents were filtered through an Acrodisc 0.45-μm filter (Fisher Scientific) before use. The column was a 5 μm, 12.5 cm × 4.6 mm Whatman Partisphere C_{18} column equipped with a Whatman reversed-phase guard column and maintained at a temperature of 25°C. The separation conditions were as follows: flow-rate, 1.5 ml/min; initial solvents, 14% solvent B; linear rise to 20% solvent B in 7 min; 20% solvent B for 3 min; linear rise to 41% solvent B in 4 min; 41% solvent B for 7 min; 100% solvent B for 4.5 min. Re-equilibration to 14% solvent B required 4.5 min for a total analysis time of 30 min.

RESULTS AND DISCUSSION

The amino acid hydrolysis procedure was a fairly standard procedure and is not dealt with in this communication. Several excellent reviews are available on this subject [6–9]. PTC derivatives of amino acids are formed from a reaction of phenylisothiocyanate (Edman reagent) with the amino group of amino acids at room temperature. This step is essentially the first step in the Edman degradation that is used in amino acid sequencing of polypeptides. Koop *et al.* [10] are credited with the first use of PTC derivative in amino acid analysis. However, Heinrikson and Meredith [2] and Bidlingmeyer *et al.* [1] are the first to describe the complete analysis of amino acids in protein hydrolysates using phenylisothiocyanate. Heinrikson and Meredith [2] used both an IBM octadecylsilane (ODS) and Altex Ultrasphere octylsilane columns for separating 18 amino acids common to protein hydrolysis within 35 min. Bidlingmeyer *et al.* [1] used a specialty column (Picotag) developed by Waters and achieved a separation time of less than 12 min. This is still the fastest separation time to our knowledge. There is considerable published literature on the Picotag hydrolysate column [1,11–18]. However, specialty columns tend to be expensive. Several other PTC-amino acid analysis systems have been developed using multipurpose columns. These columns have included Spherisorb ODS-2 [3,4,19,20]; Hypersil ODS [5,20]; Nova-Pak C_{18} [21]; Altex Narrow Bore C_{18} [22,23]; IBM C_{18} [2,20], Supersphere C_{18} [24]; Zorbax C_{18} [25] and Altex Ultrasphere C_{18} [26]. The separation times for the majority of these columns have ranged from 15 to 35 min. Separation of PTC-amino acids from a standard mixture of amino acids and from hydrolysates of a feed sample using the present Partisphere C_{18} column is illustrated in Figs. 1 and 2, respectively. The separation time is approximately 23 min and is among the faster elution times. Analyses can also be run at near room temperatures

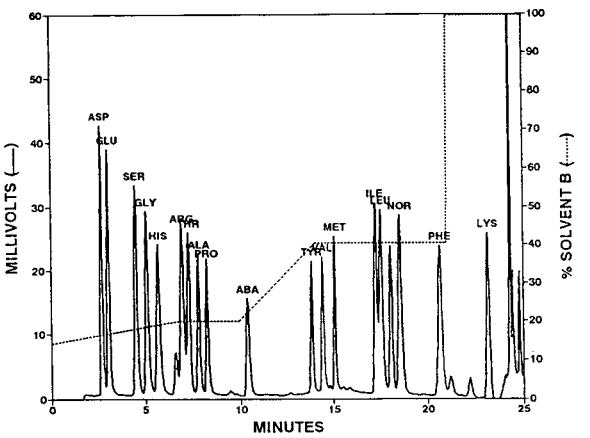

Fig. 1. Chromatogram of PTC-amino acids from standard amino acids mixture at an equimolar concentrations (100 pmol each). ABA = α-Aminobutyric acid (internal standard); NOR = norleucine (internal standard). Chromatographic conditions: column, Whatman Partisphere C_{18} (5 μm) (125 × 4.6 mm I.D.); Whatman reversed-phase guard column; column temperature, 25°C; eluent A, 50 m*M* sodium acetate, triethylamine (4 ml/l), pH 6.4; eluent B, 50% eluent A, 40% acetonitrile, 10% methanol; flow-rate, 1.5 ml/min; gradient, 0 min 14% B, 7 min 20% B, 10 min 20% B, 14 min 41% B, 21 min 41% B, 21 min 100% B; UV detection, 254 nm; injection volume, 20 μl.

eliminating the need for a column heater. Mixtures of standard amino acids were injected onto the column in the range of 10 to 1000 pmol to measure the sensitivity of the method. Linear responses in peak areas were found for all amino acids within the range of 50 to 1000 pmol. Linear responses in peak area below 50 pmol were found for alanine, methionine and norleucine but the other amino acids showed a curvilinear response within this range. The linear response of norleucine and the curvilinear responses of threonine and valine are illustrated in Fig. 3. Threonine and valine were selected in particular because they showed the greatest curvilinear response in the range of 10 to 50 pmol. This sensitivity is similar to that found with specialty columns [1]. The relative molar responses of the amino acids relative to α-aminobutyric acid and norleucine internal standards are given in Table I. These responses were consistent through at least first 300 analyses and a concentration range of 50 to 1000 pmol. The Partisphere C_{18} column is also among the less expensive columns presently on the market. Additionally, Whatman columns have void sealing capabilities as a result of movable inlet frits. These movable frits effectively remove column inlet dead volumes which causes loss of theoretical plates created by prolonged column use. As a result, theoretical plates are partially restored and the column life span increased. In our laboratory we have been able to perform over 300 runs per column with movable inlet frit adjustments at approximately 60–70 h of constant use. The amino acid analysis procedure described here will add more flexibility in analyses that can be performed in lab-

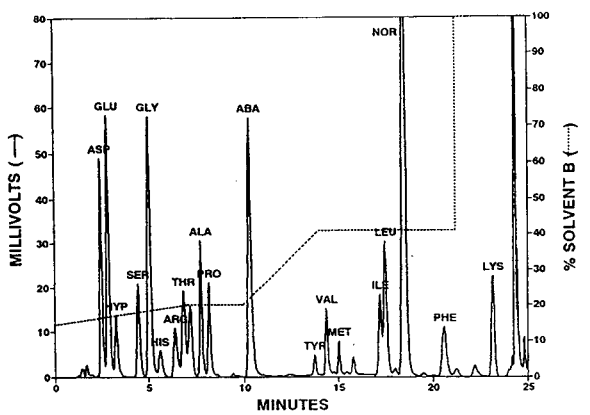

Fig. 2. Chromatogram of PTC-amino acids from a hydrolysate of a mixed fish feed (65% protein). Conditions as in Fig. 1.

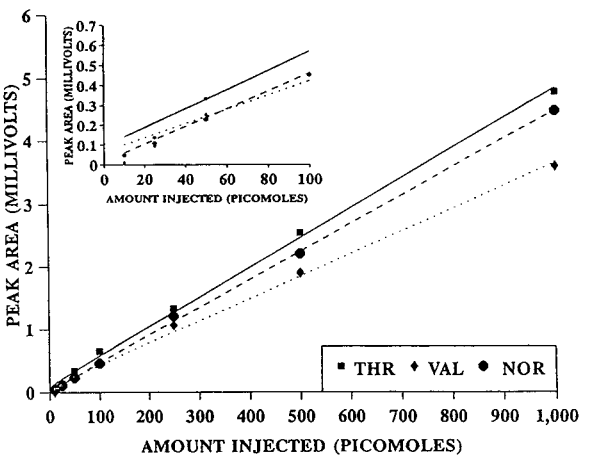

Fig. 3. Linearity of peak area responses of amino acids in the concentration range of 10 to 1000 pmol.

TABLE I

RELATIVE MOLAR RESPONSES (RMR) OF AN EQUIMOLAR MIXTURE OF AMINO ACIDS RELATIVE TO α-AMINOBUTYRIC ACID (ABA) AND NORLEUCINE (NOR) INTERNAL STANDARDS

RMR is calculated by dividing the area of the amino by the area of the internal standard at equimolar concentrations.

Amino acid	RMR_{ABA}	RMR_{NOR}
Aspartic acid	1.01	0.948
Glutamic acid	1.13	1.07
Serine	1.16	1.10
Glycine	1.31	1.23
Histidine	0.894	0.842
Arginine	1.11	1.05
Threonine	1.52	1.43
Alanine	1.23	1.16
Proline	1.33	1.26
α-Aminobutyric acid	1.00	0.941
Tyrosine	1.04	0.980
Valine	1.07	1.01
Methionine	1.16	1.10
Isoleucine	0.898	0.845
Leucine	1.35	1.27
Norleucine	1.06	1.00
Phenylalanine	1.07	1.00
Lysine	2.06	1.86

oratories which currently use the Partisphere C_{18} column.

ACKNOWLEDGEMENT

This research was supported by a University of Hawaii Research and Training Revolving Fund Seed-Money Award from the University Research Council.

REFERENCES

1 B.A. Bidlingmeyer, S.A. Cohen and T.L. Tarvin, *J. Chromatogr.*, 336 (1984) 93.
2 R.L. Heinrikson and S.C. Meredith, *Anal. Biochem.*, 136 (1984) 65.
3 R.F. Ebert, *Anal. Biochem.*, 154 (1986) 431.
4 P. Fürst, L. Pollack, T.A. Graser, H. Godel and P. Stehle, *J. Chromatogr.*, 499 (1990) 557.
5 R.A. Sherwood, A.C. Titheradge and D.A. Richards, *J. Chromatogr.*, 528 (1990) 293.
6 C.W. Gehrke, L.L. Wall, Sr., J.S. Absheer, F.E. Kaiser and R.W. Zumwalt, *J. Assoc. Off. Anal. Chem.*, 68 (1985) 811.
7 R.G. Elkin and J.E. Griffith, *J. Assoc. Off. Anal. Chem.*, 68 (1985) 1028.
8 R.G. Elkin and J.E. Griffith, *J. Assoc. Off. Anal. Chem.*, 68 (1985) 1117.
9 C.J. Rayner, *J. Agric Food Chem.*, 33 (1985) 724.
10 D.R. Koop, E.T. Morgan, G.E. Tarr and M.J. Coon, *J. Biol. Chem.*, 257 (1982) 8472.
11 G. Sarwar and H.G. Botting, *J. Assoc. Off. Anal. Chem.*, 73 (1990) 470.
12 H.P.J. Bennett and S. Solomon, *J. Chromatogr.*, 359 (1986) 221.
13 J.G. Hoogerheide and C.M. Campbell, *Anal. Biochem.*, 201 (1992) 146.
14 B.C. Pramanik, C.R. Moomaw, C.T. Evans, S.A. Cohen and C.A. Slaughter, *Anal. Biochem.*, 176 (1989) 269.
15 M. Raghavan, C.K. Smith and C.E. Schutt, *Anal. Biochem.*, 178 (1989) 194.
16 B.A. Bidlingmeyer, S.A. Cohen, T.L. Tarvin and B. Frost, *J. Assoc. Off. Anal. Chem.*, 70 (1987) 241.
17 G. Sarwar, H.G. Botting and R.W. Peace, *J. Assoc. Off. Anal. Chem.*, 71 (1988) 1172.
18 S.A. Cohen, B.A. Bidlingmeyer and T.L. Tarvin, *Nature*, 320 (1986) 769.
19 L.T. Ng, A. Pascaud and M. Pascaud, *Anal. Biochem.*, 167 (1987) 47.
20 R. Mora, K.D. Berndt, H. Tsai and S.C. Meredith, *Anal. Biochem.*, 174 (1988) 679.
21 T.-M. Chen and J.E. Coutant, *J. Chromatogr.*, 463 (1989) 95.
22 H.-S. Lu and P.-H. Lai, *J. Chromatogr.*, 386 (1986) 215.
23 H.S. Lu, M.L. Klein and P.-H. Lai, *J. Chromatogr.*, 447 (1988) 351.
24 M.M.T. O'Hare, O. Tortora, U. Gether, H.V. Nielsen and T.W. Schwartz, *J. Chromatogr.*, 389 (1987) 379.
25 G. Gimenez-Gallego and K.A. Thomas, *J. Chromatogr.*, 409 (1987) 299.
26 D.J. Strydom, *Anal. Biochem.*, 174 (1988) 679.

Journal of Chromatography A, 657 (1993) 208–212
Elsevier Science Publishers B.V., Amsterdam

CHROM. 25 555

Short Communication

Stability study of 2′-deoxyuridine by liquid chromatography

A. Van Schepdael*, E. Macken, R. Busson, G. Janssen, P. Herdewijn, E. Roets and J. Hoogmartens

Laboratorium voor Farmaceutische Chemie, Instituut voor Farmaceutische Wetenschappen, Katholieke Universiteit Leuven, Van Evenstraat 4, B-3000 Leuven (Belgium)

(Received July 16th, 1993)

ABSTRACT

Previous stability studies on 2′-deoxyuridine (dUrd) made use of UV spectrophotometry. However, this technique does not allow dUrd to be determined separately from its anomer and pentopyranosyl isomers formed during acid degradation. The anomerization and isomerization have been monitored by TLC before, but the separation between dUrd and its α-anomer was not optimal. Therefore, the aim of this study was to determine the rate constants of the degradation of dUrd, using a recently developed liquid chromatographic method. Rate constants of degradation of dUrd were determined at several pH values in the range 1–12. Studies at different temperatures showed that the Arrhenius equation is applicable at pH 1 and 7. To elucidate further the mechanism of hydrolysis in acidic media, some degradation tests were performed at pH 1 on the α-anomer and pentopyranosyl isomers of dUrd.

INTRODUCTION

The stability of dUrd has been investigated mainly by UV spectrophotometry but this method has the disdvantage that the interpretation of the spectral data is hampered by the presence of uracil, as the main degradation product, and of a chromophore formed from the 2-deoxyribose part of the nucleoside molecule in acidic media. This chromophore can be eliminated, however, by working in alkaline media [1], and dUrd can be determined separately from uracil by measuring at two different wavelengths. The following pH ranges have been covered in stability studies: H_0 (Hammett acidity function) −0.92 to −6.47 [2], pH 0.03–0.61 [3] and pH 1.9–6.5 [4]. Later studies have shown that dUrd also anomerizes and isomerizes in strongly acidic media [5]. In this case thin-layer chromatography with radioactive scintillation counting was applied to resolve and determine all compounds formed [6]. We were interested in the stability of dUrd in the frame of a comparative liquid chromatographic stability study of 5-halogenated 2′-deoxyuridines. Therefore, we tried to determine dUrd selectively using liquid chromatography (LC) with the more convenient UV detection mode.

* Corresponding author.

0021-9673/93/$06.00

EXPERIMENTAL

2′-Deoxyuridine and 2-deoxy-D-ribose were purchased from Janssen Chimica (Beerse, Belgium). 1-(2-Deoxy-α-D-*erythro*-pentofuranosyl)-uracil (α-F) was synthesized according to a previously published procedure [7] and the syntheses of 1-(2-deoxy-α-D-*erythro*-pentopyranosyl)uracil (α-P) and 1-(2-deoxy-β-D-*erythro*-pentopyranosyl)uracil (β-P) have been described elsewhere [8]. All reagents were of analytical-reagent grade (Merck, Darmstadt, Germany) and water was distilled twice before use. Tetrahydrofuran was purified by distillation in the presence of iron(II) sulphate and was stored at 5°C in the dark. Stability studies were performed in the pH range 1.09–12.23; Glycine · HCl (0.1 *M*) was used for pH 1.09 and 0.1 *M* phosphate buffer for the other pH values. The ionic strength of all the buffers used was adjusted to 0.4 with KCl. pH was measured at room temperature with a Consort (Turnhout, Belgium) P514 pH meter using a Schott (Mainz, Germany) pH electrode. Samples were incubated at various temperatures in a Memmert (Schwabach, Germany) oven. The reaction was quenched at appropriate intervals by addition of a neutralizing KOH or HCl solution and freezing. All experiments were performed in duplicate.

Samples were analysed as a series by LC, using a Hypersil C_{18} 5-μm column (250 mm × 4.6 mm I.D.) with tetrahydrofuran–0.2 *M* phosphate buffer (pH 4.0)–water (0.1:5:94.9, v/v/v) as the mobile phase. The chromatographic equipment consisted of a Milton Roy mini-pump (Laboratory Data Control, Riviera Beach, FL, USA), used at a flow-rate of 1 ml/min, a Marathon injector (Spark Holland, Emmen, Netherlands) with a 20-μl loop, a Waters (Milford, MA, USA) Model 440 detector set at 254 nm and a Hewlett-Packard (Avondale, PA, USA) Model 3396 A integrator. The column temperature was maintained at 10°C using a jacket connected to a thermostat (Julabo, Seelbach, Germany). The usual starting concentration of dUrd in the LC samples was approximately 10^{-5} *M*. A Waters Model 990 photodiode array detector was used to record the on-line UV spectra.

Merck precoated silica gel F_{254} plates were used for TLC with CH_3CN–$CHCl_3$ (19:81, v/v) as the mobile phase. Column chromatography was performed on silica gel (Merck, 0.040–0.063 nm, 35 × 5.5 cm I.D.) with $CHCl_3$–CH_3CN (95:5, v/v) as the eluent. ^{13}C and ^{1}H NMR spectra were run, at the operating temperature, on a JEOL FX90Q spectrometer in 5-mm tubes, using deuterochloroform as solvent. Mass spectra were recorded on a Kratos Concept 1H mass spectrometer.

RESULTS AND DISCUSSION

The LC system was developed previously with a test mixture of dUrd, α-F, α-P and β-P in water [9]; a typical chromatogram is shown in Fig. 1. This system was found to be valid for quantification because a linear response of the detector was obtained in the kinetic working range. During kinetic studies, however, problems of peak splitting were encountered, probably owing to the very low percentage of organic modifier present in the mobile phase. It is believed that lipophilic components of the sample were retained on the stationary phase and

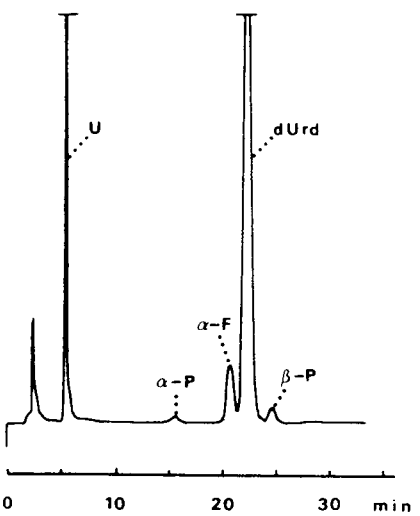

Fig. 1. Chromatogram of a sample of 2′-deoxyuridine degraded at pH 1.09 and 381 K for 4 h. Column, Hypersil C_{18}, 5 μm (250 mm × 4.6 mm I.D.); mobile phase, tetrahydrofuran–0.2 *M* potassium phosphate buffer (pH 4.0)–water (0.1:5:94.9, v/v/v); flow-rate, 1.0 ml/min; temperature, 10°C; detection, UV at 254 nm. U = Uracil.

shielded off the active silanol groups on its surface. Washing with non-polar solvents such as dichloromethane or with acidic polar mobile phases such as acetone–1 *M* perchloric acid–water (50:5:45, v/v/v) regenerated the column to its original state. To prevent these problems we looked for other types of stationary phases on which dUrd would be retained more strongly so that it would be possible to use larger amounts of organic modifier. The following columns were tested but did not improve the method: LiChrosorb diol (10 μm), RSil CN (10 μm) and RSil C_{18} HL (10 μm).

An acid degradation product of 2-deoxyribose is certainly one of the compounds retained on the column with this system, because it is seen in samples in kinetic studies, when analysed under the conditions applied previously for 5-halogenated 2′-deoxyuridines [10]. Chromatography on a Spherisorb ODS-1 (10 μm) column with methanol–0.2 *M* phosphate buffer (pH 5.0)–water (0.1:5:94.9, v/v/v) indeed revealed a substance which was identical (diode array detector; $\lambda_{max} = 262$ nm) with the compound formed through acid degradation of 2-deoxyribose under conditions described previously [1] and which differed from 2-furaldehyde or the acid degradation compounds described by Rice and Fishbein [11]. This compound was isolated by extraction of a degradation mixture of 2-deoxyribose (6 g in 500 ml of 1.2 *M* HCl, 80°C, 3 h) with chloroform. The extract was concentrated and purified by silica gel column chromatography. From mass spectrometry [electron impact ionization, *m/z* 98 ($M^{+\bullet}$), and isobutane chemical ionization, *m/z* 99 (MH^+)] and with the aid of ^1H NMR [δ 2.24 (d, $J = 0.8$ Hz, Me), 4.49 (AB, CH_2) and 5.49 ppm (q, $J = 0.8$ Hz, CH=)] and ^{13}C NMR [δ 16.6 (Me), 75.3 (CH_2O–), 104.7 (*HC*=C–O), 191.3 (=C–O–) and 202.5 ppm (conj. CO)], the compound was identified as 5-methyl-2,3-dihydrofuran-3-one, consistent with earlier results [12].

The degradation reaction of dUrd displayed first-order kinetics over the whole pH range studied. At pH 1.09 and 12.23 not only uracil was formed but also α-F, α-P and β-P, while at all other pH values only uracil was found as the degradation product. The identity of the chromatographic peaks was confirmed by comparison of retention times and by comparison of the UV spectra recorded by diode-array detection [λ_{max}(uracil) = 259 nm, λ_{max}(α-F) = 264 nm, λ_{max}(dUrd) = 262 nm, λ_{max}(α-P) = 260 nm and λ_{max}(β-P) = 260 nm]. Mass balance calculations performed on samples degraded at pH 1.09 and 7.00 fitted within a 4% deviation so that it was concluded that no major compounds were formed other than those described above. As no reference substances with known content were available for α-F, α-P and β-P, these substances were expressed as dUrd in the calculations. At pH 8.91 and 12.23, a decrease in mass occurred, probably because the pyrimidine ring opened in alkali, as has been described for uridine [13].

The hydrolysis of dUrd at various pH values and at 101°C is summarized in Table I. The ionic strength of all buffers was kept at 0.4 with KCl because of its influence on the reaction rate [2]. As the concentration of the phosphate buffer did not influence the degradation at pH 2.00 (see the data in Table I), and as previous investigators did not find buffer catalysis [4], all pH results were assessed together to determine different zones of catalysis. A previously described zone

TABLE I

OBSERVED RATE CONSTANTS FOR THE HYDROLYSIS OF dUrd AT 101°C AS A FUNCTION OF pH

0.1 *M* Glycine·HCl was used for pH 1.09 and 0.1 *M* phosphate buffer for the remaining pH studies. All buffers were of ionic strength 0.4. *N* = Total number of chromatograms; *x* = number of points on the time axis; *y* = number of independent experiments; *z* = number of half-lives during which tested.

pH	k (h^{-1})	*N*	*x*	*y*	*z*
1.09	0.060 ± 0.002	16	4	2	4
2.00	0.0207 ± 0.0005	35	9	2	4
	0.0188 ± 0.0005[a]	26	8	2	2
	0.0185 ± 0.0005[b]	28	8	2	2
2.95	0.0173 ± 0.0004	12	6	1	3
3.81	0.0159 ± 0.0003	28	8	2	3
4.57	0.020 ± 0.003	21	6	2	4
5.85	0.0219 ± 0.0007	16	8	1	4
7.00	0.025 ± 0.002	22	6	2	5
8.91	0.0086 ± 0.0001	13	7	1	3
12.23	0.023 ± 0.001	21	5	2	3

[a] 0.2 *M* phosphate buffer.
[b] 0.3 *M* phosphate buffer.

of specific acid catalysis at pH <0.7 [3] is followed by a zone of slope −0.5, which is probably a transition between the specific acid catalysis zone and the solvent catalysis zone in the pH range 3–7, where the overall slope is approximately zero. The slowest degradation was seen at pH 8.91. Previous workers had shown that the rate of hydrolysis falls off in the pH range 9–11 [4]. Our data at pH 12.23 show that k again rises at higher pH values. The degradation rate constants at pH 7.00 in 0.1 *M* phosphate buffer at 95°C, obtained with the UV spectrophotometric and the liquid chromatographic method, show a close resemblance, namely 0.011 h^{-1} (UV) and 0.012 h^{-1} (LC value calculated using the experimentally determined Arrhenius relationships below).

Fig. 2 depicts the possible mechanism of degradation at pH 1.09. The small amounts of anomer and isomers present could act as intermediates in the degradation of dUrd to uracil or could simply be side products of the degradation, not degrading to any significant extent to uracil. To elucidate this mechanism further, the anomer and isomers of dUrd were degraded under exactly the same conditions as dUrd itself and the observed degradation rate constants are given in Table II.

First it is interesting to note that α-F degrades 1.3 times faster than dUrd at pH 1.09, which is comparable to the factor of 1.4 found for 2′-deoxyadenosine and its α-anomer [14]. York [14] suggested that a reverse anomeric effect together with a steric strain from the *cis*-3′-OH was the cause of the decreased stability of the α- relative to the β-anomer. The presence of a ribopyranosyl sugar in all cases stabilizes the compound since α-F is 12.8 times more labile than α-P and dUrd is 3.2 times more labile than β-P. This is also consistent with the fact that 1-(2-deoxy-α-D-*erythro*-pentofuranosyl)adenine is 29.8 times more labile than 1-(2-deoxy-α-D-*erythro*-pentopyranosyl)adenine [14] and that the adenine and uracil nucleosides of ribo- and glucopyranose are hydrolysed more slowly than those of ribofuranose [15].

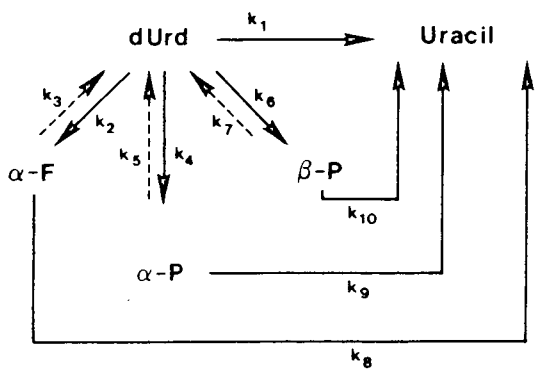

Fig. 2. Possible mechanism of degradation at pH 1.09.

TABLE II

OBSERVED RATE CONSTANTS OF DEGRADATION OF α-F, α-P, β-P AND dUrd AT pH 1.09 AND 101°C IN 0.1 *M* GLYCINE · HCl BUFFER ($\mu = 0.4$)

Compound	k (h^{-1})
α-F	0.077 ± 0.001
α-P	0.0060 ± 0.0002
β-P	0.0191 ± 0.0003
dUrd	0.060 ± 0.002

Further, during this experiment no dUrd could be detected in degradation samples of α-F, α-P or β-P, so that the equilibrium reactions in Fig. 2 can be neglected and k_3, k_5 and k_7 approximate to zero. It can also be concluded that k_8, k_9 and k_{10} are equal to the degradation rate constants observed for α-F, α-P and β-P, respectively. As the α-pyranosyl and β-pyranosyl forms degrade more slowly than dUrd and the α-furanosyl form more quickly, we tend to conclude that dUrd degrades to uracil either directly or mainly through its α-anomer. It should be possible to determine the contributions of k_1, k_2, k_4 and k_6 to the overall degradation rate constant of dUrd if standards of the intermediates were available. In that case a simulation of the experimentally obtained concentration profiles using a multiparameter computer program might be performed [16]. To achieve this, however, α-F, α-P and β-P standards of known purity must be synthesized.

The formation of the anomer and ring isomers of dUrd indicated that two pathways are followed in the degradation of dUrd: on the one hand a direct rupture of the N-glycosidic bond and on the other the formation of a Schiff base intermediate in which the opened sugar ring can recyclize in different ways, thus forming the

anomer or ring isomers [5]. As the percentage of recyclization of the Schiff base intermediate towards a five- or a six-membered sugar ring is not known, it is difficult to distinguish between the two pathways.

Table III gives the results of experiments performed at different temperatures. The following Arrhenius relationships were obtained:

$$\text{pH } 1.09: \log k = 14.6 - 5934(1/T) \quad r = 0.9998$$
$$\text{pH } 7.00: \log k = 12.7 - 5371(1/T) \quad r = 0.9977$$

Activation energies determined from the respective slopes were 26.9 and 24.6 kcal/mol (1 kcal = 4.184 kJ). These in turn yielded entropy of activation values of −11 e.u. at pH 1.09 and −19 e.u. at pH 7.00 and 75°C. The latter large negative value deviates substantially from the value of 3.5 e.u. previously determined at 75°C and pH 6.5 [4].

TABLE III

OBSERVED RATE CONSTANTS FOR THE HYDROLYSIS OF dUrd AT pH 1.09 (0.1 *M* GLYCINE · HCl, $\mu = 0.4$) AND pH 7.00 (0.1 *M* PHOSPHATE BUFFER, $\mu = 0.4$) AS A FUNCTION OF TEMPERATURE

N = Total number of chromatograms; x = number of points on the time axis; y = number of independent experiments; z = number of half-lives during which tested.

pH	T (K)	k (h^{-1})	N	x	y	z
1.09	348	0.0038 ± 0.0002	10	5	1	<1
	374	0.060 ± 0.002	16	4	2	4
	381	0.119 ± 0.005	27	7	2	5
	387	0.191 ± 0.003	24	6	2	6
7.00	338	0.00062 ± 0.00006	12	6	1	<1
	354	0.0029 ± 0.0002	30	6	2	<1
	374	0.025 ± 0.002	22	6	2	5
	387	0.056 ± 0.001	23	6	2	6

ACKNOWLEDGEMENTS

A.V.S. is a Senior Research Assistant of the Belgian National Fund for Scientific Research. The authors thank C. Vinckier (Afdeling Anorganische en Analytische Scheikunde, Katholieke Universiteit Leuven, Leuven, Belgium) for instructive discussions. A. Decoux and I. Quintens are acknowledged for secretarial help.

REFERENCES

1 J.K. Seydel and E.R. Garrett, *Anal. Chem.*, 37 (1965) 271.
2 R. Shapiro and M. Danzig, *Biochemistry*, 11 (1972) 23.
3 E.R. Garrett, J.K. Seydel and A.J. Sharpen, *J. Org. Chem.*, 31 (1966) 2219.
4 R. Shapiro and S. Kang, *Biochemistry*, 8 (1969) 1806.
5 J. Cadet and R. Téoule, *J. Am. Chem. Soc.*, 96 (1974) 6517.
6 J. Cadet and R. Téoule, *J. Chromatogr.*, 76 (1973) 407.
7 H. Aoyama, *Bull. Chem. Soc. Jpn.*, 60 (1987) 2073.
8 P. Herdewijn, A. Van Aerschot, R. Busson, P. Claes and E. De Clercq, *Nucleosides Nucleotides*, 10 (1991) 1525.
9 A. Van Schepdael, A. Van Aeroschot, P. Herdewijn, E. Roets and J. Hoogmartens, *Chromatographia*, 33 (1992) 571.
10 A. Van Schepdael, N. Ossembe, P. Herdewijn, E. Roets and J. Hoogmartens, *J. Pharm. Biomed. Anal.*, 11 (1993) 345.
11 F.A.H. Rice and L. Fishbein, *J. Am. Chem. Soc.*, 78 (1956) 1005.
12 J.K. Seydel, E.R. Garrett, W. Diller and K.-J. Schaper, *J. Pharm. Sci.*, 56 (1967) 858.
13 A.S. Jones, A.M. Mian and R.T. Walker, *J. Chem. Soc. C*, (1966) 1784.
14 J.L. York, *J. Org. Chem.*, 46 (1981) 2171.
15 F. Micheel and A. Heesing, *Chem. Ber.*, 94 (1961) 1814.
16 C. Vinckier, R. Hauchecorne, Th. Cachet, G. Van den Mooter and J. Hoogmartens, *Int. J. Pharm.*, 55 (1989) 67.

Journal of Chromatography A, 657 (1993) 213–218
Elsevier Science Publishers B.V., Amsterdam

CHROM. 25 568

Short Communication

Direct chromatographic separation of the enantiomers of phaclofen, saclofen and hydroxysaclofen

Influence of the anionic moiety

Claude Vaccher, Pascal Berthelot and Michel Debaert*

Laboratoire de Pharmacie Chimique, Université de Lille II, B.P. 83, 3 Rue du Pr. Laguesse, 59006 Lille Cédex (France)

(First received 27th July, 1993; revised manuscript received September 16th, 1993)

ABSTRACT

The direct resolution of three analogues of baclofen (phaclofen, saclofen and hydroxysaclofen), potent γ-aminobutyric acid B antagonists, is achieved by HPLC on an enantioselective crown ether column. The effects of the anionic group are discussed. Perchloric acid and methanol as organic modifier is used as mobile phase. The absolute configuration is proposed by comparison with enantiomers of baclofen (β-*p*-chlorophenyl-γ-aminobutyric acid). The above-mentioned compounds are easily and completely resolved.

INTRODUCTION

γ-Aminobutyric acid (GABA) is a major depressant neurotransmitter involved in the control of neuronal activity in mammals [1]. Receptors for GABA have been subdivided into two distinct classes designated, according to their binding properties, GABA-A and GABA-B receptors [1–4]. Baclofen [4-amino-3-(4-chlorophenyl) butyric acid] (**1**) is the only selective agonist for GABA-B receptors: its *R*-(−) enantiomer is about 100 times more active than the *S*-(+) enantiomer [5]. Selective GABA-B antagonists are of importance to understand the functions of GABA-B receptors. Phaclofen [3-amino-2-(4-chlorophenyl)propylphosphonic acid: phosphonobaclofen] (**2**), saclofen [3-amino-2-(4-chlorophenyl)propylsulphonic acid: sulphonobaclofen] (**3**) and hydroxysaclofen [3-amino-2-(4-chlorophenyl)-2-hydroxypropylsulphonic acid] (**4**) (Fig. 1) have been recently developed in this way by changing the carboxylic acid group to a phosphonic or a sulphonic group. They have proved to be potent antagonists and are currently used as biological tools. As these compounds have a chiral centre at C-3, a detailed investigation of their pharmacodynamic properties could furnish a knowledge of the behaviour of each enantiomer. In this regard there is a real need for the resolution of the enantiomers of these antagonists. As a first step to achieving this, a chromatographic method to separate the

* Corresponding author.

0021-9673/93/$06.00

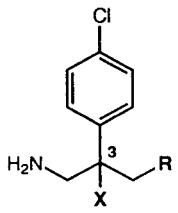

(1) R = CO_2H X = H
(2) R = PO_3H_2 X = H
(3) R = SO_3H X = H
(4) R = SO_3H X = OH

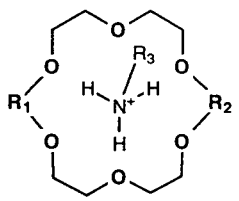

18-crown-6 ether : chiral selector of the CROWNPAK CR

Fig. 1. Chemical structures.

isomers has to be determined, preferably without a derivatization procedure.

We recently described the enantiospecific separation of the agonist baclofen (**1**) [6]. To directly resolve the enantiomeric components, we used a chiral crown ether moiety as chiral selector (Fig. 1). Our interest in the GABA-B receptors [7] prompted us to extend this study to the separation of **2**, **3** and **4**. A comparison was possible to investigate the importance of the anionic group of the molecules in the separation.

EXPERIMENTAL

Chromatography

High-performance liquid chromatography (HPLC) was developed on an LKB Model 2249 metering pump and detection was achieved with a Hewlett-Packard (HP) 1040 photodiode array spectrophotometer connected to an HP 9000 S300 computer. The routine detection wavelengths were 200, 220 and 225 nm. The column was a 150 × 4 mm I.D. Crownpak CR(+) (5 μm) column (Daicel, Baker, France). The sample loop was 10 μl and was made using a Rheodyne 7125 injector. Mobile phase elution was made isocratically using perchloric acid, diluted to obtain the required pH, and methanol as organic modifier. The flow-rate was 0.9 ml/min or 1.5 ml/min. The temperature of the column was controlled by the use of a circulating water through a jacket surrounding the column. Temperature was measured in the water bath. The temperatures used were 30 and 40°C.

TABLE I

ANALYTICAL HPLC: CAPACITY FACTORS (k'), SELECTIVITY OF RESOLUTION (α) AND RESOLUTION (R_s) OF **1–4**

Eluent: $HClO_4$ pH 2–CH_3OH (90:10).

Compound	Flow-rate (ml/min)	Temperature 30°C				Temperature 40°C			
		k'_S	k'_R	α	R_s	k'_S	k'_R	α	R_s
1	0.9	8.4	16.1	1.92	8.01	7.2	11.3	1.57	5.78[a]
	1.5					7.0	11.0	1.57	4.45
2	0.9	3.0	5.5	1.82	4.68	2.3	3.6	1.57	3.75
	1.5					2.3	3.6	1.57	2.89
3	0.9	3.5	7.5	2.15	7.31	2.6	4.9	1.85	6.04
	1.5					2.6	4.9	1.86	4.84
4	0.9	3.1	9.1	2.95	9.98	2.4	5.7	2.40	7.92
	1.5					2.4	5.7	2.40	6.64

[a] Ref. 6.

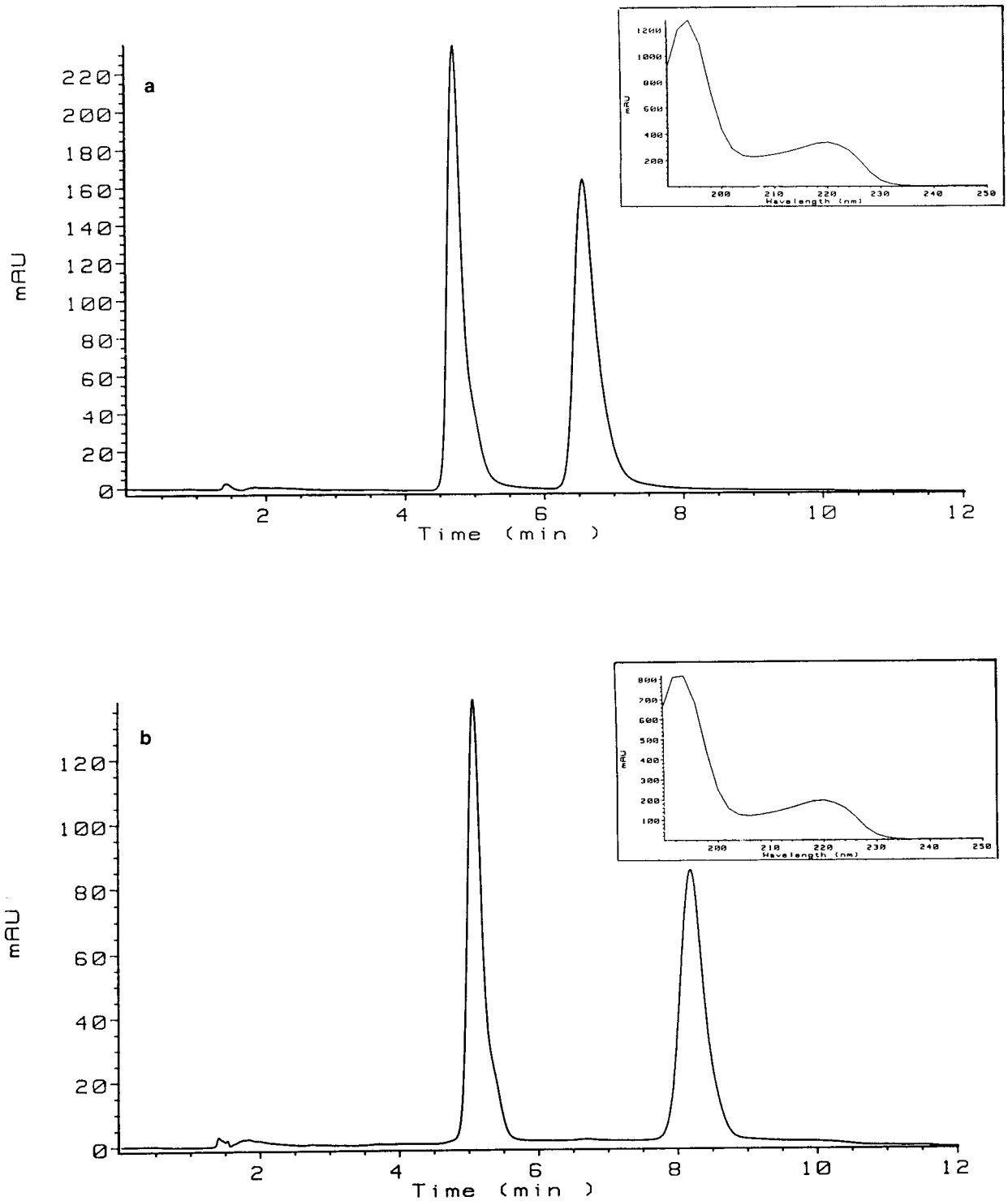

Fig. 2.

(Continued on p. 216)

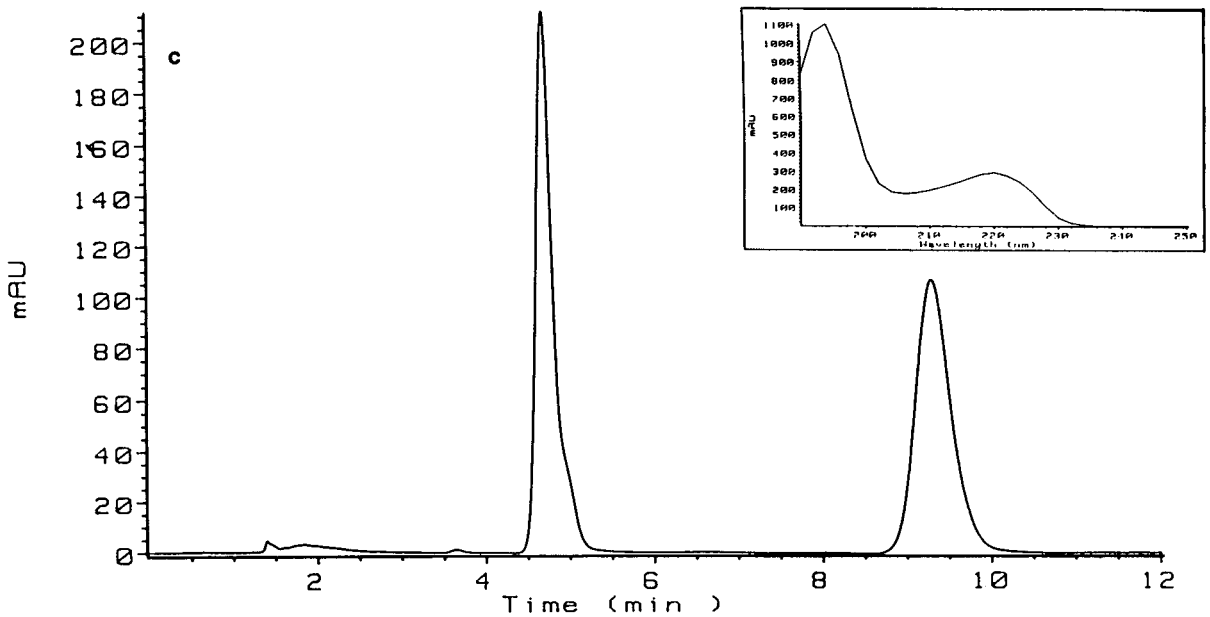

Fig. 2. Chromatographic resolution of (a) **2**, (b) **3** and (c) **4** ($\lambda = 225$ nm). Eluent: $HClO_4$ pH 2–CH_3OH (90:10). Temperature: 40°C. Flow-rate: 0.9 ml/min. The others conditions are described in the Experimental section. Inserts show the UV spectrum of the first eluted peak.

Reagents and materials

Baclofen (**1**) was kindly supplied by Ciba-Geigy. Compounds **2–4** were purchased from Tocris-Neuramin (Langford, Bristol, UK): only their racemates were available. Water used was purified through a Milli-Q unit. The methanol was gradient grade from Merck. Perchloric acid was of analytical grade from Prolabo. The required pH was obtained after dilution as described in the technical note supplied with the column: concentrated acid (70%, 13.6 g) is diluted in 1 l of water to give a pH 1.0 solution, further dilution (100 ml to 1 l) gives a pH 2.0 solution. All the solutions were filtered (0.45 μm), degassed and purged with helium. The mobile phase used was $HClO_4$ pH 2–CH_3OH (90:10). All amino acids were dissolved in the mobile phase to a concentration of about 1.6 m*M* calculated in racemate (which corresponds to $1.6 \cdot 10^{-8}$ mol injected) and passed through a 0.45-μm membrane filter prior to injection. To prevent corrosion and decomposition of the stationary phase, the column and all the apparatus were thoroughly washed with water at the end of each day.

RESULTS AND DISCUSSION

The enantiomeric separation of compounds **1–4** on the crown ether chiral stationary phase is summarized in Table I. For **2**, **3** and **4** adequate resolution can be easily achieved using a $HClO_4$ pH 2–CH_3OH (90:10) solution as mobile phase and representative chromatograms ($\lambda = 225$ nm) are shown at a flow-rate of 0.9 ml/min and 40°C (Fig. 2). The UV spectrum is shown in Fig. 2 for the first eluted peak: as expected, the UV absorbance of the separate enantiomers was identical. Moreover, the UV spectra of compounds **2–4**, are, of course, very similar due to the same conjugation.

The designation of k'_S and k'_R as the first and the second peaks respectively was proposed by analogy with the chromatography, under similar conditions, of authentic samples of the enantiomers of baclofen.

The lower the temperature, the better the resolution becomes (α, R_s increase). The factors α and R_s were found to decrease with increasing temperature from 30 to 40°C: as expected, the resolution increased at the expense of increased

retention times as well as broadened peak shape. The separation remained very satisfactory even at high temperature (40°C), at high-flow-rate (1.5 ml/min) and with an organic modifier in the mobile phase ($R_s \geqslant 1$).

Under identical eluting conditions the order of elution was (Table I) (Fig. 3): **1** (7.0) > **3** (2.6) > **2** (2.3) (40°C, k'_S in parentheses), and **1** (11.0) > **3** (4.9) > **2** (3.6) (40°C, k'_R in parentheses). The same observations can be made at 30°C. So **2** and **3** are much less retained. These compounds are certainly more hydrophilic than baclofen. The substituted constant Π is a good measure of hydrophobicity [8] and the increment values can be calculated for the –COOH, $-SO_3H$, $-PO_3H_2$ moieties: −0.32 (**1**), −1.76 (**3**) and −2.48 (**2**), respectively. They are in perfect accordance with capacity factor order: **2** and **3** constitute a group quite different from **1**. Similar chromatographic behaviour was observed between glutamic acid and its phosphono analogue where the phosphono function is considerably more hydrophilic than the carboxylic one [9]. The factors α and R_s follow the order: α **1**, **2** (1.57) < **3** (1.86), and R_s **2** (3.75) < **1** (5.78) < **3** (6.04) (Fig. 3).

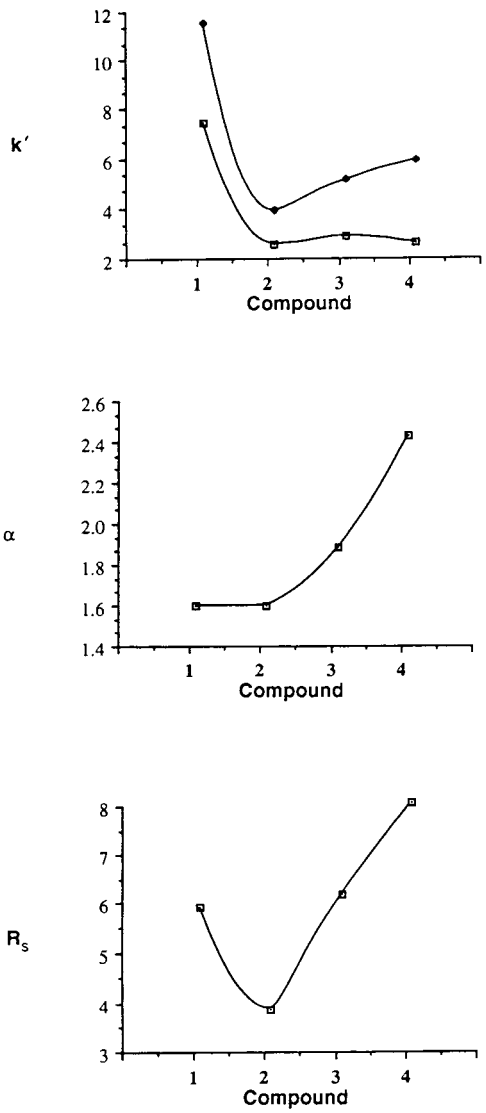

Fig. 3. Variation of the capacity factor k' (□ = k'_1; ◆ = k'_2), enantioselectivity α and resolution R_s of compounds **1–4**. Eluent: $HClO_4$ pH 2–CH_3OH (90:10). Temperature: 40°C. Flow-rate: 0.9 ml/min. (λ = 225 nm). Other conditions are described in the Experimental section.

Between **3** and **4** the presence of a polar OH substituent increases the possibility of chiral discrimination due to the "three-point" interaction, which may involve a supplementary hydrogen bonding and/or dipole interactions between **4** and the chiral stationary phase. In this case steric bulk may also be a factor that affects separation on the column. It can either enhance or decrease enantioselectivity. This depends on whether or not a bulky group prevents the ammonium group from forming a strong inclusion complex. It has been observed that when the primary amine is further removed from the stereogenic centre, steric bulk (due to OH in hydroxysaclofen) seems to enhance the enantioselectivity [10]: **3** (1.86) < **4** (2.40) (40°C, α in parentheses), and **3** (4.84) < **4** (6.64) (40°C, R_s in parentheses). But if a bulky substituent and the amino group are α to the stereocentre, this induces a decrease in enantioselectivity [10].

The good separation of optical isomers of **2–4** make this chromatographic method suitable (i) to quantify optical purity and for studies in pharmacological distribution and (ii) for preparative separation of the enantiomers. In the second case better resolution could, if necessary, easily be obtained at lower pH or without organic modifier or at lower temperature. This method has the advantage of being less time-consuming and less troublesome than the derivatization procedures.

ACKNOWLEDGEMENTS

We wish gratefully to acknowledge Ciba-Geigy (Rueil-Malmaison, France; Basle, Switzerland) for the generous loan of (*RS*)-(±)-baclofen, (*R*)-(−)-baclofen hydrochloride and (*S*)-(+)-baclofen hydrochloride.

REFERENCES

1 H. Möhler, *Arzneim. Forsch./Drug Res.*, 42 (1992) 211.
2 N.G. Bowery, *Trends Pharmacol. Sci.*, 3 (1982) 400.
3 N.G. Bowery and G.D. Pratt, *Arzneim. Forsch./Drug Res.*, 42 (1992) 215.
4 N.G. Bowery, *Trends Pharmacol. Sci.*, 10 (1989) 401.
5 H.R. Olpe, H. Demiéville, V. Baltzer, W.L. Bencze, W.P. Koella, P. Wolf and H.L. Hass, *Eur. J. Pharm.*, 52 (1978) 133.
6 C. Vaccher, P. Berthelot and M. Debaert, *J. Chromatogr.*, 645 (1993) 95.
7 P. Berthelot, C. Vaccher, A. Musadad, N. Flouquet, M. Debaert and M. Luyckx, *J. Med. Chem.*, 30 (1987) 743.
8 C. Hansch and A. Leo, *Substituent Constants for Correlation Analysis in Chemistry and Biology*, Wiley, New York, 1979, p. 48.
9 P.M. Udvarhelyi, D.C. Suntear and J.C. Watkins, *J. Chromatogr.*, 519 (1990) 69.
10 M. Hilton and D.W. Armstrong, *J. Liq. Chromatogr.*, 14 (1991) 3673.

Journal of Chromatography A, 657 (1993) 219–222
Elsevier Science Publishers B.V., Amsterdam

CHROM. 25 596

Short Communication

Gas chromatographic and mass spectrometric investigation of seven carbamate insecticides and one metabolite

Y.Y. Wigfield*, R. Grant and N. Snider

Laboratory Services Division, Agriculture Canada, Ottawa, Ontario K1A 0C6 (Canada)

(First received July 29th, 1993; revised manuscript received September 28th, 1993)

ABSTRACT

Eight thermally labile N-methylcarbamates, aldicarb, carbaryl, carbofuran methiocarb, methomyl, oxamyl and propoxur, the active ingredients of insecticides, and 3-hydroxycarbofuran, the metabolite of carbofuran were separated on a gas chromatographic column, detected by a mass spectrometer and confirmed by positive ion electron impact (PIEI) spectra and ammonium positive ion chemical ionization spectra. The characteristic ions suitable for selected ion monitoring using PIEI are presented. The fragmentation patterns of these carbamates demonstrated that thermal degradation has not occurred under the reported conditions.

INTRODUCTION

To demonstrate food safety, Agriculture Canada has a program to monitor annually the residues of over 120 pesticides and metabolites in many samples of fruits and vegetables using a multi-residue method [1,2]. The sample extract in acetonitrile, after being cleaned up with a Nuchar–Celite column, can be analyzed by gas chromatography coupled with mass-selective detection (GC–MS) using the selected ion monitoring (SIM) mode. Automation allows for the rapid analysis of a large number of samples for residues of organochlorines, organophosphates and nitrogen-containing pesticides. However, N-methylcarbamate insecticides, being thermally labile, have to be analyzed separately by high-performance liquid chromatography with post-column fluorescence detection [3]. This analytical method is time consuming involving a separate analytical system and preparation of post-column reaction reagents.

GC determination of certain carbamates using various temperature profiles and injection techniques [4–6], GC–MS determination of carbamates after derivatization with acetic anhydride [7] and with trimethylsulfonium hydroxide in a programmed-temperature vaporizer (PTV) [8] have been reported. In an effort to increase the output of this program by shortening the analysis time, a preliminary study of their GC behaviour and MS fragmentation was necessary. This paper reports the results of the investigation of seven carbamates (aldicarb, carbaryl, carbofuran, methiocarb, methomyl, oxamyl and propoxur)

* Corresponding author.

and three metabolites (aldicarb sulfoxide, aldicarb sulfone and 3-hydroxycarbofuran). Aldicarb, aldicarb sulfoxide and aldicarb sulfone have been analyzed by GC using a packed column and very low column temperatures (95°C for aldicarb and 130°C for aldicarb sulfoxide and aldicarb sulfone) [6]. On the other hand, direct GC of aldicarb, methiocarb, 3-hydroxycarbofuran and oxamyl using a capillary column and higher column temperatures (50–230°C) has not been previously reported.

EXPERIMENTAL

Analytical standards

Aldicarb (99.9%), aldicarb sulfoxide (99.2%) and sulfone (99.4%) were obtained from Union Carbide (Research Triangle, NC, USA); carbaryl, methomyl, oxamyl and propoxur (all 99.0%) from Caledon (Georgetown, Canada), carbofuran (99.5%) and 3-hydroxycarbofuran (99.0%) from FMC (Middleport, NY, USA) and methiocarb (98.7%) from Mobay (Kansas City, MO, USA).

Stock standard solutions of individual carbamates (100 ng/μl) were prepared in acetone. Composite standard solution 1, which contained aldicarb (20 ng/μl), carbaryl, methiocarb and propoxur (10 ng/μl each) was prepared by combining and diluting appropriate aliquots of the stock solutions with acetone. Composite standard 2, containing methomyl, 3-hydroxycarbofuran (21 ng/μl each), carbofuran (11 ng/μl) and oxamyl (47 ng/μl) was prepared in the same manner as for composite standard 1.

Instrumentation

For GC–MS a Varian Model 3400 gas chromatograph was used with Varian Model 1095 on-column capillary injector and direct capillary coupling to a MAT 90 (Finnigan-MAT) mass spectrometer. The analytical parameters were: column, DB-5 (10 m × 0.32 mm I.D. with 0.25 μm coating); temperatures: injector, 60–200°C at 20°C/min; oven, at 50°C for 7 min, increased to 150°C at 20°C/min, at 150°C for 1 min, to 230°C at 10°C/min and held at 230°C for 4 min; interface, 230°C; source, 250°C for positive ion electron impact (PIEI) mode and 150°C for positive ion chemical ionization (PICI) mode; source presssure for PICI, $3 \cdot 10^{-4}$ Torr (1 Torr = 133.322 Pa); emmission current, 0.35 mA for PIEI and 0.20 mA for PICI; carrier gas, helium at 4 ml/min; injection volume, 1 μl.

RESULTS AND DISCUSSION

GC investigation of these carbamates began with injection of individual carbamates on a gas chromatograph with a flame ionization detector using two different 30-m columns coated with 0.25 μm film thickness of (a) SE-54 (0.32 mm I.D.) or (b) DB-5 (0.2 mm I.D.). Two different temperature profiles were used, (a) injection, splitless, 260°C; oven, 60–260°C at 18°C/min and (b) injection splitless, 250°C; oven, 70°C (2 min),

TABLE I

EIGHT N-METHYLCARBAMATES [R–O–C(O)–NHCH$_3$] ANALYZED BY GC–MS

M_r = Molecular mass.

No.	Carbamate	R	M_r
1	Aldicarb	$CH_3S(CH_3)_2CCH=N-$	190
2	Carbaryl	α-Naphthyl	201
3	Carbofuran	2,3-Dihydro-2,2-dimethyl-7-benzofuranyl	221
4	Methiocarb	4-(Methylthio)-3,5-dimethylphenyl	225
5	Methomyl	$CH_3S(CH_3)C=N-$	162
6	Oxamyl	$(CH_3)_2NC(O)C(SCH_3)=N-$	219
7	Propoxur	2-Isopropoxyphenyl	209
8	3-Hydroxycarbofuran	2,3-Dihydro-2,2-dimethyl-3-hydroxy-7-benzofuranyl	237

increased to 130°C at 25°C/min, to 220°C at 2°C/min, to 280°C at 10°C/min and held there for 4.6 min. The latter temperature profile is normally used for the multiresidue analysis of all other pesticides by GC–MS in our laboratory. Separate injections of individual pesticides showed that all carbamates were degraded except carbaryl, carbofuran, methiocarb and propoxur while 3-hydroxycarbofuran was not degraded when a DB-5 column and the second temperature profile was used. Suzuki *et al.* [4] have demonstrated that when a short wide-bore column (10 m × 0.52 mm I.D.) was used, due to the short column residence time, degradation of carbamates could be avoided; thus a short DB-5 (10 m × 0.32 mm I.D.) column was investigated. A short column with 0.32 mm I.D. offers the advantages of higher resolution and fast analysis time and can result in performance improvement. In addition, to further prevent thermal degradation, a PTV injection technique was used. Under these conditions, regular single peaks were achieved for 7 carbamates and 1 metabolite (Table I) with aldicarb sulfoxide and sulfone showing slow degradation into broad overlapping multiple peaks which were not identified.

Because flame ionization detection is non-selective, a GC–MS system was substituted. The GC–MS chromatograms (Fig. 1A and B) show baseline separation with symmetrical peak shape. Using the PIEI mode, molecular ions were detected for all carbamates except aldicarb, methomyl and oxamyl (see Table II). However,

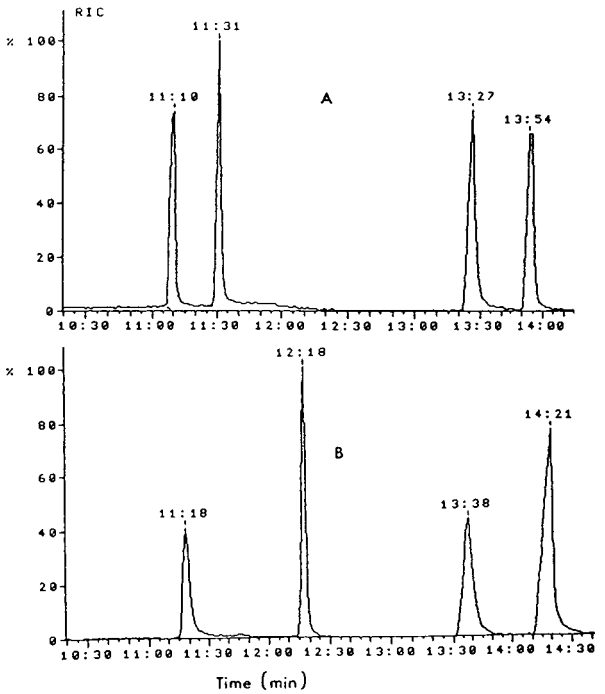

Fig. 1. GC–MS chromatograms of (A) aldicarb (11 min:10 s), propoxur (11 min:31 s), carbaryl (13 min:27 s) and methiocarb (13 min:54 s) and (B) methomyl (11 min:18 s), carbofuran (12 min:18 s), 3-hydroxycarbofuran (13 min:38 s) and oxamyl (14 min:21 s).

TABLE II

INTENSITY AND THE CHARACTERISTIC *m/z* OBSERVED IN EIGHT N-METHYLCARBAMATES

m/z for (a) $[M - SCH_2]^+$, (b) $[M - SCH_2 - 58]^+$, (c) $[CH_3NHCO]^+$, (d) $[CH_3NCO]^+$ in PIEI, and (e) $[M + NH_4]^+$ in ammonium PICI.

Carbamate	Intensity (%)						
	M^+	144 (a)	$[R - OH]^+$	86 (b)	58 (c)	57 (d)	$[M + 18]^+$ (e)
Aldicarb	0	43		92	50	20	30
Carbaryl	1.8		100		0	10	100
Carbofuran	6		100		0	42	40
Methiocarb	4		100		0	10	100
Methomyl	0		75		80	100	100
Oxamyl	0		20		20	80	10
Propoxur	0.3		20		2	6	100
3-Hydroxycarbofuran	0.08		42		0	48	25

TABLE III

RELATIVE STANDARD DEVIATION (R.S.D.) ($n = 4$) OF GC–MS INJECTIONS FOR EIGHT N-METHYLCARBAMATES BY AREA COUNTS (A)

Carbamate	Mass (ng)[a]	Mean ($A \times 10^6$)	S.D. $\times 10^6$	R.S.D. (%)
Aldicarb	20	52.9	3.4	6.5
Carbaryl	10	71.0	4.0	5.7
Carbofuran	11	35.0	6.2	17.6
Methiocarb	10	60.5	3.8	6.3
Methomyl	21	26.0	3.1	11.8
Oxamyl	47	69.9	4.0	5.7
Propoxur	10	70.9	6.0	8.5
3-Hydroxycarbofuran	21	33.3	6.8	20.5

[a] Mass of carbamates injected onto GC–MS.

using the PICI mode with ammonia, the ammonium adducts of these molecular ions, $[M + 18]^+$, were detected (see Table II). These characteristic masses together with the single sharp GC–MS peaks observed in the chromatograms supported the fact that all eight carbamates were eluted from the GC column without undergoing degradation. The acceptable relative standard deviation (R.S.D.) (see Table III) suggested that these carbamates can be quantitated using GC–MS. The R.S.D.s for carbofuran and 3-hydroxycarbofuran were relatively high (17.6 and 20.5%, respectively); however, using GC–flame ionization detection the corresponding R.S.D.s were 6.0 and 7.6% ($n = 6$). In addition, carbofuran has also been analyzed directly using GC with a nitrogen-specific detector [9].

When highly selective and sensitive detection of carbamates is desired, as in the case of residue analysis, the use of MS to monitor pre-selected ions is advantageous. In most cases, except for aldicarb, the ions from the C–O bond cleavage giving the m/z corresponding to $[ROH]^+$ can be utilized for this purpose. For aldicarb, the m/z 144 representing $[M - SCH_2]^+$ can be used instead.

REFERENCES

1 W. Liao, T. Joe and W.G. Cusick, *J. Assoc. Off. Anal. Chem.*, 74 (1991) 554.
2 *L.S.D. Method No. P-RE-023-92(4)-DFV,* Agriculture Canada, Ottawa, 1992.
3 R.T. Krause, *J. Assoc. Off. Anal. Chem.*, 63 (1980) 1114.
4 O. Suzuki, H. Hattori, J. Liu, H. Seno and T. Kumazawa, *Forensic Sci. Int.*, 46 (1990) 169.
5 H.-M. Muller and H.-J. Stan, *J. High Resolut. Chromatogr.*, 13 (1990) 759.
6 S.M. Waliszewski and G.A. Szmczyński, *Fresenius' J. Anal. Chem.*, 338 (1990) 75.
7 H.-J. Stan and Klaffenbach, *Fresenius' J. Anal. Chem.*, 339 (1991) 151.
8 H. Färber and H.F. Schöler, *J. Agric. Food Chem.*, 41 (1993) 217.
9 C.F. Ling and G.P. Melian, *J. Chromatogr.*, 519 (1990) 359.

Journal of Chromatography A, 657 (1993) 223–226
Elsevier Science Publishers B.V., Amsterdam

CHROM. 25 565

Short Communication

Mixed adsorbent for cleanup during supercritical fluid extraction of three carbamate pesticides in tissues

B. Murugaverl, Ahmad Gharaibeh and Kent J. Voorhees*

Department of Chemistry and Geochemistry, Colorado School of Mines, Golden, CO 80401 (USA)

(First received June 16th, 1993; revised manuscript received September 15th, 1993)

ABSTRACT

A mixed selective adsorbent composed of 7% diol and 93% C_{18} has been used in a cleanup column to remove the supercritical fluid lipid extractables from tissues containing carbamate pesticides. Fatty acid and sterols observed in supercritical fluid chromatographic analysis of supercritical fluid extracts of tissues were essentially eliminated. The supercritical fluid extraction recoveries of three carbamate pesticides (Bendiocarb, Methiocarb and Carbaryl) from chicken muscle ranged from 71 to 96%.

INTRODUCTION

The selective extraction of an analyte from a lipid containing material using supercritical carbon dioxide is extremely difficult. Supercritical carbon dioxide readily solubilizes lipid matter, including free fatty acids, glycerides, and sterols. Since co-extraction of the lipid matter is unavoidable and adversely affects the separation and detection of the analytes, procedures to cleanup the extracts are required before analysis. Murugaverl and Voorhees [1] have employed a solid-phase extraction procedure using a C_{18} column in conjunction with an on-line supercritical fluid extraction (SFE)–supercritical fluid chromatography (SFC) system to retain the co-extracted fat components while passing carbamate pesticides. Similarly, France *et al.* [2] have used a cleanup column packed with deactivated alumina or silica in an off-line application for the analysis of chlorinated pesticides in fat. Other investigators have also reported the use of post-extraction solid-phase cleanup columns [3,4]. Each of these analyses varied in the type of analytes and matrices used, but all employed an analytical scheme involving gas chromatography. The reported stationary phases used in the cleanup step in these studies have performed adequately on sample sizes usually less than 100 mg. For example, 5.7 ng of Bendiocarb in 8.7 mg of fat could be analyzed without significant interferences using the C_{18} cleanup column on the on-line system with flame ionization detection [1]. An increase in the fat sample size above 15 mg on this system resulted in significant interferences in the chromatography from the extracted fat components. The following paper

* Corresponding author.

0021-9673/93/$06.00

discusses the development of a new mixed selective adsorbent that can be used for cleanup with SFE on tissue samples greater than 100 mg.

EXPERIMENTAL

Sample preparation

Tissue samples were chopped into very small pieces and then spiked with a standard solution containing about 1.5 μg/μl levels of Bendiocarb, Methiocarb or Carbaryl (Ultra Scientific) in methanol. The spiked muscle was then ground using a mortar and pestle. Hydromatrix (Varian) (30%, w/w) [5] was then added and grinding continued until a uniform consistency was obtained. All reported ppm and ppb values are w/w.

Cleanup column

Stainless-steel column blanks, 4 cm × 3 mm I.D. with 2 μm frits (Keystone Scientific), were partially packed with about 100 mg of a stationary phase containing 7% diol in C_{18} (Keystone Scientific). The cleanup column was flushed with supercritical CO_2 (Air Products) at 219 atm (1 atm = 101 325 Pa) and 90°C for 30 min. The tissue sample was then placed on top of the stationary phase in the cleanup column and attached to the supercritical fluid carbon dioxide.

Extraction condition

Tissue samples were extracted at 90°C and 219 atm for about 30 min, resulting in the use of about 4 ml of supercritical CO_2. In the on-line mode, the extracts were trapped in a cryogenic trapping device (Fig. 1), while in the off-line experiments, extracts were collected into 2 ml of ice-cooled methanol. A 25 μm I.D. fused-silica capillary restrictor was used in both cases. The methanol solutions from the off-line extractions were evaporated to dryness and then reconstituted to 100 μl with methanol for SFC–mass spectrometry (MS) analysis.

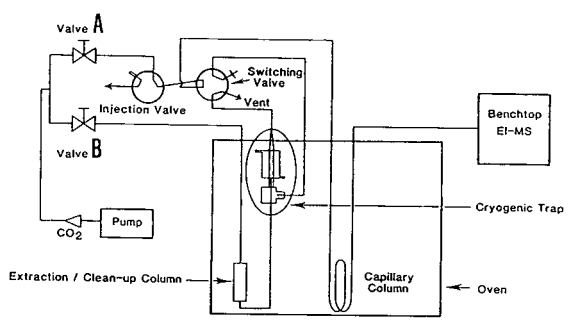

Fig. 1. The on-line SFE–clean-up–capillary SFC–benchtop EI-MS system.

SFC–MS

SFC analysis of off-line extracts was accomplished using a 1.5 m × 50 μm I.D. SB-Biphenyl-30 column (Dionex) with density programming of the CO_2 at 70°C from 0.2 g/ml to 0.7 g/ml at a ramp rate of 0.015 g/ml per min. Extracts were introduced into the SFC system via a Valco injection valve with a 60-nl sample loop. The mass spectrometer (Perkin-Elmer) was operated in the electron ionization mode either in the selected ion monitoring mode or in the full scan mode with a scan range of 75 to 250 u [6].

SFE–cleanup–SFC–MS

The on-line SFE–cleanup–SFC system has been previously discussed [1] and the schematic diagram of this system is shown in Fig. 1. This analysis employed the same Biphenyl column and operating parameters as previously discussed for the SFC–EI-MS analyses.

RESULTS

Several stationary phases including divinylbenzene–styrene, alumina, silica, C_{18}, cyanopropyl, amino and diol, were investigated in this study. Individually, none of these worked satisfactorily. The diol, amino, alumina and silica completely retained the carbamate pesticides investigated, while most of the other phases allowed too much fatty materials through the clean-up column. The optimum stationary phase for the cleanup of fat extracts was found to be a diol–C_{18} (7:93) mixture.

Fig. 2 shows an example of the interferences observed in a total ion chromatogram from 55 mg of beef muscle spiked with 5.5 ppm of Bendiocarb using the on-line system with a C_{18} cleanup column. Analysis of the interference peaks revealed that they consisted mainly of fatty acids and sterols. Selected ion monitoring

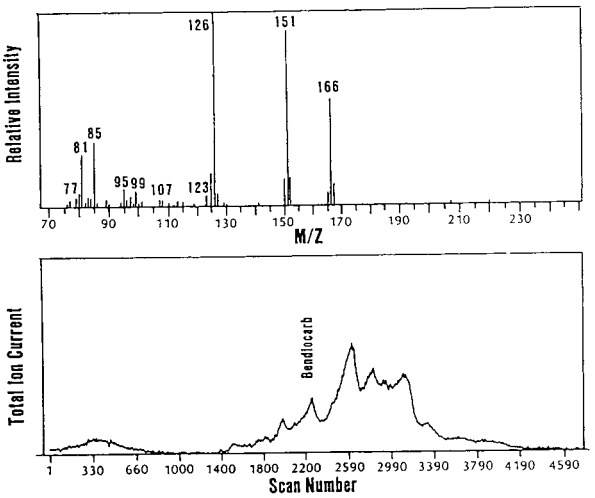

Fig. 2. The on-line SFE–clean-up–SFC–EI-MS total ion chromatogram of 5.5 ppm Bendiocarb in 55 mg beef muscle sample.

of the major Bendiocarb mass spectral peaks, m/z 126, 151 and 166, did not reduce the background signal. This level of interference inhibits a detection level much lower than the observed 5 ppm from Bendiocarb.

Fig. 3 shows the total ion chromatogram of 50 mg of beef muscle spiked with 4.4 ppm Bendiocarb run on the SFE–cleanup–SFC–MS system using a diol–C_{18} (7:93) cleanup column. A

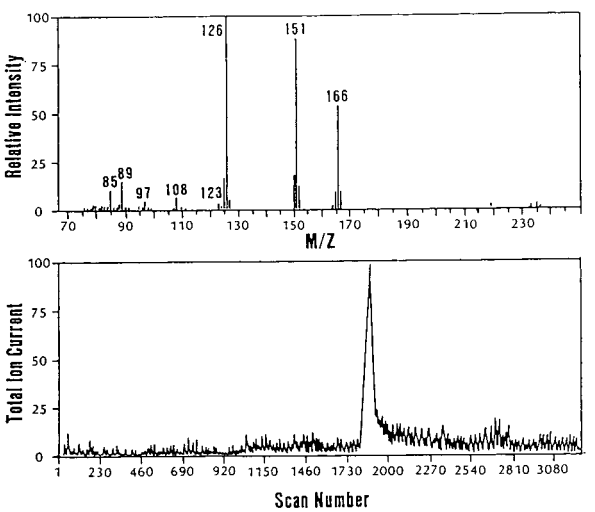

Fig. 3. Total ion chromatogram of the on-line analysis of 50 mg beef muscle sample spiked with 4.4 ppm of Bendiocarb using the diol–C_{18} mixed sorbent in the clean-up column.

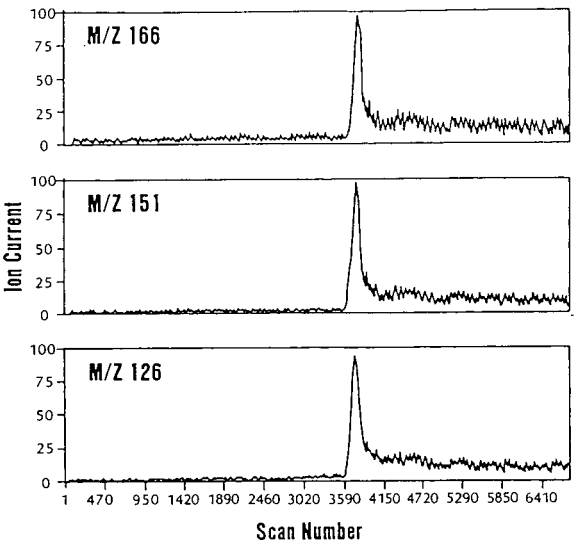

Fig. 4. On-line analysis of 75 mg beef muscle spiked with 1.5 ppm of Bendiocarb using the diol–C_{18} mixed sorbent in the clean-up column. MS operated in the selected ion mode.

comparison between Figs. 2 and 3 clearly shows a dramatic reduction of the background due to the fat components. Fig. 4 illustrates the selected ion trace of m/z 126, 151 and 166 for 1.5 ppm Bendiocarb in 75 mg beef muscle obtained under similar conditions. Using the on-line SFE–cleanup–SFC–MS, muscle samples ranging from 50 to 130 mg spiked with 1 ppm of Bendiocarb have been successfully analyzed. The detection limit for Bendiocarb for these experiments was about 200 ppb.

A series of off-line SFE experiments have been conducted using 95 to 150 mg of chicken muscle. Table I summarizes the means and R.S.D.s from selected ion chromatography results of a 100 mg chicken muscle sample spiked with 260 ppm of Bendiocarb and Carbaryl, and 180 ppm of Methiocarb. Because of the limitations of the injection loop (0.06 μl), higher concentrations of pesticides were used than would normally be analyzed with the on-line system. Using this injection volume, roughly 10 ng of each analyte was injected onto the column. The high R.S.D.s can be attributed to the mass spectrometer integration software. Because of the large peak areas, a slight change in the setting of the baseline by the operator had a

TABLE I

DATA FOR REPETITIVE SFC–MS RUNS OF CARBAMATE PESTICIDES IN 100 mg CHICKEN MUSCLE

	Bendiocarb	Methiocarb	Carbaryl
Sample mass 100 mg			
No. of runs	4	4	4
Mean peak area[a]	$1.91 \cdot 10^6$	$1.05 \cdot 10^6$	$1.41 \cdot 10^6$
R.S.D. (%)	17	22	24
Sample mass 150–300 mg			
No. of runs	5	5	5
Mean peak area[a]	$1.41 \cdot 10^5$	$7.30 \cdot 10^4$	$1.48 \cdot 10^5$
R.S.D. (%)	13	14	15

[a] All peak areas were normalized to a sample mass of 100 mg.

drastic effect on the calculated areas. No effort was made to optimize reproducibility. The signal-to-noise ratio for the peaks was about 20:1. Extraction efficiencies of 85% (Methiocarb), 96% (Bendiocarb) and 71% (Carbaryl) were calculated by comparing the individual means of the extract concentrations against an external standard.

Table I also summarizes similar mean and R.S.D. data for the repetitive off-line analyses using 150 to 300 mg chicken muscle samples spiked with the pesticides at 13 ppm Methiocarb, 19 ppm Bendiocarb and 19 ppm Carbaryl. Following cleanup and the other sample preparations, the quantities of pesticides injected in the 0.06 μl volume onto the SFC was 0.8 to 1.14 ng. A signal-to-noise ratio of 10:1 was observed for the SIM data. The calculated extraction efficiencies for Bendiocarb, Methiocarb and Carbaryl were 77, 80 and 83% respectively.

CONCLUSIONS

The combination of 7% diol and 93% C_{18} is an effective stationary phase for cleanup of supercritical fluid extracts of tissues containing carbamate pesticides. Extraction efficiencies between 71 and 96% were observed. Chicken muscle samples as large as 580 mg containing low ppm levels of pesticides were successfully extracted and then cleaned up using 100 mg of the diol–C_{18} stationary phase. Similar results were also observed for beef muscle.

ACKNOWLEDGEMENT

The authors wish to thank Food Safety and Inspection Service/US Department of Agriculture for their support of this study.

REFERENCES

1 B. Murugaverl and K.J. Voorhees, *J. Microcol. Sep.*, 3 (1991) 11.
2 J.E. France, J.W. King and J.M. Snyder, *J. Agric. Food Chem.*, 39 (1991) 1871.
3 K.S. Nam, S. Kapila, A.F. Yanders and R.K. Puri, *Chemosphere*, 23 (1991) 1109.
4 M.L. Hopper and J.W. King, *J. Assoc. Off. Anal. Chem.*, 74 (1991) 661.
5 N. Alexandrou, M.J. Lawrence and J. Pawliszyn, *Anal. Chem.*, 64 (1992) 301.
6 B. Murugaverl, S. Deluca and K.J. Voorhees, *J. Chromatogr.*, 633 (1933) 195.

Journal of Chromatography A, 657 (1993) 227
Elsevier Science Publishers B.V., Amsterdam

CHROM 25 579

Book Review

Gas–liquid–solid chromatography (*Chromatographic Science Series*, Vol. 56), by V.G. Berezkin, Marcel Dekker, New York, 1991, VIII + 231 pp., price US$ 99.75 (US + Canada), US$ 114.50 (elsewhere), ISBN 0-8247-8425-1.

This work has been prepared by an author who has studied extensively various adsorption effects in gas chromatography and been one of the leading workers in the area. It is suggested that the existing nomenclature gas–liquid chromatography is largely inadequate and a proposal to describe it more adequately as gas–liquid–solid chromatography and liquid–liquid chromatography as liquid–liquid–solid chromatography is developed.

The first chapter is entitled absolute retention and considers a model for the sorbent, the influence of the sorbent surface and equilibrium theories. Standardization of chromatographic nomenclature has been the subject of discussion for decades and it is probably a pity that this work does not indicate the relation of the nomenclature used to the developing situation.

Chapter 3 considers adsorption effects on both relative and invariant relative values, the discussion being developed in Chapter 4 where the effect of the solid support on the efficiency of separation is considered.

Special features of separation form Chapter 5 and phase ratios applicable to packed and capillary columns are detailed. Catalytic effects and adsorption of the solid support and the determination of the equilibrium parameters due to interaction between solutes and solvents form Chapters 6 and 7.

The final chapters consider physicochemical properties related to adsorption and the effect of the solid support on conditioning and ageing of columns.

The author has assembled an extensive bibliography exceeding 700 references on an important topic which chromatographers frequently choose to neglect. Essentially mathematical and requiring careful reading the work will be of value to serious practitioners wishing to extend their knowledge of the chromatographic processes.

While the description of the book indicates an explanation of new trends based on advancement over the last decade it is apparent as with many contributions from Eastern European workers that the work is far from timely. Barely 10% of the citations have appeared in the last decade while over one third appeared during the period of rapid development of gas chromatography in the 1950s and 1960s.

Kensington (Australia) J.K. Haken

Journal of Chromatography

Request for Manuscripts

Ralph Riggin and Gregory Davis will edit a special, thematic issue of the *Journal of Chromatography* entitled "**Analytical Biotechnology**". Both reviews and research articles will be included.

Topics such as the following will be covered:

- Sequencing
- Host Cell Protein Determination
- Peptide Mapping
- Electrophoretic Methods
- Capillary Electrophoresis/Electrokinetic Chromatography
- Protein Mass Spectrometry
- Glycoprotein Characterization
- High-Speed Separations
- Chromatographic Methods
- Residual DNA Determination
- Immunochemical Assays
- Moisture Determination

Potential authors of reviews should contact Roger Giese, Editor, prior to any submission. Address: Mugar Building Rm 122, Northeastern University, Boston, MA 02115, USA; tel.: (617) 373-3227; fax: (617) 373-8720.

The deadline for receipt of submissions is **April 30, 1994**. Manuscripts submitted after this date can still be published in the Journal, but then there is no guarantee that an accepted article will appear in this special, thematic issue. Four copies of the manuscript, citing this issue, should be submitted to the Editorial Office, Journal of Chromatography, P.O. Box 681, NL-1000 AR Amsterdam, The Netherlands. All manuscripts will be reviewed and acceptance will be based on the usual criteria for publishing in the *Journal of Chromatography*.

PUBLICATION SCHEDULE FOR THE 1994 SUBSCRIPTION

Journal of Chromatography A and *Journal of Chromatography B: Biomedical Applications*

MONTH	O 1993	N 1993	D 1993	J	F	
Journal of Chromatography A	652/1 652/2 653/1	653/2 654/1 654/2 655/1	655/2 656/1 + 2 657/1 657/2	658/1 658/2 659/1 659/2	660/1 + 2 661/1 + 2 662/1 662/2	The publication schedule for further issues will be published later.
Bibliography Section						
Journal of Chromatography B: Biomedical Applications				652/1	652/2 653/1	

INFORMATION FOR AUTHORS

(Detailed *Instructions to Authors* were published in Vol. 609, pp. 437–443. A free reprint can be obtained by application to the publisher, Elsevier Science Publishers B.V., P.O. Box 330, 1000 AH Amsterdam, Netherlands.)

Types of Contributions. The following types of papers are published: Regular research papers (Full-length papers), Review articles, Short Communications and Discussions. Short Communications are usually descriptions of short investigations, or they can report minor technical improvements of previously published procedures; they reflect the same quality of research as Full-length papers, but should preferably not exceed five printed pages. Discussions (one or two pages) should explain, amplify, correct or otherwise comment substantively upon an article recently published in the journal. For Review articles, see inside front cover under Submission of Papers.

Submission. Every paper must be accompanied by a letter from the senior author, stating that he/she is submitting the paper for publication in the *Journal of Chromatography A* or *B*.

Manuscripts. Manuscripts should be typed in **double spacing** on consecutively numbered pages of uniform size. The manuscript should be preceded by a sheet of manuscript paper carrying the title of the paper and the name and full postal address of the person to whom the proofs are to be sent. As a rule, papers should be divided into sections, headed by a caption (*e.g.*, Abstract, Introduction, Experimental, Results, Discussion, etc.) All illustrations, photographs, tables, etc., should be on separate sheets.

Abstract. All articles should have an abstract of 50–100 words which clearly and briefly indicates what is new, different and significant. No references should be given.

Introduction. Every paper must have a concise introduction mentioning what has been done before on the topic described, and stating clearly what is new in the paper now submitted.

Experimental conditions should preferably be given on a *separate* sheet, headed "Conditions". These conditions will, if appropriate, be printed in a block, directly following the heading "Experimental".

Illustrations. The figures should be submitted in a form suitable for reproduction, drawn in Indian ink on drawing or tracing paper. Each illustration should have a legend, all the *legends* being typed (with double spacing) together on a *separate sheet*. If structures are given in the text, the original drawings should be supplied. Coloured illustrations are reproduced at the author's expense, the cost being determined by the number of pages and by the number of colours needed. The written permission of the author and publisher must be obtained for the use of any figure already published. Its source must be indicated in the legend.

References. References should be numbered in the order in which they are cited in the text, and listed in numerical sequence on a separate sheet at the end of the article. Please check a recent issue for the layout of the reference list. Abbreviations for the titles of journals should follow the system used by *Chemical Abstracts*. Articles not yet published should be given as "in press" (journal should be specified), "submitted for publication" (journal should be specified), "in preparation" or "personal communication".

Vols. 1–651 of the *Journal of Chromatography*; *Journal of Chromatography, Biomedical Applications* and *Journal of Chromatography, Symposium Volumes* should be cited as *J. Chromatogr.* From Vol. 652 on, *Journal of Chromatography A* (incl. Symposium Volumes) should be cited as *J. Chromatogr. A* and *Journal of Chromatography B: Biomedical Applications* as *J. Chromatogr. B.*

Dispatch. Before sending the manuscript to the Editor please check that the envelope contains four copies of the paper complete with references, legends and figures. One of the sets of figures must be the originals suitable for direct reproduction. Please also ensure that permission to publish has been obtained from your institute.

Proofs. One set of proofs will be sent to the author to be carefully checked for printer's errors. Corrections must be restricted to instances in which the proof is at variance with the manuscript. "Extra corrections" will be inserted at the author's expense.

Reprints. Fifty reprints will be supplied free of charge. Additional reprints can be ordered by the authors. An order form containing price quotations will be sent to the authors together with the proofs of their article.

Advertisements. The Editors of the journal accept no responsibility for the contents of the advertisements. Advertisement rates are available on request. Advertising orders and enquiries can be sent to the Advertising Manager, Elsevier Science Publishers B.V., Advertising Department, P.O. Box 211, 1000 AE Amsterdam, Netherlands; courier shipments to: Van de Sande Bakhuyzenstraat 4, 1061 AG Amsterdam, Netherlands; Tel. (+31-20) 515 3220/515 3222, Telefax (+31-20) 6833 041, Telex 16479 els vi nl. *UK*: T.G. Scott & Son Ltd., Tim Blake, Portland House, 21 Narborough Road, Cosby, Leics. LE9 5TA, UK; Tel. (+44-533) 753 333, Telefax (+44-533) 750 522. *USA and Canada*: Weston Media Associates, Daniel S. Lipner, P.O. Box 1110, Greens Farms, CT 06436-1110, USA; Tel. (+1-203) 261 2500, Telefax (+1-203) 261 0101.

Intelligent Software for Chemical Analysis

Edited by **L.M.C. Buydens** and **P.J. Schoenmakers**

Data Handling in Science and Technology Volume 13

Various emerging techniques for automating intelligent functions in the laboratory are described in this book. Explanations on how systems work are given and possible application areas are suggested. The main part of the book is devoted to providing data which will enable the reader to develop and test his own systems. The emphasis is on expert systems; however, promising developments such as self-adaptive systems, neural networks and genetic algorithms are also described.

Contents:

1. Introduction. Automation and intelligent software. Expert systems. Neural networks and genetic algorithms. Reader's guide. Concepts. Conclusions.

2. Knowledge-based Systems in Chemical Analysis (P. Schoenmakers). Computers in analytical chemistry. Sample preparation. Method selection. Method development. Instrument control and error diagnosis. Data handling and calibration. Data interpretation. Validation. Laboratory management. Concluding remarks. Concepts. Conclusions. Bibliography.

3. Developing Expert Systems (H. van Leeuwen). Introduction. Prerequisites. Knowledge acquisition. Knowledge engineering. Inferencing. Explanation facilities. The integration of separate systems. Expert-system testing validation and evaluation. Concepts. Conclusions. Bibliography.

4. Expert-System-Development Tools (L. Buydens, H. van Leeuwen, R. Wehrens). Tools for implementing expert systems. Tool selection. Knowledge-acquisition tools. Concepts. Conclusions. Bibliography. **5. Validation and Evaluation of Expert Systems for HPLC Method Development - Case Studies** (F. Maris, R. Hindriks). Introduction. Case study I: Expert systems for method selection and selectivity optimization. Case study II: System-optimization expert system. Case study III: Expert system for repeatability testing, applied for trouble-shooting in HPLC. Case study IV: Ruggedness-testing expert system. General comments on the evaluations. Concepts. Conclusions. Bibliography.

6. Self-adaptive Expert Systems (R. Wehrens). Introduction - maintaining expert systems. Self-adaptive expert systems: Methods and approaches. The refinement approach of SEEK. Examples from analytical chemistry. Concluding remarks. Concepts. Conclusions. Bibliography.

7. Inductive Expert Systems (R. Wehrens, L. Buydens). Introduction. Inductive classification by ID3. Applications of ID3 in analytical chemistry. Concluding remarks. Concepts. Conclusions. Bibliography. **8. Genetic Algorithms and Neural Networks** (G. Kateman). Introduction. Genetic algorithms. Artificial neural networks. Concepts. Conclusions. Bibliography. **9. Perspectives.** Limitations of Intelligent Software. Dealing with intelligent software. Potential of intelligent software. **Index.**

© 1993 366 pages Hardbound
Price: Dfl. 350.00 (US $ 200.00)
ISBN 0-444-89207-9

ORDER INFORMATION

For USA and Canada
ELSEVIER SCIENCE PUBLISHERS
Judy Weislogel, P.O. Box 945
Madison Square Station
New York, NY 10160-0757
Fax: (212) 633 3880

In all other countries
ELSEVIER SCIENCE PUBLISHERS
P.O. Box 330
1000 AH Amsterdam
The Netherlands
Fax: (+31-20) 5862 845

US$ prices are valid only for the USA & Canada and are subject to exchange rate fluctuations; in all other countries the Dutch guilder price (Dfl.) is definitive. Customers in the European Community should add the appropriate VAT rate applicable in their country to the price(s). Books are sent postfree if prepaid.

ELSEVIER
SCIENCE PUBLISHERS

0021-9673(19931224)657:1;1-R